Influence of Iron Supplementation on Gut Microbiota and the Natural History of Inflammatory Bowel Disease

Dr Awad Mahalhal

A thesis submitted to the University of Liverpool in accordance with the requirements for award of the degree of Doctor of Philosophy

Gastroenterology Research Unit,
Department of Cellular and Molecular Physiology,
Institute of Transitional Medicine
Faculty of Health and Life Sciences,
University of Liverpool

March 2017

Author's Declaration

I declare that the work in this dissertation was carried out in accordance with the requirements of the University's Regulations and Code of Practice for Research Degree Programmes and that it has not been submitted for any other academic award. Except where indicated by specific reference in the text, the work is the candidate's own work. Work done in collaboration with, or with the assistance of others, is indicated as such. Any views expressed in the dissertation are those of the author.

Signed:…… Date:……. 2017

Copyright Declaration

Abstract

Inflammatory bowel disease (IBD) is idiopathic in origin and is associated with damaged mucosa which may bleed and result in anaemia. Iron deficiency is common in IBD and has been shown to be involved in the pathogenesis of the anaemia of patients with IBD. Treatment of iron deficiency with oral iron supplementation may intensify inflammation and tissue damage, and there is evidence that iron supplementation induces inflammation both in normal rats and in rodent models of IBD.

The intestinal microbiota is considered to play a vital role in the pathogenesis of IBD, and various studies have confirmed the presence of intestinal dysbiosis in IBD patients compared to healthy controls. Furthermore, iron supplementation has been shown to influence microbial diversity. This thesis studies the effect of iron on gut microbial composition in the presence of mucosal inflammation.

These aims were addressed using acute and chronic (DSS) murine models of IBD using wild-type C57BL/6 mice receiving diets differing in iron content. Bacterial gDNA was extracted from faeces, and the microbiota composition was determined by sequencing the V4 region of 16S rDNA on the Illumina MiSeq platform. DSS-induced colitis in all treated mice, but a low iron consumption was clinically (body weight ($p<0.001$) and histology ($p<0.0001$)) more influential on colitis. Whereas, high iron intake was more prominent regarding intestinal microbiota disturbance (reduction in *Bacteroidetes* and *Firmicutes* and an increase in *Proteobacteria* and *Actinobacteria*).

This thesis demonstrates that changes in nutritional luminal iron (100ppm and 400ppm iron) exacerbate colitis and cause dysbiosis in mice with acute or chronic colitis. Iron, therefore, appears to contribute to the dysbiosis which is associated with IBD.

Acknowledgements

First and foremost, I would like to express my genuine gratitude to my supervisor Professor Chris Probert who has supported me throughout my thesis, and without his patience, guidance, and encouragement during the last four years, this doctoral thesis would not have been completed. Also, I would like to thank him for teaching me scientific writing and giving me the opportunity to contribute at international conferences.

My sincere thanks also, to my supervisors, Professors D Mark Pritchard and Barry Campbell for their supervision, advice and insightful comments. I would also like to thank Dr Michael Burkitt and Dr Carrie Duckworth for taking the time to train and support me with some experiments as well as for their valuable advice and discussions. I would like to acknowledge Jonathan Williams for his reporting of DSS colitis-associated features and all members of the Henry Welcome Laboratories at the University of Liverpool for their help, motivation and most of all for making sure that I took time out of work to de-stress and enjoy life during the last four years. I would like to acknowledge the University of Benghazi via the Ministry of Higher Education in Libya for my PhD funding.

All my love and thanks go to my wife, Dr Heba Karosh for her sincere enduring love, support, tolerance, patience and faith in me. Without her, I would not be where I am today. My heartfelt thanks go to my missed parents for raising me to reach this stage in my life. Lastly, thanks to my family and friends for their encouragement and inspiration throughout this study.

List of figures

List of Tables

Table of Contents

1 Introduction

1.1 Inflammatory bowel disease

Inflammatory bowel disease (IBD) is a group of disorders affecting the gastrointestinal tract (GIT). Ulcerative colitis (UC) and Crohn's disease (CD) represent the principal types of inflammatory bowel disease (IBD), and they are idiopathic in nature. In general, IBD patients complain of abdominal pain, diarrhoea, weight loss, and rectal bleeding. Chronic inflammation of the intestinal tract is the main feature of IBD. UC and CD are manageable, but incurable diseases. They often begin in patients in their teens to 20s, and then they frequently show a relapsing and remitting clinical course [1].

At present, the prevalence of IBD in the UK is 0.5–1%, with an estimated 620 000 people believed to be affected. Men and women are diagnosed in similar numbers. The rising incidence of the condition, young age of onset and severe nature mean that treatment of IBD has significant implications [2, 3].

In Crohn's disease, the inflammation may occur anywhere along the digestive tract, whereas in UC the colon is the only affected site. The inflammation disturbs the mucosal layer only in UC, whereas CD shows transmural involvement [4].

IBD patients go through numerous investigations and procedures to make the diagnosis before they can receive appropriate treatment. Medical management of inflammatory bowel disease seeks to induce and maintain remission using corticosteroids, immunosuppressive and biologic agents. As a result of their symptoms, their medication and its side effects,

patients often lack confidence and face significant impacts on their lives, such as loss of jobs, disrupted education and health insurance issues.

1.1.1 Aetiology and pathogenesis

1.1.1.1 Aetiology

IBD is characterised by immunoregulatory defects in the mucosa. Some theories have been proposed regarding the causes of IBD, such as a dysfunctional immune host response to normal intestinal luminal microbes; infection with a particular pathogen; and an impaired mucosal barrier to luminal antigens. Immune responses to the intestinal microbiota in inflamed tissues are thought to result from a failure of tolerance to the commensal microbiota. A dysregulated and inappropriately persistent inflammatory response is central to the development of both types of IBD [5, 6].

1.1.1.2 Pathogenesis

Inflammation is advantageous when it is physiological and stops spontaneously without causing any tissue damage, clearing the trigger of that inflammation. However, in IBD the inflammation is pathological, chronic, and out of control [7].

Existing aetiological concepts of IBD focus on environmental causes (microbial factors), genetic influences, and immunoregulatory defects as it's shown in figure 1-1.

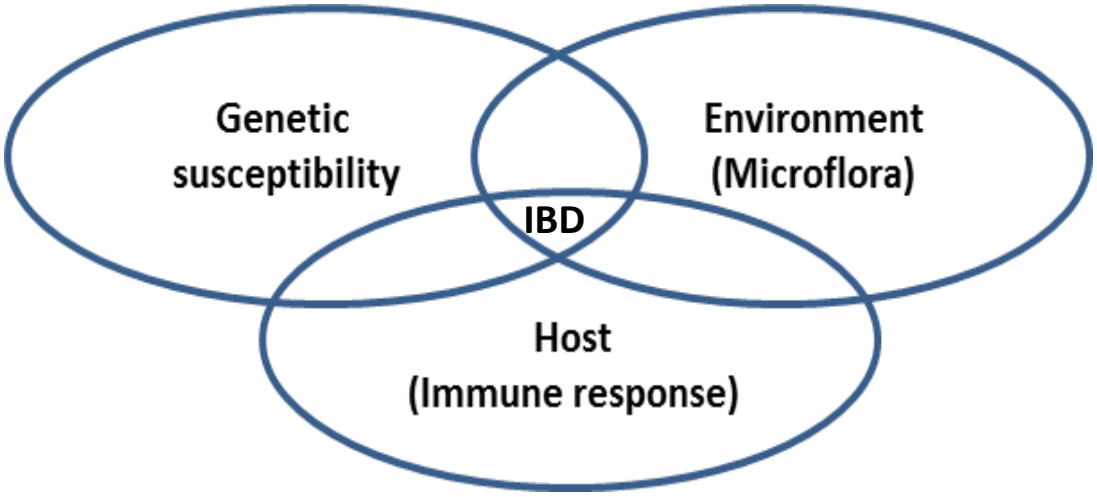

Figure 1-1: The factors contributing to the development of IBD (adapted from [8])

The concept of the impact of environmental factors in IBD came from epidemiologic studies: changes in diet, smoking, alterations in sunlight, pollution, and industrial chemicals are important influences [8]. Hygiene and exposure to infection are risk factors. Poor sanitation seems to protect against IBD since the prevalence of UC and CD in higher socioeconomic communities is greater than in poorer communities. UC and CD are more common in white-collar workers compared with those with blue-collar jobs, and mortality from IBD is low among farmers and builders [9]. Researchers in a German study proposed that working outdoors and physical activity may protect against IBD. Such hypothesis may explain why IBD is more common in northern latitudes and among immigrants from developing countries [10].

Diet is considered to have a major influence on the gut microbiota [11]. A diet rich in high fatty acids increases the risk of IBD, and fast-food consumption causes a 3-4 fold greater risk for IBD [12].

Smoking is the strongest environmental risk factor for IBD. Smoking has the opposite effect on each form of IBD; for example, non-smoking is a feature of UC, whereas smoking is a risk for CD [13]. Moreover, smoking can aggravate the clinical and endoscopic recurrence of CD as well as affecting disease activity (37% among non-smokers, 46% of patients who smoked less than 10 cigarettes/d, and 48% among heavy smokers) after surgery [14]. Maintenance treatment with azathioprine is also more effective in non-smokers than smokers with CD (Figure1-2) [13].

The elements in tobacco that cause these effects are undefined. A modulatory effect of nicotine on immune reactions *in vitro* has previously been detected, so the different association between UC and CD, in particular, is mystifying and may be related to differences in the pathogenesis of the two illnesses [15, 16].

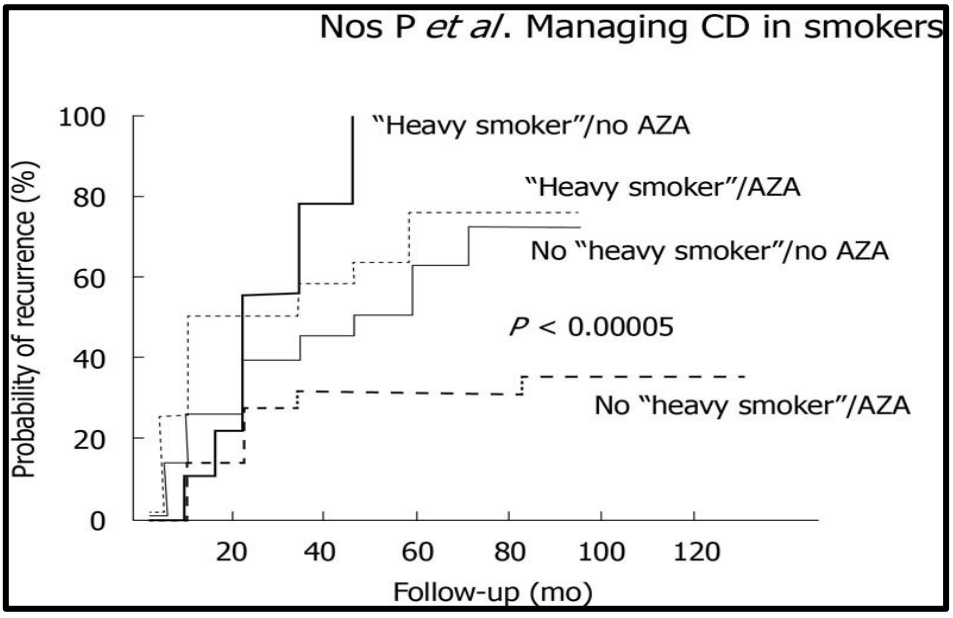

Figure 1-2: Cumulative probability of recurrence depending on the preventive use of azathioprine and active smoking (Reproduced with permission from the author [12])

1.1.1.2.1 Genetic factors

Genetic factors are important in the susceptibility to IBD. UC and CD are polygenic diseases sharing some but not all susceptibility loci [17]. There is an increased rate of IBD in first- and second-degree relatives of patients and a higher relative risk among siblings. The occurrence of IBD among family members ranges from 20% to 30% in referral-based studies and from 5% to 10% in population surveys [17]. The increased risk of IBD in the Jewish community also supports the role of genetic factors in the aetiology of IBD [18].

In families with a high incidence of IBD among first-degree relatives, 75% of those affected are concordant for either UC or CD, whereas 25% are discordant, with some members having UC and others having CD; this finding indicates that the genetic factors may overlap [17]. Furthermore, there is a greater concordance in monozygotic twins with CD or UC, compared with dizygotic twins [19]. Interestingly, immunologic abnormalities, for example, antibodies to *Escherichia coli* O: 14 antigens and intestinal epithelial antigens occur in healthy first-degree families of IBD patients [20, 21].

In fact, there are no individual genes that can cause either CD or UC, although many predisposing genes have been identified. A recent study identified about 163 genes that contribute to the risk of IBD [22]. A genome-wide meta-analysis study found 39 loci involved in Crohn's disease-relevant pathways such as IL-10, IL-27 and TYK2, which emphasises the significant genetic overlap with loci involved in other immune-related diseases [23]. By contrast, another meta-analysis revealed 29 loci containing genes that strengthen the role of epithelial barrier function, intracellular defence and cytokine-dependent signalling in UC, as well as

showing a genetic overlap with Crohn's disease. Besides looking at some complex diseases, genome-wide association studies have identified 99 non-overlapping genetic risk loci, including 28 that are common to Crohn's disease and ulcerative colitis [24].

1.1.1.2.2 Immune response

It is proposed that impaired regulation of the mucosal intestinal immune cascade could be a factor in the development of IBD. Intestinal epithelial cells (IECs) provide a single superficial layer on the intestinal mucosa and act as the first defensive barrier against the luminal content of the gut and protector of the underlying tissues. IECs have important roles, secreting antimicrobial substances [defensins] and communicating with intestinal immune cells through soluble mediators, chemokines and cytokines [25, 26]. In patients with IBD a disruption in function of the epithelial and mucosal barrier occurs; ultimately this will cause chronic recurrence of inflammation in the intestinal mucosa. It has become evident that IECs play a significant part as the first line of defence and as a signal inducer for underlying immune cells. One of the most important features of IECs is the tight regulation of pro- and anti-inflammatory signalling, which is defective in the case of chronic intestinal inflammation [27].

1.1.1.2.3 Microbiota (Bacteria mainly)

Gut bacteria are an ecosystem, which changes over time, as the diet changes, and as general health changes. The colon harbours a complex microbial population of approximately 10^{11} microorganisms per gram of intestinal content: and most of these bacteria are anaerobic. The

most dominant bacteria are *Bacteroides*, *Bifidobacterium*, *Lactobacillus*, *Clostridium*, *Eubacterium*, *Escherichia*, *Enterococcus*, *Streptococcus*, and *Klebsiella*. *Bifidobacterium* and *Lactobacillus* are thought to be the most important health-beneficial bacteria for the human host [28]. The microbiota has many important biological functions such as tissue repair, digestion and protection against pathogens (colonisation resistance), by challenging for space and making anti-bacterial substances such as bacteriocins. The primary function of the helpful bacteria is the synthesis of (SCFA) short-chain fatty acids, which are considered to be essential as a source of energy. The intestinal microbiota plays a key role in the production of essential vitamins such as B groups and K and preserve the acidic environment, aiding immune functions [29].

However, not all intestinal microbes are beneficial. Others are pathogenic for example; some *Clostridia*, *Staphylococci*, *Coliforms*, and *yeasts* or *fungi* [28]. Some non-pathogenic microbes may also contribute to diseases such as IBD [30]. It is still not proven that IBD develops as a result of infection i.e. that there is an association between a single microorganism and inflammation [31].

Most bacterial pathogens enter the host body via mucosal surfaces, as in the gastrointestinal tract. There are many mechanical as well as immunological barriers that protect mucosal surfaces from infection. Colonisation resistance is an additional important protective mechanism [29].

Ordinary gut epithelium contains proinflammatory luminal bacteria, without neutrophil recruitment. About 50% of these bacteria may activate neighbouring gut-specific

macrophages: thus, in the presence of intestinal inflammation, these bacteria may augment degranulation and secretion of proinflammatory cytokines, which result from activating TREM-1 (the receptor expressed on myeloid cells). TREM-1 is a cell surface molecule existing on neutrophils, monocytes, and macrophages within the intestinal lamina propria. Less than 10% of macrophages express TREM-1, suggesting that this is a system to avoid extreme inflammatory reactions [32].

There is little information about colonisation resistance at the molecular level, and how pathogenic bacteria overcome this process. However, recent research in IBD and animal models of enteric disease has found some answers to colonisation resistance. Perturbations of gut microbiota (dysbiosis) can result from gut disturbance, which upsets colonisation resistance and increases pathogen survival [28].

1.2 Anaemia in IBD

Anaemia is a common blood disorder with either too little haemoglobin in the red blood cells or too few red blood cells. Anaemia has a prevalence of around 3% in middle-aged men and 14% in middle-aged women in the United Kingdom, but it is more common in the developing world [33]. Anaemia-specific symptoms include fatigue, breathlessness, headache, dizziness, and palpitations. Iron deficiency (ID)-associated symptoms include impaired nail growth, skin defects, sleeping disorders, loss of libido and erectile dysfunction [34]. There are several kinds of anaemia, and they can be classified by morphology or aetiology as shown in Table 1-1.

(a) Morphology of RBCs		**(b) Underlying aetiology (pathogenic)**
Normocytic: MCV 80-100 fl		Excessive blood loss (haemorrhage).
Microcytic: MCV < 80 fl		Excessive RBC destruction (haemolysis).
Macrocytic: MCV > 100 fl		A defect in blood cell production mechanism (haematopoiesis).

Table 1-1: Classification of anaemia per (a) morphology and (b) aetiology

Anaemia is a common manifestation of inflammatory bowel disease (IBD) affecting about one-third of patients [34]. There are four types of anaemia in IBD patients; iron deficiency, vitamin B12 deficiency, folate deficiency, and anaemia of chronic disease (ACD). Together iron deficiency anaemia (IDA) and anaemia of chronic disease (ACD) are the most common types of IBD-associated anaemia, and these two disorders often coexist [35].

Iron deficiency is the most common cause of anaemia in IBD, as it results not only from constant or repeated blood loss from ulceration of the bowel mucosa but also from decreased iron intake or malabsorption which causes a negative iron balance leading to iron deficiency anaemia [35].

In chronic inflammatory diseases, such as IBD, cytokines, interleukin-1 (IL-1), interleukin-6 (IL-6), tumour necrosis factor-α (TNF-α), and interferon-ɣ (IF-ɣ) concentrations may be elevated, causing adverse effects at different stages of erythropoiesis and inhibition of erythropoietin (EPO) production. In addition, there is retention of iron within macrophages and monocytes (the reticuloendothelial system) because of hepcidin effects (Figure 1-3). The result of this process is termed “anaemia of chronic disease (ACD)” [36, 37].

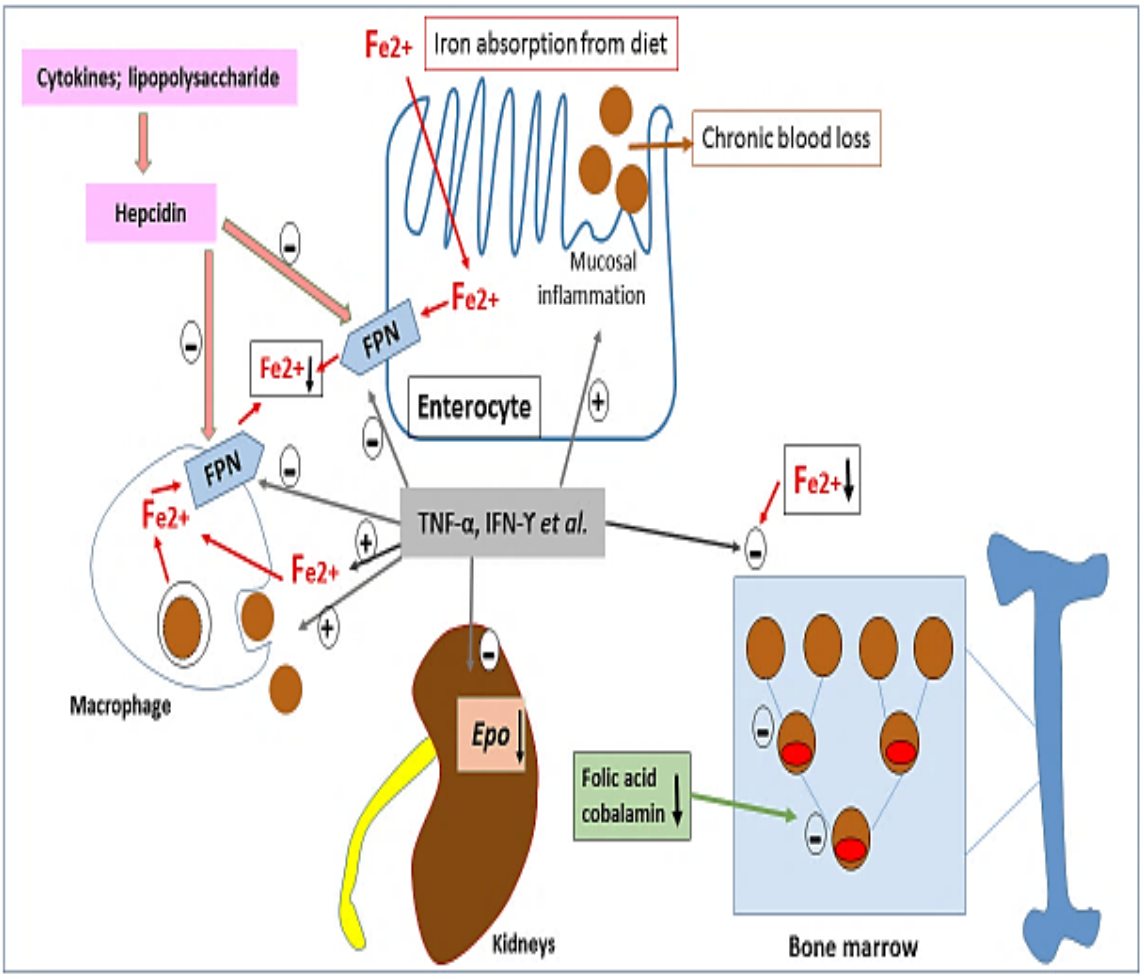

Figure 1-3: Pathophysiological mechanisms of anaemia in IBD patients. Cytokines induce the formation of hepcidin which then blocks cellular iron (Fe2+) export via ferroportin (FPN) from macrophages and inhibits the transfer of absorbed iron from the intestine to the circulation. This will result in a drop of circulating iron and limits its availability for erythroid progenitors, thus blocking erythropoiesis. Some cytokines, such as tumour necrosis factor (TNF)-α and interferon (IFN)-ɣ, will restrict iron in macrophages by stimulating iron uptake, promoting phagocytosis and inhibit iron export via repression of ferroportin transcription. Iron deficiency can also worsen by chronic luminal blood loss in active IBD cases. Further inhibition of the erythropoiesis will further occur due to a reduction in erythropoietin (Epo) formation along with some vitamins deficiencies that can impair erythroid differentiation (adapted from [35]).

1.2.1 Treatment of anaemia in IBD

The persistence of anaemia associated with impaired cardiac and renal function will cause decreased systemic oxygen delivery, reduced physical activity, fatigue, and a declining quality of life. The quality of life in anaemic patients with CD may be the same as that in those who suffer from advanced cancer [38]. Treatment of IBD-associated anaemia should be taken seriously as its correction will improve the quality of life. The best therapy for anaemia of chronic disease (ACD) is to cure the underlying disease. However, this may not always be possible [35].

1.2.1.1 Iron therapy

1.2.1.1.1 Oral iron preparations

There are two types of oral iron supplements; ferrous salts (ferrous sulphate, ferrous gluconate, and ferrous fumarate) and iron polysaccharides (iron polymaltose complex). Oral iron supplementation is frequently used to treat IDA because of its relative safety, efficacy, and cost. However, compliance often declines with time because of gastrointestinal side effects. Patients frequently complain of gastrointestinal symptoms such as nausea, bloating, diarrhoea, constipation and upper abdominal pain. However, the exact cause of these symptoms is still not completely understood; it may be due to the intestinal formation of free oxygen radicals [33]. The goal is to replenish iron stores as well as to treat the anaemia [37].

1.2.1.1.2 Intravenous iron preparations

The parenteral route may be used to avoid the issues with oral iron supplementation. Intravenous iron should be given slowly to avoid cellular toxicity of iron salts [39]. There are several products available.

1- ***Iron dextran:*** this is a stable form of parenteral iron product that may be given as a single dose. This product has a molecular weight (MW) of 100-500 KD; its plasma half-life is 3-4 days, and it has high structural homogeneity. Iron dextran complexes are taken up by the reticuloendothelial system (RES) cells such as macrophages, through phagocytosis, where intracellular degradation occurs and releasing iron into the plasma. The dextran molecule can, however, cause dextran-induced anaphylactic reactions.

2- ***Iron sucrose:*** this has the same molecular weight as iron saccharate (30-100 KD). It is partially stable and has a half-life of about 90 minutes. Cells of the RES and additionally apotransferrin or apoferritin might take up iron sucrose. It is less likely to lead to an allergic reaction than iron dextran.

3- ***Iron gluconate:*** this type of intravenous iron product is unstable with fast dynamic degradation and direct uptake of plasma proteins (apotransferrin, apoferritin, others). Iron gluconate may also be toxic due to oversaturation of transferrin (Tf) binding capacity.

4- ***Ferumoxytol:*** this is used for the treatment of iron deficiency anaemia in adult patients with chronic kidney disease (CKD).

Iron preparation	Brand name	Recommended dose
Oral Iron		
Ferrous sulphate	Feospan, ironorm Drops, ferrogard	300mg (60mg elemental iron) three times a day
Ferrous gluconate	Non-proprietary	300mg (35mg elemental iron) three times a day
Ferrous fumarate	Fersaday, Fersamal, Galfer	200mg (65mg elemental iron) three times a day
Intravenous iron		
Iron sucrose	Venofer	2% (20mg/ml) of iron by slow IV injection or IV infusion, calculated according to body weight and iron deficit.
Iron dextran	CosmoFer (Vitaline)	5% (50mg/ml) of iron by slow IV injection or IV infusion, calculated according to body weight and iron deficit.
Ferric carboxymaltose	Ferinject	5% (50mg/ml) of iron by slow IV injection or IV infusion, calculated according to body weight and iron deficit.

Table 1-2: Iron formulations adapted from BNF

The amount of iron needed to correct anaemia and the best way to administer it is still a subject of debate. Both routes of administration can effectively increase the haemoglobin level in an iron-deficient patient; however, there is no evidence to show that intravenous iron is superior to oral iron. Some side effects of oral iron may result from the high doses prescribed, and a lower iron dose has been suggested to have equal benefits along with fewer side effects [40]. In conclusion, both oral iron and intravenous iron supplements are very effective in IBD [41].

1.2.2 Iron homoeostasis and metabolism

Iron is an essential metal that is required by all organisms. Iron has a transition ability between 2 redox states, which makes it very helpful as a catalyst. Biological functions that require iron include DNA synthesis, oxygen and electron transport, and respiration. The same characteristics that make iron useful also make it toxic. Unbound (free) iron can produce free oxidative radicals, which may damage lipids, proteins, and DNA [42]. In many organisms, iron uptake and storage is regulated by the iron load. In humans, this regulation happens between the amounts of iron that are absorbed, rather than the amount that is excreted. Any disruption will result in anaemia or iron overload [43].

Iron homoeostasis happens mainly in the epithelial cell layer of the duodenum, where about 1-2mg of iron is absorbed from gut each day: iron passes through the apical and basolateral membranes of the enterocytes of the duodenum and upper jejunum. 1-2mg of iron is lost by the skin and gut epithelial turnover process. This mechanism maintains iron balance in the body. The iron, when it is absorbed, will bind to transferrin (Tf) in the plasma. It is subsequently released in the bone marrow for erythropoiesis. The amount of free iron in plasma is very low (3.5-5 mg) compared with the total body amount. Most iron is attached to haemoglobin [43].

Transferrin has two binding sites for iron; about 30-40% of these are occupied under normal physiological conditions. Iron binds to Tf, and it is then taken up by the Tf Receptor (TfR) into target cells by the process of endocytosis and subsequently, at a low pH, disassociation occurs. Iron is then released to perform its functions, which include acting as a cofactor for

many enzymes and intracellular proteins (Figure 1-4) [43]. TfR can be detected in human serum after cleavage of its cytoplasmic and transmembrane domains. This soluble form of TfR (sTfR) is produced when TfR leaves the cell surface. An increase in sTfR level indicates iron deficiency and a high-rate of erythropoiesis. Consequently, sTfR may be used to distinguish between iron deficiency (ID) alone and a combination of ID and ACD [43].

When intracellular iron decreases, TfR expression is upregulated. However, TfR expression is controlled by the interaction of iron regulatory protein (IRP) and iron-responsive element (IRE) post-transcriptionally at the 3`-untranslated region of its mRNA. The affinity of IRP binding to IRE changes with the intracellular concentration of iron, i.e. when iron concentration is low, affinity is high and vice versa. So, binding of IRP to IRE at the 3`-untranslated end of TfR mRNA saves it from degradation and enhances TfR expression. However, binding of IRP to IRE at the 5`-untranslated end of ferritin or 5-aminolevulinic acid (ALA-S) will inhibit the translation and stop protein synthesis. In the case of high intracellular iron, TfR degradation occurs causing an induction of ferritin and ALA-S expression [40].

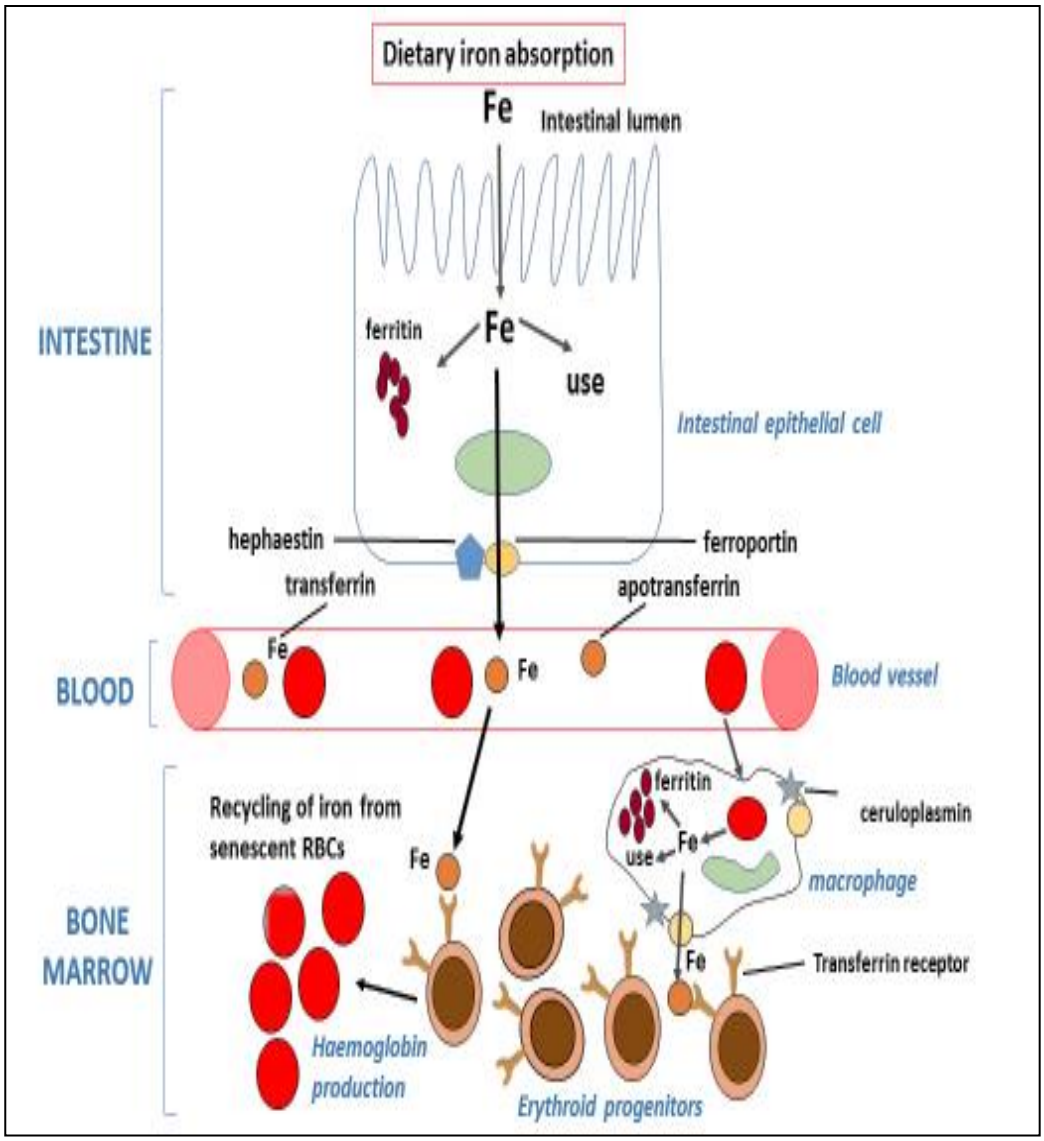

Figure 1-4: Iron homoeostasis and metabolism. Once dietary is iron absorbed from the intestine, it is stored as ferritin in the intestinal epithelial cells or conveyed to plasma as transferrin. Haemoglobin synthesis happens when erythroid progenitors attain iron either from plasma transferrin or reutilizing iron of old erythrocytes which destroyed by macrophages in bone marrow, spleen, and liver. When iron quantity is more than its requirement, it is then stored in macrophages as ferritin, which is then oxidised to hemosiderin. These stores will be released from macrophages in times of need (increased erythropoiesis) adapted from [44].

There is a linear relationship between intracellular and circulating ferritin, which reflects the iron resources. During inflammation or neoplasia serum ferritin levels are increased, giving ferritin the characteristics of an acute phase protein. Thus, in inflammation, a rise in serum ferritin concentrations may obscure iron deficiency [45].

Iron molecules are essential for haemoglobin (Hb) synthesis which depends on the availability of intracellular iron in erythroid precursor cells (Figure 1-4). Haemoglobin holds about 60% of total body iron. Haemoglobin biosynthesis does not begin until the intracellular iron concentration is high. Iron controls the synthesis of some associated proteins, and its metabolism can be detected by measurement of these proteins, which include Hb, Tf, sTfR, and ferritin. Plasma iron concentration on its own is often unhelpful [46].

Preservation of cellular iron homoeostasis is also essential for many vital biological processes, the development of many microorganisms, and for immune functions. Both iron deficiency and iron overload can apply indirect effects on immune status by changing the proliferation of T and B cells [47].

Immunological properties of iron can be seen in macrophage-mediated cytotoxicity by catalysing the construction of reactive oxygen species (ROS); in contrast, oxidative stress and nitric oxide (NO) excite the binding of IRP to IRE process and interact with an expression of TfR and ferritin. Iron-rich macrophages similarly demonstrate a reduction in interferon-ɣ responsiveness, TNF-α production, and (NO) formation [47, 48].

IBD patients have a combination of IDA and ACD because of chronic intestinal blood loss during flares of their disease. Sometimes iron absorption may be impaired in the duodenum and upper jejunum in CD, but in general iron absorption in both CD and UC is normal. However, when chronic intestinal bleeding exceeds the body's absorptive capacity, a negative iron balance will result in [43].

When total body iron has decreased, chronic inflammation triggers iron trapping from the plasma pool. This reaction is an acute response, which will provoke up-regulation of ferritin and down-regulation of Tf assembly. This will reduce Tf-bound plasma iron, which is referred to as a functional iron deficiency. This term means a failure of iron transport to supply an adequate amount of iron from the storage pool to the bone marrow [49].

1.3 Bacteria, iron, and pathogenicity

Over the last decade, there have been many publications on microbial iron metabolism. These have shown the role that iron plays in the *in vivo* growth of infectious pathogens. For many microorganisms, it is vital that they acquire iron to maintain themselves within animals. Without this ability, they will be unable to grow, and eventually, they will be eradicated by the host, or die from nutrient starvation.

Not all bacteria are pathogenic, but they can become so when they find a suitable environment in which to grow within the animal. Bacteria need warmth and nutrients that are necessary for their growth. The human 'host' may provide warmth and nutrients,

including organic carbon, which can found in body fluids and tissues. These molecules are easy for bacteria to use, but iron cannot be found freely in the body [50].

In the human body, iron can be present in two forms, the ferric form (Fe III) and ferrous form (Fe II). In an aerobic environment, iron exists in the oxidised, ferric form. The concentration of free iron in solution at pH 7.0 is usually very low (10^{-18} M), so pathogens have to find a specific mechanism to obtain iron from their host [50].

Generally, in human and other developed vertebrates, iron from the diet is absorbed by mucosal cells of the jejunum then passed into the circulation via attachment with a glycoprotein transferrin (Tf) [34]. There are three types of Tf; serum transferrin (serotransferrin); Lactoferrin (Lf) or lactotransferrin, which is found in several extracellular fluids; and ovotransferrin, previously called conalbumin, which was, initially, discovered in the albumen of eggs. All three types of Tf convey iron to different cells to be used in the synthesis of certain proteins. All kinds of Tf have two similar binding sites for iron; these sites have a binding constant for iron of ~10^{20}. Ideally, this binding capacity should not be fully saturated: leaving some "spare capacity" is essential to take up any extra iron into the blood during infection. This surplus iron-binding capacity of Tf then ensures that no free iron is left in the circulation [34, 51].

The withholding of iron from infecting bacteria is a significant means of host protection, and the virulence of numerous pathogens (investigational infections) has been noticeably enhanced in the laboratory by injecting iron into host animals. A list of such organisms includes *Aeromonas spp*., *Clostridium spp*., *Corynebacterium spp*. and *Enterobacteria spp*.

Escherichia coli, *Klebsiella spp*., *Salmonella spp*., *Listeria spp*., *Neisseria spp*., *Pasteurella spp*., *Pseudomonas spp*., *Staphylococcus spp*., *Vibrio spp*., and *Yersinia spp*. *Mycobacterium avium* and *Mycobacterium tuberculosis* [52, 53] may also be added to this list.

Pathogenic bacteria cannot multiply *in vivo* because of the "iron-withholding" defence mechanism of the infected host. If pathogenic bacteria grow in the host, this suggests that they have developed methods to obtain iron from available sources. For example, bacteria, may bind to transferrin and/or lactoferrin to use the iron associated with these proteins. Bacteria may also obtain iron from haemoglobin (by the destruction of erythrocytes) or ferritin [54].

The main iron storage complex is ferritin. Ferritin is not confined to animals but also occurs in plants (phytoferritin) and many microorganisms (as bacterioferritin). Bacterioferritins can also be found in fungi. Ferritin, characteristically, is composed of 24 protein subunits that form a hollow sphere that can house > 4000 atoms of Fe (III). However, bacterioferritin differs from ferritins and phytoferritin, by possessing haem groups that store iron in iron-replete cells and make it available to the cell whenever it is needed [55].

Bacteria can use two methods to obtain iron from their host tissues. The first is direct contact with iron sources such as Tf or iron proteins (haem and haem proteins) where the iron is then removed by reduction and uptake. In the second, microorganisms, such as bacteria and fungi, synthesise an ultra-high-affinity composite that has a superior binding strength. This binding capacity can physically capture iron from the host protein (ferritin or Tf): such compounds, known as siderophores, play key roles in the microbial iron acquisition. These two methods

are crucial to the understanding of the relationship between the host's response to infection and iron metabolism disturbance [55, 56].

1.4 Iron supplements and IBD activity

Oral iron supplements can increase intestinal tissue injury by catalysing the production of reactive oxygen species (ROS). Inflamed intestinal mucosa contain activated neutrophils which produce ROS in excess which in turn aggravates the injured mucosal tissues. As free iron is considered to be a strong catalyst for ROS production, oral iron therapy such as ferrous sulphate tablets may be harmful to IBD patients. Oral ferrous sulphate tablets are poorly absorbed and lead to a high faecal iron concentration where it will be ready for catalytic activity [57].

It is believed that many iron supplements can affect the immune system as well as intestinal inflammation in IBD. Iron inhibits interferon ɣ (INF-ɣ) activity which has disabling effects on macrophage function and T helper one cell (Th1) reaction. Therefore, giving parenteral iron will reduce Th1-driven intestinal inflammation in Crohn's disease [38].

1.5 Human-associated microbiota

The human body is home to multiple groups of microbes. It is an ecosystem of many different niches or a metacommunity. Human-associated microorganisms are estimated to number 10^{14} in total; this is about ten times the number of human cells per individual. These microbial

populations reside in the mouth, nose, ears, vagina, skin, and in the intestinal tract. As an ecosystem, it is comparable to ecological sources where microbes are present, for example, seawater and soil. Each anatomical site has unique physiochemical features, and each location is occupied by specific types of microbes [58]. The mainstream of the human-associated microbes and the most diverse community is in the intestinal tract, where microbial abundance increases from the stomach to the colon. The highest number of microbes is found in the stool (10^{11} per mL), in which the complex ecosystem contains bacteria, archaea, yeasts, and other eukaryotes [59].

1.5.1 Composition and function

Human microbiota is a term referring to the total number of microorganisms. These microbes include bacteria, fungi, yeast, and archaea, in different abundances and diversities, depending on location and local environment. A study of the human skin bacteria found that the greatest numbers of types were allocated to the *Actinobacteria*, *Firmicutes*, and *Proteobacteria* phyla. However, in the same study, the structure of the skin microbiota was the same between samples from the left and right forearm of most participants, but highly variable at different time-points and between different individuals [60].

The idea that all microbes are harmful to humans has been replaced by the concept that the majority of microbe-host interactions are non-pathogenic, i.e. commensal where microorganisms benefit without causing any harm to human, or, mutualistic, in which both partners benefit. How extra-intestinal microbes may be beneficial is unknown. According to many recent studies, it is clear that the gut microbiota benefits the host in several different

ways. Intestinal symbionts have been shown to have important roles in nutrient digestion and synthesis, vitamin synthesis, energy metabolism, epithelial development, and immune responses. In turn, the intestinal bacteria are provided with steady growth conditions and a continuous stream of nutrients [59].

The human vagina is occupied by a range of microbes from a pool of over 50 species. *Lactobacilli* are very common, mostly in healthy women. Changes in the microbiota can cause infection such as bacterial vaginosis (BV); this condition is characterised by a depletion of the *lactobacillus* population. However, *in vitro* studies have found that *Lactobacillus* strains can interrupt BV and yeast biofilms and prevent the growth of urogenital pathogens [61].

1.5.2 Gut microbiota

The gut microbiota, previousely known as the gut flora, consists of trillions of microorganisms in human intestines; these microbes participate in some metabolic activities like those of an organ. Gut microbiota also contributes to immune system development: changes in its composition can be associated with many chronic diseases including obesity and diabetes [11]. However, it is possible that around 99% of the bacteria come from 30 or 40 species. Moreover, fungi, protozoa, virus and archaea also make up a part of the gut microbiota, but their activities are still not fully understood [62].

1.5.2.1 Normal gut microbiota

The oral microbiota has been linked to local (periodontal) as well as systemic diseases such as bacterial endocarditis and preterm labour. The composition of the oral microbiota varies depending on the site as well as between individuals. The most abundant genera found include *Streptococcus*, *Gemella*, *Granulicatella*, and *Veillonella* [63].

A study of bacteria present in the oesophagus of four healthy participants showed the presence of nearly 100 bacterial species. The upper oesophagal microbiota was similar to those in the oral cavity (*Streptococcus*, *Prevotella*, and *Veillonella*). In the lower part of the oesophagus, the microbiota was closer to that found in the stomach despite its high acidic environment. *Helicobacter pylori* (*H. pylori*) may reside in the stomach and play a role in the development of many gastric diseases. A study analysing the bacterial 16S rDNA of gastric biopsies in 23 individuals found 128 phylotypes. The majority of the sequences belonged to *Proteobacteria*, *Firmicutes*, *Actinobacteria*, *Bacteroidetes*, and *Fusobacteria* phyla, suggesting that the human stomach harbours a distinct microbiota [64].

Regarding the microbiota in the large intestine and faeces, around 395 phylotypes were identified from 11,831 bacterial 16S rDNA sequences in an extensive study which analysed multiple colonic sites and the faeces of three healthy individuals. However, there was only one phylotype, *Methanobrevibacter smithii* that was detected among the 1524 sequences amplified with archaeal primers. The majority of phyla were assigned to the *Firmicutes* and *Bacteroidetes*; while the minor phyla were *Proteobacteria*, *Actinobacteria*, *Fusobacteria*, and

Verrucomicrobia. The intersubject variation was greater than that between different sites within a single individual [65].

1.5.2.2 Intestinal microbiota and disease

To understand the intestinal microbiota and its role in human health and disease, we should increase our knowledge of the function and composition of the human-associated microbiota as well as the consequences of its perturbation on the host and its symbionts.

For example, a connection between intestinal microbiota and obesity has been reported; the faeces of an obese mouse model has a lower energy value than that of a wild-type mouse, signifying that the obese mouse is better able to extract energy from its diet. The gut microbiota of obese mice was given to germ-free (GF) mice, and this resulted in weight increase, although repeating the same experiment using gut microbiota from lean mice caused no reduction of the weight of GF obese mice. The intestinal microbiota of obese mice demonstrated fewer *Bacteroidetes* and more *Firmicutes*; similar findings occur in lean and obese humans [66, 67].

Recent studies in rodents have shown changes in bacterial composition in the case of colonic inflammation and infection. Advanced molecular techniques have demonstrated changes in mucosal bacterial composition and faecal microbiota in patients with Crohn's disease and ulcerative colitis. There is a decrease in specific phyla in CD and UC such as *Bacteroidetes* and *Firmicutes* [68].

1.5.2.3 Physiological interactions between the microbiota and host

In the healthy intestine, commensal gut microbiota contributes to homeostatic responses by epithelial cells and different types of immune cells such as macrophages, dendritic cells (DC), T lymphocytes, and B cells, thus allowing cohabitation with potentially toxic microbial products. The most important homeostatic responses include down-regulating bacterial receptors, promoting intracellular and secreted molecules that stop adaptive and innate immune responses and stimulating protective fragments that facilitate mucosal barrier function. Bacteria have unique ways of entering cells i.e. transmembrane design recognition receptors, such as intracellular nucleotide-binding oligomerization domain (NOD) receptors, Toll-like receptors (TLR) and, NOD-like receptor (NLR) family. The central signalling cascade starts once these bacterial receptors have been occupied. The recognition cascade is inhibited by stimulation of interferon (IFN), interleukin (IL)-10, and transforming growth factor (TGF). In order to regulate such inhibition, paracrine exchanges between epithelial cells and lamina propria regulatory lymphocytes that secrete TGF and IL-10 are needed (Figure 1-5) [69-71].

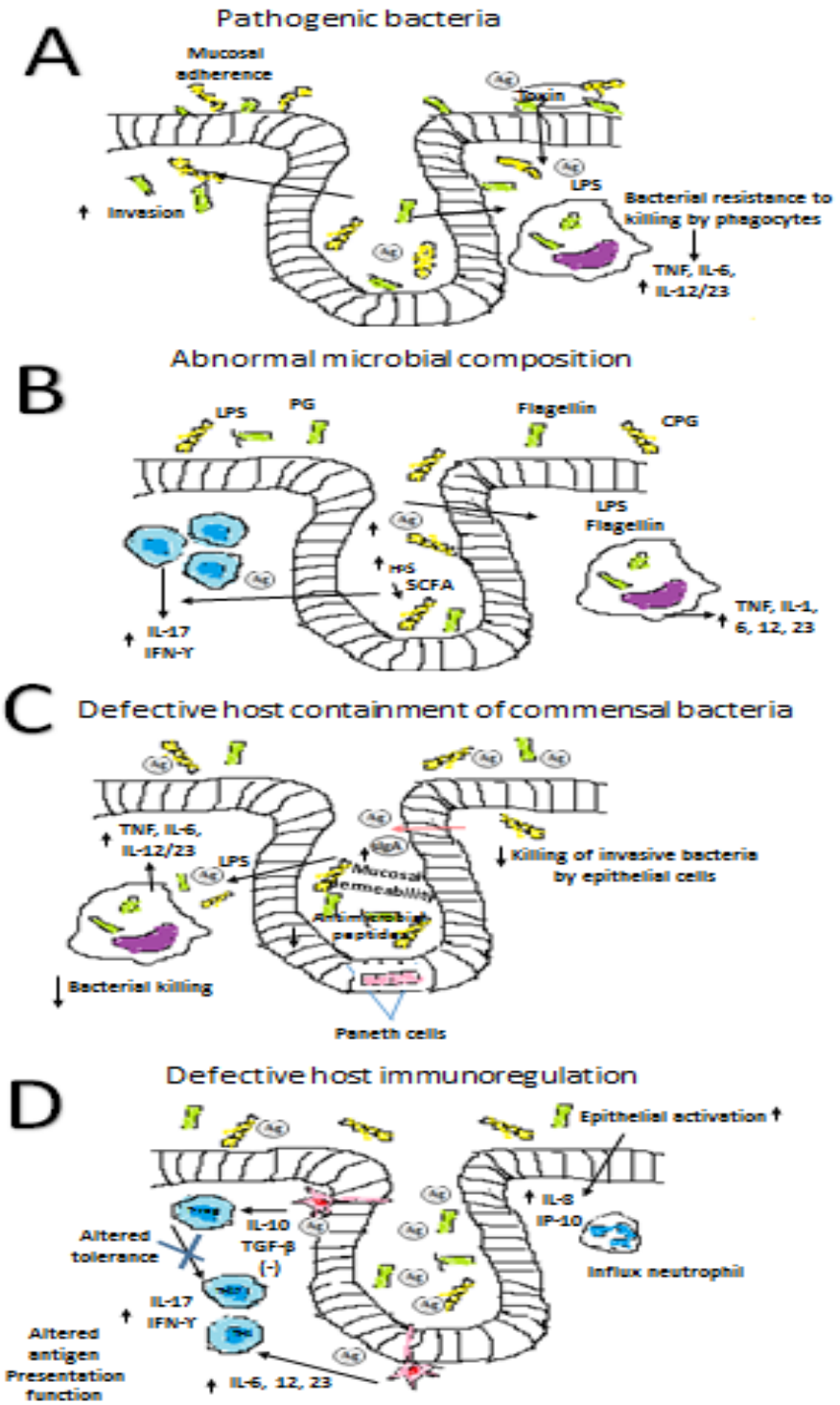

Figure 1-5: Possible mechanisms of inducing chronic immune-mediated intestinal injury by enteric bacteria. (A) A common pathogen or dysbiosis will increase bacterial stimulation of innate and adaptive immune responses. (B) a reduction in the bacteria that produce SCFA such as butyrate may increase mucosal permeability to toxic metabolites such as hydrogen sulphide (H_2S). (C) inadequate secretion of antimicrobial peptides or secretory IgA will cause bacterial mucosal overgrowth creating flawed killing of phagocytosed bacteria increasing mucosal permeability. (D) Failed down-regulation of innate immune response in epithelial and antigen-presenting cells (APC), can stimulate inflammation. However, dysfunction of regulatory T cells or APC will aggravate T cells response to universal microbial antigens (i.e., loss of tolerance) (Adapted from [69])

1.5.2.4 Flawed bacterial killing mechanism in Crohn's disease

There are pathophysiologic similarities between CD and chronic granulomatous diseases, such as defective phagocyte function and polymorphisms of genes that regulate the clearance of intracellular pathogens. There are defects in innate antimicrobial function in subtypes of CD triggered by defective clearance of commensal, opportunistic or pathogenic bacteria. This, followed by initiation of compensatory antibacterial effector T cells resulting in tissue damage [71].

Some of the genetic polymorphisms that are found in CD are associated with failed killing and include autophagy-related protein 16-1 (ATG16L1) and immunity-related GTPase family M protein (IRGM), NOD2, and Neutrophil cytosol factor 2 (NCF2) [72]. Deletion of the autophagy gene ATG16L1 results in Paneth cell morphologic changes and reduced expression of antimicrobial peptides (Figure 1-6). A reduction in antimicrobial peptide secretion might cause bacterial overgrowth, the rise of mucosal adherent bacteria and translocation of commensal bacteria, whereas a defective clearance of invasive or phagocytized bacteria encourages persistence of viable intracellular bacteria. These two mechanisms increase antigenic stimulation of pathogenic TH1/TH17 cells and promote chronic granulomatous inflammation and increase susceptibility to infection by opportunistic pathogens [73].

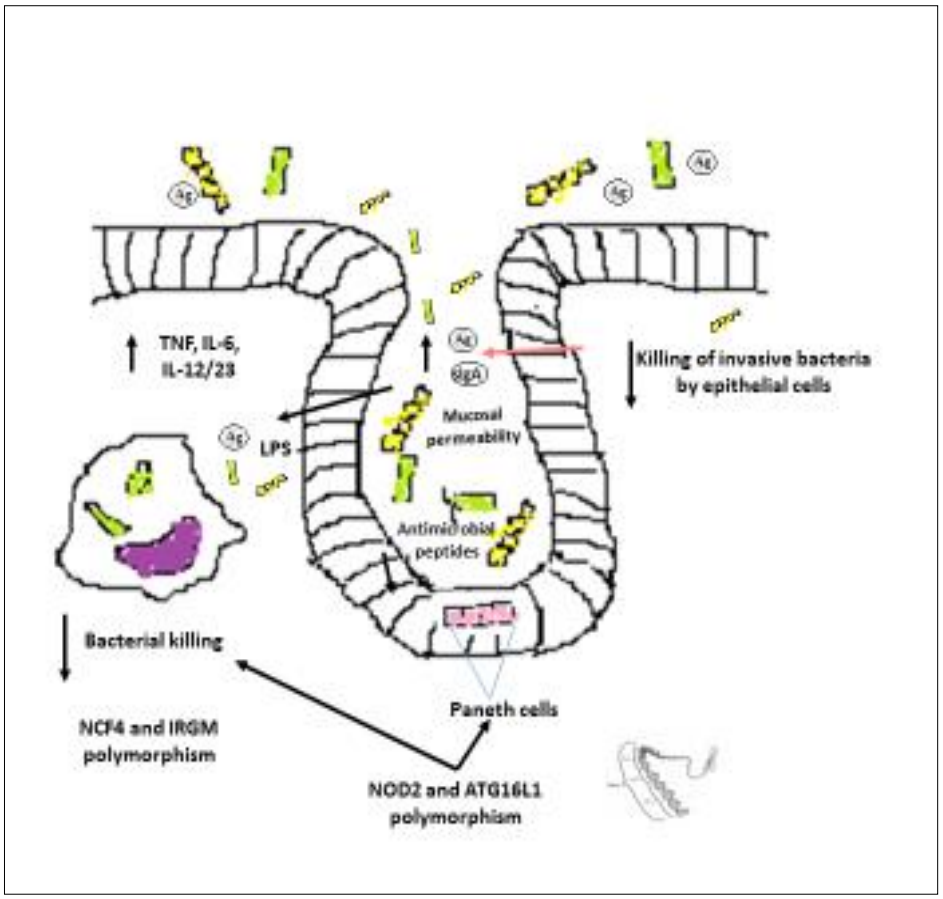

Figure 1-6: Flawed control of commensal bacteria in IBD. (Adapted from [73]).

Crohn's disease associated genetic mutations may impair bacterial recognition potentially leading to the poor control of commensal bacteria. An increase in mucosal bacterial growth may result from the defective secretion of antimicrobial peptides (NOD2 and ATG16L1 polymorphisms) or secretory IgA. However, a reduction in bacterial killing (NOD2, ATG16L1, NCF4 and IGRM polymorphisms) can cause intracellular bacteria to persist and the unsuccessful clearance of bacterial antigens. When mucosal permeability is increased, an overwhelming exposure to bacterial TLR ligands and antigens occurs, which then activates pathogenic innate and T-cell immune responses [74].

1.6 The relationship between iron and gut microbiota

Iron is a growth-limiting nutrient for many gut bacteria, which compete for unabsorbed dietary iron in the colon [75]. *Lactobacilli*, considered to be beneficial barrier bacteria, do not require iron. *Lactobacilli* play a significant role in the inhibition of colonisation by enteric pathogens [76]. For other bacteria, acquiring iron is an essential step for their virulence; such bacteria include Gram-negative bacteria (*Salmonella*, *Shigella*, or pathogenic *Escherichia coli*) [77]. In animal studies, increasing amounts of iron in diets causes a linear rise in diarrhoea. The proportion of *Bifidobacterium* and *Lactobacilli* to *Enterobacteria* can be a guide to gut health: a higher proportion of *Bifidobacterium* and *Lactobacilli* is associated with resistance to infection. Consequently, an increase in unabsorbed dietary iron in humans could alter the composition of the colonic microbiota and favour the growth of pathogenic strains over barrier strains [78].

1.7 Murine models of IBD (colitis)

There are many different animal models of IBD, which are valuable tools for examining factors that are involved in IBD pathogenesis. Recent studies have used 20 experimental models with a diverse range of clinical features similar to human IBD. These models have contributed advances to the understanding of the pathogenesis of IBD. These models support the idea that the induction of IBD is affected by environmental factors in genetically susceptible individuals [79].

The animal model used should, ideally, display structural changes, inflammation, symptoms and signs, pathophysiology, and disease course comparable to those observed in human IBD. The animal used should also have a distinct and defined genetic background.

Animal models of IBD are classified into four broad classes (examples of which in mice are shown in Table 1-3). The majority of these models are based on chemical induction, free cell transfer or gene targeting. However, in some models, the illness is spontaneous [80, 81].

Model	Pathology	Site	Pathogenesis	Cost
1- Spontaneous colitis: SAMP/Yit	Chronic	Ileum	Activation of Th1 T cells toward luminal antigen in ileum only	High
2- Inducible colitis:				
DSS	Acute/Chronic Mainly mucosal	Colon	Toxic intestinal damage plus activation of the mucosal immune system (TH1/TH2). The addition of azoxymethane induces cancer.	Low
TNBS	Acute/Chronic Transmural	Colon	Activation of the immune system (TH1-mediated; hapten-specific). Optimisation of TNBS dosage is required in certain strains.	Low
3- Adoptive transfer: CD45RB CD62L+ cell transfer into SCID Mice	Acute/Chronic Transmural	Colon/ duodenum	IL-12 driven TH1 T cells. Induction of colitis requires 6-12 weeks. Animal facility for SCID mice required.	High
4- Genetically modified:				
IL-2 knockout mice	Acute/Chronic Mucosal	Colon	IFN-gamma production T cells. Colitis develops 6-15 weeks after birth, variability between mice.	Medium
STAT-4 transgenic	Acute/Chronic Transmural	Colon/ Ileum	TH1 T cells in response to bacterial antigens. Requires immunisation of mice.	Medium

Table 1-3: Types of animal models of IBD (adapted from [79], [80]).

DSS-induced colitis model has some advantages in comparison with others. For example, it is relatively simple, has similarity to human IBD and has acute/chronic or relapsing variants which can be produced easily by changing the concentration of DSS and numbers of cycles administered to mice and rats.

Also, dysplasia, similar to that in human UC, occurs frequently in the chronic phase of DSS-induced colitis [82]. DSS models respond to some of the therapeutic agents that are used to treat human IBD, suggesting that DSS-induced colitis is an appropriate model for many experimental purposes [83].

1.7.1 Dextran sulphate sodium (DSS) colitis

DSS is a colitogenic chemical with anticoagulant properties. It is a sulphated polysaccharide with a highly variable molecular weight, ranging from 5KDa to 1400KDa. The molecular weight is a critical factor in the induction of colitis or colitis-induced dysplasia (carcinogenicity) [84, 85].

There are numerous elements peculiar to the DSS including concentration, duration, frequency, molecular weight, manufacturer and batch. Murine factors also influence response: these include genetic modification, strain, substrain and gender. C57BL/6J mice have a more severe IBD phenotype following DSS than other mice [86]. Furthermore, the intestinal microbiota may influence DSS-induced colitis [87].

The severity of both colitis and dysplasia differs according to the use of DSS of different molecular weights. There is a failure of induction of colitis when high molecular weight 500

KDa DSS is used. The location of colitis can also be affected by the molecular weight of DSS. For example, 40KDa DSS causes colitis in the distal colon whereas 5KDa DSS causes patchy lesions more proximally in the colon [84]. The peak of carcinogenic activity of DSS occurs with 54KDa DSS, while DSS of smaller or larger molecular weights has no carcinogenic activity [85]. DSS is mainly excreted in the urine and faeces as it is resistant to degradation by the intestinal microbiota and pH [88].

1.7.2 Initiation of colitis using DSS

In the DSS model, mice are given drinking water supplemented with DSS for several days. This is believed to be directly toxic to colonic epithelial cells. Treatment with 3.5% to 5% DSS causes a rapid loss of body weight. Due to the severity of the 5% DSS model, saline is administered intravenously on day-10 to treat dehydration; saline administration is not required in the ≤3.5% DSS model. The procedures for acute DSS colitis can be completed in about two weeks, but the protocol for chronic DSS colitis takes around two months [89].

Acute colitis can be induced by giving DSS [molecular weight 36,000–50,000 KDa (MP Biomedicals, LLC, UK) in acidified drinking water [2–2.5% (wt. /v)] for 4 to 5 days followed by 5-7 days of plain drinking water (Figure 1-7). By contrast, chronic colitis can be induced by administering 3-4 DSS cycles of 5 days with intervals of 5 to 16 days between cycles when plain drinking water is administered**.** The acute DSS colitis model, despite its limitations, has increased our understanding of the pathophysiology of intestinal inflammation. The chronic DSS model represents a powerful means with which to study the impact of recurrent episodes of inflammation in IBD [89].

Mice are weighed on arrival and then daily after the DSS cycle has been initiated. Both weight loss and later weight gain are useful indicators of DSS-induced colitis and recovery. Mice are observed daily and clinical measurements, including an IBD severity scoring, are conducted twice weekly. The IBD scoring system contains severity scores of zero to three for three parameters:

1. Stool consistency
2. Faecal blood
3. Anal prolapse

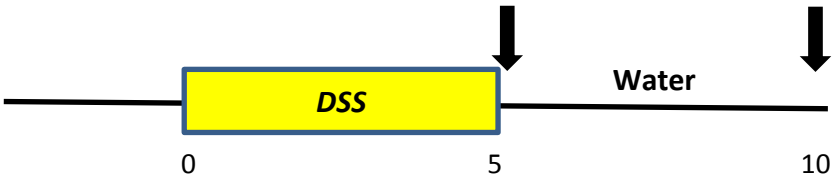

Figure 1-7: Study timeline for acute DSS induction

1.7.3 Clinical and histological signs of DSS colitis

In all animals, body weight, rectal bleeding, stool consistency and survival should be monitored daily. Intestinal bleeding can be detected by using a Hem-occult test (Beckman Coulter, Inc., Fullerton, CA) as well as by watching for signs of bleeding at the anus or indeed the presence of gross bleeding. Disease activity index (DAI) can be calculated as shown in Table 1-4. The scores are combined then divided by three to obtain the final disease activity index. Depending on DSS colitis type, whether it is acute or chronic, 10 to 30 days following

disease induction, the mice are euthanised, and the large intestine is collected and evaluated for colonic length and microscopic colonic changes [90].

Score	Weight loss	Stool consistency	Bleeding
0	None	Normal	-
1	1-5%	Loose	-
2	5-10%	Loose	+
3	10-15%	Diarrhoea	+
4	>15%	Diarrhoea	Gross bleeding

Table 1-4: DAI Scoring System adapted from [89]

Acute histological changes in the colon can be seen as mucosal erosions or destruction and inflammatory cell infiltration. Chronic DSS colitis results in mononuclear leukocyte infiltration, crypt architectural disarray and a widening of the gap between the base of the crypt and muscularis mucosae with deep mucosal lymphocytosis also commonly observed [91].

Assessment of colonic histological damage can be made from distal colonic tissues after processing them by standard methods, embedding them in paraffin wax before staining them with haematoxylin-eosin (H&E). Total histology scores are calculated according to the scale shown in Table 1-5. The two equally weighted subscores (cellular infiltration and tissue damage) are added, and the combined histological colitis severity score is reported ranging from zero to six.

Score	Cell infiltration	Tissue damage
0	None	None
1	Focally increased numbers of inflammatory cells in the lamina propria	Discrete epithelial lesions
2	Confluence of inflammatory cells extending into the submucosa	Mucosal erosions
3	Transmural extension of the infiltrate	Extensive mucosal damage and/or extension through deeper structures of the bowel wall

Table 1-5: Colitis Scoring System adapted from [90]

1.7.4 Significance of iron on DSS-induced colitis

A short-term study was performed to investigate the consequences of alimentary iron supplementation on DSS-induced acute colitis in 2002 by Seril *et al.* Acute DSS (1%) colitis was used to induce mild to moderately severe colitis. This acute colitis was enough to allow evaluation of the influence of iron on inflammation. Colons underwent histopathology scoring to assess the changes. The study found that iron given in the diet significantly increased DSS-induced acute colitis severity. Colons from animals given 2, 5, or 10-fold increased oral iron displayed more severe inflammation and more extensive areas of inflammation (more than 50% of the colorectal mucosa) than those fed the control diet. However, colons from the control mice administered a 10-fold enhanced iron containing diet without 1% DSS were normal. The authors concluded that the effect of iron supplementation on acute DSS colitis is dose-dependent [92].

In another study, iron supplementation increased disease activity in DSS-induced colitis: it was linked with oxidative stress, neutrophilic infiltration, augmented cytokines and activation of NF-κB. However, this damaging effect was moderately reduced by vitamin E [93].

1.8 Bacterial life characteristics

Bacteria are present everywhere - in the air, soil, water, inside an animal's body and on its skin. They have a habit of multiplying rapidly under favourable conditions, creating colonies of millions or even billions of organisms within a space as small as a drop of water. Bacteria assemble in various distinctive ways. Most microbes are one of three common shapes: a rod (*bacillus*), round (*coccus*), or winding (*spirillum*). An additional group, *vibrios*, show up as incomplete spirals. A cell wall encompasses the cytoplasm and plasma film of most bacterial cells; further characterisation of microbes depends on cell wall features (e.g. using a Gram's stain). Aerobic bacteria are metabolically active in oxygen; anaerobes require no oxygen.

1.8.1 Symbiosis

Humans are colonised by four groups of commensal organisms (Eubacteria, Archaebacteria, Fungi and Protista) of the six kingdoms of life (Figure 1-8). The human gastrointestinal tract houses helpful and theoretically pathogenic microorganisms. Symbiosis is a constant beneficial interaction between two or more organisms. The most prominent human symbiont is *Bacteroides fragilis*, which protects animals from experimental colitis [94]. In typical environments, microbiota survives in a state of symbiotic tolerance (eubiosis) with its host and stays fairly constant over time [95].

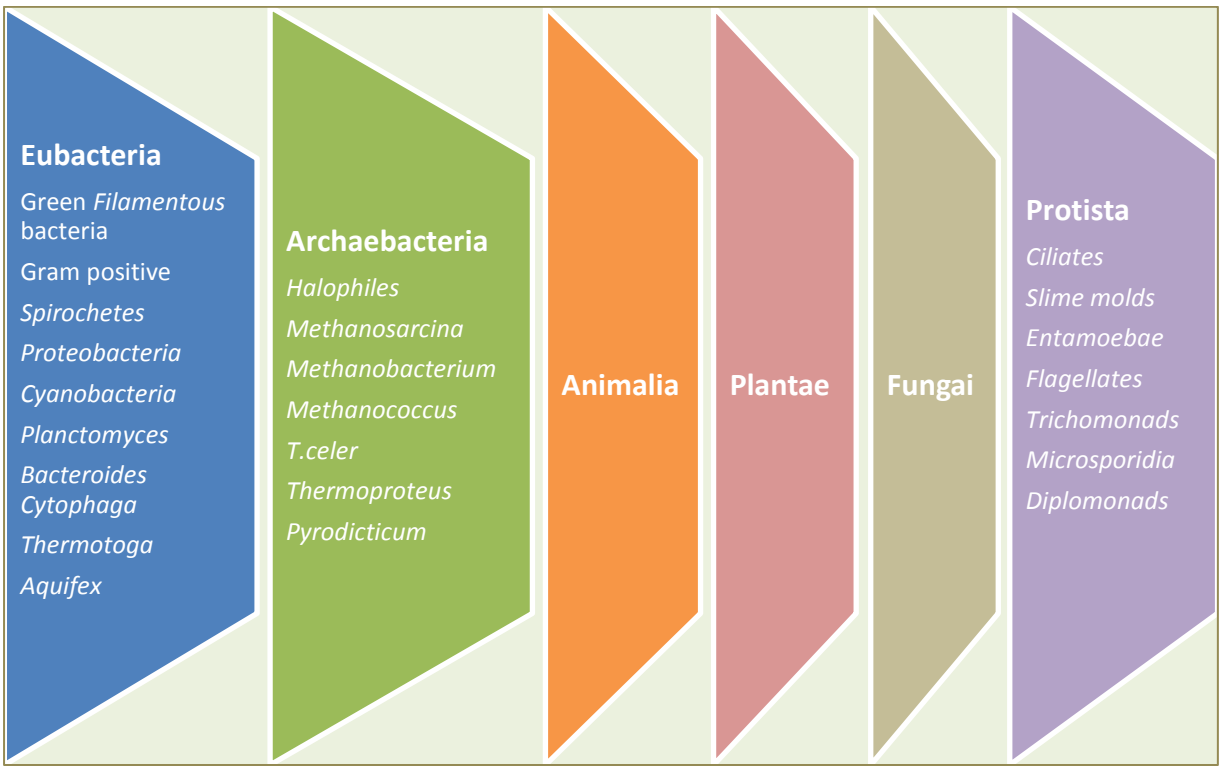

Figure 1-8: Kingdoms of life

1.8.2 Dysbiosis

Changes in bacterial populations within the gut will cause imbalances in the composition of the bacterial microbiota, a condition known as dysbiosis. The change in the normal gut microbiome associated with a failure of host- microbial mutualism may represent what happens in IBD. It is established that there is a shift from main "symbiont" bacteria to potentially harmful "pathobiont" bacteria [96]. These changes in microbiota are thought to be a major factor in human illnesses such as inflammatory bowel disease [97]. Some of these alterations in the gut microbiota have been identified in the common subgroup of IBD

patients: some changes have been particularly defined either in CD or UC patients. The most distinct alteration in IBD patients is the reduction in *Firmicutes* abundance [96].

Different agents may cause dysbiosis e.g. continuous and improper antibiotic use, alcohol abuse, or a change in diet. A recent study revealed that taurine-conjugated bile acids, produced by an interaction between milk (fats) and bile acids, increased the intraluminal growth of *Bilophilia wadsworthia*. This bacterium induces macrophages and dendritic cells to release immune cytokines, which stimulate bacterial-antigen-specific TH1 cells to secrete interferon-gamma (IFN-ɣ) causing colitis [97]. Another pathway that may include *B. wadsworthia* may lead to deconjugation of taurine and hydrogen sulphide formation. Hydrogen sulphide production may interfere with the mucosal barrier and inhibit colonic epithelial metabolism (Figure 1-9). In inflammatory bowel disease, dysbiosis may be a key component in immunopathogenesis by disrupting the host immune defences against commensal microbes at the mucosal border [97].

Immunomodulators, dietary contributions, and exposure to antibiotics disturb the gut microbiome to a varying extent. However, antibiotics have the most significant outcome on microbial community assembly [97].

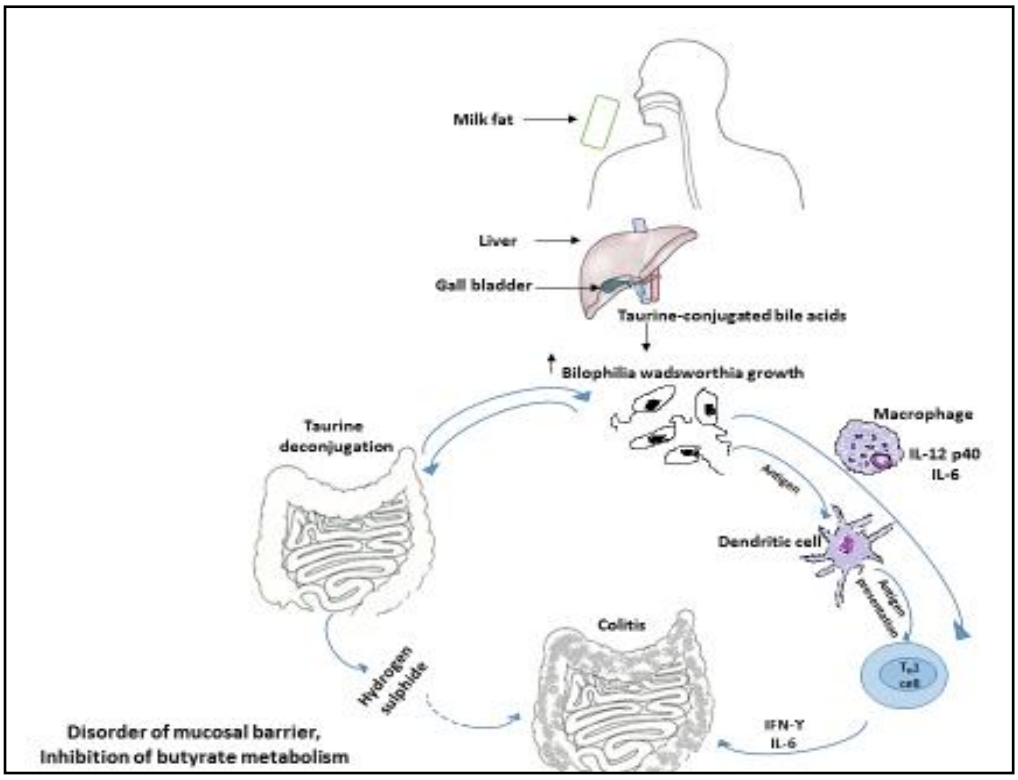

Figure 1-9: Diet promotes dysbiosis and colitis in susceptible hosts (adapted from [94])

1.8.3 Diversity and abundance

The variety of microorganisms in a specific anatomical body site can define the number and abundance distribution of discrete types of microbes. A reduction in diversity is associated with many human systemic illnesses, such as obesity and inflammatory bowel disease [98].

Alterations in microbial composition in inflammatory bowel disease patients occur during disease activity. They are more marked in CD than in UC [99].

1.9 The Great Anomaly

In 1985, Staley and Konopka established that the biodiversity of a complex microbial community observed by microscopy was greater than that by culturing it on agar plates. Therefore, they called this phenomenon The Great Anomaly. More recently, as a consequence of the widespread usage of PCR and DNA sequencing, 16S ribosomal DNA (rDNA) sequencing has played an essential role in the precise identification of bacterial isolates and the discovery of novel microscopic organisms in clinical microbiology research facilities [100].

1.9.1 16S rRNA

16S rDNA genes code for 16S rRNA. 16S rDNA is around 1,500 bp long and represents one of the components of the small subunit (30S) of prokaryotic ribosomes. These genes are very useful for evaluating phylogenetic relationships among microorganisms, as the degree of conservation varies significantly. All bacteria share the conserved regions, whereas the variable regions contain specific sequences which are characteristic to individual bacteria. This uniqueness enables taxonomic identification (Figure 1-10) [101]. Regarding the microbial diversity of the gastrointestinal tract, through a random sequencing of 16S rRNA genes, Hold *et al. 2002* [102] showed in a study that only 25% of sequences were > 97% sequence identity with current species type strains, and 28% were < 97% linked to any database entry, which indicating our incomplete knowledge of bacterial diversity in the colon. Also, Hold observed a sequence identity was above 97% of 21 out of the 110 of the colonic 16S rDNA sequences with butyrate-producing strains that been extracted from human faeces [102].

1.9.2 Variable regions

Bacterial 16S ribosomal RNA (rRNA) genes cover nine "hypervariable regions" (V1 – V9), which have significant sequence diversity between different bacteria. Species-specific sequences in a given hypervariable region are useful targets for diagnostic assays and other scientific investigations. However, there is no single region that can distinguish all bacteria; so numerous systematic studies that associate the relative advantage of each region with specific diagnostic goals have been performed [101].

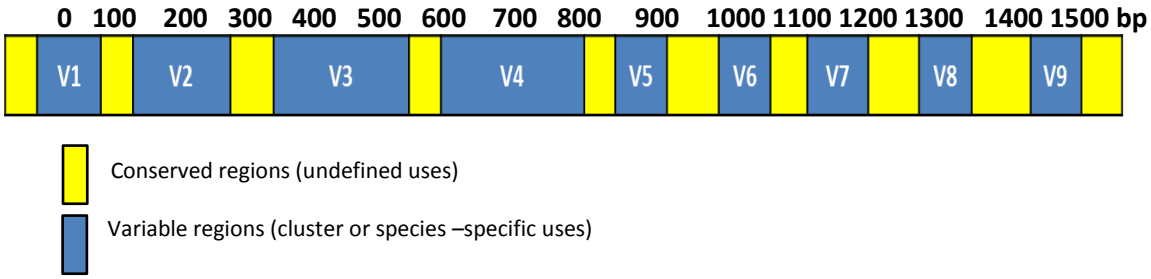

Figure 1-10: 16S ribosomal DNA gene

1.9.3 V4 region

The most widely used variable region of 16S rRNA is V4. It is around 291 bp in size. The disadvantage of V4 is that it is a small fragment. V4 primers could be designed to suit the best arrangement/library when sequencing is performed. For instance, utilising MiSeq Illumina needs 250bp every route (forward and reverse), so the V4 region is suitable for this machine. However, adding adapters and barcodes should also be taken into consideration (Table 1-6).

Region	Product size (bp)	+ 150 adapters + barcodes
V4	291	441

Table 1-6: V4 primer size

1.10 Sequencing an amplicon library

The processing and sequencing of amplicons are entirely adaptable and allow for a broad range of experimental designs. Variables include the number of amplicons pooled together, the length of amplicons, the number of reads required for a given amplicon pool, and whether to read from the A end, the B end or both. So each project will have its specific variables as well as objectives.

The choice of 16S rRNA region to sequence is an area of discussion, and the area of interest might vary depending on experimental objectives, design, and sample type. The protocol in Figure 1-11 illustrates a strategy for preparing samples for sequencing the variable V4 region of the 16S rRNA gene. This protocol can similarly be applied to different sequencing regions with various region-specific primers. This protocol combined with a benchtop sequencing framework, on board initial analysis, and secondary analysis using MiSeq Reporter or Base Space, provides a comprehensive workflow for 16S rRNA amplicon sequencing.

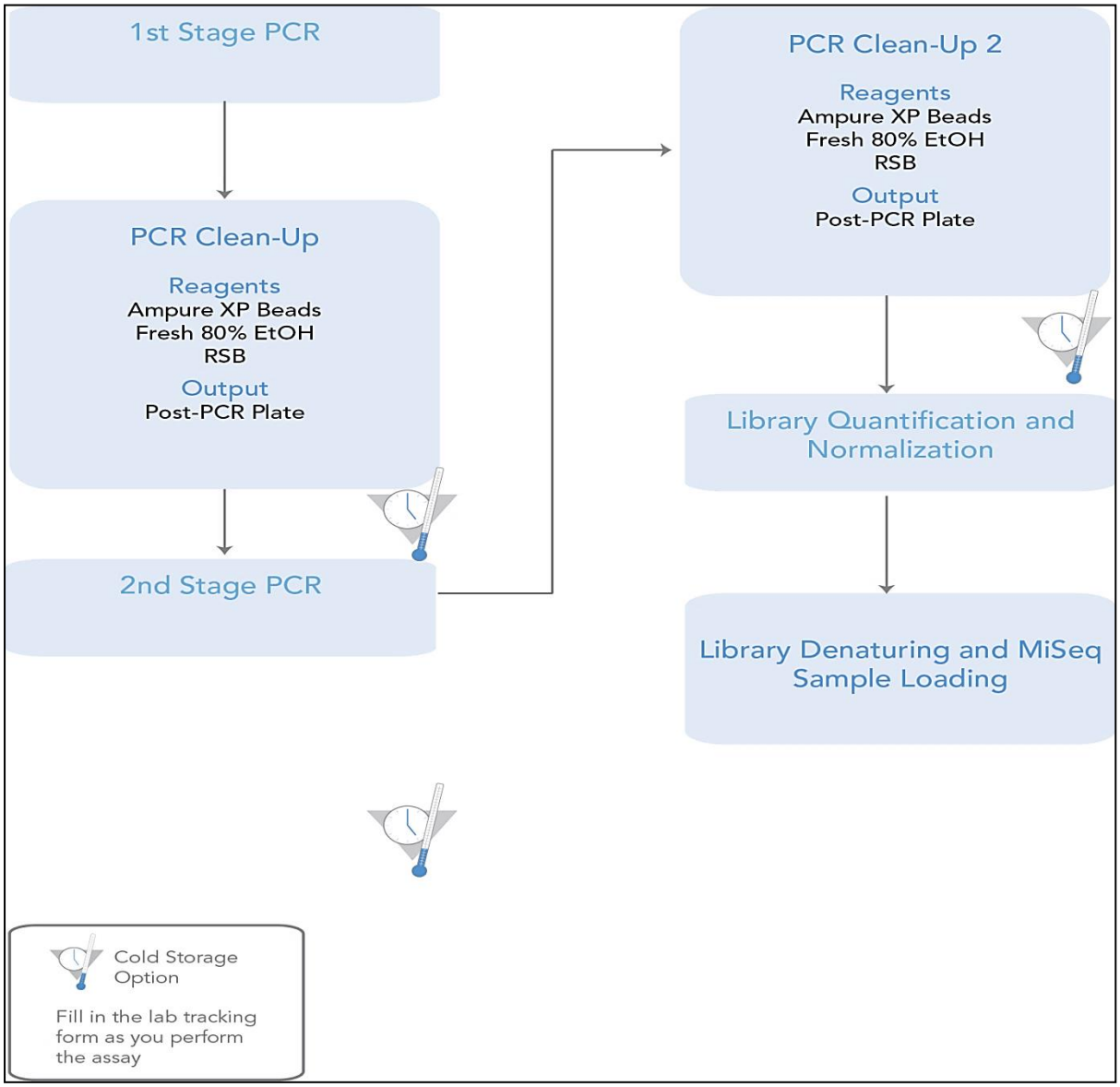

Figure 1-11: 16S library preparation workflow (reproduced with permission from CGR)

1.11 Hypothesis

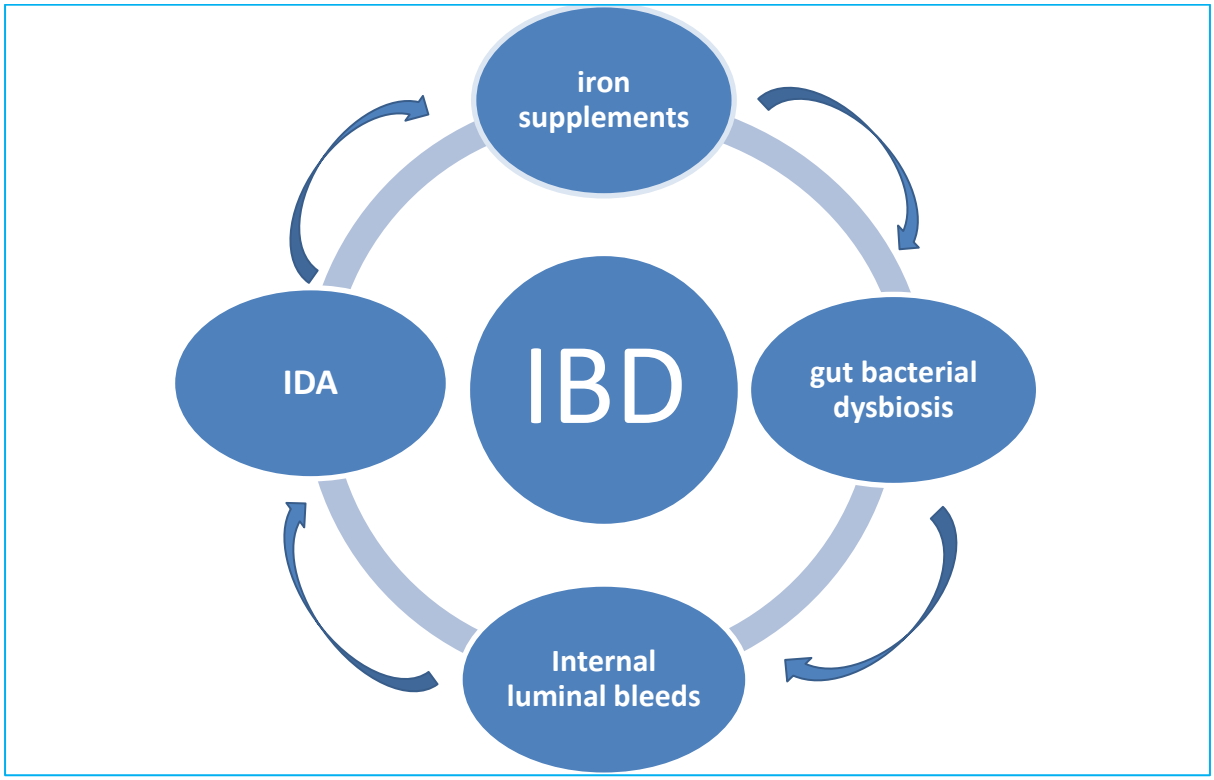

The hypothesis under investigation is that iron supplementation (and or bleeding) in IBD patients can change the composition of the gut microbiota and influence the natural history of IBD.

1.12 Aims and objectives

1.12.1 Aims

The purpose of this research project is to investigate the influence of iron on the gut microbiota in inflammatory bowel disease (IBD).

1.12.2 Objectives

To characterise the intestinal microbiota in murine models of inflammatory bowel disease, and in mice given different doses of iron supplements.

2 Materials and methods

2.1 Mice

Unless otherwise mentioned, all mice were purchased from Charles River Laboratories (Margate, UK).

2.1.1 Animal conditions

All mice used in animal experiments were wild-type C57BL/6 female mice, aged 8-9 weeks old, purchased from Charles River Laboratories (Margate, UK). They were acclimatised under typical animal house conditions for at least seven days before the experiments began. The mice were fed standard mice chow pellets (during the acclimatisation period only) and water *ad libitum.* They were individually caged in a room with controlled temperature, humidity and a pre-set dark-light cycle (12 h: 12 h).

2.2 Experimental procedures

For each group of experiments, mice were matched for age, sex, and body weight. The care of, and experimentation on, mice was carried out in accordance with the UK Home Office regulations. The animal work was done under a project licence as specified by the Animals (Scientific Procedures) Act 1986, as well as with institutional guidelines under protocols approved by the Biomedical Services Unit (BSU) at the University of Liverpool for the proper use of animals in biomedical research. The author as a UK Home Office personal licence holder conducted every animal procedure.

2.2.1 Dietary intervention and group classification

Unless otherwise stated, the animals were administered chow pellets throughout the experiments (all diets purchased from Special Diets Services [SDS], Witham, Essex, UK).

2.2.1.1 Dietary intervention

The conventional breeding diet utilised in the Biomedical Services Unit (BSU) at the University of Liverpool is the Rat and Mouse Breeder and Grower Pelleted CRM (P). It contains 200ppm [part per million] iron and appears as a 10mm compression pellet. These pellets were used for all experiments which required a normal iron diet. There were two modifications of this diet: the first was CRM (P) 100ppm iron Fe (P) where the CRM (P) formulation was used but had reduced iron content (0.01% Fe). This was called the low iron diet (100ppm iron). The second was CRM (P) 400ppm iron Fe (P): again the CRM (P) formulation was used, but the iron content was increased (0.04% Fe). This was called the high iron (400ppm iron) as shown in Figure 2-1.

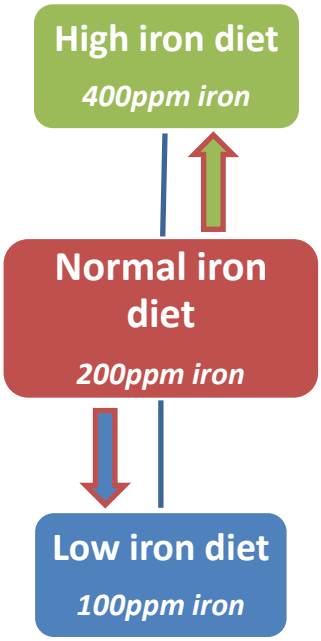

Figure 2-1: Mice dietary modifications.

2.2.2 Induction of colitis

Dextran sulphate sodium (DSS) was used to induce colitis: this being a commonly used murine model of human ulcerative colitis. Usually, only the acute phase is used to study the innate immune response, but CD and UC are chronic pathologies, and so chronic intestinal inflammation was induced by the used of repeated cycles of DSS, thus enabling the study of the adaptive immune system.

2.2.2.1 Acute DSS

Mice were given a 2% solution [1000ml sterile water + 20g DSS] of dextran sulphate sodium (M.W. 36,000 – 50,000Da; Catalogue number: 160110; Lot number: 6683K; MP Biomedicals, LLC, UK) in their drinking water for 5 days to induce colitis (~150ml/mouse over 5 days),

followed by another 5 days of DSS-free water. Mice were euthanised on day-10, measured from the start of the experiment. The gastroenterology research team at the University of Liverpool approved this protocol (Acute DSS cycle). Mice were monitored daily for signs of disease (clinical observation), and their body weight was recorded as illustrated in Figure 2-2.

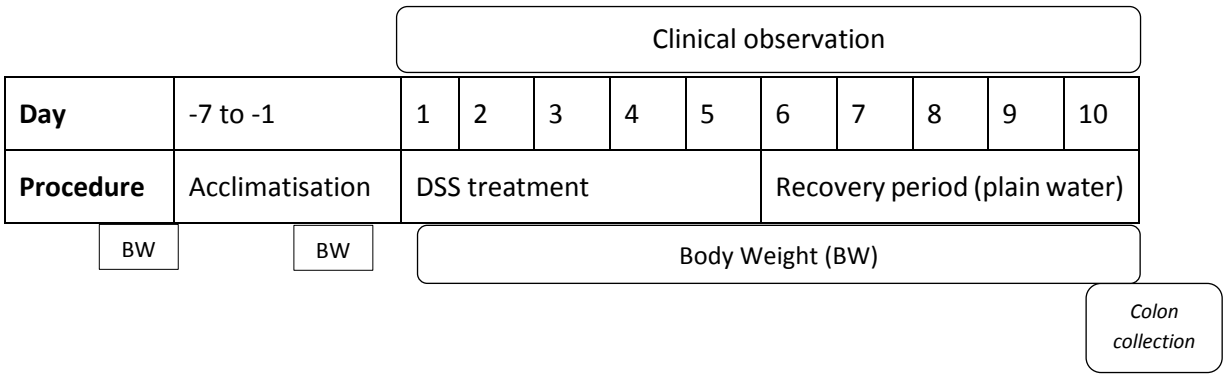

Figure 2-2: Induction of acute colitis protocol using DSS

2.2.2.2 Chronic DSS

Chronic colitis can be induced by applying 3-4 cycles of 5 days of DSS treatment with intervals of between 5 to 16 days when plain drinking water is provided. Mice were given 1.25% DSS solution [1000ml sterile water + 12.25g DSS (as above)] to drink for 5 days to induce acute colitis (~150ml/mouse over 5 days), followed by 16 days of DSS-free water (full recovery period). The cycles were repeated twice to give 3 cycles of 21 days each (total 63-days) as illustrated in Figure 2-3. The gastroenterology team approved this protocol (Chronic DSS). All mice were euthanised on day-63 counting from the start of the experiment. During the whole period (63 days) mice were weighed and monitored daily for any signs of disease by clinical observation.

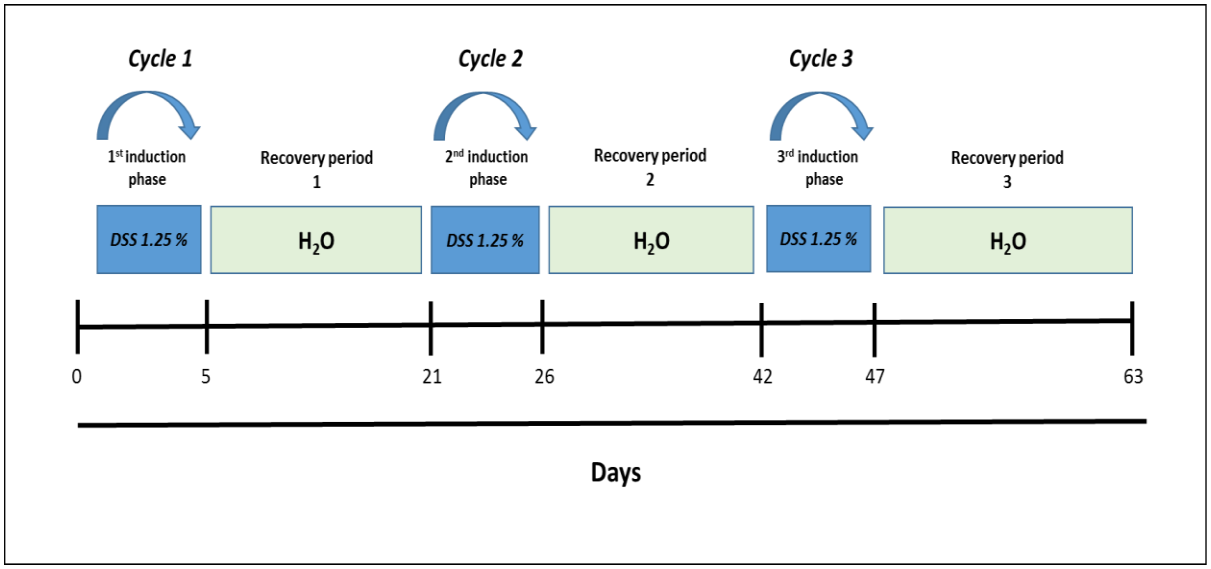

Figure 2-3: Chronic DSS schedule

2.3 Tissue sampling and preparation

Mice were killed by using a CO_2 chamber with 2 cycles of 60% CO_2 for 5 minutes, followed by 100% CO_2 for 1 minute to enable blood extraction by cardiac puncture. Death was then confirmed by a neck dislocation technique (this is a Home Office approved Schedule 1 procedure). Subsequently, after spraying with 70% ethanol, a ventral midline incision was performed. The colon was grasped with forceps and pulled until the caecum could be identified. The colon, from the colocaecal junction to the anal verge, was removed: particular care was taken as the inflamed colon of DSS-treated animals is delicate, shortened and attached to surrounding tissues. Colonic faecal contents were removed by squeezing the colon, using a pair of forceps, onto a clean histology slide before transferring the contents into a 2ml Eppendorf tube containing stool stabiliser (supplied from Startec Kit [PSP® Spin Stool DNA Plus Kit]).

2.3.1 Fixation / Preservation

Fixation is a major step in histological specimen preparation. The intestine was rinsed (dipped in a dish) with cold (4°C) Phosphate-buffered saline (PBS) and then wrapped in filter paper and fixed in freshly prepared 4% formalin solution for a maximum of 24hrs. The tissue was then stored in 70% ethanol before the bundling step.

2.3.2 Gut bundling and processing

Tissues were removed from the ethanol and rinsed with cold (4°C) PBS, and divided into 2 parts: proximal and distal colon. The distal colon tissue segment, located approximately 10 mm, from the anal verge was identified and cut into 2-3 small parts before being placed into loops of 3M Micropore surgical tape in a process called 'gut bundling'. After bundling, the tape around the tissues was squeezed to hold the tissues in loops together, and the bundles were trimmed by removing excess tissues and any extra tape using a Swann-Morton size 22-scalpel blade (VWR International Ltd, Lutterworth, UK) [103]. Each bundle was placed individually into a histology cassette, and this was stored in 70% ethanol until the processing step. All of the cassettes were placed in the processor machine [Thermo Shandon Hypercentre] overnight.

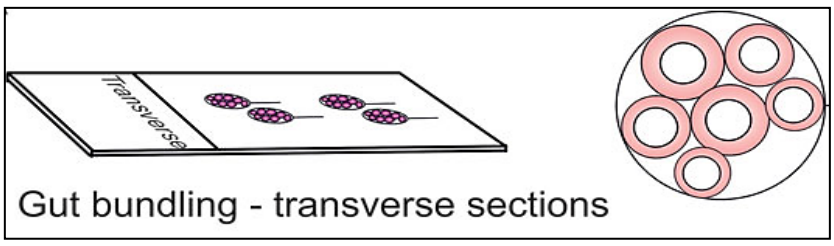

Figure 2-4: Schematic diagram for gut bundling [103].

2.3.3 Embedding in paraffin and cutting

After retrieving cassettes from the processor, the paraffin-embedding stage was begun. Tissues were held in a vertical position in the centre of a stainless steel or plastic mould, to enable transverse section during tissue cutting, before pouring the melted paraffin wax and then allowing the blocks to cool and harden. Finally, transverse tissue sections of 4µm thickness were obtained by cutting the paraffin blocks using a manual microtome (Leica RM2235 manual microtome). Tissue sections were then placed on glass microscope slides. Slides were drained vertically for a brief time to get rid of excess water before they were placed in an oven (at 37°C for 24hrs).

2.3.4 Haematoxylin and eosin staining

Paraffin is poorly permeable to stains, so the slide was de-waxed using fresh Xylene I for 5 minutes and fresh Xylene II for another 5 minutes. The sections were then transferred through a series of alcohol gradients starting with absolute ethanol and finishing with distilled water to avoid diffusion currents.

Slides were placed in haematoxylin (Sigma-Aldrich Co, Dorset, UK) for 3 minutes and then rinsed in tap water for 10 minutes. The slides were placed in eosin (Sigma-Aldrich Co, Dorset, UK) for 4 minutes, before dipping them in tap water several times. Sections were then dehydrated by immersion in 95% ethanol and (twice) in 100% ethanol.

After dehydration, slides were cleared using Xylene I and II for 5 minutes each. Finally, the slides were removed from the rack, wiped, and mounting medium (DPX) and coverslips were applied. Air bubbles were removed using tweezers or a pipette tip. The slides were allowed to cool for 10 minutes at room temperature and were then examined under a light microscope.

2.3.5 Masson's trichrome staining

Intestinal fibrosis in chronic DSS-induced colitis was investigated by staining the sections with the Masson's trichrome method: NovaUltra™ Masson's Trichrome Stain Kit (Fisher Scientific UK Ltd) was utilised. The sections were dipped in 2 Xylene dishes [I and II] for 5 minutes each to remove paraffin; then the slides were rehydrated in 2 changes of 100% alcohol for 5 minutes each, 95% and 70% alcohol for 1 minute each. Then the slides were rinsed in distilled water before staining them in a dish filled with Weigert's Iron Haematoxylin Solution for 10 minutes. The slides were then placed in running tap water for 10 minutes, before being washed with distilled water and stained in Biebrich Scarlet-Acid Fuchsin Solution for 10-15 minutes, before being washed again in distilled water. The sections were then placed in phosphomolybdic-phosphotungstic (PP) Acid Solution for 10-15 minutes to differentiate or until the red colour of the collagen disappeared. At that time, the sections were laid into aniline blue solution, without rinsing, and stained for 5-10 minutes and rinsed briefly with distilled water and acetic acid solution for 2-5 minutes, before washing again in distilled water.

This was followed by quick dehydration using 95% alcohol, two changes of 100% alcohol for 1 minute each to wash off the Biebrich Scarlet-Acid Fuchsin stain before, finally, clearing the slides again using 2 changes of xylene, 5 minutes each, before mounting medium and coverslips were applied. Slides were allowed to cool before being visualised using the microscope.

2.4 Faecal bacterial DNA extracted from mouse pellets

The intestinal microbiota is considered to play a vital role in the pathogenesis of IBD, and various studies have confirmed the presence of intestinal dysbiosis in IBD patients compared to healthy controls [68]. Furthermore, iron supplementation has been shown to influence microbial diversity, and therefore this should be considered when studying the intestinal microbiota [104]. This research aimed to assess the relationship between the faecal microbiota and the presence of gastrointestinal mucosal inflammation.

There are significant differences in relative abundance of bacteria when DNA is extracted using different techniques from mock groups of bacteria and measured by 16S rRNA sequencing [105]. However, in another study, reported differences in the yield and relative abundance of main bacterial families for different kits used to extract bacterial DNA from faeces. This highlights the importance of ensuring that all samples are prepared with the same DNA extraction technique (kit), and careful consideration when comparing studies that have used different approaches [106].

Therefore, in this research, to evaluate bacterial diversity in faeces, bacterial DNA was extracted using the Startec Kit [PSP® Spin Stool DNA Plus Kit] throughout the study. The extracted DNA was sent to the Centre for Genomic Research (CGR) at the University of Liverpool to carry out 16S Metagenomic Sequencing Library Preparation. Data was extracted from the sequencing machine [Miseq] followed by bioinformatics analysis.

2.4.1 Faecal sampling

In the murine studies, to avoid cross-contamination between samples, each mouse was put in a bowl previously wiped with 70% ethanol. The presence of the animal in the bowl for a couple of minutes was usually sufficient for it to excrete 5-6 faecal pellets. This amount is sufficient for DNA extraction. The faecal samples were placed into 2ml Eppendorf tubes filled with a stool stabiliser (supplied with the extraction kit) using sterile forceps.

Figure 2-5: Stool Stabilizer Tube

2.4.2 PSP® Spin Stool DNA Plus Kit

This kit is a combined kit for the collection, transportation and storage of faecal samples and consequent DNA purification; it is designed for the separation of DNA from microorganisms, as well as from the host organism. The PSP® Spin Stool, DNA Plus Kit (Figure 2-6), delivers fast and easy purification of DNA from frozen or fresh stool samples using Invisorb® technology. The kit utilises a stabilising reagent (Stool DNA Stabilizer in tubes; Figure 2-4) for collection, storage and stabilisation of the stool sample to prevent DNA degradation, prelysing bacteria and stopping further bacterial growth, thus preserving the microbial community. The kit is effective for both Gram positive and negative bacteria.

Figure 2-6: PSP® Spin Stool DNA plus 250 extractions Kit

2.4.3 Assay procedure

1. The required amount of the stool sample was collected and transferred to the stool collection tube, which contained stool DNA stabiliser. The tube was closed, and the contents were mixed by shaking.
2. 1.4ml of the stabilised stool sample was pipetted into a 2.0ml Safe-Lock Tube.
3. The sample was incubated for 10 minutes at 95°C on a thermomixer, then shaken at 900 rpm.
4. 5 Zirconia Beads II was added, the sample was vortexed for 2 minutes, then centrifuged at 11.000 x g for 1 minute.
5. The supernatant was transferred to the InviAdsorb-Tube before mixing by vortex for 15 seconds.
6. The sample was incubated for about 1 minute at room temperature then centrifuged again for 3 minutes at full speed (15.000 x g).
7. The supernatant was transferred to a new 1.5ml receiver tube before being centrifuged again at full speed for 3 minutes.
8. 800µl of the sample supernatant was added to a new 2.0ml Safe-Lock-Tube, 25µl Proteinase K was added, and this was mixed briefly by vortexing.
9. The sample was incubated for 10 minutes at 70°C on a thermomixer while shaking (900 rpm).
10. 400µl of Binding Buffer A was added to the sample, and this was mixed by pipetting up and down.
11. The whole mixture was transferred to the RTA Spin Filter and was incubated at room temperature for about 1 minute.

12. The RTA Spin Filter was centrifuged at 11.000 x g for 2 minutes before disposing of the filtrate and the RTA Receiver Tube.
13. The RTA Spin Filter contents were placed in a new RTA Receiver Tube, 500µl of Wash Buffer I was added to the RTA-Spin Filter, and this was then centrifuged at 11.000 x g for 1 minute before discarding the flow-through and the RTA Receiver Tube.
14. Again, the RTA Spin Filter was placed in a new RTA Receiver Tube and 700µl Wash Buffer II was pipetted onto the RTA Spin Filter, then this was centrifuged at 11.000 x g for 1 minute before disposing of the flow-through and reusing the RTA Receiver Tube.
15. An additional centrifuge step for 4 minutes at maximum speed was applied to remove any traces of ethanol.
16. After centrifugation, the RTA Receiver Tube was removed, and the RTA Spin Filter was placed into a new 1.5ml Receiver Tube. 100-200µl of elution buffer, heated up to 70°C (Stuart Scientific heater block) was added to the centre of the membrane of the filter before it was incubated for 1 minute at room temperature.
17. The tube was then centrifuged at 11.000 x g for 1 minute; the RTA-Spin Filter was removed, and two aliquots were prepared for use. One aliquot was placed directly into a refrigerator and the second was stored in the freezer at –20°C.

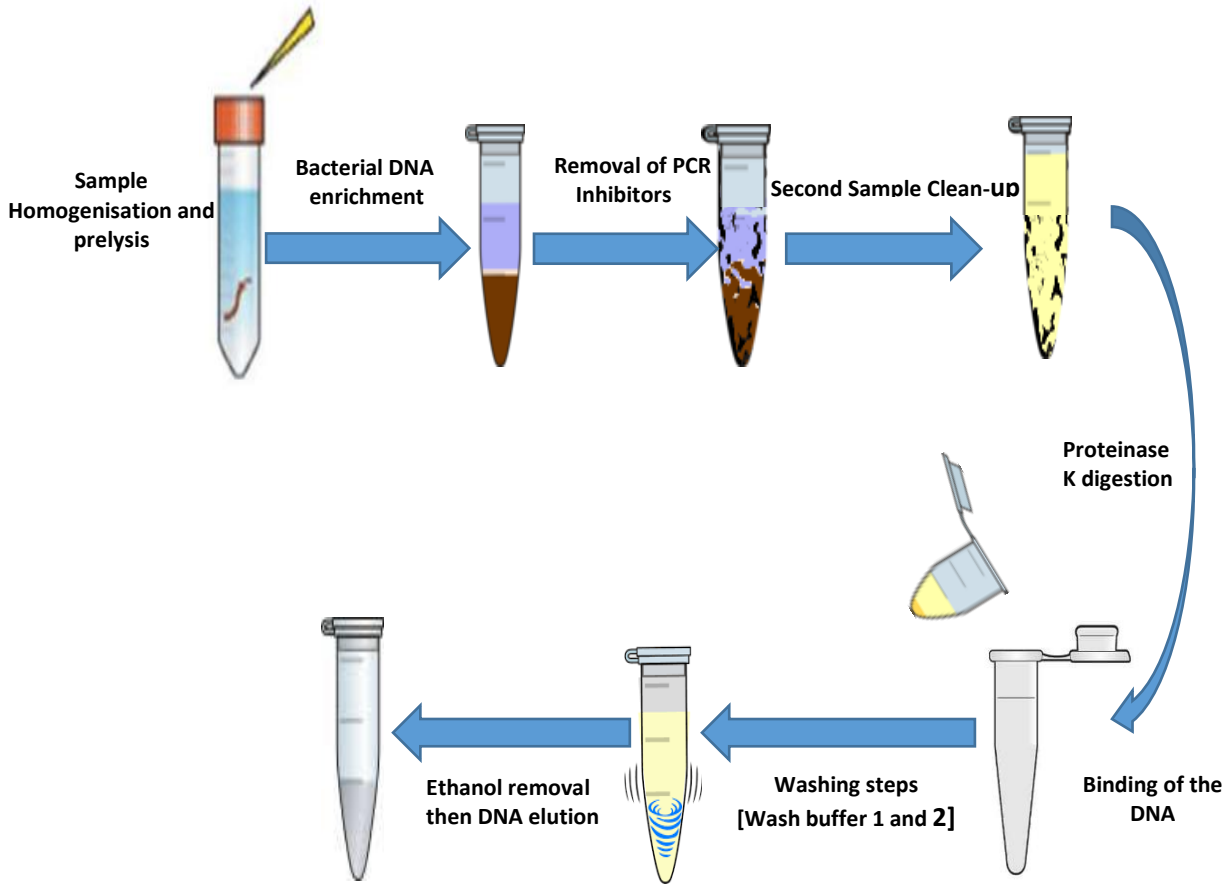

Figure 2-7: Scheme of the PSP® Spin Stool DNA plus Kit

2.5 ELISA for faecal calprotectin analysis

ELISA (enzyme-linked immunosorbent assay) is a plate-based assay procedure aimed at finding and measuring elements such as peptides, proteins, antibodies, and hormones. In ELISA assay, an antigen is immobilised on a solid surface and then complexes with an antibody linked to an enzyme. Detection is achieved by evaluating the conjugated enzyme activity via incubation with a substrate to produce a measurable product. Calprotectin is a calcium-binding protein which is secreted predominantly by neutrophils and monocytes. It is a marker for neoplastic and inflammatory gastrointestinal diseases such as IBD.

2.5.1 S100A8/S100A9 ELISA [Murine]

The S100A8/S100A9 ELISA by Immundiagnostik Germany is designed for experimental animal studies i.e. mouse or rat and is not suitable for human samples. This ELISA kit was designed for the quantitative determination of calprotectin S100A8/S100A9 (Calprotectin, MRP (8/14)) in stool, urine, plasma, serum, tissue samples and cell culture.

Figure 2-8: S100A8/S100A9 ELISA Kit

2.5.1.1 Faecal samples prepared and stored for analysis

Mouse faecal samples (pellets) were allowed to thaw slowly at 2–8°C, if they were frozen, and were warmed to room temperature before analysis. For long term storage of up to 12 months, samples were stored at -20°C and repeated freezing and thawing of the sample was avoided as much as possible. Each faecal sample was extracted 1:50 in extraction buffer (e.g. 100mg faeces + 5ml extraction buffer), then centrifuged for 10 minutes at 3000 x g.

2.5.1.2 Assay procedure

100µl of the supernatant was pipetted into each well. All reagents and samples were brought to room temperature (15–30°C) and mixed well. The experiments were performed in duplicate, and the assay procedure steps were completed according to the protocol supplied with S100A8/S100A9 ELISA kit. First, each well in the plate was washed 5 times by dispensing 250µl of diluted WASHBUF (wash buffer) using an automatic microplate washer (Mikura Autura 1000), then residual buffer was removed by tapping the plate on absorbent paper. 100µl of STD (Standard) SAMPLE (Sample/supernatant) CTRL (Controls) was pipetted into each corresponding well. An adhesive plastic sheet was placed to cover the plate tightly before it was incubated for 1 hour at 37°C on a single plate horizontal shaker (Mikura Orbis). The contents of each well were removed, then washed again 5 times with diluted WASHBUF (wash buffer) before tapping the plate on absorbent paper to remove residual buffer. 100µl of diluted AB (detection antibody) was added to each well, the strips covered firmly, and this was re-incubated again for 1 hour at 37°C on a horizontal shaker.

The plate's content was discarded, and it was washed 5 times again with 250µl wash buffer and slapped four times onto absorbent paper. 100µl of diluted CONJ (conjugate) was pipetted into each well then the plate was covered tightly before being re-incubated once more for 1 hour at 37°C on a horizontal shaker. Similarly, the contents of each well were removed and washed another 5 times, with diluted wash buffer, and then the plate cleaned using the same tapping technique.

100µl of SUB (substrate) was pipetted into each well, however, this time, the plate was incubated for 10–20min at room temperature (15–30°C) in the dark. Lastly, 100µl of STOP (stop solution) was added to each well, and this was mixed before the absorption was measured immediately with an ELISA reader (TECAN Sunrise™) at 450nm.

2.5.1.3 Calprotectin results filtered and analysed

The absorbance was measured directly at 450nm only as no reference wavelength was available on the ELISA reader (TECAN Sunrise™). For a 4-parameter algorithm, a logarithmic abscissa was used for the concentration and a linear ordinate for the optical density. However, using a logarithmic abscissa, the zero standards were specified with a value less than 1 (e.g. 0.001). All data from the ELISAs were reduced using special software either MasterPlex ReaderFit (Hitachi Solutions America, Ltd. USA) or [Gen5 Image+ (BioTek Instruments, Inc., USA)].

The reduced data from the calprotectin test used the dilution factor 50. However, as the standards are ng/ml but were reported in ug/g, the following calculation was applied to the observed result:

$$\frac{(\text{Result} \times 5000 = \text{Final concentration in } \mathbf{ng/ml})}{1000} = \text{Final result in } \mathbf{\mu g/g}$$

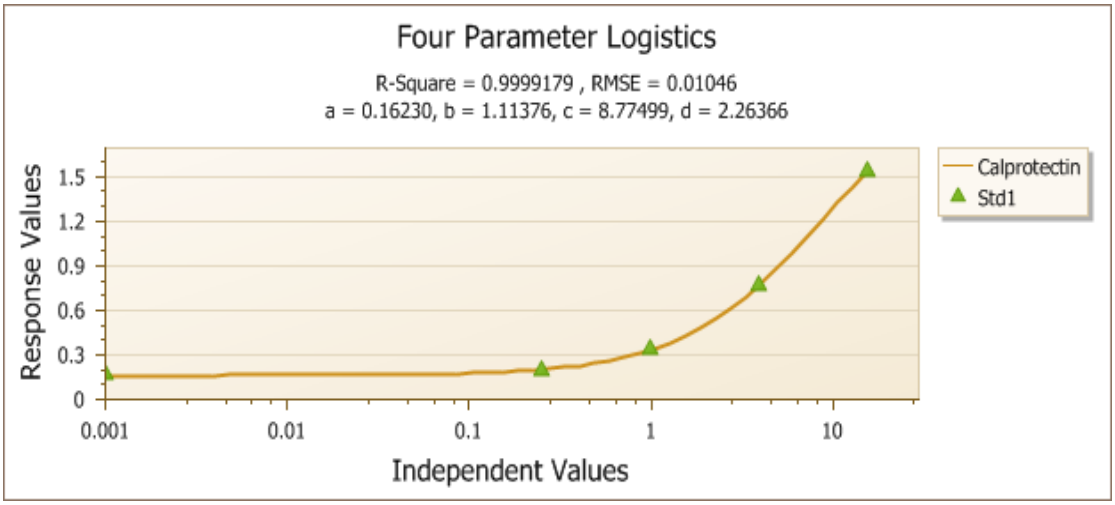

Figure 2-9: Standard curve using MasterPlex ReaderFit Software [(a) the minimum value that can be obtained, (d) the maximum value that can be obtained (i.e. what happens at infinite dose), (c) the point of variation (i.e. the point on the S-shaped curve halfway between a and d) and (b) Hill's slope of the curve (i.e. this is related to the sharpness of the curve at point c)

450	= Absorbance reading at 450nm
[Concentration]	= Calculated concentration in ng/ml (I.e. concentration before applying the dilution factor of 0.05)
[Concentration] x Dil.	= Calculated concentration in ug/g (I.e. concentration after applying the dilution factor of 0.05)

2.6 Faecal iron concentration

Iron deficiency anaemia (IDA) is common in inflammatory bowel disease (IBD). Iron plays a critical role in numerous biological pathways. The biological action of iron is largely governed by its transition ability: redox reactions control its ferric (Fe^{3+}) and ferrous (Fe^{2+}) forms. Free reduced iron is toxic as it reacts with hydrogen peroxide (H_2O_2) or lipid peroxide to produce highly reactive radicals that can damage lipids, proteins, and nucleic acids. In inflammatory bowel disease, reactive oxygen species (ROS) are formed by neutrophils in inflamed intestinal mucosa which participate in the mechanism of tissue injury: free iron is a strong catalyst for ROS production [107, 108].

There is some doubt about how to treat patients with iron deficiency, who have haemoglobin readings in the normal range. Oral iron supplementation usually consists of ferrous (Fe^{2+}) salts, which are linked to gastrointestinal side effects, often resulting in poor compliance. Treatment with oral ferrous salts may even be harmful to IBD patients as they are poorly absorbed and lead to an increase in faecal iron concentration. A significant portion of faecal iron will be available for catalytic activity when iron reaches the inflamed intestinal mucosa causing more ROS production and thus aggravating tissue damage [109].

2.6.1 Faecal iron immunoassay

To calculate faecal iron concentration, an iron assay kit [MAK025, Sigma-Aldrich Company Ltd. Dorset, England] was utilised. This assay gives the option to measure Fe^{2+} directly or to measure total iron (Fe^{2+} and Fe^{3+}). Iron is released by adding an acidic buffer; freed iron reacts with a chromogen causing in a colorimetric (593 nm) product, proportional to the amount of iron present. The MAK025 Assay Kit, therefore, offers a suitable means of calculating iron in diverse biological samples (tissues, cells, serum and other liquids).

Figure 2-10: Iron assay kit**.**

2.6.1.1 Storage and preparation of samples

Fresh specimens [mouse faecal samples (pellets)] were used and stored correctly until used, then allowed to thaw slowly at 2–8°C from frozen, and warmed to room temperature before analysis. To calculate the best size for the faecal sample, three weights (10, 20 and 30mg of fresh specimens) were used to ensure that readings were within the linear range of the standard curve. The best reading (standard curve) was found to be with 20mg samples. Therefore all faecal iron immunoassay tests (animal) used this weight of starting material. 20mg of faecal samples were added to a 2ml Eppendorf tube with 5 mm stainless steel beads and 100µl of Iron Assay Buffer. For rapid homogenisation, a bead beater (TissueLyser II/ QIAGEN) was used at frequency 30 1/S for about 2 minutes; then the tubes were centrifuged at 13,000 x g for 10 minutes at 4°C to remove any insoluble material.

2.6.1.2 Assay procedure

This assay was performed in triplicate for all wells (samples and standard) using 96 well clear flat-bottom plates.

1) 0, 2, 4, 6, 8, and 10µl of the 1 mM standard solution were added into a 96 well plate to create 0, 2, 4, 6, 8, and 10 nmol/well standards, then Iron Assay Buffer was added to each well to bring the volume to 100µl.
2) 20µl of the samples (homogenised) was added into respective wells, before adding Iron Assay Buffer to each well to bring the volume to 100µl.

3) To measure total iron, 5µl of Iron Reducer was added to each of the wells (sample and standard) to reduce Fe^{3+} to Fe^{2+}.

4) Solutions were pipetted up and down to mix all the contents in each well before the plate was incubated for 30 minutes at room temperature.

5) 100µl of Iron Probe was added to each well and samples were then mixed well by pipetting, and the reaction was re-incubated for about 60 minutes at room temperature. The plate was wrapped in aluminium foil to protect it from light during each incubation.

6) The absorbance was measured using a spectrophotometric multi-well plate reader (TECAN Sunrise™) at 593 nm (A_{593}).

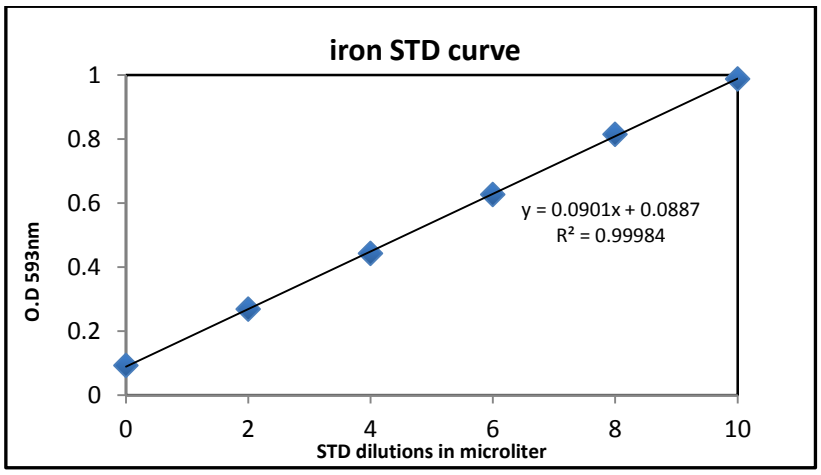

Figure 2-11: An example of a standard iron curve in 96-well plate assay (the calibration curve obtained by plotting the absorbance of identified concentrations)

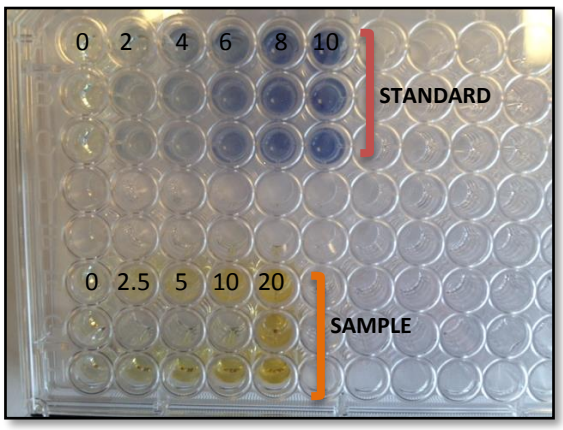

Figure 2-12: Standard curve and dilution optimization

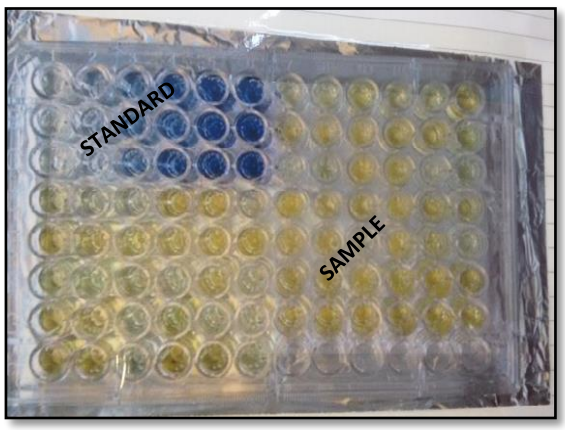

Figure 2-13: Assay micro-plate model

Iron changes colour by reduction during the reaction. The different oxidation states have the following colours, Fe^{2+} (Very pale green) to Fe^{3+} (Very pale violet (as in the standard)/brown). Then, once chloride ions bind Fe^{3+} in a complex, it forms a yellow/brown colour. These colorimetric products are followed by measuring absorbance at 593 nm.

2.6.1.3 Faecal iron results and analysis

It is important to have a blank (0) for the iron standard for use as a background for the assay. The background is removed from the sample values by deducting the 0 (blank) value from all readings. A standard curve was prepared from a known concentration of iron. A new standard curve was made for each assay run.

$$\textbf{Concentration of iron in sample (C)} = \frac{\textbf{Sa} \text{ (Amount of iron in unknown sample (more) from standard curve)}}{\textbf{Sv} \text{ (Sample volume (µl) added into the wells)}}$$

Example for sample calculation:

Assuming the amount of iron (Sa) = 5.84 moles (from standard curve) and the sample volume (Sv) = 100µl, then by applying the equation above.

Concentration of iron in sample = 5.84 nmole/100µl = 0.0584 nmol/µl

Now converting from nmol/µl to ng/µl by multiplying the concentration of iron in sample by the iron atomic mass is 55.85 g/mole

0.0584 nmole/µl x 55.85 ng/nmole = 3.26 ng/µl

2.7 Microbiome studies

Metagenomic studies are accomplished by analysing the prokaryotic 16S ribosomal RNA gene (16S rRNA), which is around 1,500 bp long and covers nine variable regions sprinkled between conserved regions. Variable regions of 16S rRNA are often used in phylogenetic classifications such as genus or species in diverse microbial populations.

Previous animal research has shown that there are changes in bacterial composition with colonic inflammation and/or infection [30]. Current molecular techniques have enabled the description of the change in the composition of the faecal microbiota, as well as mucosally-associated bacteria, in patients with CD and UC. This research has explored the impact of disease activity and iron on the faecal microbiota. The mucosal microbiota play a crucial role in maintaining microbiome equilibrium, however in this research it was difficult to obtain samples (mucosal) from day-1 without killing the animals, as the aim is to compare pre- and post-treatment samples together.

2.7.1 DNA sample preparation and storage

Bacterial DNA was extracted from murine faecal samples using the Startec Kit [PSP® Spin Stool DNA Plus Kit]. To validate the efficiency of the PCR assay for detection of the presence of the prokaryotic V4 region (16S rDNA), the DNA extracted was quantified by Qubit® 2.0 Fluorometer [Invitrogen by life technologies] to 1 ng/µl into Aliquots of 50µl.

2.7.1.1 DNA samples were quantified using Qubit® 2.0 Fluorometer

- Aliquot 199 x n µl of Quant-iT™ Buffer was added into the 45ml tube, and 1 x n µl for the Quant-iT™ Reagents to make Quant-iT™ Working Solution (master mix). [n= number of Standards plus number of Samples].
- Aliquot 199µl of Quant-iT™ Working Solution was added into 0.5ml tubes (molecular probe tubes for the Qubit) for the samples, and 190µl was added to the two standards.
- 1µl of the sample was added and 10µl of the standards to a separate 0.5ml tube.
- The samples and standards were mixed by vortex.
- The samples and standards were incubated for 2 minutes at RT in the dark.
- The Qubit machine was switched on then standards were placed in for calibration before the samples were placed in for reading. All the reading data were recorded in an Excel file.

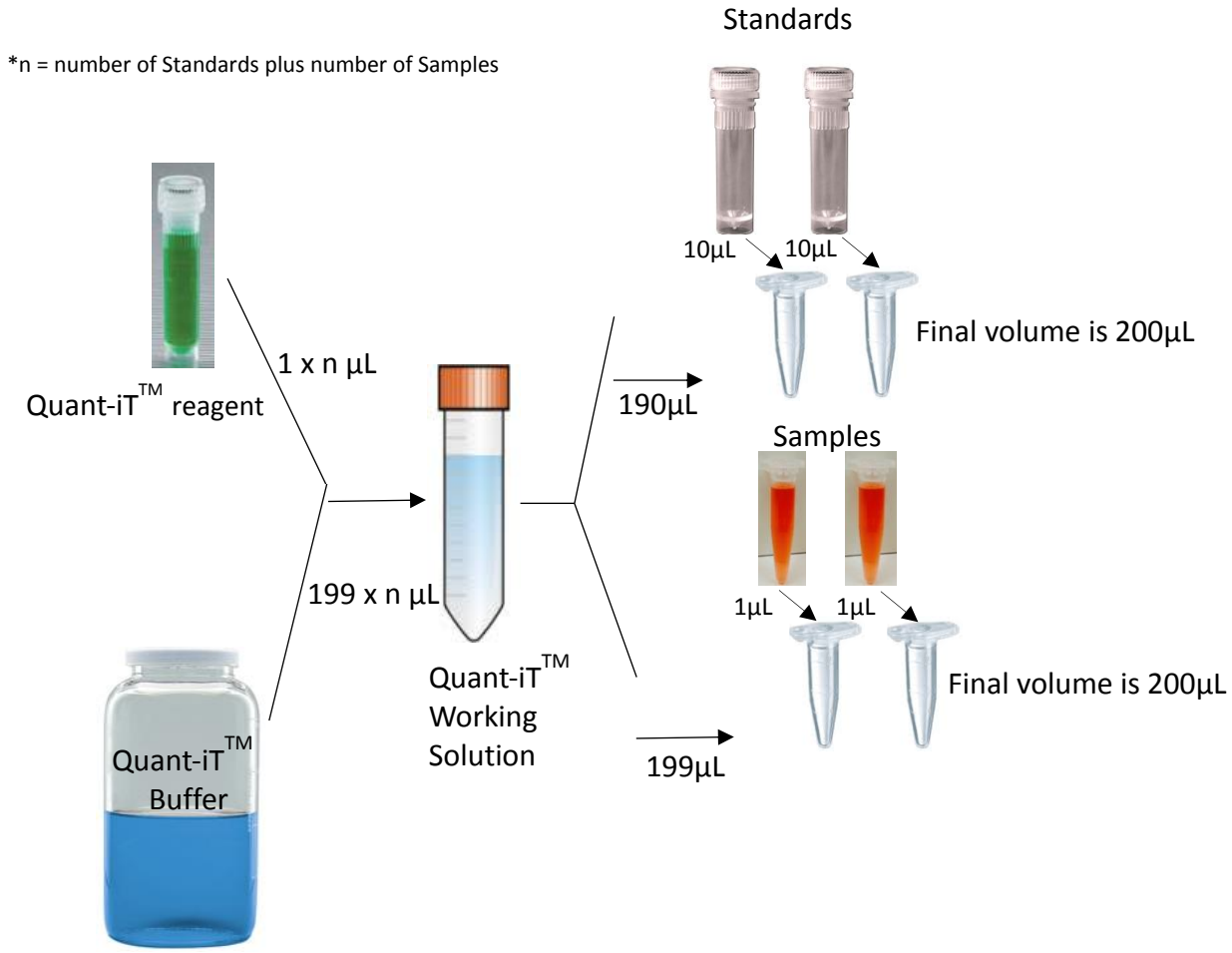

Figure 2-14: Qubit's process

2.7.1.2 Assessing DNA quality

To assess the quality of the extracted DNA before sequencing, a basic PCR was performed to detect the V4 region band on an agarose gel. This was done for one out of every five DNA extracted samples. V4 primers [Forward: F515: 5'-GTG-CCA-GCM-GCC-GCG-GTA-A-3', and Reverse: 806R: 5'-GGA-CTA-CNN-GGG-TNT-CTA-AT-3'] were used. A KAPA HiFi HotstartReadyMix PCR Kit [Kapabiosystems, Boston, Massachusetts, United States] was used as recommended by the CGR (Centre for Genomic Research).

Reaction component	**Final concentration**	**Per 25µl reactions**
PCR grade water	_	Up to 25µl
KAPA HiFi Hot start	1x	12.5µl
Fw V4 primer	0.3µM	1.5µl
Rv V4 primer	0.3µM	1.5µl
Template DNA	1 ng/µl	1.5µl

Table 2-1: KAPA HiFi reaction setup for routine high-fidelity PCR

Reactions were performed using a MultiGene™ OptiMax Thermal Cycler (Labnet International, Inc.) under the cycling conditions listed in Table 2-3, below.

Cycling step	Temperature and Time	
Initial denaturation	2 min at 95°C	1
Denaturation	20 sec at 98°C	X 30 cycles
Annealing	15 sec at optimal 60°C	
Extension	40 sec/kB at 72°C	
Final extension	1 min at 72°C	1

Table 2-2: KAPA HiFi cycling parameters for routine high-fidelity PCR

To detect the amplified band, a 2% agarose gel was placed in a bath of running buffer ((Tris-acetate-EDTA) TAE 1x) with 5µl of Hyperladder IV and 12.5µl of PCR product. The gel was run for 2 hours at 80 Volts. After 90 minutes, it was possible to visualise the gel in a ChemiDoc™ MP System (BIO-RAD) where the band size should be around 300 bp.

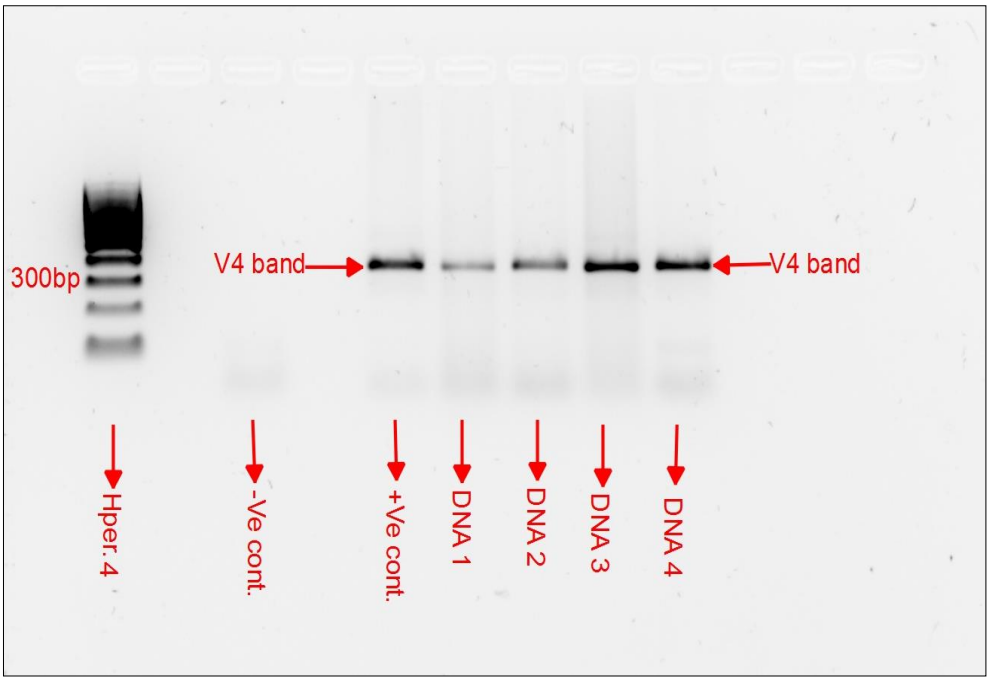

Figure 2-15: example of 2% agarose gel showing V4 bands [-ve CTR. (water), +ve CTR (healthy control), DNA 1, 2, 3 and 4 (IBD samples)] all samples are faecal bacterial DNA from humans

Once the DNA quality had been assured, 96 well plates were prepared with 25µl of quantified samples (genomic DNA) per well. Negative controls were also applied.

2.7.2 16S Metagenomics Sequencing Library Preparation

All of the following work was done at the Centre for Genomic Research labs and by their staff.

The Centre for Genomic Research (CGR) used a standard protocol as shown in Figure 2-16 for preparing samples and sequencing the variable V4 region of the 16S rRNA gene. This protocol combined with a benchtop sequencing system, initial onboard analysis, and secondary analysis using MiSeq Reporter, provided a comprehensive workflow for 16S rRNA amplicon sequencing.

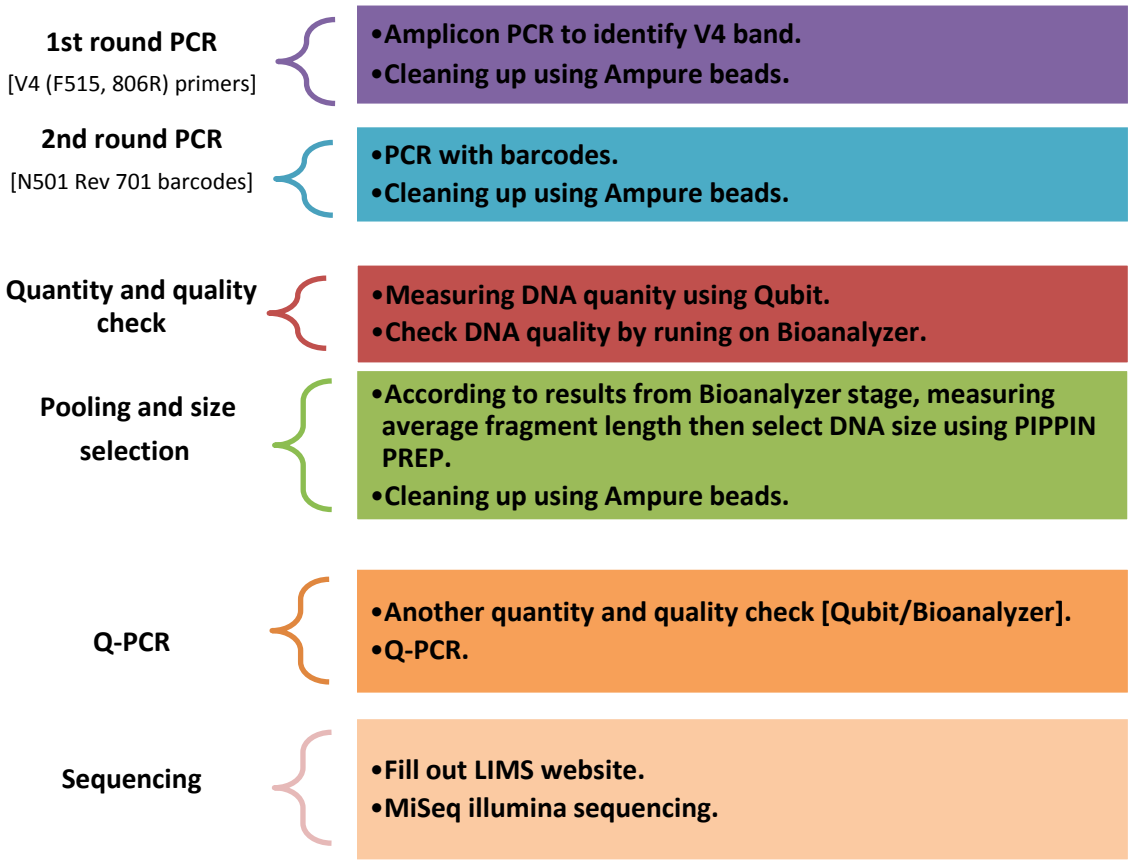

Figure 2-16: V4 sequencing protocol (2-steps PCR Dual Indexes)

2.7.2.1 Amplicon PCR

In this step, PCR was used to amplify DNA of interest using specific primers with extended adapters attached.

1. The following components of DNA, 2 x KAPA HiFi Hot Start Ready-mix, and primers were added together to make a reaction mix of 25µl per each sample:

Reaction components	**Volume**
Microbial DNA (5 ng/µl)	2.5µl
V4 Forward Primer 1µM	5µl
V4 Reverse Primer 1µM	5µl
2x KAPA HiFi Hot Start Ready-mix	12.5µl
Total	**25µl**

2. 25µl of each reaction components (each sample) was added to a 96-well PCR plate. The plate was then sealed, and the PCR reaction was performed in a thermal cycler using the following program:

Cycling step	**Temperature and Time**	
Initial denaturation	3 min at 95°C	1
Denaturation	30 sec at 95°C	X 25 cycles
Annealing	30 sec at optimal 55°C	
Extension	30 sec/kB at 72°C	
Final extension	5 min at 72°C	1

The size was verified by running 1µl of the PCR product on a Bioanalyzer DNA 1000 chip using the V4 primer pairs in the protocol. The expected size on a Bioanalyzer trace after the Amplicon PCR step was ~550 bp.

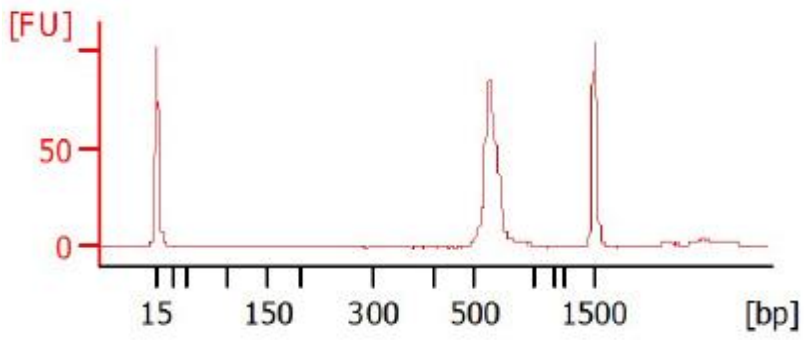

Figure 2-17: Example of Bioanalyzer trace after Amplicon PCR Step

2.7.2.2 PCR Clean-Up 1

In this step, AMPure XP beads were used to purify the 16S V4 amplicon away from free primers and primer dimer species. The kit was prepared by bringing the AMPure XP beads to room temperature.

Consumables

Item	Quantity
10 mM Tris pH 8.5	52.5µl per sample
AMPure XP beads	20µl per sample
96-well 0.2ml PCR plate	1 plate
Freshly Prepared 80% Ethanol (EtOH)	400µl per sample

2.7.2.2.1 Procedure

1) The Amplicon PCR plate was centrifuged at 1,000 × g at 20°C for 1 minute.

2) Then the AMPure XP beads were vortexed for 30 seconds to make sure that the beads were evenly dispersed before adding some to a trough.

3) About 20µl of AMPure XP beads was added to each well of the Amplicon PCR plate; this was then mixed by pipetting up and down a few times before incubating at room temperature for 5 minutes.

4) The plate was placed on a magnetic stand for 2 minutes until the supernatant had cleared.

5) While the Amplicon PCR plate was on the magnetic stand, the supernatant was removed and discarded using a pipette.

6) The beads were washed with freshly prepared 80% ethanol while the Amplicon PCR plate was on the magnetic stand. First, 200µl of freshly prepared 80% ethanol was added to each sample well. Next, the plate was incubated on the magnetic stand for 30 seconds. Then, the supernatant was removed and discarded.

7) Again, the second ethanol wash was performed while the Amplicon PCR plate was on the magnetic stand. So, 200µl of freshly prepared 80% ethanol was added to each sample well. Next, the plate was incubated on the magnetic stand for 30 seconds. Then the supernatant was removed and discarded before removing excess ethanol with pipette tips.

8) The beads were allowed to air-dry for 10 minutes then the Amplicon PCR plate was removed from the magnetic stand before 52.5µl of 10 mM Tris pH 8.5 was pipetted into each well of the Amplicon PCR plate.

9) Gentle mixing was performed by pipetting up and down 10 times, before incubation at room temperature for 2 minutes.

10) The plate was placed on the magnetic stand for 2 minutes or until the supernatant had cleared.

11) 50µl of the supernatant was transferred from the Amplicon PCR plate into a new 96 well PCR plate.

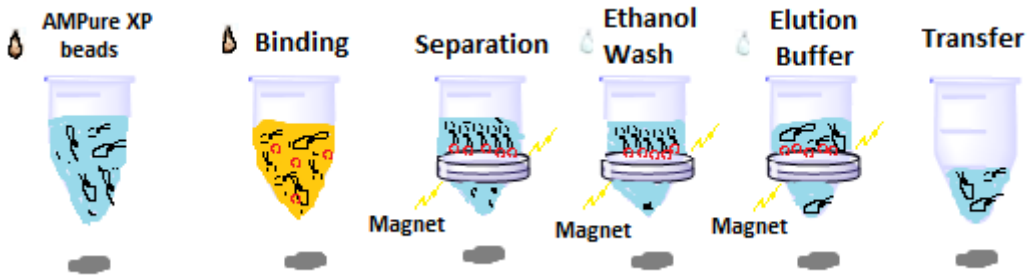

Figure 2-18: Standard workflow of AMPure XP reagents (adapted from manufacturer's catalogue)

2.7.2.3 Index PCR

In this step dual indices and Illumina sequencing adapters were attached using the Nextera XT Index Kit.

Consumables

Item	Quantity
2x KAPA HiFi Hot Start Ready-mix	25µl per sample
Nextera XT Index 1 Primers (N7XX)	5µl per sample
Nextera XT Index 2 Primers (S5XX)	5µl per sample
PCR Grade Water	10µl per sample
TruSeq Index Plate Fixture (FC-130-1005)	1
96-well 0.2ml PCR plate	1 plate
Microseal 'A' film	1

Table2-3: Nextera XT Index Kit contents

2.7.2.3.1 Procedure

1) About 5µl of suspended PCR product DNA was transferred from each well to a new 96-well plate.

2) The Index 1 and 2 primers were positioned in a rack (i.e. the TruSeq Index Plate Fixture) as follows:

[a] Index 2 primer tubes (white caps, clear solution) were placed vertically, aligned with rows A-H.

[b] Index 1 primer tubes (orange caps, yellow solution) were placed horizontally, aligned with columns 1-12.

3) The 96-well PCR plate containing the 5µl of DNA had been put in the TruSeq Index Plate Fixture.

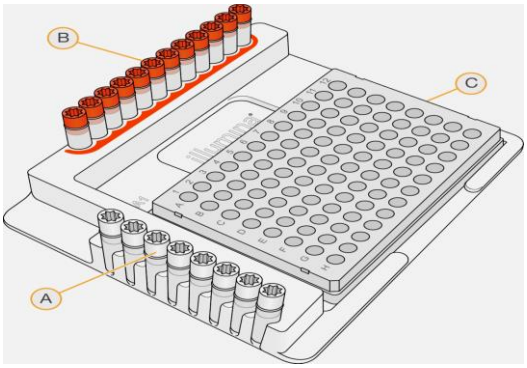

A Index 2 primers (white caps)
B Index 1 primers (orange caps)
C 96-well plate

Figure 2-4: TruSeq Index Plate Fixture

4) The following components of DNA, Nextera XT Index Primers [1 (N7xx), 2 (S5xx)], 2x KAPA HiFi Hot Start Ready-mix, and PCR Grade water were added together to make a reaction mix of 50µl per each sample:

Reaction components	Volume
DNA	5µl
Nextera XT Index Primer 1 (N7xx)	5µl
Nextera XT Index Primer 2 (S5xx)	5µl
2x KAPA HiFi Hot Start Ready-mix	25µl
PCR Grade water	10µl
Total	**50µl**

5) All components were mixed by pipetting up and down; then the plate was covered with micro seal 'A' before it was centrifuged at 1,000 × g at 20°C for 1 minute.

6) PCR reaction was performed in a thermal cycler using the following cycling conditions:

Cycling step	Temperature and Time	
Initial denaturation	3 min at 95°C	1
Denaturation	30 sec at 95°C	X 8 cycles
Annealing	30 sec at optimal 55°C	
Extension	30 sec/kB at 72°C	
Final extension	5 min at 72°C	1

2.7.2.4 PCR Clean-Up 2

In this step, AMPure XP beads were used again to clean up the last library before quantification.

Consumables

Item	Quantity
10 mM Tris pH 8.5	27.5µl per sample
AMPure XP beads	56µl per sample
96-well 0.2ml PCR plate	1 plate
Freshly Prepared 80% Ethanol (EtOH)	400µl per sample

2.7.2.4.1 Procedure

1) The Index PCR plate was centrifuged at 280 × g at 20°C for 1 minute to gather condensation.

2) The AMPure XP beads were vortexed for 30 seconds to make sure that the beads were evenly dispersed before adding some to a trough.

3) Around 56µl of AMPure XP beads was added to each well of the Index PCR plate, mixed by pipetting up and down few times before incubating at room temperature for 5 minutes.

4) The plate was placed on a magnetic stand for 2 minutes until the supernatant had cleared.

5) While the Amplicon PCR plate was on the magnetic stand, the supernatant was removed and discarded using a pipette.

6) The beads were washed with freshly prepared 80% ethanol while the Amplicon PCR plate was on the magnetic stand. First, 200µl of freshly prepared 80% ethanol was added to each sample well; the plate was placed on the magnetic stand for 30 seconds before the supernatant was removed and discarded.

7) Again, another ethanol wash was performed during the Amplicon PCR plate on the magnetic stand. 200µl of freshly prepared 80% ethanol was added to each sample well; then the plate was placed on the magnetic stand for 30 seconds before the supernatant was removed and discarded and any excess ethanol was removed with fine pipette tips.

8) The beads were allowed to air-dry for 10 minutes before the Amplicon PCR plate was removed from the magnetic stand. 27.5µl of 10 mM Tris pH 8.5 was added to each well of the Amplicon PCR plate.

9) Gentle mixing by pipetting up and down 10 times, before incubating at room temperature for 2 minutes.

10) The plate was placed on the magnetic stand for 2 minutes or until the supernatant had cleared.

11) 25µl of the supernatant was transferred from the Index PCR plate to a new 96-well PCR plate.

2.7.2.5 Library Quantification, Normalization, and Pooling

Illumina recommends quantifying libraries using a fluorometric quantification method that uses dsDNA-binding dyes.

The following equation is used to calculate DNA concentration in nM, based on the size of DNA amplicons as determined by an Agilent Technologies 2100 Bioanalyzer trace:

$$\frac{\text{(Concentration in ng/µl)}}{\text{(660 g/mol x average library size)} \times 10^6} = \text{concentration in nM}$$

The concentrated final library was diluted by using Resuspension Buffer (RSB) or 10 mM Tris pH 8.5 to 4 nM, then 5µl of diluted DNA from each library was aliquoted, and all aliquots for pooling libraries were mixed with unique indices.

However, depending on coverage needed, up to 96 libraries can be pooled for one MiSeq run. In the case of metagenomics samples, >100,000 reads per sample are adequate to survey the bacterial composition fully. This number of reads permits sample pooling to the maximum level of 96 libraries, given the MiSeq output of > 20 million reads.

2.7.2.6 Library Denaturing and MiSeq Sample Loading

To prepare a cluster generation and sequencing, pooled libraries were denatured with NaOH, diluted with hybridization buffer, and then heated before MiSeq sequencing. To each run, a minimum of 5% PhiX was added to serve as an internal control for these low diversity libraries.

Consumables

Item	Quantity
10 mM Tris pH 8.5 or RSB (Resuspension Buffer)	6µl
HT1 (Hybridization Buffer)	1540µl
0.2 N NaOH (less than a week old)	10µl
PhiX Control Kit v3 (FC-110-3001)	4µl
MiSeq reagent cartridge	1 cartridge
1.7ml microcentrifuge tubes	3 tubes
2.5 L ice bucket	

Before denaturing the DNA, a heat block suitable for 1.7ml microcentrifuge tubes sat at 96°C. Then the MiSeq reagent cartridge was thawed at room temperature. Finally, an ice-water bath in an ice bucket was prepared by combining 3 parts ice and 1 part water.

2.7.2.6.1 Denature DNA

1) 5µl of 4nM pooled final DNA library and 5µl of freshly diluted 0.2 N NaOH were combined in a microcentrifuge tube.

2) The remaining dilution of 0.2 N NaOH was retained to prepare a PhiX control within the next 12 hours.

3) The sample solution was mixed by vortex, and centrifuged for 1 minute at 280 × g, before being incubated for 5 minutes at room temperature to denature the DNA into single strands.

4) 990µl of the pre-chilled HT1 was added to a tube containing 10µl of the denatured DNA. Consequently, adding the HT1 resulted in a 20 pM denatured library in 1 mM NaOH, this denatured DNA was then placed on ice until proceeding to final dilution.

2.7.2.6.2 Dilute Denatured DNA

1) Dilution of the denatured DNA to the preferred concentration used the following example:

Final concentration	**2 pM**	**4 pM**	**6 pM**	**8 pM**	**10 pM**
20 pM denatured library	60µl	120µl	180µl	240µl	300µl
Pre-chilled HT1	540µl	480µl	420µl	360µl	300µl

2) The DNA solution was mixed by inverting the tubes several times and pulse centrifuging and then placing the denatured and diluted DNA on ice.

2.7.2.6.3 Denature and Dilution of PhiX Control

This step was to denature and dilute the 10 nM PhiX library to the same loading concentration as the Amplicon Library. However, the final library mixture must contain at least 5% PhiX.

1) 2µl of the 10 nM PhiX library was added to 3µl of 10 mM Tris pH 8.5 to dilute the PhiX library to 4 nM.

2) Then 5µl of the 4 nM PhiX library was added to 5µl of the 0.2 N NaOH in a microcentrifuge tube.

3) About 2 nM PhiX library solution was mixed gently by vortex before the solution was incubated for 5 minutes at room temperature to denature the PhiX library into single strands.

4) 990µl of pre-chilled HT1 was added to the tube containing 10µl of the denatured PhiX library to result in a 20 pM PhiX library.

5) The denatured 20 pM PhiX library was diluted to the same loading concentration as the Amplicon Library using the same example above.

6) The DNA solution was mixed by inverting the tubes several times and pulse centrifuging and then placing the denatured and diluted Phix on ice.

2.7.2.6.4 Combine Amplicon Library and PhiX Control

1) 30µl of the denatured and diluted PhiX control was added to 570µl of the denatured and diluted amplicon library in a microcentrifuge tube.

2) The combined sample library and PhiX control were placed on ice until it was time to denature the mixture, immediately before loading it onto the MiSeq v3 reagent cartridge.

3) The combined library and PhiX control tube were incubated in a heat block at 96°C for 2 minutes.

4) After incubation, the solution was mixed by inverting the tube a couple of times, and this was immediately placed in ice water for about 5 minutes.

2.7.2.7 MiSeq Reporter Metagenomics Workflow

Once the samples had been loaded, a secondary analysis was provided by the MiSeq system using the MiSeq Reporter software (MSR). This software provides several selections for analysing MiSeq sequencing data. Therefore, for the 16S protocol, the Metagenomics workflow was selected.

By following this protocol, the Metagenomics workflow classifies organisms from a V4 amplicon using a database of 16S rRNA data. The classification will be based on the Greengenes database (http://greengenes.lbl.gov/). The production of this workflow is a ranking of reads at several taxonomic levels: Kingdom, phylum, class, order, family, genus, and species.

This analysis includes:

1- Clusters Graph – displays numbers of the raw cluster, clusters passing filter, clusters that did not align, clusters not related with an index, and duplicates.

2- Sample Table – summarises the sequencing outcomes for each sample.

3- Cluster Pie Chart – a graphical illustration of the classification breakdown for each sample.

2.8 Statistical analysis of physiological and microbiota data

To test the statistical significance of the physiological and biochemical data, normally distributed data were assessed by analysis of variance followed by multiple comparisons Dunn's test, whereas not normally distributed data were assessed by Kruskal-Wallis test followed by multiple comparisons Dunn's test (StatsDirect version 3.0.171). Differences were considered significant when $P<0.05$.

For the bioinformatic analysis of microbiota data, Welch's t-test was used in acute DSS experiments, and Kruskal-Wallis H-test was used in chronic DSS experiments (the software [STAMP] guidelines recommendations). The false discovery rate (FDR) Storey's (multiple correction tests) was used to produce a prioritised list of OTUs that summarise observed differences between two user-defined populations. The q-value is the adjusted p-value based on FDR calculation, where statistical significance was declared at $P<0.05$.

3 The effect of different iron diets on acute course of dextran sulphate sodium (DSS)-induced colitis in wild-type mice C57BL/6

3.1 Introduction

Iron deficiency is common in IBD. Iron supplementation appears to exacerbate symptoms: this may be because all ferrous compounds are oxidised and release activated hydroxyl radicals (reactive oxygen species (ROS)) within the lumen of the gut or the mucosa. These particles will damage the intestinal wall and produce a variety of gastrointestinal symptoms and discomfort [110].

There is a dysbiosis in patients with IBD. Also, there is a possibility that components of the normal intestinal microbiota might cause, activate, or in some way contribute to IBD [111]. Variations in microbial ecology among people with UC and CD and normal individuals have been demonstrated by recent studies, in which the diversity of bacteria is changed [112]. The gut microbiota of healthy individuals is occupied by *Firmicutes* and *Bacteroidetes*, and contain less *Proteobacteria*, *Actinobacteria* and *Verrucomicrobia* [99]. However, in IBD patients, *Firmicutes* appear to be reduced [113], [114], [115] whereas *Gammaproteobacteria* was increased [116], [117]. In CD patients there was a reduction in the *Clostridia* cluster IV group, in particular *Faecalibacterium prausnitzii* [118], [119]. Some members of *Clostridia* group XIVa (*Roseburia* genus), also appear to be reduced in all IBD patients [119]. In addition to these alterations in relative abundances of specific phylotypes, there appears to be a general reduction in biodiversity in IBD patients [120], [121].

Most invading pathogens require iron for rapid growth during infection. Consequently, most mammals aim to resist infection by reducing (sequestering) free iron: this tight regulation

protects the body during infection [111]. Increasing available iron, by iron supplementation, increases the growth of *Escherichia coli, Salmonella enterica serovar*, *Yersinia enterocolitica*, *Typhimurium* and *Staphylococcus epidermidis* [122]**.** Therefore, regulating free iron may be used to control the constitution of the microbiome.

The take-up of iron from dietary components occurs in the small intestine: however excess iron in the diet remains in the small intestine and passes into the colon. There is a correlation between the amount of dietary iron consumed and faecal iron excretion in healthy individuals [123].

This study investigated the hypothesis that changing the amount of dietary iron would influence the development of IBD in a murine model. Dietary iron was both increased and decreased in groups of mice in which DSS-induced colitis was induced. This chapter reports the impact of different oral iron diets on colitis features in wild-type mice.

3.2 Aims

The aims were to investigate the impact of varying dietary iron on acute DSS-induced colitis in mice.

3.3 Preliminary experiments

36 individually housed, wild-type C57BL/6 female mice aged 8-9 weeks were divided into 6 groups of 6 mice. Group (A) mice were given a 100ppm iron diet; Group (B) a 200ppm iron diet and Group (C) a 400ppm iron diet. All groups were given 2% DSS treatment. Control mice were given distilled water without DSS; Group (D) had a 100ppm iron diet; Group (E) a 200ppm iron diet and Group (F) mice a 400ppm iron diet (Figure 3-1).

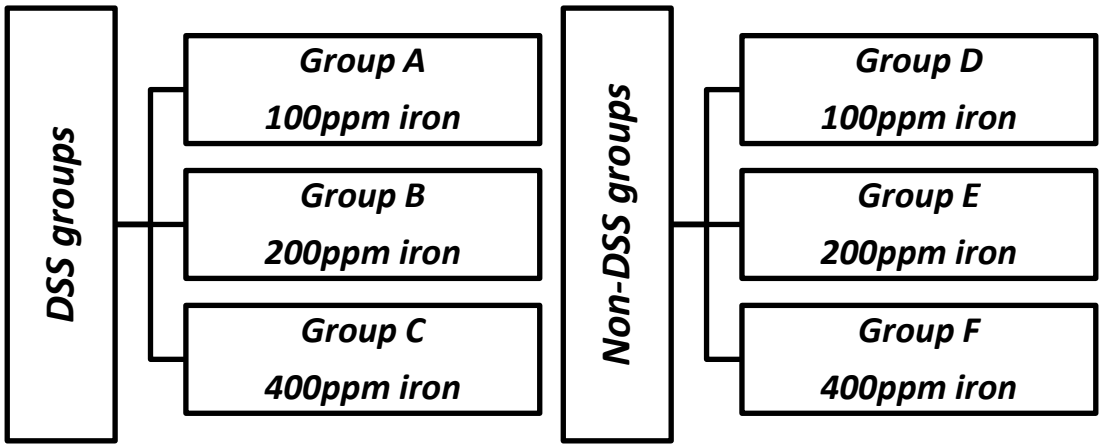

Figure 3-1: Different diet groups with and without DSS treatment

3.3.1 Induction of Colitis in three different iron diet groups

The 2% DSS colitis model (5 days DSS in drinking water) induces disease that may be recognised by the development of the clinical signs such as loss of body weight, loose faeces/watery diarrhoea and faecal blood/rectal bleeding. This colitis model, established in our department, has been documented in previous publications [124].

DSS-treated animals (Group (A) 100ppm iron, (B) 200ppm iron and (C) 400ppm iron) were fed each corresponding diet from day-1 until day-10 of the DSS cycle. All mice were administered 2% DSS in distilled water as the sole source of drinking fluid for 5 days, and then normal drinking water for the subsequent 5 days (the 10-day period was defined as an acute DSS cycle as illustrated in Figure 2-2, Chapter 2). During the entire 10-day experiment the mice were caged separately and placed on paper bedding, which was changed daily to collect fresh samples and observe any signs of colonic bleeding. Daily body weight was recorded in addition to any clinical observations at the end of the experiment (day-10) when all mice were euthanised using a schedule 1 method.

3.3.1.1 The effect of dextran sulphate sodium (DSS) on the body weight of wild-type C57BL/6 mice in DSS-treated mice supplemented with different iron diets

The body weight of the DSS-treated mice was recorded daily to monitor the percentage of body weight change as outlined in Figures 3-2, 3-3 and 3-4. Strikingly, mice on 400ppm iron only lost 2.3% of their starting body weight on day-9; this was significantly less than mice taking 100 and 200ppm iron diets which lost 9% and 5% of their starting body weight, respectively on day-8. However, the mice on 400 and 200ppm iron both showed a significant increase in the percentage of body weight gain compared to 100ppm iron mice on day-10. In other words, 400 and 200ppm iron mice showed 8.3% and a 2.8% weight gain while 100ppm iron mice showed a 0.03% weight gain on day-10 (Figures 3-2, 3-3 and 3-4). Control mice group (E), taking a 200ppm iron diet without DSS treatment had a steady increase in body weight during the 10-day period (Figure 3-5).

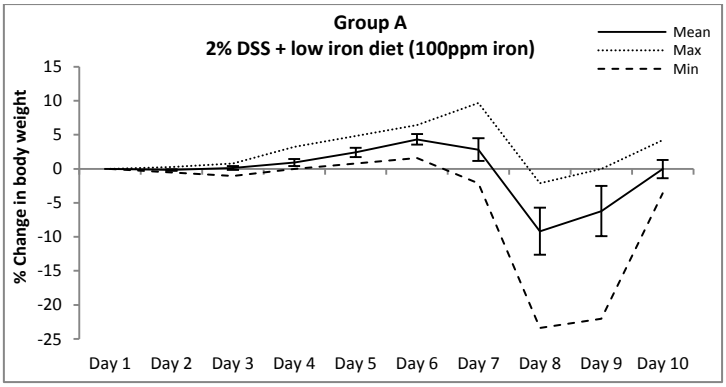

Figure 3-2: Percentage of weight change in mice received 100ppm iron diet during 2% DSS-induced colitis. Data are presented as mean (solid line) ± standard error of the mean, maximum (dotted line) and minimum (dashed line).

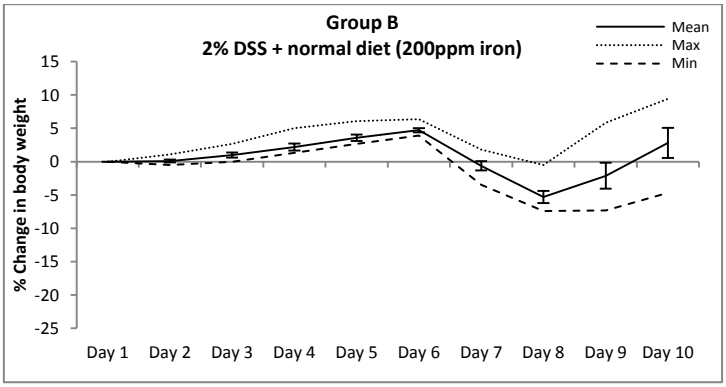

Figure 3-3: Percentage of weight change in mice received 200ppm iron. Data are presented as mean (solid line) ± standard error of the mean, maximum (dotted line) and minimum (dashed line).

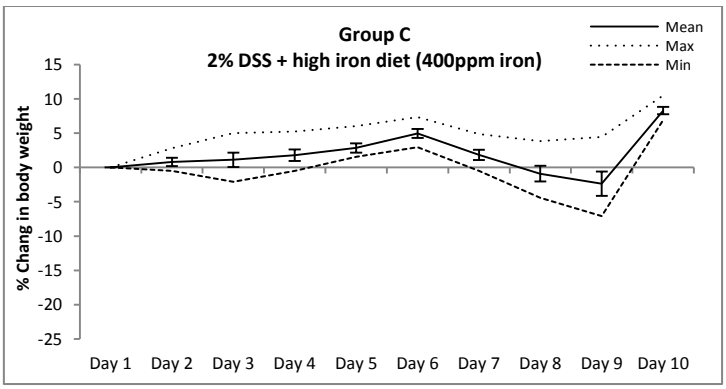

Figure 3-4: Percentage of weight change in mice received 400ppm iron. Data are presented as mean (solid line) ± standard error of the mean, maximum (dotted line) and minimum (dashed line).

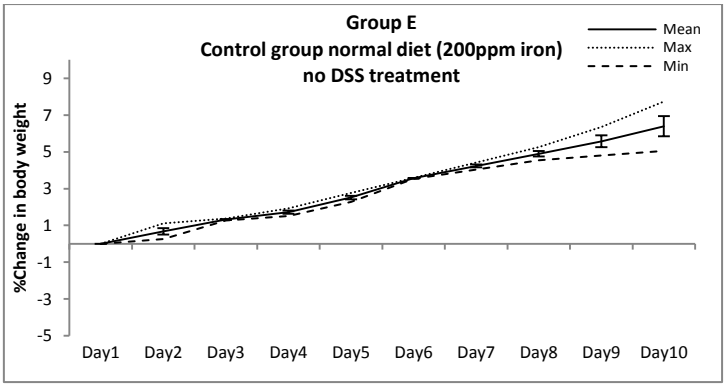

Figure 3-5: Percentage of weight change in mice received 200ppm iron diet during the 10-day period. Data are presented as mean (solid line) ± standard error of the mean, maximum (dotted line) and minimum (dashed line).

Acute colitis was induced in the mice that received 2% DSS in their drinking water for 5 days, and they recovered during the following 5 days on plain drinking water. All DSS-treated mice lost body weight from day-6 with the maximal loss occurring on day-8. Group (A) 100ppm iron mice lost significantly more weight than other groups (Figure 3-6).

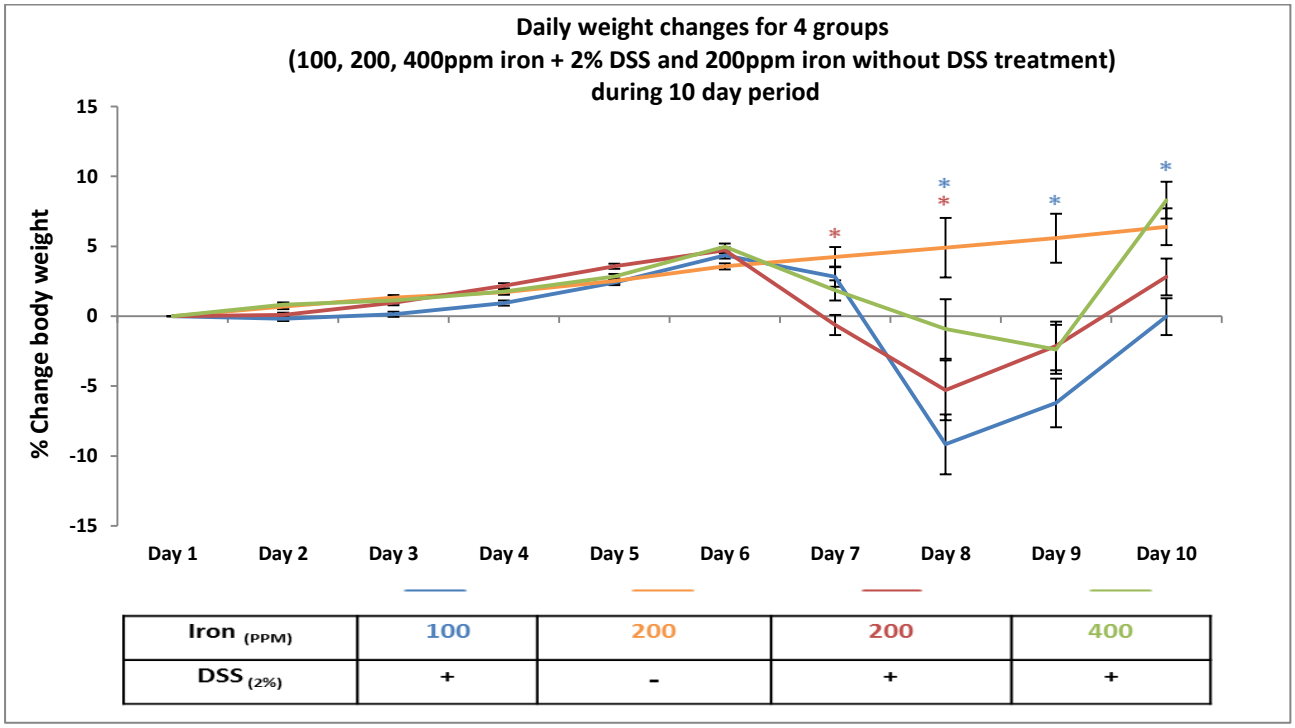

Figure 3-6: Percentage of weight change in mice (100 (blue), 200 (red), and 400ppm iron (green)) during dextran sulphate sodium-induced colitis and mice receiving 200ppm (orange) iron diet without DSS treatment during the 10-day period. Data are presented as a mean ± standard error of the mean. Statistical differences were assessed by Kruskal–Wallis test followed by Dunn's multiple comparison tests (*P<0.05). (n=6 female mice per group).

3.3.1.2 The influence of different iron diets on the body weight of wild-type C57BL/6 mice without DSS treatment

Control mice (Groups D-F) received drinking water without DSS, but with varying amounts of dietary iron, as described above. Daily observations and measures were completed in the same way as for the mice receiving DSS.

Group (E) mice (200ppm iron) were euthanised at day-10 to allow comparison with the DSS-treatment groups. However, the rest of the untreated mice (Group D (100ppm iron) and Group F (400ppm iron)) were maintained on their diets for a total of 28 days. They were then euthanised using a Home Office approved schedule 1 method.

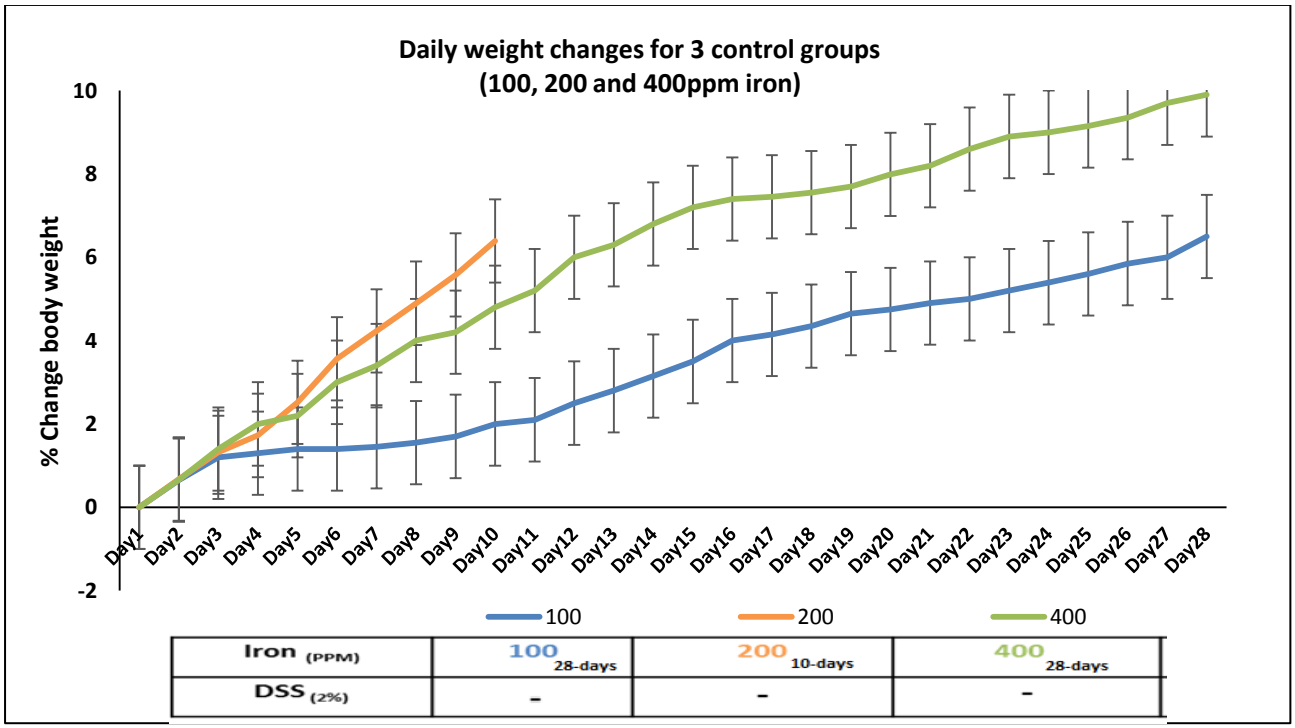

Figure 3-7: Percentage of weight change in mice (100 (blue), 200 (orange), and 400ppm iron (green)) without DSS treatment during the 10-days for 200ppm and 28-days for 100 and 400ppm iron groups. Data are presented as a mean ± standard error of the mean. Statistical differences were assessed by Kruskal–Wallis test followed by Dunn's multiple comparison tests. (n=6 female mice per group).

3.3.2 Histopathological changes resulted from colonic inflammation following dextran sulphate sodium administration

The colons of the mice were examined for the features of colitis by light microscopy after staining with haematoxylin and eosin (H&E).

3.3.2.1 100ppm iron diet DSS-treated mice displayed more severe colonic inflammation compared with mice receiving 200 and 400ppm iron diets

After 10 days of DSS administration, all DSS-treated mice along with the 200ppm iron diet controls were killed by exposure to rising concentrations of CO_2. A specimen of the whole distal colon was removed, fixed in 4% neutral buffered formalin, dehydrated, and wax-embedded and was then cut into 4µm sections. The sections were stained with haematoxylin and eosin (H&E) to observe under light microscopy. Untreated mice distal colon showed no colitis features at all i.e. had similar histological findings to normal with normal crypts and no inflammation (Figure 3-8 I, II and III). In contrast to this, all the mice that were treated with 2% DSS developed bloody diarrhoea within the last 5 days of the study, but there was no mortality. Histological examination established the presence of DSS-induced colitis, which was mainly located in the distal part of the colon. Histological features included areas of mucosal loss, increased muscle thickness, oedema and inflammatory cell infiltration (Figure 3-8 IV, V and VI).

Using the histological inflammatory scoring system (Table 3-1) [91], H and E stained slides were scored in a blinded fashion by two investigators; the researcher and an accredited veterinary pathologist Jonathan Williams (Diplomate of the European College of Veterinary Pathologists). Histological damage was scored using the criteria of Bauer [91], which considers the loss of mucosal architecture and cellular infiltration (maximum score = 6).

The 100ppm iron + DSS mice showed a significant increase in intestinal inflammation (significant increase in the colitis score) compared with the DSS + 400 or 200ppm iron diet groups.

Score	Cell infiltration	Tissue damage
0	None	None
1	Focally increased numbers of inflammatory cells in the lamina propria	Discrete epithelial lesions
2	Confluence of inflammatory cells extending into the submucosa	Mucosal erosions
3	Transmural extension of the infiltrate	Extensive mucosal damage and/or extension through deeper structures of the bowel wall

Table 3-1: Colitis scoring system adapted from [91]

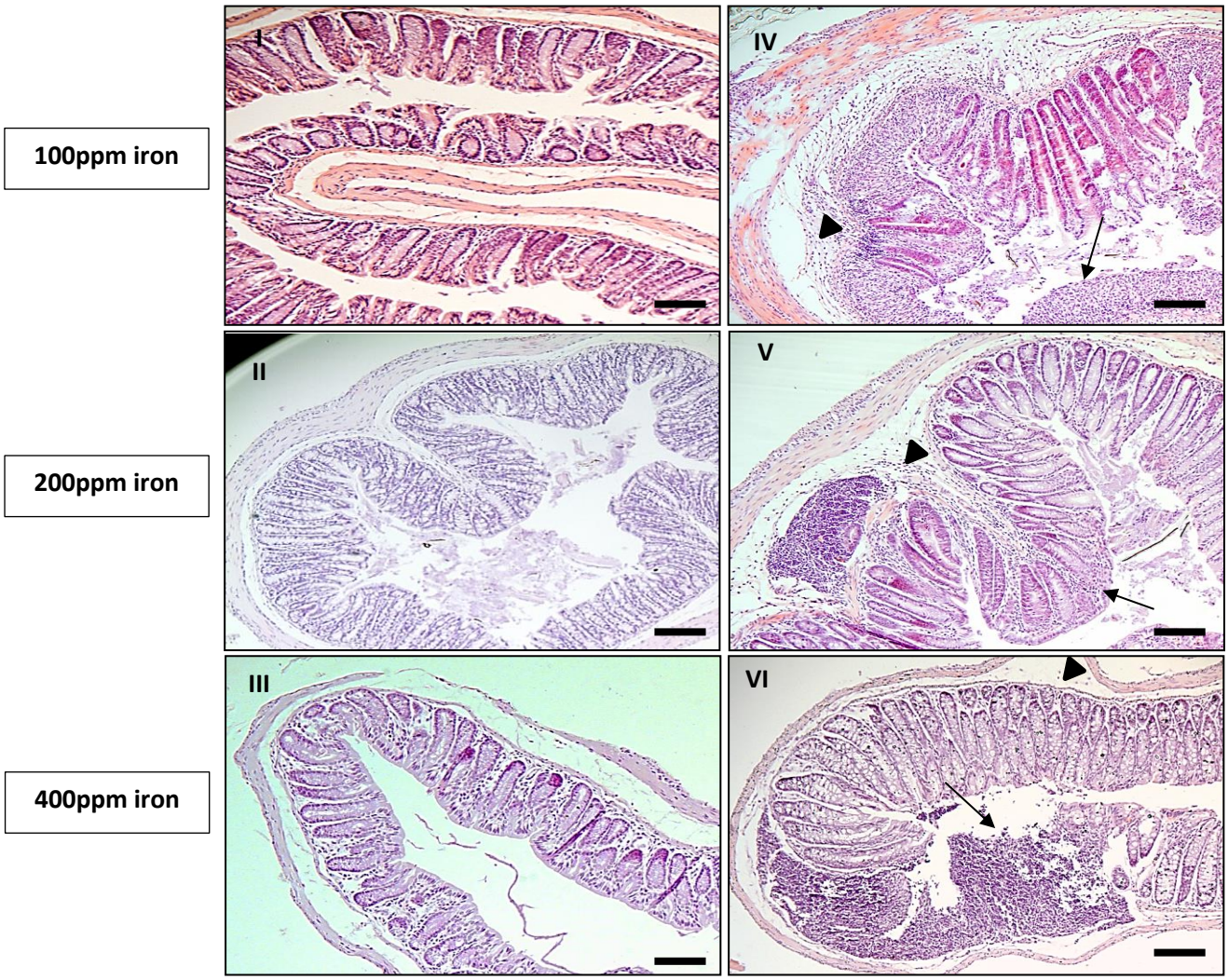

Figure 3-8: Representative H&E-stained sections of distal colon from untreated and 2% DSS-treated mice (6 mice per group). Mice received either water (control) (I, II, III) or 2% DSS for 5 days followed by another 5 days on plain drinking water (IV, V, VI) before all mice were euthanised on day-10. Arrowheads highlight submucosal oedema; arrows highlight almost complete loss of colonic epithelium. (20x magnification).

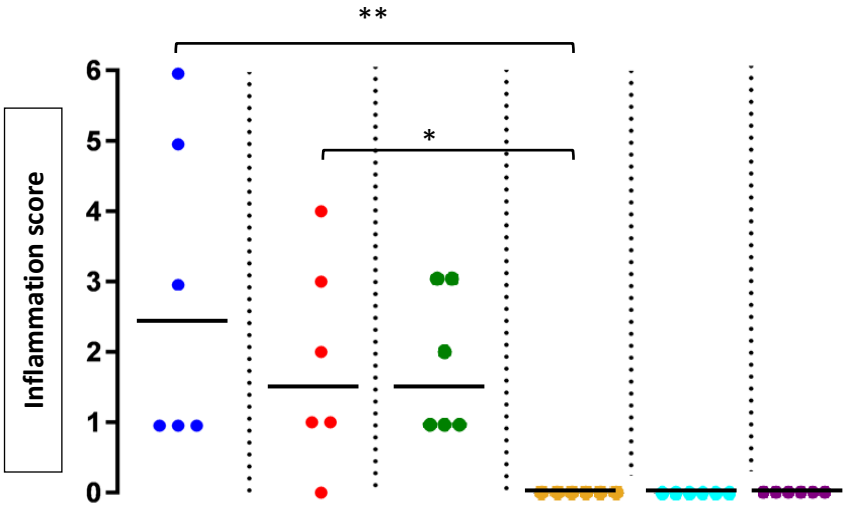

Iron (ppm)	100	200	400	200	100	400
DSS (2%)	+	+	+	-	-	-
Duration (days)	10	10	10	10	28	28

Figure 3-9: Inflammation (colitis) scores for all groups, DSS-treated and untreated (controls) mice on different iron diets. Horizontal lines at the median. Differences tested by One-way ANOVA followed by multiple comparisons Dunn's test. * P<0.05, **P<0.01 (vs. 200ppm iron).

3.3.3 Faecal calprotectin in colitis and its role as an inflammatory marker

Faecal calprotectin is a sensitive and non-invasive biomarker to identify active inflammation in the gastrointestinal tract of IBD patients and to distinguish IBD from irritable bowel syndrome (IBS) [125]. Calprotectin represents about 60% of the neutrophil cytosolic proteins which are present in all body fluids. Its concentration is directly proportional to the amount of neutrophil migration into the intestinal tract (at sites of inflammation) [126].

3.3.3.1 Assessing the degree of gut inflammation at the molecular level by measuring faecal calprotectin in wild-type (C57BL/6) DSS-treated mice during the 10-day course

Faecal calprotectin was measured by an ELISA designed for animals such as mice (S100A8/S100A9 ELISA). Initially, a standard test was performed, and data for 4 parameter logistics were plotted (Figure 3-10).

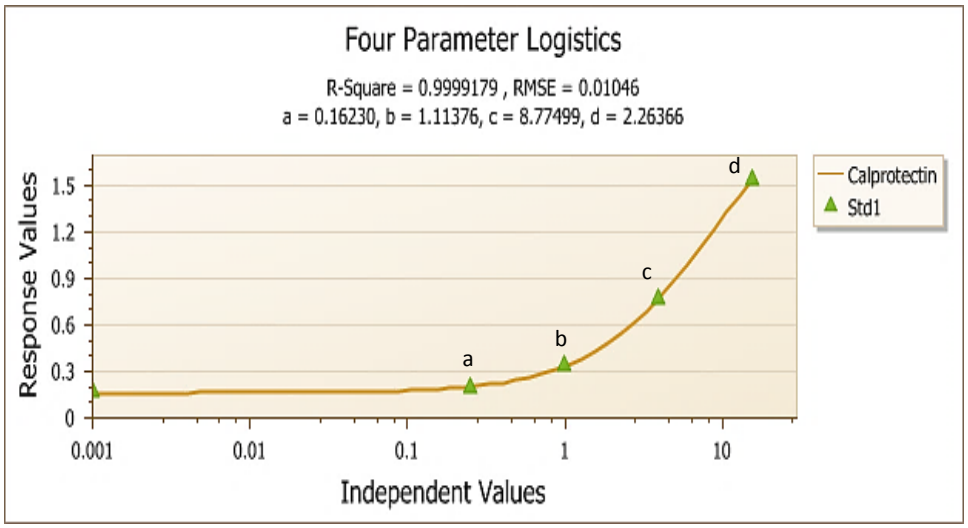

Figure 3-10: Standard curve using MasterPlex ReaderFit Software [(a) the minimum value that can be obtained, (d) the maximum value that can be obtained (i.e. what happens at infinite dose), (c) the point of variation (i.e. the point on the S-shaped curve halfway between a and d) and (b) Hill's slope of the curve (i.e. this is related to the sharpness of the curve at point c)

Faecal pellets (6) were collected from the cage of each mouse in all groups at day-1 and day-10. Faecal calprotectin was measured by the S100A8/S100A9 ELISA kit using 100µl per sample where the final concentration was applied in ng/ml. The difference between samples taken at two different time points, for example at day-1 the start of the diet and DSS treatment and at day-10 after the onset of the experiments, reflects the degree of inflammation in DSS-

treated animals. However, the difference in untreated groups would show the impact of the diet on intestinal cells and their response (Figure 3-11).

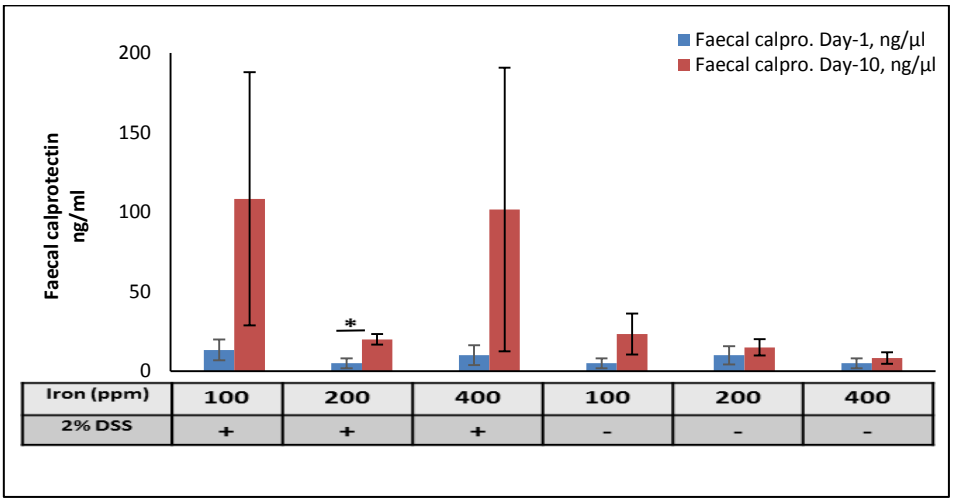

Figure 3-11: Faecal calprotectin concentrations at two different time points (day-1 and 10) for six groups (n=6 mice each), three DSS-treated and three untreated. Data are presented as a mean ± standard error of the mean. Differences were tested by Kruskal–Wallis test followed by multiple comparison Dunn's test. * P<0.05.

The figure shows that the standard iron diet (200ppm iron) for DSS-treated mice resulted in a statistical difference in between day-1 and day-10 (P<0.05). However, low and high iron diet DSS-treated and all untreated mice did not show any significance (Figure 3-11), although the degree of variability between mice was high in some groups.

3.3.3.2 The influence of different iron diets (100 and 400ppm iron) on faecal calprotectin concentration in untreated mice during 28-day course

Faecal pellets were collected at day-1 and day-28 from untreated mice taking low (100ppm iron) and high (400ppm iron) iron diets. The samples were analysed with the same ELISA kit as described above using 100µl per sample. The result showed that there was no significant difference between the two different time points in either group (Figure 3-12).

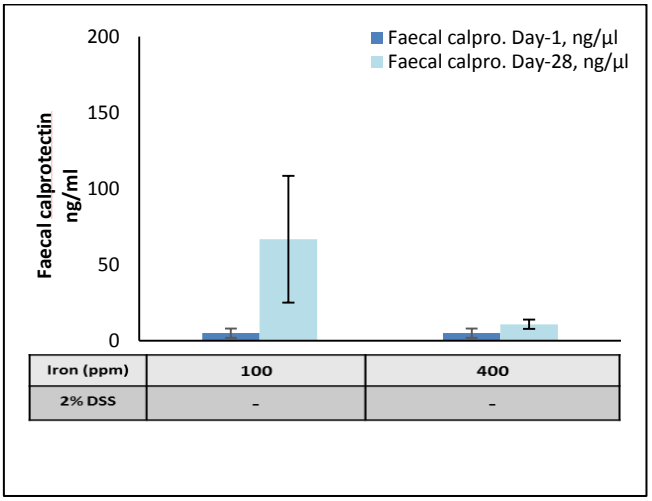

Figure 3-12: Faecal calprotectin concentrations at day-1 and day-28 in two untreated groups (100 and 400ppm iron) 6 mice each. Data are presented as a mean ± standard error of the mean. Differences were tested by Kruskal–Wallis test followed by multiple comparison Dunn's test.

There was no statistical significance found in day-1 vs. day-28 for 100 and 400ppm iron untreated groups (Figure 3-12), although the faecal calprotectin concentration at day-28 in the low iron diet appeared to have increased.

3.3.4 The importance of dietary iron and its effect on intestinal inflammation as well as its impact on the gut microbiota

One possible source of iron to the intestinal microbial community is likely to be excess iron that is not absorbed from the diet. Thus, changes in luminal iron concentrations will potentially have an impact on intestinal microbiome structure [127]. Iron replacement therapy is a common treatment in patients with anaemia and IBD such as Crohn's disease. Oral iron supplements are sometimes less well tolerated, and may also influence intestinal inflammation as well as intestinal microbial community structure and function [93].

3.3.4.1 Total faecal iron concentrations in DSS-treated and untreated mice during 10-day course

Measuring faecal iron concentrations would help to assess the severity of inflammation (bleeding) during colitis. However, it is hard to distinguish between the iron that comes from the diet and that which has been released from RBCs during luminal bleeding during colitis. Therefore, we collected faecal pellets at different time points from each mouse and calculated the total iron (ferric and ferrous) (dietary and bleeding source) and compared the results between groups (treated and untreated). To use the correct amount of samples we initially tested standard curves using three sample concentrations (5, 10 and 20µl), at six different dilutions. The 20µl volume gave the best standard curve (Figure 3-13).

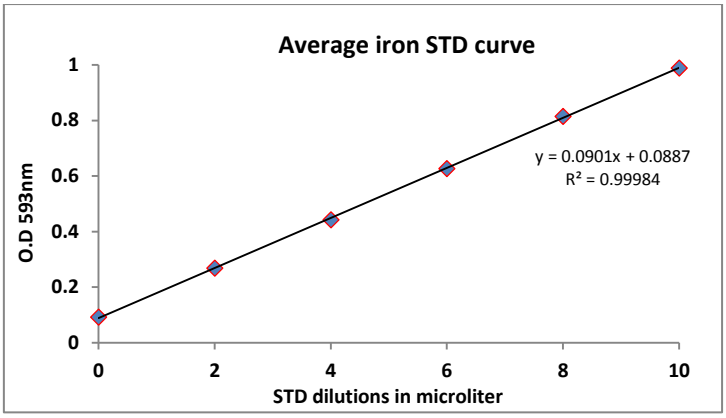

Figure 3-13: Iron standard curve at six dilutions points using 20µl volume of the raw sample

Faecal pellets were collected from the cage of each mouse in all groups at day-1 and day -10. The total faecal iron concentration was measured using an iron immunoassay kit [MAK025, Sigma-Aldrich]. The difference between samples taken at two different time points, day-1 at the start of the diet and DSS treatment and day-10 after the completion of the experiment can reflect colitis severity (luminal bleeding) in DSS-treated animals. However, the difference in untreated groups will show the change in faecal iron as a result of dietary depletion/supplementation (Figure 3-14).

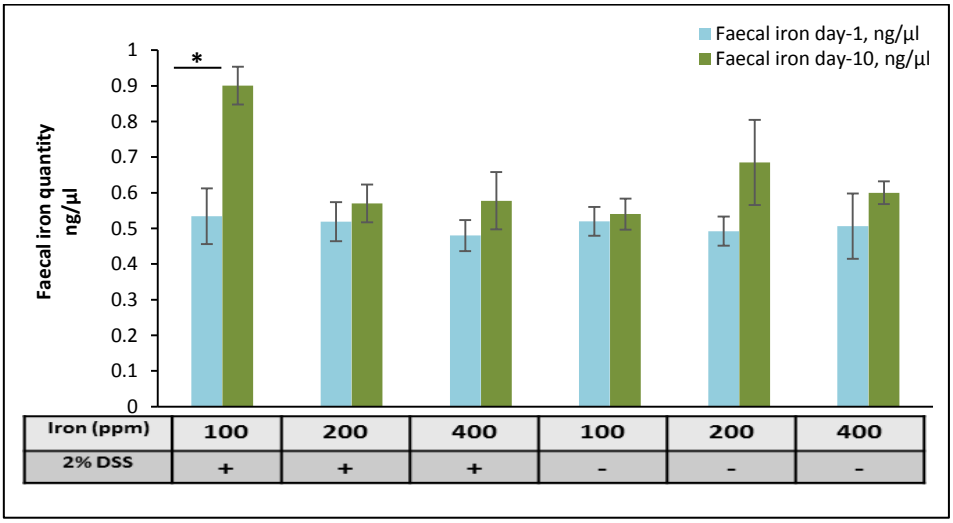

Figure 3-14: Faecal iron concentration at two different time points (day-1 and 10) for six groups (n=6 mice each) three DSS-treated and three untreated. Data are presented as a mean ± standard error of the mean. Differences were tested by Kruskal–Wallis test followed by multiple comparison Dunn's test. * P<0.05.

The 100ppm iron DSS-treated group showed a significant difference (P<0.05) between day-10 and day-1. By contrast, the 200 and 400ppm iron DSS-treated and all untreated groups did not show any statistical differences (Figure 3-14).

3.3.4.2 Total faecal iron concentration in untreated (100 and 400ppm iron) mice during 28-day course

Faecal pellets were also collected at day-1 and day-28 from untreated mice (100 and 400ppm iron) to investigate the effect of iron diet modification on faecal iron concentration. The samples were analysed with the same iron assay kit above using 20µl per sample. The result showed a significant increase (P<0.05) between day-1 and 28 for the 400ppm iron mice (Figure 3-15).

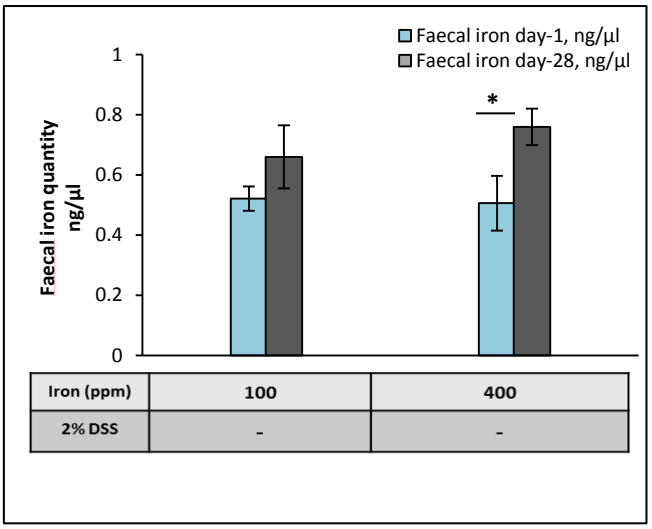

Figure 3-15: Faecal iron concentration at day-1 and day-28 in untreated groups (100 and 400ppm iron) n=6 mice each. Data are presented as a mean ± standard error of the mean. Differences were tested by Kruskal–Wallis test followed by multiple comparison Dunn's test. *P<0.05.

3.4 Investigating the effect of different iron diets during 8-day course of dextran sulphate sodium

The clinical signs [loss of body weight, loose faeces and rectal bleeding] that develop after exposure to DSS for 5 days have been established in previous work. The most weight loss and histological changes were found at day-8 (as it been shown in Figure3-6 and 3-9). In order to confirm results from previous work, four groups of C57BL/6 female 8-9-week-old mice (N=8 per group) were therefore used in a second experiment. Three DSS-treated groups (100, 200 and 400ppm iron) received 2% DSS in their drinking water for 5 days followed by 3 days on plain drinking water. The control group took a 200ppm iron diet and received plain drinking water for all 8-days of the experiment (Figure 3-16).

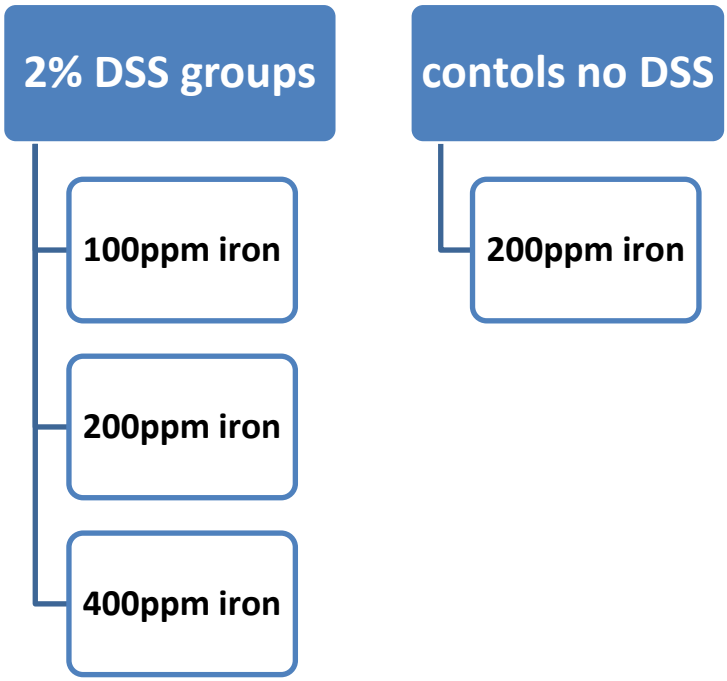

Figure 3-16: Different diet groups with and without DSS treatment during 8-day course

3.4.1 The effect of iron modification diets on the body weight of wild-type mice (C57BL/6) during 8-day period of dextran sulphate sodium (DSS) induced colitis course

The body weight of the DSS-treated mice was recorded daily (8-day course) (Figures 3-17, 3-18 and 3-19). All DSS-treated mice developed colitis and lost weight from day-5 until the day-8, when all animals were culled. The most significant weight loss was recorded for mice on 100ppm iron followed by 400ppm iron and 200ppm iron diets: weight loss was 18%, 14% and 12% of their starting body weight, respectively. However, the (control group) mice on 200ppm iron without DSS treatment showed a steady increase in body weight during the 8-day period (Figure 3-20).

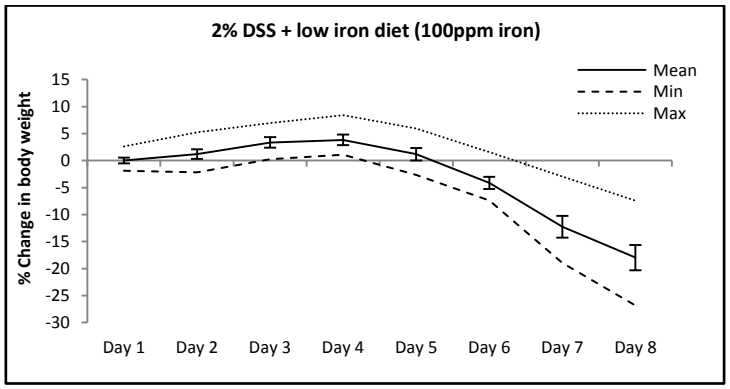

Figure 3-17: Percentage of weight change in mice that received 100ppm iron diet during 2% DSS-induced colitis. Data are presented as mean (solid line) ± standard error of the mean, maximum (dotted line) and minimum (dashed line).

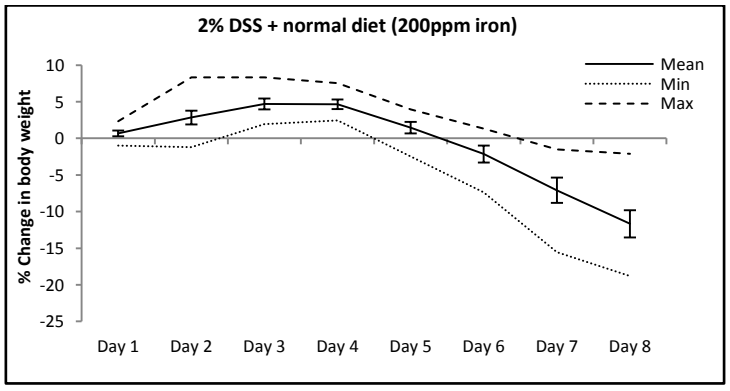

Figure 3-18: Percentage of weight change in mice that received 200ppm iron diet during 2% DSS-induced colitis. Data are presented as mean (solid line) ± standard error of the mean, maximum (dotted line) and minimum (dashed line).

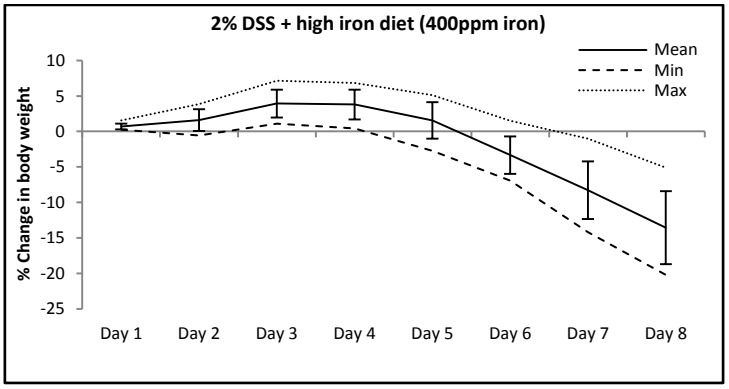

Figure 3-19: Percentage of weight change in mice that received 400ppm iron diet during 2% DSS-induced colitis. Data are presented as mean (solid line) ± standard error of the mean, maximum (dotted line) and minimum (dashed line).

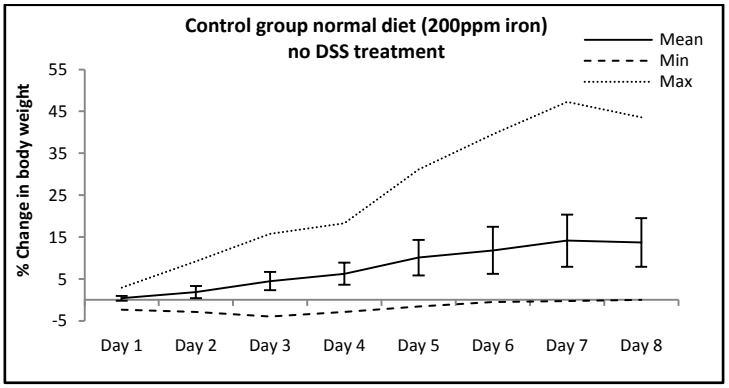

Figure 3-20: Percentage of weight change in mice that received 200ppm iron diet without DSS induction. Data are presented as mean (solid line) ± standard error of the mean, maximum (dotted line) and minimum (dashed line).

All weight changes in each group are summarised in Figure 3-21.

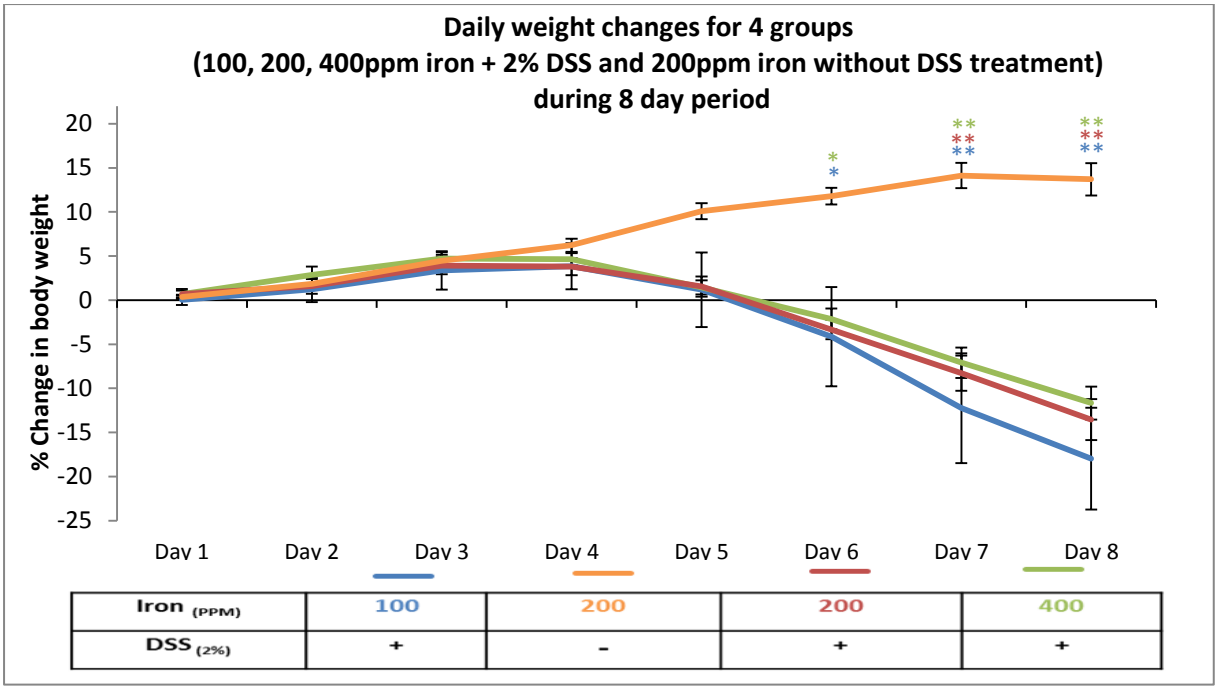

Figure 3-21: Percentage of weight change in mice (100ppm iron (blue), 200ppm iron (red) and 400ppm (green) iron diet) during dextran sulphate sodium-induced colitis and mice receiving 200ppm iron (orange) diet without DSS treatment during the 8-day period. Data are presented as a mean ± standard error of the mean. Statistical differences were assessed by Kruskal– Wallis test followed by multiple comparison Dunn's test (*P<0.05, **P<0.01). (N=8 female mice per group).

3.4.2 100ppm iron and 400ppm iron diet DSS-treated mice displayed more severe colonic inflammation compared with mice on 200ppm iron diet

After 8-days of DSS administration, all mice were killed, and tissues were obtained and processed using the same methods as have been described above. The untreated mice had no features of colitis (Figure 3-22 a). In contrast with this, all mice treated with 2% DSS developed bloody diarrhoea within the 8-day study duration, but again there was no mortality. Histological examination showed DSS-induced colitis, which was mainly located in the distal part of the colon with areas of loss of mucosal architecture and inflammatory cell infiltration (Figure 3-22 b, c and d).

The same scoring method was used as has been described above [91] (Section 3.3.2.1: Table 3-1). All mice treated with DSS showed a significant increase in intestinal inflammation compared with the untreated mice. The low (100ppm iron) iron group had the most severe colitis among all groups.

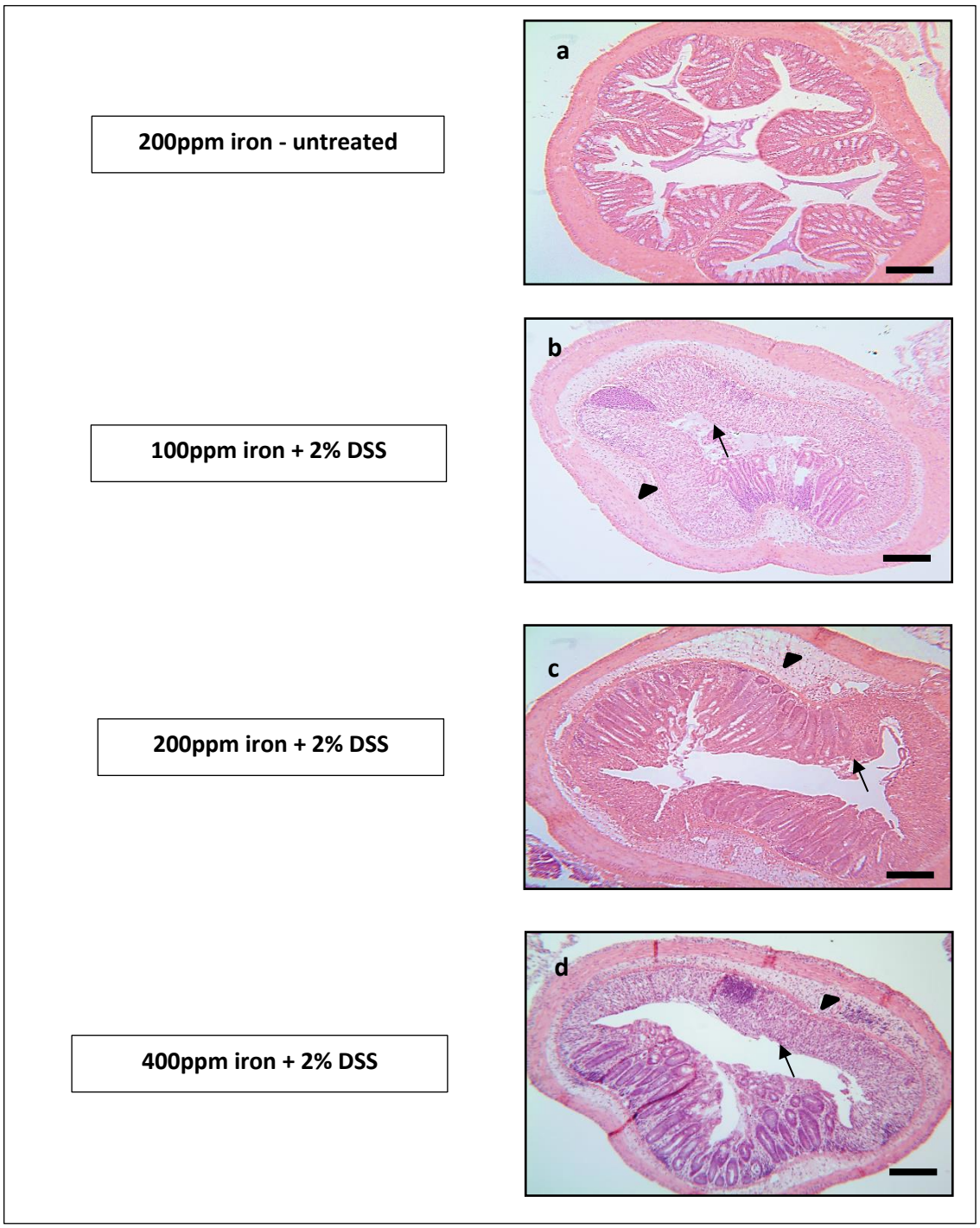

Figure 3-22: Representative H&E-stained sections of distal colon from untreated and 2% DSS-treated mice (8 mice per group). Mice receiving either water (control) (a) or 2% DSS for 5 days and followed by another 3 days on plain drinking water (b, c, d) before all mice were sacrificed on day-8. Arrowheads indicate submucosal oedema; arrows indicate almost complete loss of colonic epithelium. (20x magnification).

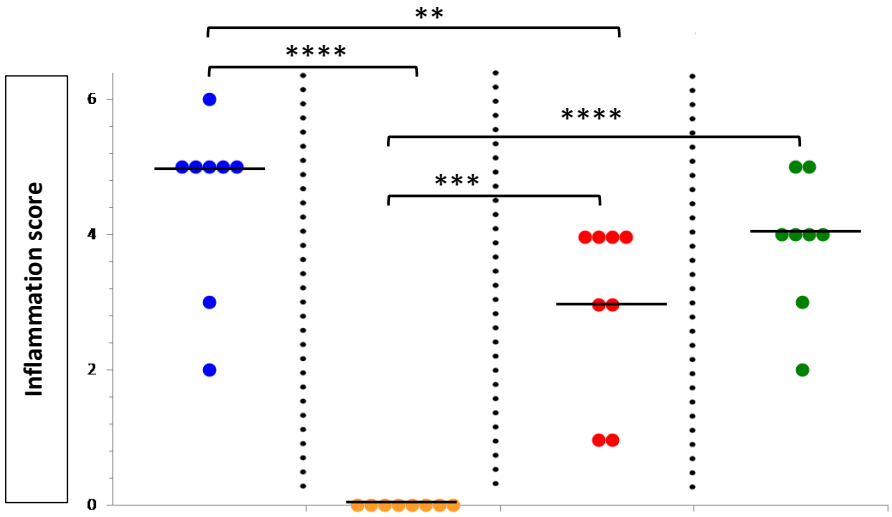

Iron (ppm iron)	100	200	200	400
DSS (2%)	+	-	+	+

Figure 3-23: Inflammation (colitis) scores for all DSS-treated mice and untreated (controls) mice. Horizontal lines at the median. The score of low (100ppm iron) iron DSS mice was significantly worse than that 200ppm iron DSS-treated mice, whereas all DSS-treated mice were statistically significantly different compared to untreated mice. Differences tested by Kruskal-Wallis followed by multiple comparisons. ** P<0.01, *** P<0.001, **** P<0.0001 versus control (200ppm iron).

3.4.3 Assessing the degree of gut inflammation by measuring faecal calprotectin in wild-type (C57BL/6) DSS-treated and untreated mice during the 8-day course

Faecal calprotectin was measured using the S100A8/S100A9. Once again, a standard test was run, and 4 parameter logistics were plotted (Figure 3-24).

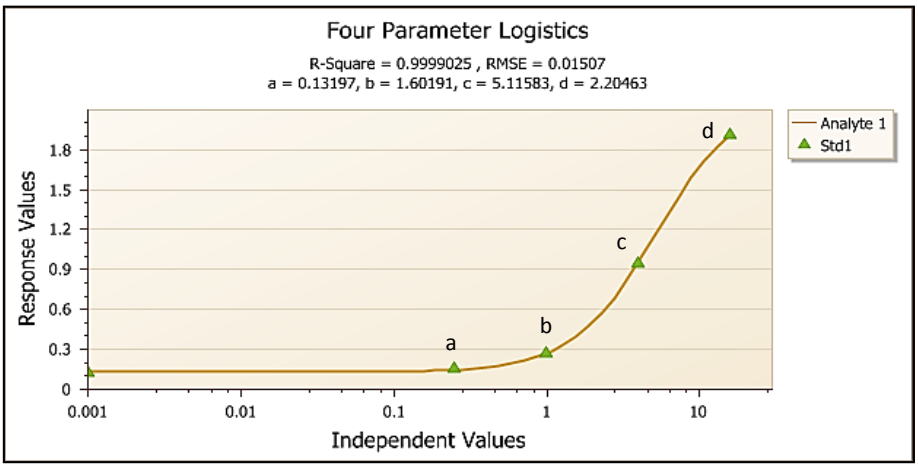

Figure 3-24: Standard curve using MasterPlex ReaderFit Software [(a) the minimum value that can be obtained, (d) the maximum value that can be obtained (i.e. what happens at infinite dose), (c) the point of variation (i.e. the point on the S-shaped curve halfway between a and d) and (b) Hill's slope of the curve (i.e. this is related to the sharpness of the curve at point c).

Faecal pellets were collected from the cages of each mouse in all groups at day-1 and day-8. The difference between samples taken at two different time points, day-1 at the start of the diet and DSS treatment and day-8, when mice were euthanised, can reflect the degree of inflammation in DSS-treated animals. However, the difference in untreated mice used as control will explain the dietary effects of standard diet (200ppm iron) on intestinal cells and their response as it is shown in Figure 3-25.

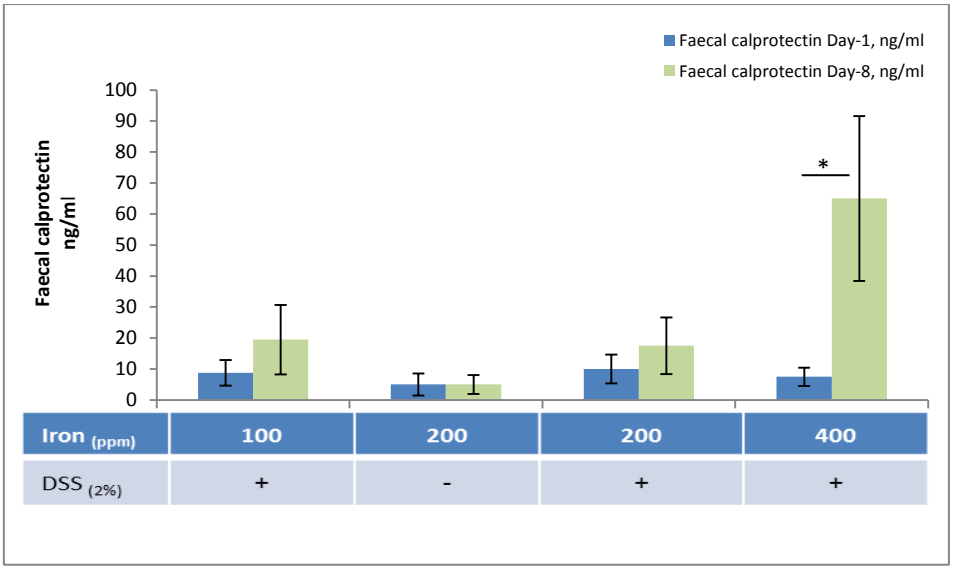

Figure 3-25: Faecal calprotectin concentrations at two different time points (day-1 and 8) for four groups of mice (n=8 each) three DSS-treated and one untreated. Data are presented as a mean ± standard error of the mean. Differences were tested by Kruskal– Wallis test followed by multiple comparison Dunn's test. * P<0.05.

The high iron diet (400ppm iron) DSS-treated mice showed a statistical difference in faecal calprotectin concentration between day-1 and day-8 (P<0.05). However, the low (100ppm iron) and standard (200ppm iron) iron diet DSS-treated mice and 200ppm iron untreated mice did not show any significant difference between these two time points (Figure 3-25).

3.4.4 Measurement of total faecal iron concentration in DSS-treated and untreated mice during 8-day course

Faecal iron concentrations were measured using the same kit [MAK025, Sigma-Aldrich] and technique as described above. A new standard curve was created (Figure 3-26).

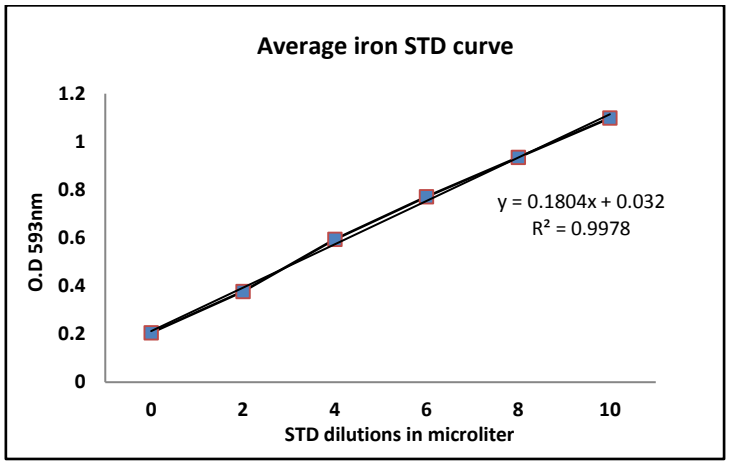

Figure 3-26: Iron standard curve at six dilution points using 20µl volume of the raw sample.

Faecal pellets were collected from the cages of each mouse in all groups at day-1 and day-8. The difference between samples taken at two different time points, day-1 at the start of diet and DSS treatment and day-8 where mice were euthanised can reflect colitis severity (luminal bleeding) in DSS-treated animals. However, any difference in untreated mice can be used as a control as illustrated in Figure 3-27.

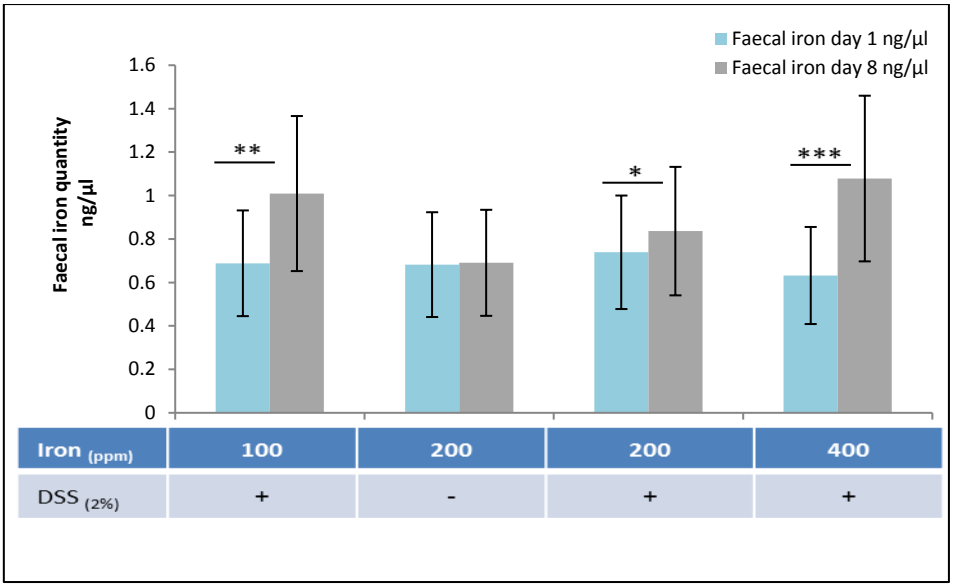

Figure 3-27: Faecal iron concentration at two different time points (day-1 and 8) for four groups of mice (n=8 each) three DSS-treated and one untreated control. Data are presented as a mean ± standard error of the mean. Differences were tested by Kruskal– Wallis test followed by multiple comparison Dunn's test * P<0.05, ** P<0.01, *** P<0.001.

The 400ppm iron DSS-treated group showed the highest significant difference (P<0.001) between day-8 and day-1 readings. The 100ppm iron and 200ppm iron DSS groups also showed significant differences (P<0.01 and P<0.05 respectively). However, the untreated group did not show any significant difference between the two times points tested (Figure 3-27).

3.5 The influence of iron modifications on weight changes in DSS-treated mice

A larger third study was subsequently performed to validate the findings from all previous preliminary experiments (changes in luminal iron exacerbates colitis mainly for low iron group). Therefore, 14 groups of 4 mice (female wild-type C57BL/6 mice aged 8-9 weeks) were individually housed and divided into two bigger sets of seven groups each. Set 1 consisted of Groups (A and E) containing mice on a 100ppm iron diet; Groups (B and F) contained mice on 200ppm iron diet and Groups (C and G) consisted of mice on a 400ppm iron diet. All these mice received 2% DSS treatment. The control Group (D) were given only distilled water and 200ppm iron diet (for 10-days). Set 2 was a repeat of set 1 with the experiment being conducted two weeks later (see Figure 3-28). DSS groups A, B and C were treated with 2% DSS for 5 days followed by another 5 days on normal drinking water and were euthanised at day-10. Groups E, F and G were treated with 2% DSS for 5 days followed by 3 days on normal drinking water only and were euthanised at day-8.

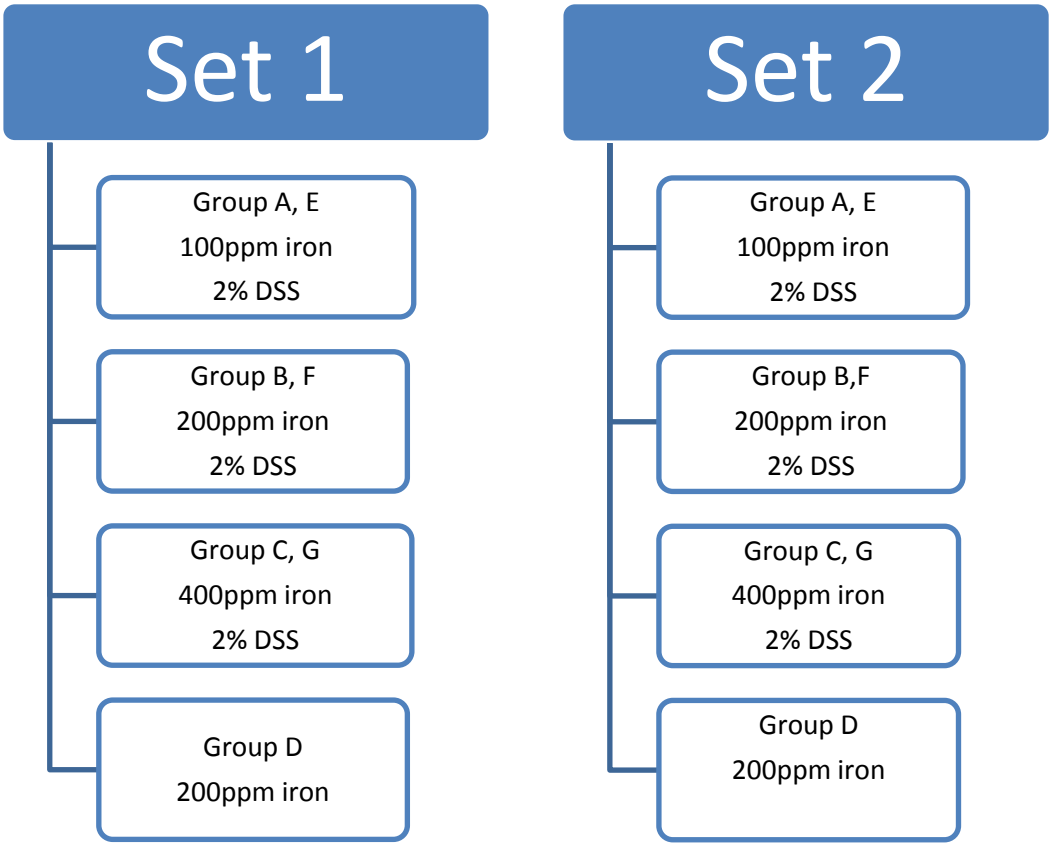

Figure 3-28: Classification of all animal experiments (DSS-treated and control groups). 14 groups of mice 4 mice per group. Two sets; 1 and 2 each consisted of 7 groups of mice. 4 groups underwent a 10-days DSS experiment and 3 groups underwent an 8-days DSS experiment. Group D received no DSS.

As mentioned in the paragraph above, each set of animal groups was experimented upon separately. Two weeks later the second experiment started. All data and results were combined (set 1 and 2) and the final data analysis and results are presented in the following pages.

3.5.1 The effect of different iron diets on the body weight of wild-type C57BL/6 mice treated with dextran sulphate sodium (DSS) during a 10-day course

The body weight of the DSS-treated mice was recorded daily (Figures 3-29). All DSS-treated mice developed colitis. Weight loss was seen from day-6 and was most significant at day-8, especially for group A (100ppm iron) (Figure 3-29).

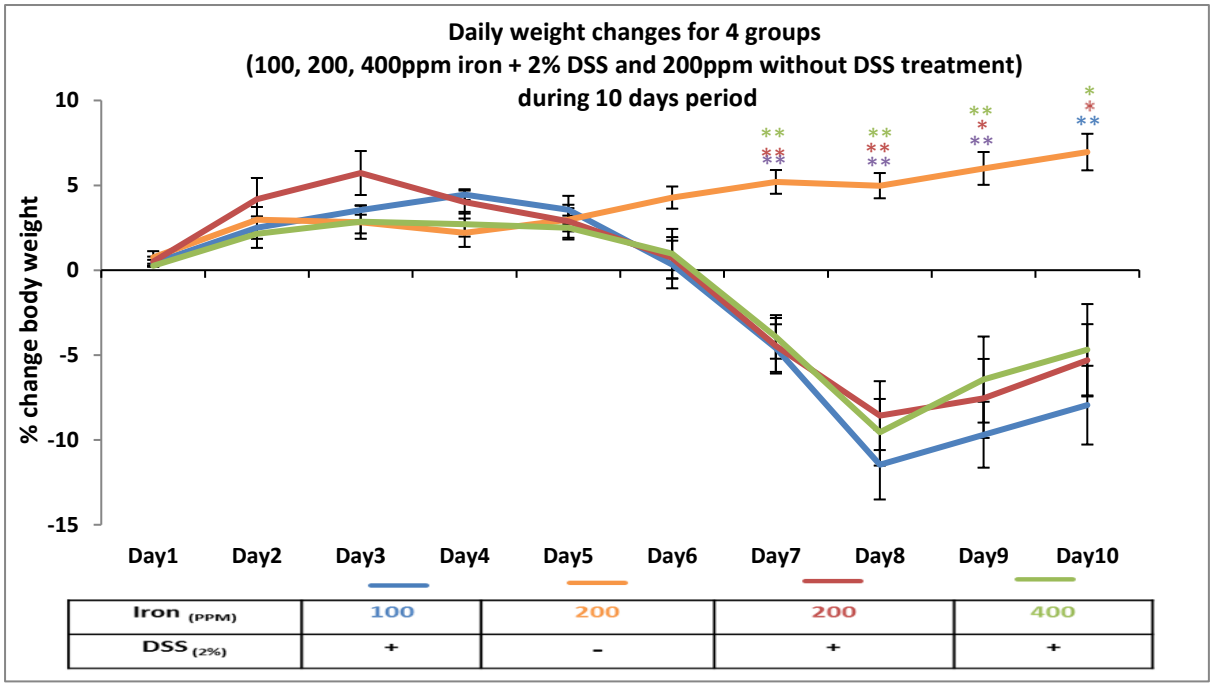

Figure 3-29: Percentage of weight change in mice (100ppm iron (blue), 200ppm iron (red) and 400ppm iron (green)) during dextran sulphate sodium-induced colitis and mice receiving 200ppm (orange) iron diet without DSS treatment during the 10-day period. Data are presented as a mean ± standard error of the mean. Statistical differences were assessed by Kruskal–Wallis test followed by multiple comparison Dunn's test (*P<0.05, **P<0.01) (N=8 female mice per group).

3.5.2 The effect of different iron diets on the body weight of wild-type C57BL/6 mice treated with dextran sulphate sodium (DSS) during an 8-day course

The most significant weight loss was recorded for mice on 100ppm iron followed by 400ppm iron and 200ppm iron-diets with 14%, 12% and 11% loss, respectively. As expected, the control group, consuming 200ppm iron without DSS treatment, showed a steady increase in body weight during the same 8-day period (Figure 3-30).

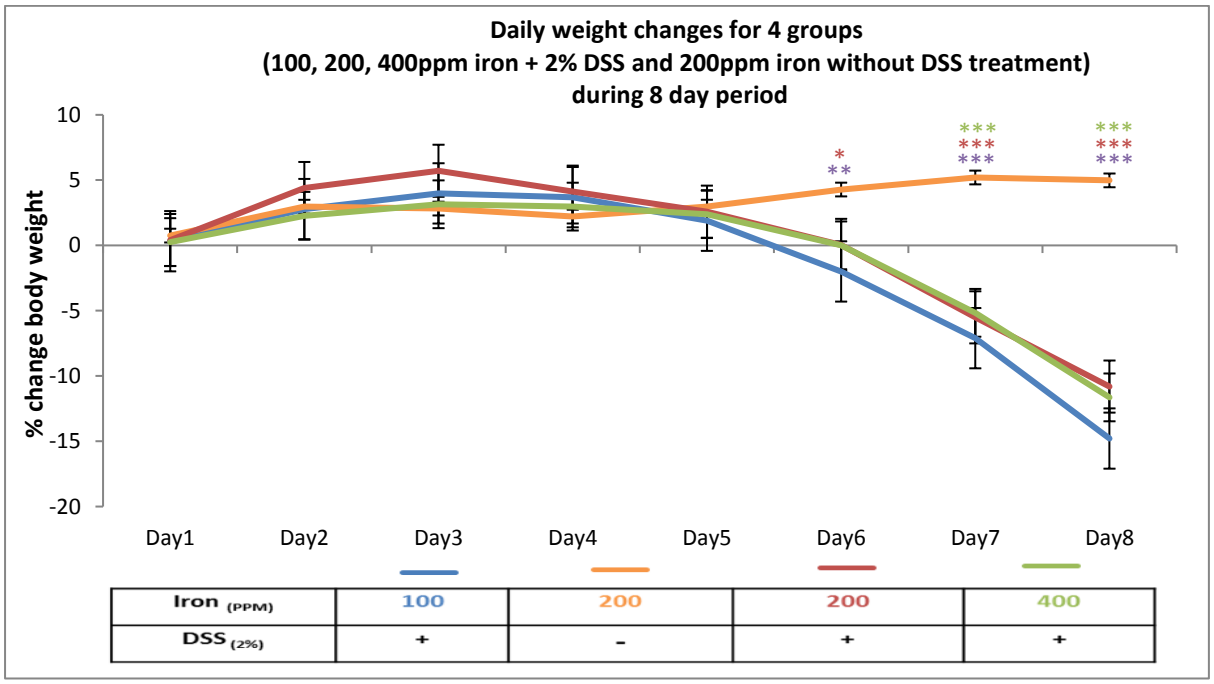

Figure 3-30: Percentage of weight change in mice (100ppm iron (blue), 200ppm iron (red) and 400ppm iron (green)) during dextran sulphate sodium-induced colitis and mice receiving 200ppm (orange) iron diet without DSS treatment during the 8-day period. Data are presented as a mean ± standard error of the mean. Statistical differences were assessed by Kruskal–Wallis test followed by multiple comparison Dunn's test (*P<0.05, **P<0.01, ***P<0.001). (n=8 female mice per group).

3.5.3 100ppm iron diet DSS-treated mice displayed severe colonic inflammation compared with mice on 200ppm iron diet for 10-day course treatment

After 10-days of DSS administration, tissues were harvested at necropsy following carbon dioxide euthanasia and were processed as described above. The slides were inspected by light microscopy, and in untreated mice, the distal colon showed no features of colitis (Figure 3-31 II). On the other hand, all the mice that had been treated with 2% DSS developed bloody diarrhoea within the 10-days' study duration. Again, there was no mortality. Histological examination established the presence of DSS-induced colitis, with areas of loss of mucosal architecture and inflammatory cell infiltration (Figure 3-31 I, III and IV).

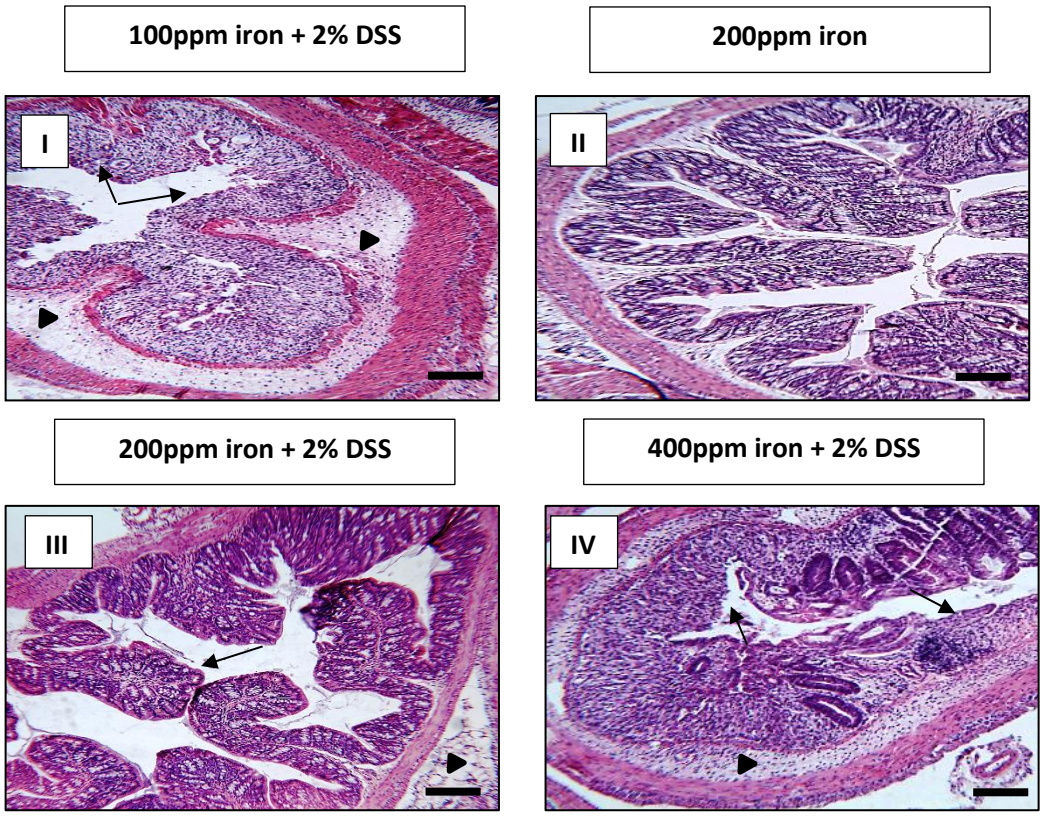

Figure 3-31: Representative H&E-stained sections of distal colon from untreated and 2% DSS-treated mice (8 mice per group). Mice received either water (control) (II) or 2% DSS for 5 days, and this was followed by another 5 days on plain drinking water (I, II and IV) before all mice were killed on day-10. Arrowheads highlight submucosal oedema; arrows highlight almost complete loss of colonic epithelium. (20x magnification).

Using the histological inflammatory scoring system (Table 3-1) [91], H and E stained slides were scored in a blinded fashion by the researcher (Figure 3-32). Histological damage was scored using the criteria of Bauer [91], which considers the loss of mucosal architecture and cellular infiltration (maximum score = 6).

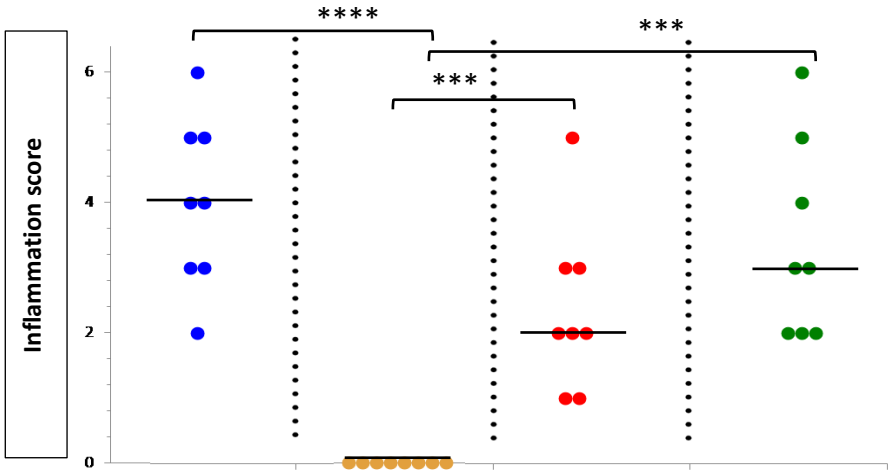

Iron (ppm iron)	100	200	200	400
DSS (2%)	+	-	+	+

Figure 3-32: Inflammation (colitis) scores for all groups DSS- treated and untreated (controls) mice on different iron diets (10-day course). Horizontal lines at the median. Differences tested by One-way ANOVA followed by multiple comparisons Dunn's test. *** P<0.001, **** P<0.0001 versus control (200ppm iron).

All DSS-treated mice showed significant differences compared with the untreated mice. Again, the 100ppm iron DSS-treated group showed the most marked difference compared to controls (P<0.0001).

3.5.4 100ppm iron diet DSS-treated mice displayed more severe colonic inflammation compared with mice on 200ppm iron diet for 8-day course of treatment

After 5-days of DSS administration and 3 days on normal drinking water, all mice were euthanised, and tissues were obtained and stained (H&E) using the same method mentioned previously. The slides were inspected by light microscopy and again the untreated mice distal colon showed no features of colitis (Figure 3-33 II). On the other hand, all the mice that had been treated with 2% DSS developed bloody diarrhoea. Histological examination showed the presence of DSS-induced colitis, with areas of loss of mucosal architecture and inflammatory cell infiltration (Figure 3-33 I, III and IV).

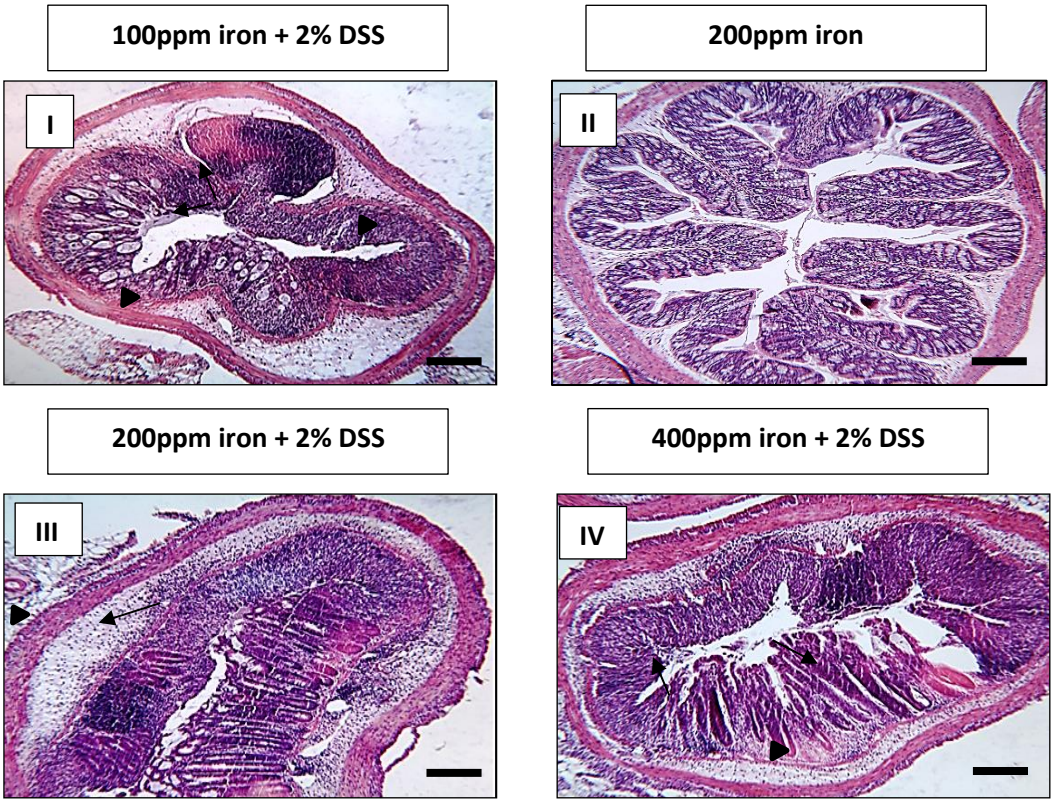

Figure 3-33: Representative H&E-stained sections of distal colon from untreated and 2% DSS-treated mice (8 mice per group). Mice received either water (control) (II) or 2% DSS for 5 days followed by another 3 days on plain drinking water (I, II and IV) before all mice were euthanised on day-8. Arrowheads highlight submucosal oedema; arrows highlight almost complete loss of colonic epithelium. (20x magnification).

Using the histological inflammatory scoring system (Table 3-1) [91], H and E stained slides were scored in a blinded fashion by the researcher (Figure 3-34). Histological damage was again scored using the criteria of Bauer [91], which considers the loss of mucosal architecture and cellular infiltration (maximum score = 6).

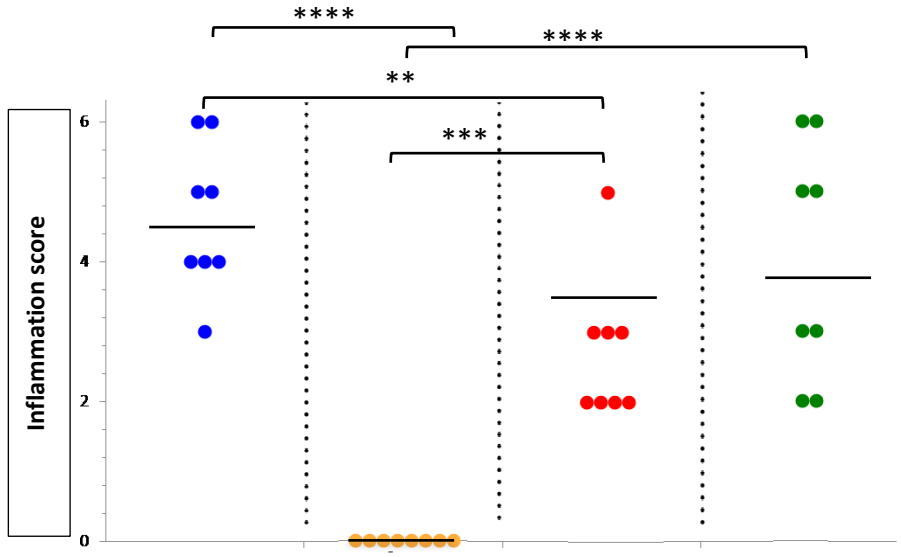

Iron (ppm iron)	100	200	200	400
DSS (2%)	+	-	+	+

Figure 3-34: Inflammation (colitis) scores for all groups DSS-treated and untreated (controls) mice on different iron diets (8-day course). Horizontal lines at the median. Differences tested by Kruskal– Wallis test followed by multiple comparisons Dunn's test. ** P<0.01, *** P<0.001, **** P<0.0001 versus control (200ppm iron).

All DSS-treated groups showed statistically significant differences vs. 200ppm iron DSS-untreated group. Interestingly, the 100ppm iron DSS-treated mice also showed a significant difference (P<0.01) compared with the 200ppm iron DSS-treated group.

3.5.5 Assessing the degree of gut inflammation at the molecular level by measuring faecal calprotectin concentrations in DSS-treated and untreated mice during 10 and 8-day experiments

All identically treated groups from each animal set (1 and 2) were combined to make the total number of samples per group as follows: DSS- treated groups' 16 samples at day-1 and day-8 then 8 samples at day-10 (each group). However, the untreated controls only had 8 samples at days-1, 8 and 10. Faecal calprotectin as with all previous work was measured using the S100A8/S100A9 ELISA kit.

Faecal pellets were collected from the cages of each mouse in all groups at days-1, 8 and 10. The difference between samples taken at three different time points, day-1 at the start of diet and DSS treatment and days-8 and 10 when mice were killed can reflect the level of colitis in DSS-treated animals. However, any difference in untreated groups will explain the dietary effects on gut response as illustrated in Figure 3-35.

In mice treated with DSS, faecal calprotectin concentrations were increased significantly at day-8 with each DSS-treated group. However, in those mice receiving 100 and 400ppm iron the difference in each case was $P<0.001$ (day-1 vs. day-8), whereas for mice receiving 200ppm iron $P<0.05$ (day-1 vs. day-8). No significant difference over time was observed in the untreated group as illustrated in (Figure 3-35).

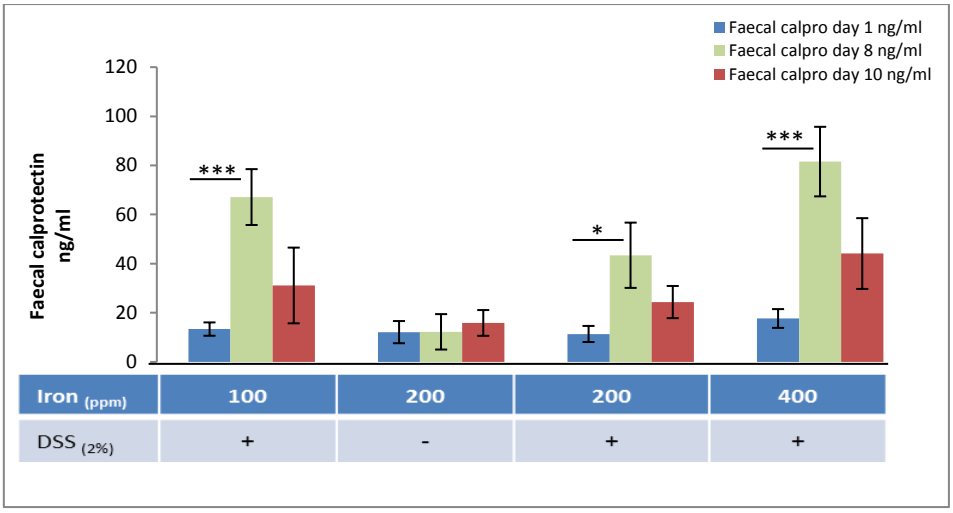

Figure 3-7: Faecal calprotectin at three different time points (day-1, 8 and 10) for n=16 mice each of the three DSS-treated and n=8 mice of the untreated group. Data are presented as a mean ± standard error of the mean. Differences were tested by Kruskal– Wallis test followed by multiple comparison Dunn's test. * P<0.05, *** P<0.001.

Further analysis compared all groups together at individual time points namely at days-1, 8 and 10. There were no any significant differences between the groups at day-1 and 10. However at day-8 the 400ppm iron (P<0.001) and 100ppm iron (P<0.01) DSS-treated groups were significantly different from the 200ppm iron untreated mice (Figure 3-36).

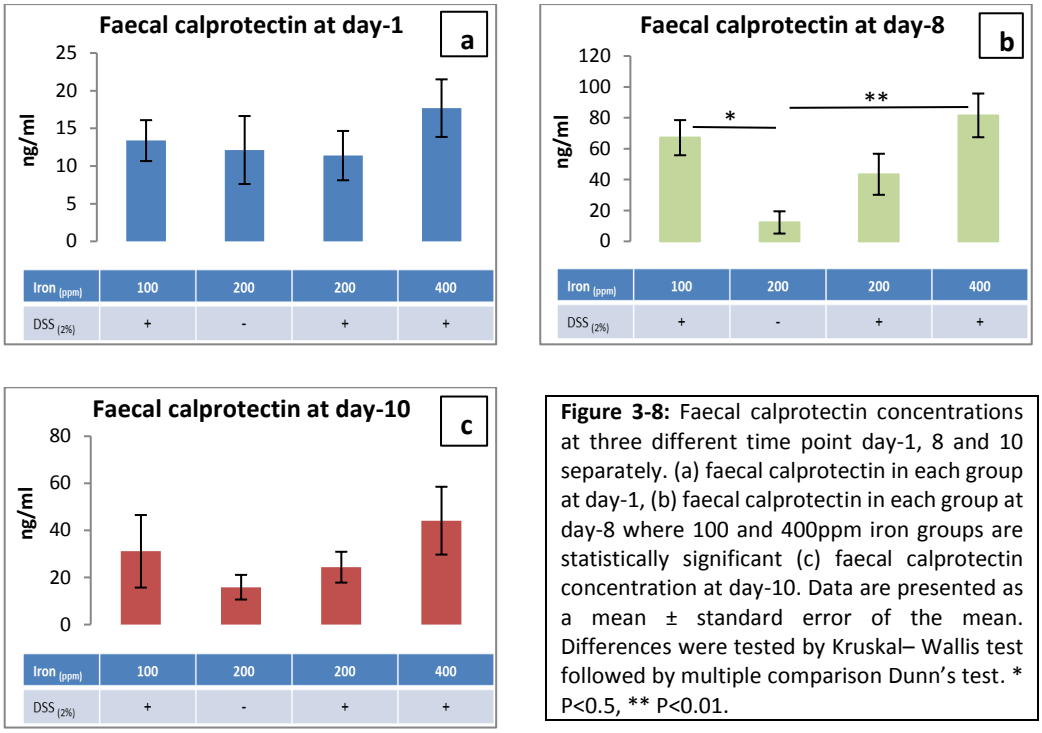

Figure 3-8: Faecal calprotectin concentrations at three different time point day-1, 8 and 10 separately. (a) faecal calprotectin in each group at day-1, (b) faecal calprotectin in each group at day-8 where 100 and 400ppm iron groups are statistically significant (c) faecal calprotectin concentration at day-10. Data are presented as a mean ± standard error of the mean. Differences were tested by Kruskal– Wallis test followed by multiple comparison Dunn's test. * P<0.5, ** P<0.01.

3.5.6 Measurement of total faecal iron concentration in DSS-treated and untreated mice during 10- and 8-day experiments

All identical groups from each animal set (1 and 2) were combined to make the total number of samples per group as follows: DSS-treated groups 16 samples at days-1 and 8 then 8 samples at day-10. Untreated controls had 8 samples at days-1, 8 and 10. The total faecal iron concentration was again measured using the iron immunoassay kit [MAK025, Sigma-Aldrich] where the final concentration was applied in ng/µl. Faecal pellets were collected from the cages of each mouse in all groups at day-1, 8 and day-10. To use the correct amount of sample a standard curve was run with every kit.

The difference between samples taken at three different time points on day-1 at the start of diet and DSS treatment and on days-8 and 10 when mice were euthanised can reflect colitis severity (luminal bleeding) in DSS-treated animals. However, any difference in untreated groups will explain the dietary effects of iron on gut response as illustrated in Figure 3-37.

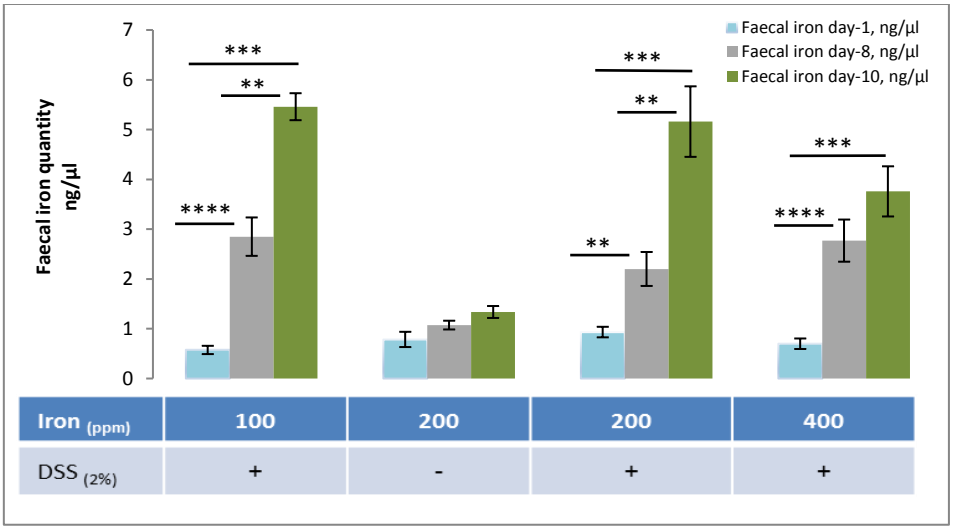

Figure 3-37: Faecal iron concentration at three different time points (day-1, 8 and 10) for four groups n=16 mice each for the three DSS-treated and n=8 mice for the untreated group. Data are presented as a mean ± standard error of the mean. Differences were tested by Kruskal– Wallis test followed by multiple comparison Dunn's test. ** P<0.01, *** P<0.01 **** P<0.0001.

Total faecal iron concentration was significantly increased in all DSS-treated mice compared to baseline at both 8 and 10-days. The highest significance in the 100 and 400ppm iron groups occurred at day-1 vs. day-8 (P<0.0001), whereas, for 200ppm iron DSS-treated mice the most significant difference was at day-1 vs. day-10 (P<0.001) (Figure 3-37).

Further analysis compared all the groups at individual time points. At day-1 no significant difference was found, whereas at day-8 there was a similar difference ($P<0.05$) for both low and high iron (100 and 400ppm iron) DSS groups versus 200ppm iron untreated mice (Figure 3-38). However, at day-10, total faecal iron concentration showed the same significant difference ($P<0.05$) for all DSS-treated mice versus untreated controls (Figure 3-38).

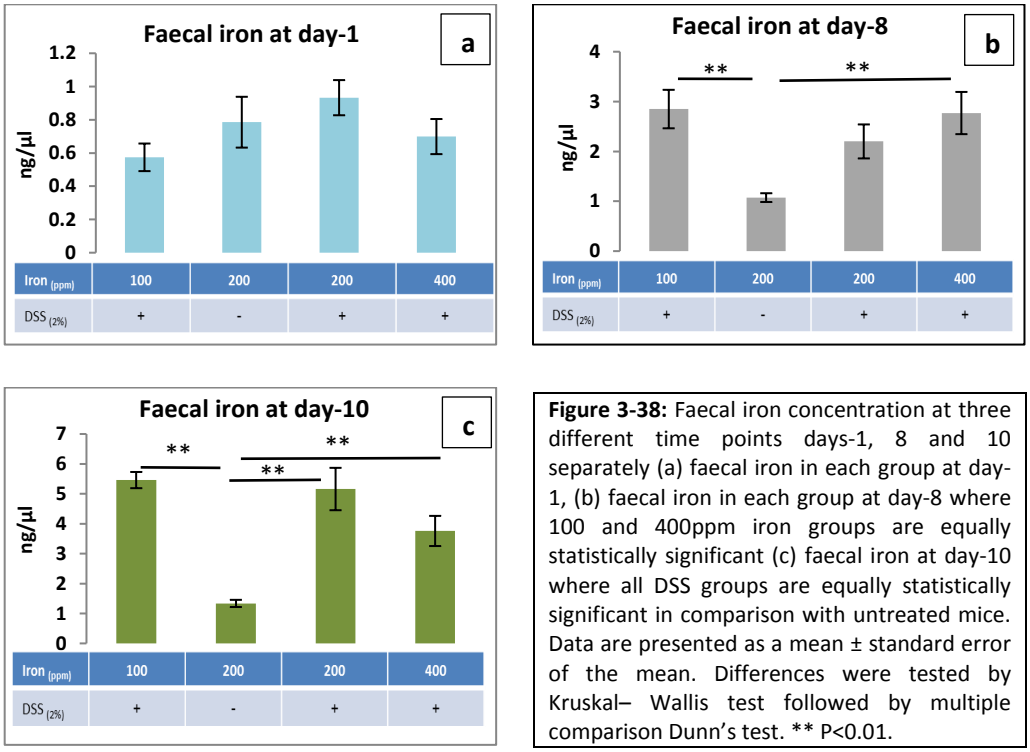

Figure 3-38: Faecal iron concentration at three different time points days-1, 8 and 10 separately (a) faecal iron in each group at day-1, (b) faecal iron in each group at day-8 where 100 and 400ppm iron groups are equally statistically significant (c) faecal iron at day-10 where all DSS groups are equally statistically significant in comparison with untreated mice. Data are presented as a mean ± standard error of the mean. Differences were tested by Kruskal– Wallis test followed by multiple comparison Dunn's test. ** $P<0.01$.

3.6 Discussion

Our hypothesis investigated whether that luminal iron can cause changes in gut microbiota in IBD patients as well as influence the nature of colitis. Data from this research shown that oral consumption of dextran sulphate sodium (DSS) (2%) in drinking water induced colitis in wild-type C57BL/6 female mice, whereas changing the oral iron intake influenced the severity of colitis induced. However, DSS-treated mice lost body weight starting from day-6 and reaching the maximum body weight loss at day-8 predominantly for mice that received 100ppm iron than the other groups. In addition, high iron diet (400ppm iron group) came second after low iron mice in terms of exacerbated colitis. While untreated mice gained weight, Indeed control mice consuming the most iron gained the most weight. These observations agree with the findings of a study by Carrier *et al.* which emphasised the role of iron in changing inflammation, which appeared to be dependent on the amount of iron consumed, however, Carrier did not investigate low dose iron in her work [93].

In the current study, any disruption of the intestinal mucosa or extensive infiltration by inflammatory cells was measured by a histological inflammatory scoring system (Table 3-1) [91]. The mice that received low iron diets (100ppm iron) showed more inflammation regarding mucosal ulceration, cellular infiltration and oedema within the lamina propria. This is also consistent with the previous study by Erichsen *et al.* which demonstrated that low-dose oral ferrous fumarate in rats with DSS-induced colitis increased intestinal inflammation [128].

In colitis, calprotectin is released by neutrophils that infiltrate inflamed tissues, raising faecal calprotectin levels [129]. In the present study, all DSS-treated mice showed rises in faecal calprotectin concentrations by day-10, but this was only significant in the 200ppm iron group. However, when assessed at day-8, all DSS-treated groups showed more calprotectin at day-8 vs. day-1, ($P<0.001$ for 100 and 400ppm iron and $P<0.05$ for 200ppm iron). This supports the view that both low and high doses of iron exacerbate the severity of DSS-colitis.

Total faecal iron concentration was measured for all groups and compared at three different time points (days-1, 8 and 10). DSS-treated groups showed significant differences in total faecal iron levels between day-1 vs. day-8 and day-10 for each group individually. However, 100 and 400ppm iron DSS groups showed a greater significance at day-8 ($P<0.0001$) than the 200ppm iron group ($P<0.01$). However, at day-10 all DSS-treated mice had similar changes ($P<0.001$ for each group). This emphasises the contribution of bleeding to faecal iron loss: the amount of faecal iron was raised even in mice receiving 100ppm iron. The only controls that showed statistically significant differences were the 400ppm iron group with $P<0.05$.

To conclude, in the present study, changes (increases or decreases) in the amounts of dietary iron appeared to enhance colonic inflammation in a DSS mouse model of inflammatory bowel disease. There appeared to be synergistic effects between iron and DSS on colonic inflammation and calprotectin levels. Inflammation, as well as oral iron increased faecal iron concentrations [127]. This can explain the paradox in the low iron group where luminal bleeding during colitis caused an increase in the faecal iron concentration despite low levels of iron in the diet.

4 The influence of iron on gut microbial composition in a 10-day DSS-induced colitis experiment in wild-type C57BL/6 mice

4.1 Introduction

Inflammatory bowel disease (IBD) is associated with alterations in gut microbial communities and dysregulated mucosal immune responses [74]. The vertebrate microbiota is extremely variable, especially at the lower taxonomic ranks. Although there are four dominant phyla*:* *Firmicutes*, *Bacteroidetes*, *Actinobacteria* and *Proteobacteria,* the *Firmicutes* and *Bacteroidetes* comprise >90% of the bacterial inhabitants in the colon, whereas *Actinobacteria* and *Proteobacteria* (*Enterobacteriaceae*) are present at 1%–5% [65].

In patients with IBD, there is a reduction in microbial diversity and enhancement of some bacteria from the family *Enterobacteriacea*e and a decline in bacteria from the phyla *Bacteroidetes* and some *Firmicutes* [68]. The mechanisms responsible for the development of this dysbiosis and its contribution to IBD are not well defined. Thus, defining which aspects of the gut microbiome change during relapse and remission may provide significant information with therapeutic potential.

Murine models of IBD offer an opportunity to investigate bacteria and their pathways implicated in IBD and host–microbiota responses to treatments. This can be difficult to investigate in humans due to several factors such as genetic diversity and variability in environmental and treatment exposures [130]. However, dysbiotic microbiota can induce murine colitis [131].

To identify approaches that promote and preserve beneficial intestinal microbes, a series of studies of the microbial community in colitis, with diets containing different amounts of iron, were undertaken as follows:

1- Mice were treated with DSS dissolved in their drinking water, for 5 days, to induce colitis, followed by a recovery period, see Methods chapter.

2- Dietary iron consumption was manipulated, see Methods chapter.

3- Microbial DNA was prepared from the stool collected and was homogenised in stool stabiliser [PSP® Spin Stool DNA Plus Kit], for details on DNA extraction, see Methods chapter.

4- 16S rRNA gene sequencing was performed: operational taxonomic unit (OTU) selection, microbial composition and community structure analyses and metagenome inference were undertaken in collaboration with CGR, see Methods chapter.

5- Finally, statistical analysis in this chapter was undertaken by using the STatistical Analysis of Metagenomic Profiles (STAMP) software package for analysing metagenomic profiles, such as phylogenetic profiles. This represents the number of indicator genes allocated to different taxonomic units or functional outlines representing the number of sequences assigned to various subsystems or pathways [132].

4.2 Aims

The aims were to:

1- Analyse gut microbial communities following treatment of mice with DSS alongside dietary interventions (100, 200 and 400ppm iron).

2- Investigate the effects of longer supplementation with various iron diets on the gut microbial structure.

4.3 Bioinformatic and Statistical analysis of metagenomic profiles

Initial processing and quality assessment of the sequence data was performed using an in-house (CGR) pipeline. Briefly, basecalling and de-multiplexing of indexed reads was performed by CASAVA version 1.8.2 (Illumina) to produce 71 samples from the single flow cell, in fastq format. The raw fastq files were trimmed to remove Illumina adapter sequences using Cutadapt version 1.2.1 (Martin, 2011). The option "-O 3" was set, so the 3' end of any reads which matched the adapter sequence over at least 3 bp was trimmed off. The reads were further trimmed to remove low quality bases, using Sickle version 1.200 with a minimum window quality score of 20. After trimming, reads shorter than 10 bp were removed. If both reads from a pair passed this filter, each was included in the R1 (forward reads) or R2 (reverse reads) file. If only one of a read pair passed this filter, it was included in the R0 (unpaired reads) file. Figure 4-1 summarise the read counts before and after adapter and quality trimming. Figure 4-2 shows the read length distributions after adapter and quality trimming.

Later analysis used only R1 and R2 reads. Both Figures 4-1 and 4-2 indicate that only few samples matched to the expected number of reads, and that many samples should be excluded from the analysis. In particular, any samples with less than 100 read pairs were excluded from the analysed dataset.

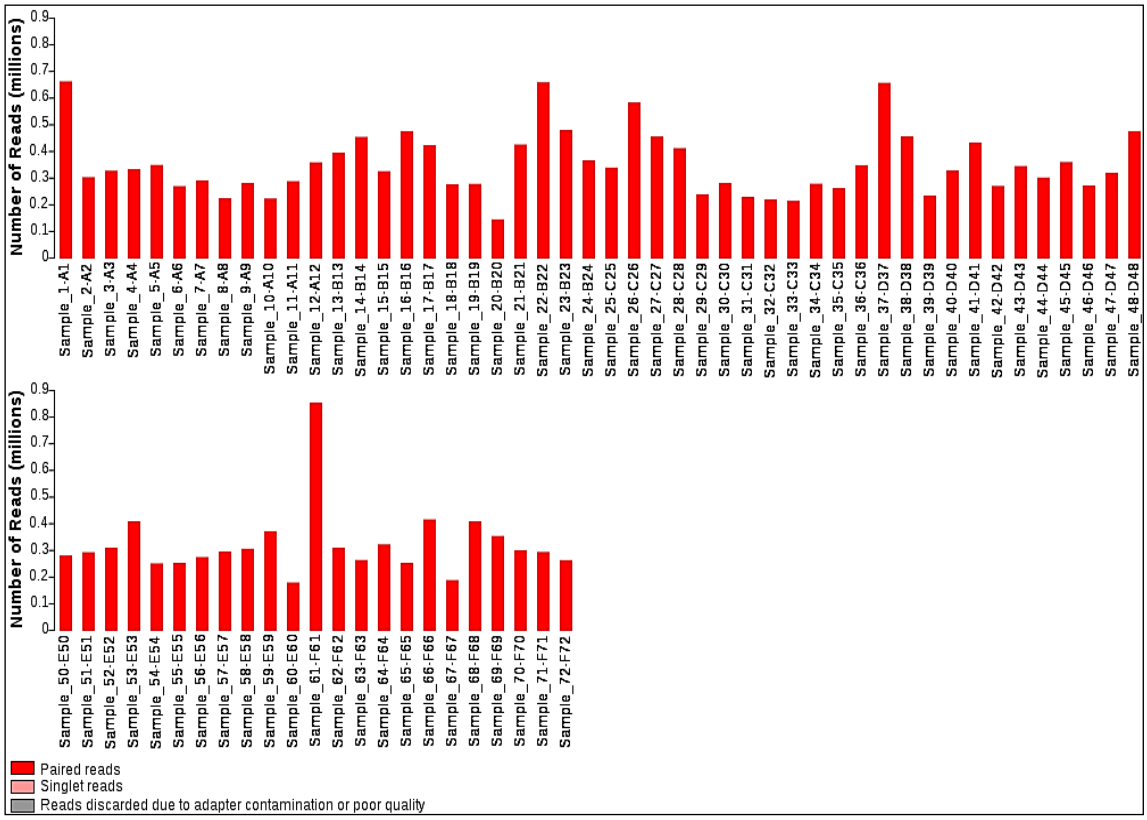

Figure 4-1: Diagram illustrating the total number of reads obtained for each sample.

Note: all samples identifications are listed in appendix 10-1

Figure 4-2: Box plot showing the distribution of trimmed read lengths for the forward (R1), reverse (R2) and singlet (R0) reads. Note that it is common for a small number of reads to consist of mostly adapter-derived sequence, so it is expected that the distribution will show a long tail. **(All samples identifications are listed in appendix 10-1)**

For the bioinformatic analysis of microbiota data, Welch's t-test was used in each group to compare day-1 vs. day-10. The false discovery rate (FDR) (multiple correction tests) was used to produce a prioritised list of OTUs that summarise observed differences between two user-defined populations. The q-value is the adjusted p-value based on FDR calculation, where statistical significance was declared at $P<0.05$.

In this chapter, we investigated the effects of different iron diet interventions on colitis status and gut microbial structure in wild-type mice. Using 16S ribosomal RNA (rRNA) gene surveys, we analysed gut microbial communities pre- and post-treatment with 2% DSS (100, 200 and 400ppm iron) groups. Also, three control groups, fed 100-, 200- and 400-ppm iron from the start day of the experiment until the day of euthanasia, were studied (Section 3.3, Chapter 3).

4.3.1 Bacterial diversity data analysis at phylum level (Summary and plot of the taxonomic content of each sample)

The community composition of each sample for a given taxonomic rank (from Kingdom to Species) was summarised using Qiime. From these summaries, bar plots were generated. An example of such a bar plot, showing the relative abundance of different phyla among the samples, as it been shown in Figure 4-3.

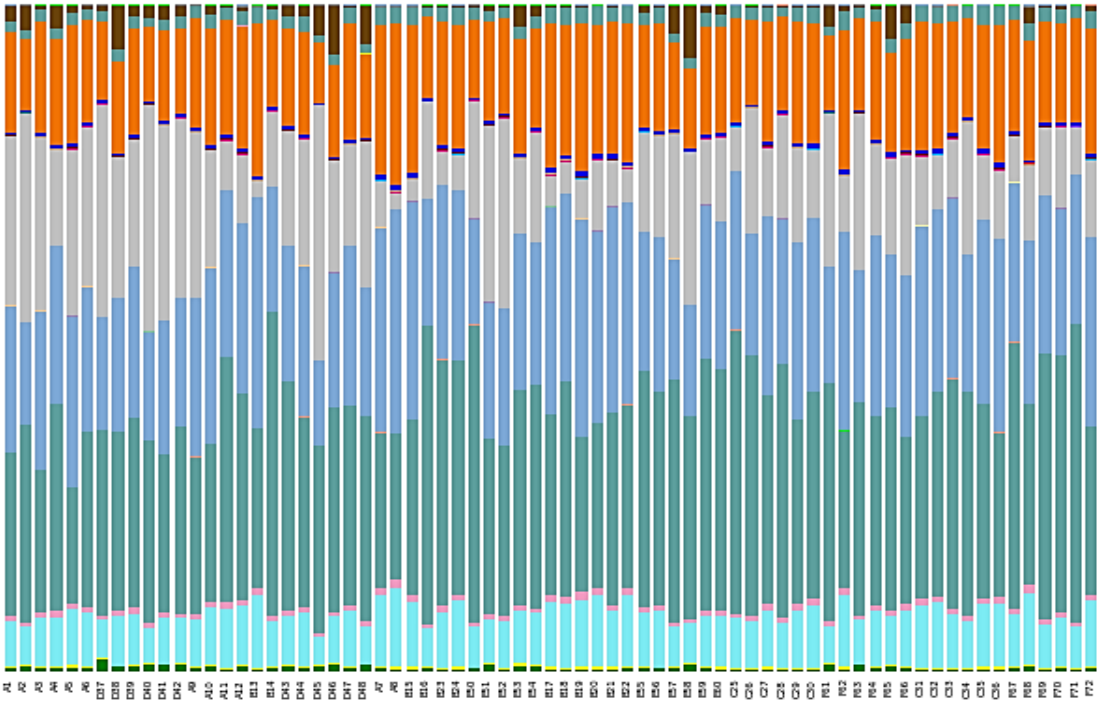

Figure 4-3: Phylum-level taxonomic composition of all samples (relative abundance).
Note: all samples identifications are listed in appendix-1 and legend in appendix -2

4.3.1.1 Alpha diversity estimation and alpha rarefaction analyses

To negate the effect of sample size and to estimate species richness within each sample (alpha diversity), OTU tables were repeatedly sub-sampled (rarefied). For each rarefied OTU table, three measures of alpha diversity were estimated: chao1, the observed number of species, and the phylogenetic distance. These estimates were plotted as rarefaction curves using Qiime (Figures 4-4,-5 and -6 show the rarefaction plot).

Chao1

Chao1 is a nonparametric estimator that predicts the minimum species richness of a sample.

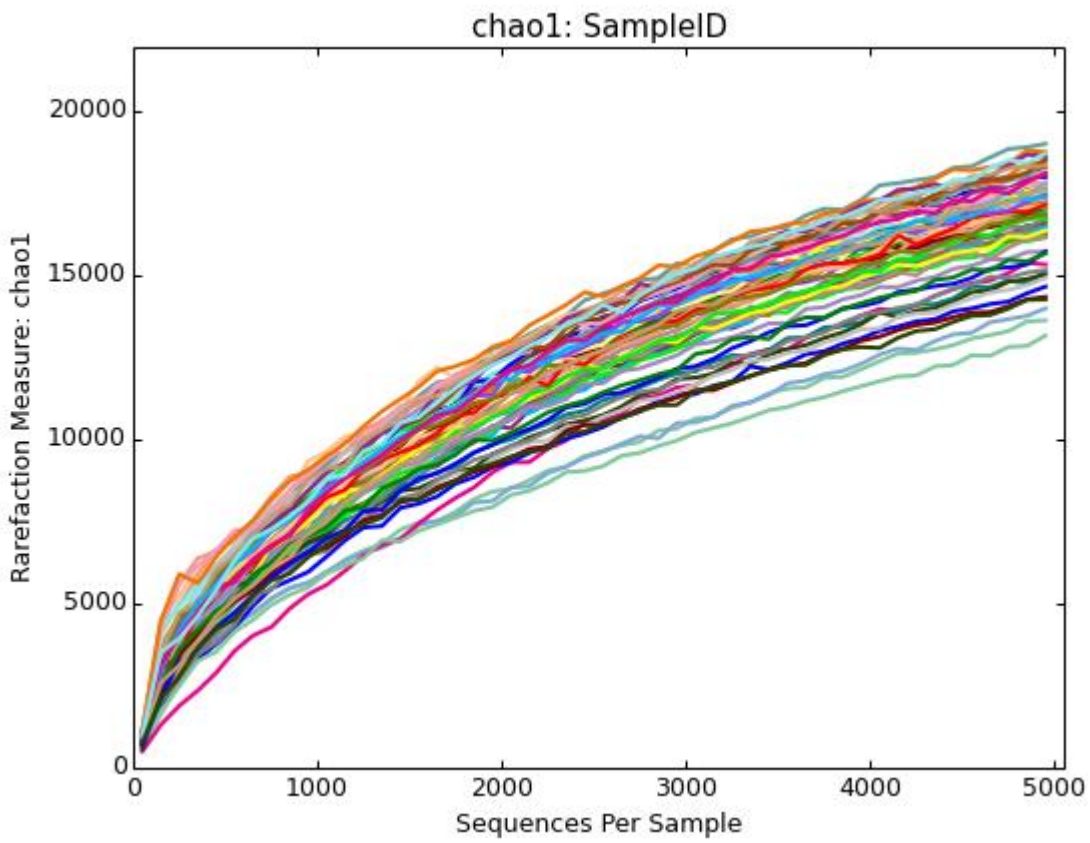

Figure 4-4: Rarefaction curves of the observed number of species metric for all samples (> 500 reads). The plot shows the average number of distinct OTUs found in sub-samples of increasing number of sequences.

Observed species

The observed number of species is defined as the number of distinct OTUs within a sample.

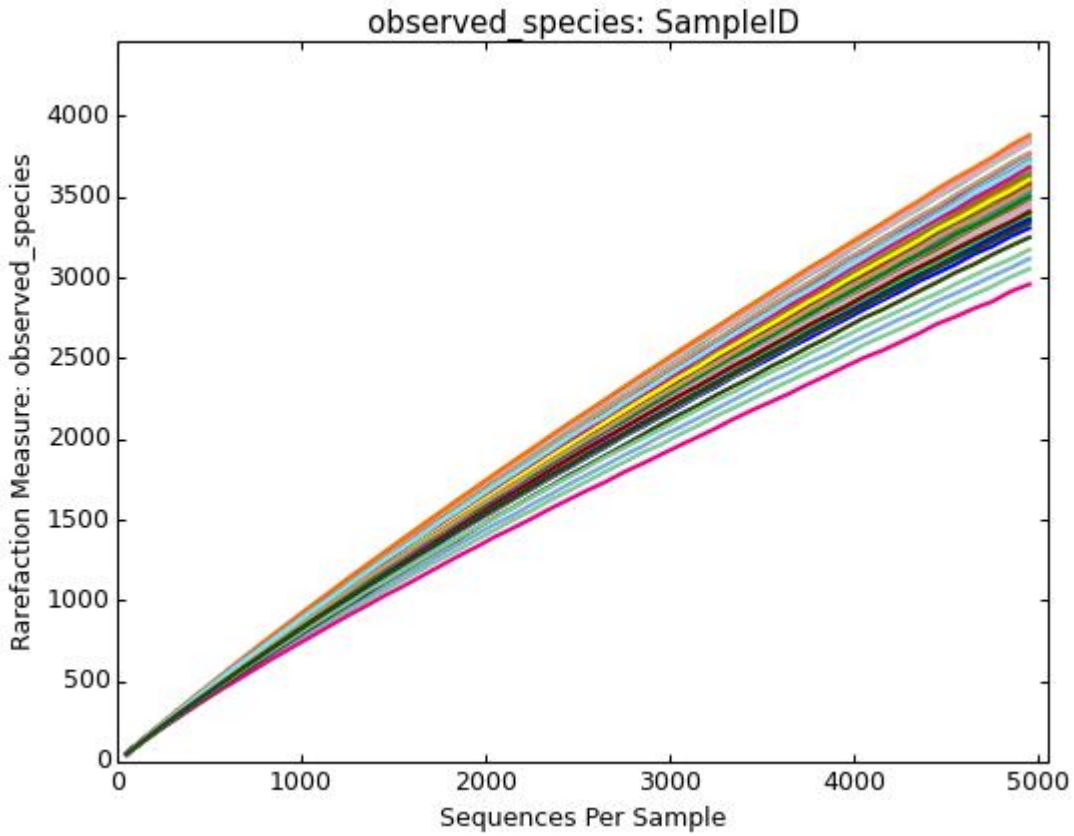

Figure 4-5: Rarefaction curves of the observed number of species metric for all samples (> 500 reads). The plot shows the average number of distinct OTUs found in sub-samples of increasing number of sequences.

PD (phylogenetic diversity)

The PD metric represents the minimum total branch length that covers all taxa within the sample on a phylogenetic tree (Faith *et. al., 1992*). A smaller PD value therefore indicates a reduced expected taxonomic diversity whilst a large PD value indicates a higher expected diversity.

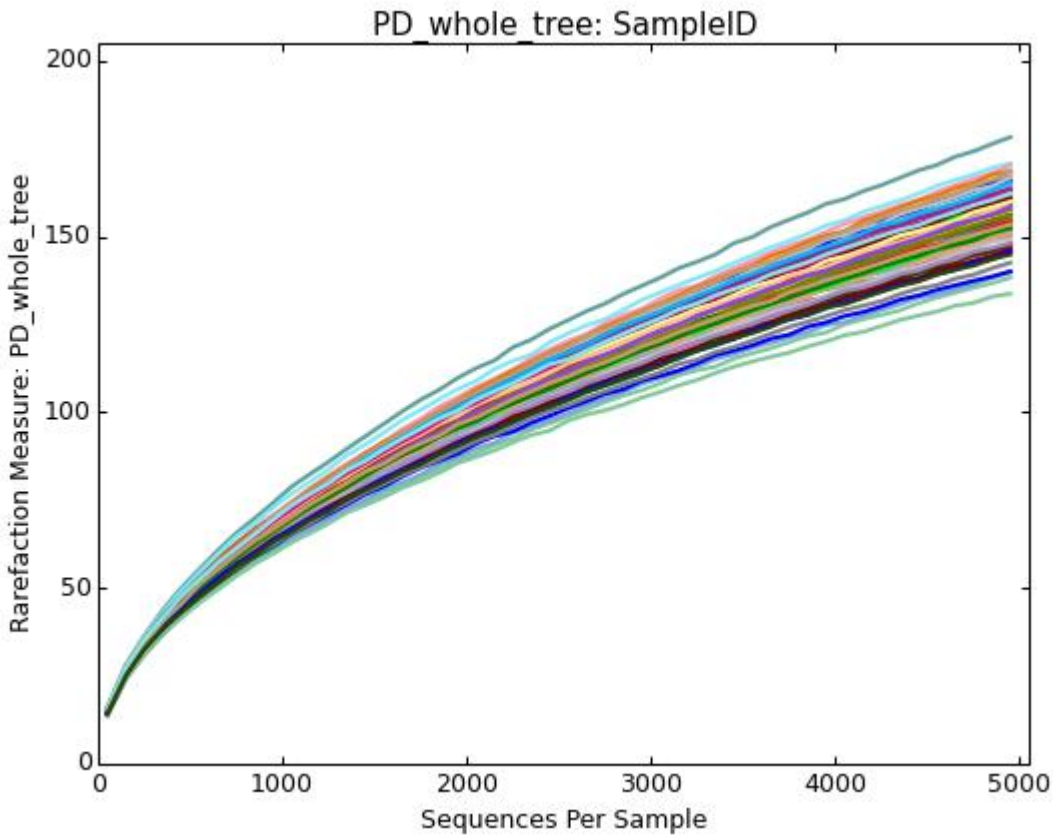

Figure 4-6: Rarefaction curves of the PD metric represents the minimum total branch length that covers all taxa within the sample on a phylogenetic tree. The plot shows the average number of distinct OTUs found in sub-samples of increasing number of sequences.

4.3.1.2 Estimate beta diversity, generate UPGMA trees and 2D PCoA plots

To allow inter-sample comparisons (beta-diversity), all datasets were sub-sampled (rarefied) using the Qiime script. Rarefied OTU tables were used to calculate weighted and unweighted pair-wise UniFrac matrices using Qiime. UniFrac matrices were then used to generate UPGMA (Unweighted Pair-Group Method with Arithmetic mean) trees and 2D principal coordinates plots (PCoA).

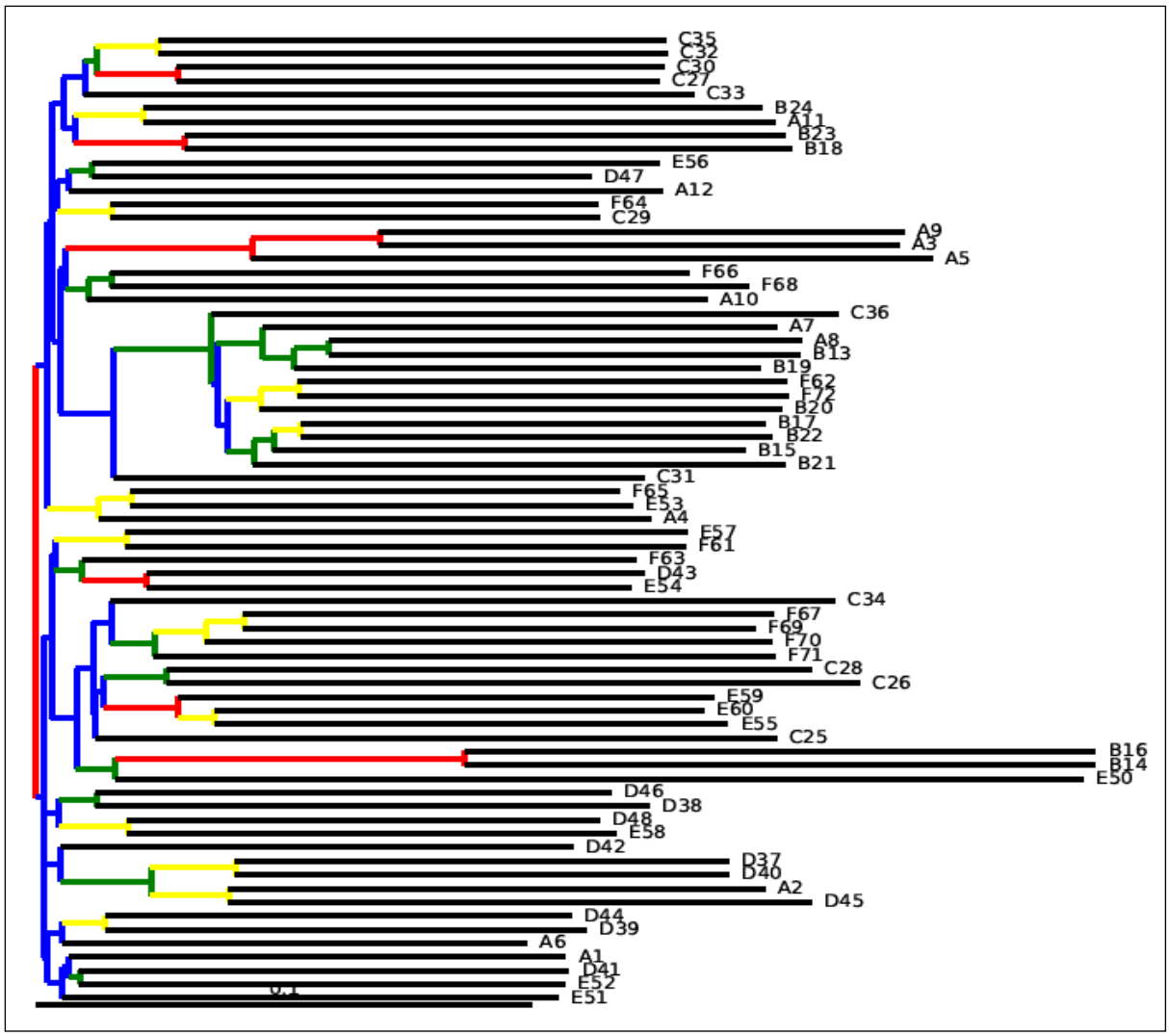

Figure 4-7: UPGMA (Unweighted Pair-Group Method with Arithmetic mean) trees.

The multidimensionality of the data was reduced first by an OTU-based method-Principal Component Analysis (PCA) for each group separately. Principal component analysis was used to identify linear combinations of gut microbial taxa that were associated with duration on a diet. The phylogeny-based method UniFrac was applied to the data, where UniFrac accounts for the phylogenetic divergence between the OTUs. A clear overlap of samples was shown in PCA on unweighted (qualitative) UniFrac distances for the 100, 200 and 400ppm iron untreated iron groups and 100 and 200ppm iron DSS-treated mice (Figure 4-8: a-e). However, there was a clear separation of samples for the 400ppm iron DSS-treated group. In this group, there was good clustering of samples pre and post-DSS treatment (Figure 4-8: f).

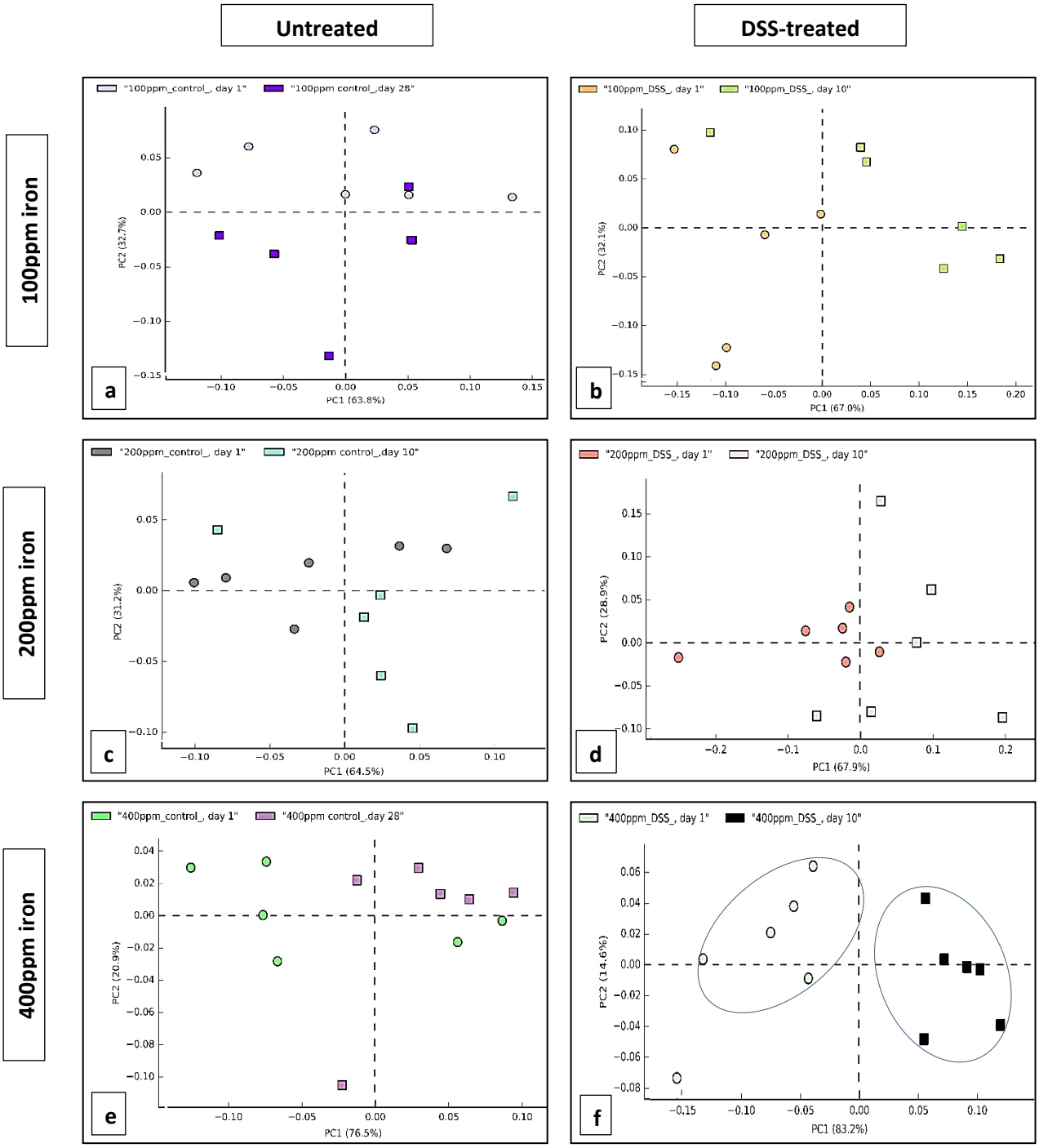

Figure 4-8: PCA plots of the unweighted UniFrac distances of pre-and post DSS-intervention stool samples from DSS-treated mice (b, d, and f) and (a, c and e) untreated mice at Phylum-level, phylogenetic classification of 16S rRNA gene sequences. Symbols represent data from individual mice, colour-coded by the indicated metadata. Statistical differences were assessed by Welch's t-test followed by Storey's FDR multiple test correction.

Heatmaps are extremely useful for the visual display of data from 16S rRNA high-throughput sequencing studies such as microbial analysis. Therefore, the heat map (Figure 4-9) below, represents the relative abundance (0.0-37.7%) of a collection of 12 phyla for 400ppm iron DSS-treated mice at day-1 vs. day-10. A noticeable reduction was observed in the proportion of *Bacteroidetes* and *Firmicutes* from day-1 to day-10. By contrast, a significant increase was demonstrated in the sequences assigned for other phyla (*Proteobacteria* and *Actinobacteria)* between these two-time points.

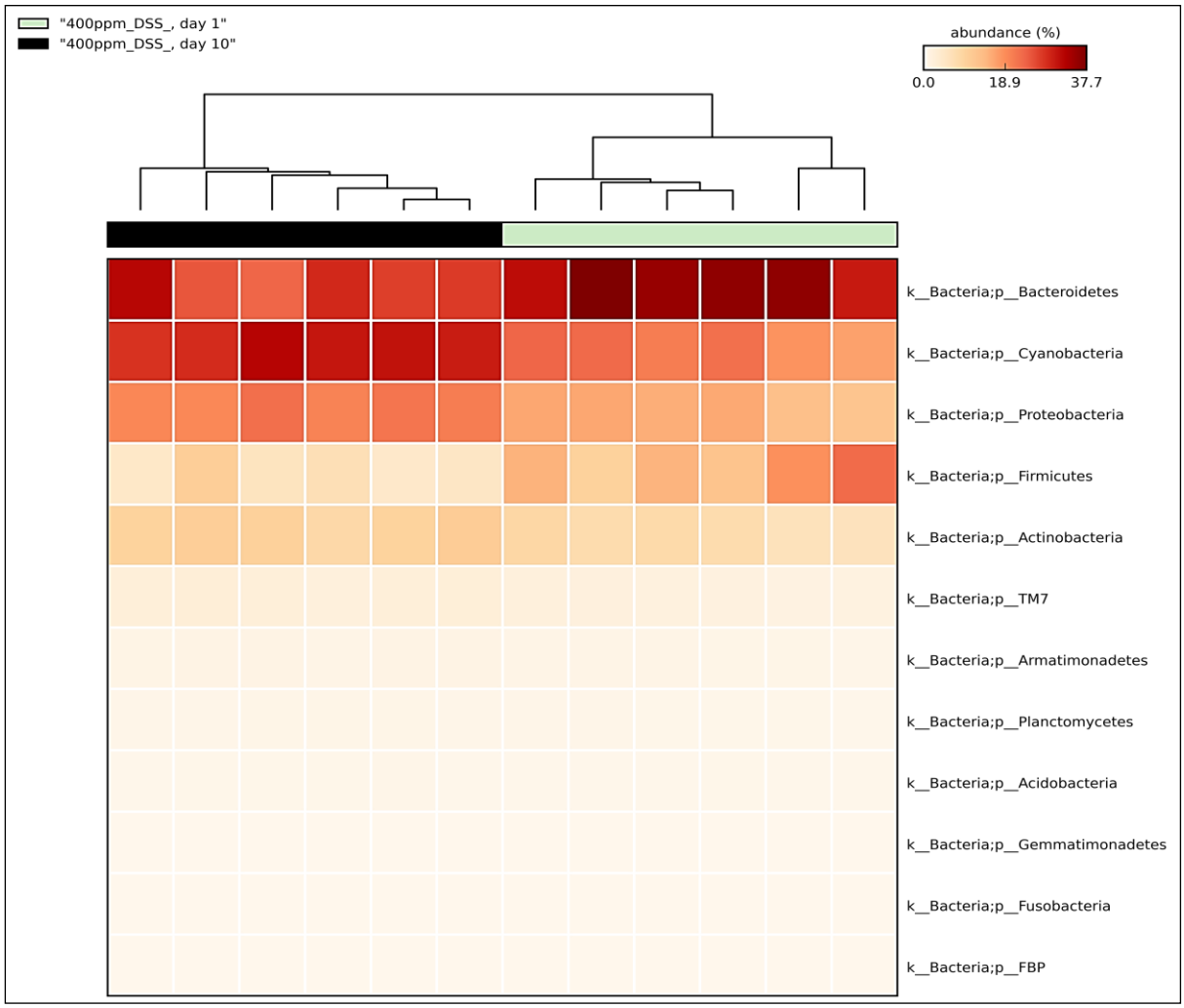

Figure 4-9: Heat map at Phylum-level, phylogenetic classification of 16S rRNA gene sequences representing relative abundances for each pre- or post-DSS intervention for the 400ppm iron group. Statistical differences were assessed by Welch's t-test followed by Storey's FDR multiple test correction.

The extended error bar plot for the 400ppm iron DSS-treated group (Figure 4-10), illustrates the mean proportion of sequences assigned to each phylum at day-1 vs. day-10. This plot also indicates the difference in mean proportion between the two-time points along with the associated confidence interval of this effect size and the p-value of the specified statistical test. The error bars signify standard error of the mean (SEM).

On the other hand, a significant statistical difference between day-1 and day-10 for all phyla was found. Whereas a reduction in *Bacteroidetes* and *Firmicutes* was noted, the opposite effect was observed for *Proteobacteria*, *Actinobacteria* and *Fusobacteria*, between day-1 and day-10.

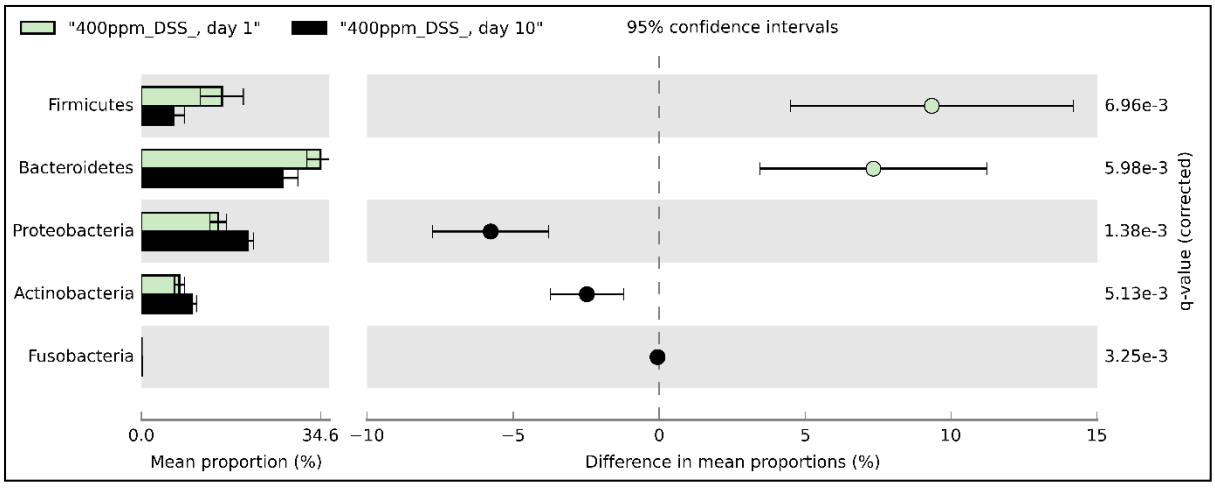

Figure 4-10: Extended error bar plot for the five phyla (*Firmicutes*, *Bacteroidetes*, *Proteobacteria*, *Actinobacteria* and *Fusobacteria*) that have a difference between the proportions of day-1 and day-10 for 400pm iron DSS-treated mice. Post-hoc plot for each phylum indicating *1)* the mean proportion of sequences at day-1 and-10, *2)* the difference in mean proportions for each phylum comparing pre-and post-DSS treatment, and *3)* a p-value indicating whether the mean proportion is equal for each time point. Statistical differences were assessed by Welch's t-test followed by Storey's FDR multiple test correction.

In the box plot graphs, the distribution of proportions (day-1 and day-10) within each phylum in the 400ppm iron DSS-treated group was indicated using a box-and-whiskers graphic (Figure 4-11) to give a more concise summary of the allocation of the proportions. There was a variation in all phyla within the 400ppm iron DSS-treated group when comparing day-1 and day-10. There were differences between the pre- and post-DSS intervention: analysis of the experimental murine microbiota at the phylum level indicated that the proportion was reduced significantly at day-10 vs. day-1 for *Bacteroidetes* (P<5.98-e3) and *Firmicutes* (P<6.98-e3). Conversely, greater proportions of *Proteobacteria* (P<1.38-e3), *Fusobacteria* (P<3.25-e3) and *Actinobacteria* (P<5.13-e3) were more frequently observed in day-10 samples as it presented in Figure 4-11.

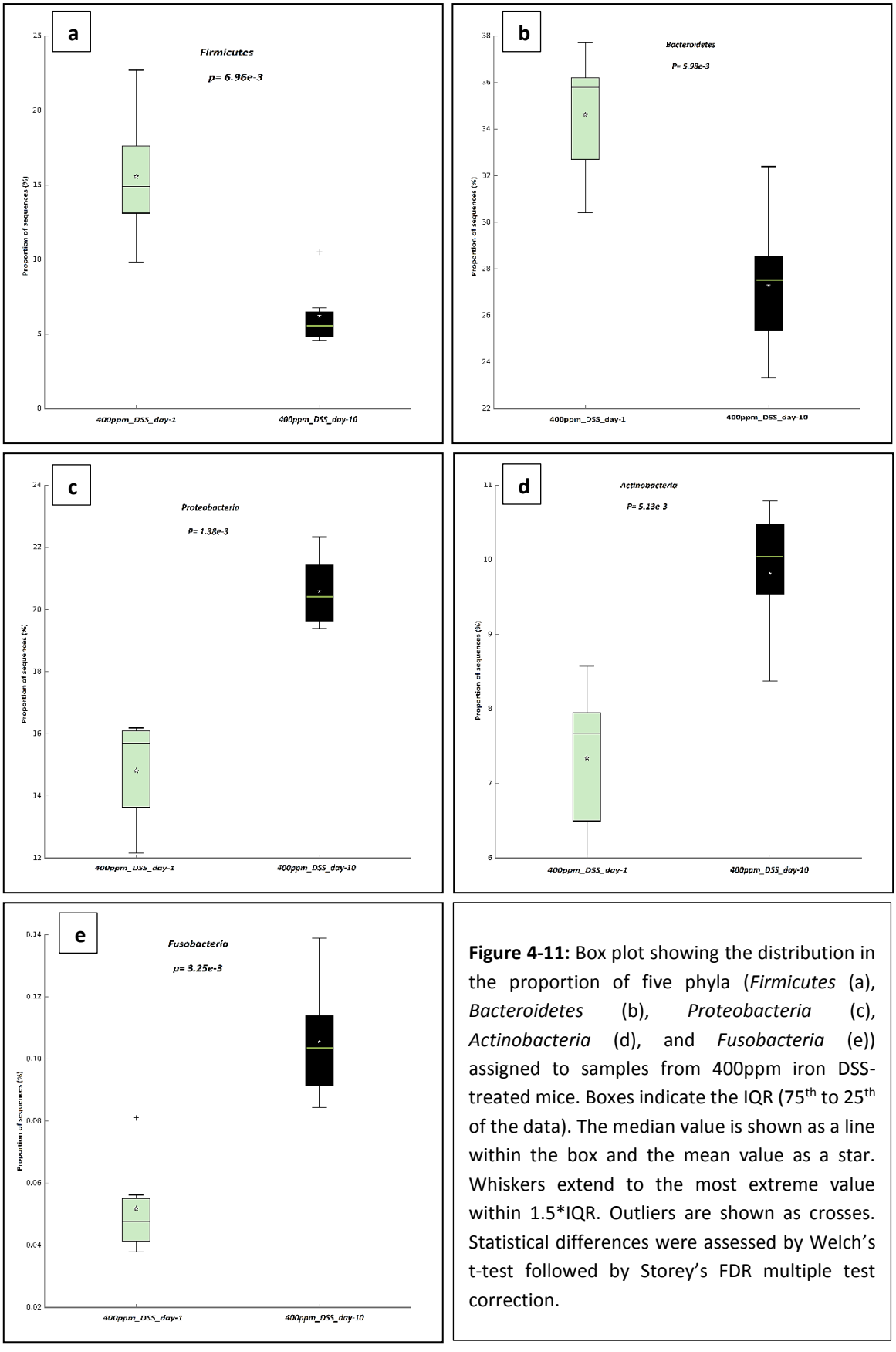

Figure 4-11: Box plot showing the distribution in the proportion of five phyla (*Firmicutes* (a), *Bacteroidetes* (b), *Proteobacteria* (c), *Actinobacteria* (d), and *Fusobacteria* (e)) assigned to samples from 400ppm iron DSS-treated mice. Boxes indicate the IQR (75^{th} to 25^{th} of the data). The median value is shown as a line within the box and the mean value as a star. Whiskers extend to the most extreme value within 1.5*IQR. Outliers are shown as crosses. Statistical differences were assessed by Welch's t-test followed by Storey's FDR multiple test correction.

4.3.2 Bacterial diversity data analysis at family level

Any variable region of a genome is good for distinguishing between closely related organisms. If a region is not under strong negative selection (most mutations lethal or detrimental) the sequence drifts as mutations accumulate. But many other considerations are also involved with choosing one variable region as being very good for identifying what type of organism is in your sample. One of the considerations is having the variable region flanked by highly conserved regions so that it is easy to design PCR primers and sequencing primers that will work across a wide variety of organisms. Another consideration is having a reasonable size of the variable region such as something between 50 and 1,000 bases length which makes PCR and sequencing inexpensive and reliable [133, 134].

Plenty of 16S rRNA sequence data for microbial communities is provided by next-generation sequencing techniques with primers (e.g. V4). However, if we want to compare whether bacterial communities are different among samples, at what taxonomic level should we compare? Unfortunately, resolution based on amplification of the V4 16S region is not the best way to determine bacterial species with a high degree of confidence [134]. However, it provides a useful tool to characterise microbial community structure based on a higher taxonomic level such as phyla or family. Though, if the project does not have sequence fragments larger than 1kb, the taxonomic assignation even at genus level will remain elusive. In our case, it was recommended to get the taxonomy at the family level thus providing results with a high degree of certainty for such identifications.

The community composition of each sample for a given taxonomic rank (from Kingdom to Species) was summarised using Qiime. From these summaries, bar plots were generated. An example of such a bar plot, showing the relative abundance of different families among the samples, is shown in Figure 4-12.

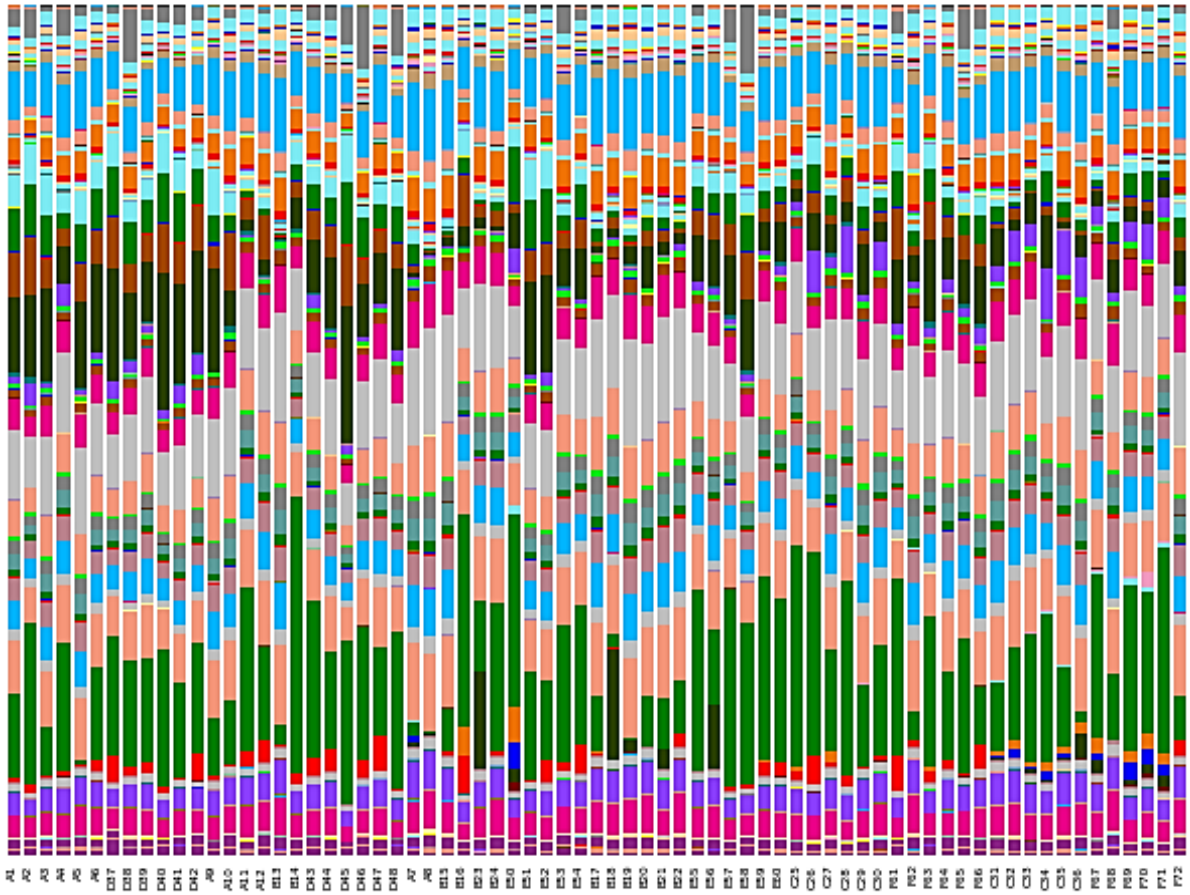

Figure 4-12: Family-level taxonomic composition of all samples (relative abundance).
Note: all samples identifications are listed in appendix-1 and legends in appendix -3

the heat map (Figure 4-13) below, represents the relative abundance (0.0-39.4%) of a collection of 32 families for 400ppm iron DSS-treated mice at day-1 vs. day-10. A noticeable reduction was observed in the proportion of *S24.7*, *Lachnospiraceae*, *Ruminococcaceae*, and *Lactobacillaceae.* By contrast, a significant increase was demonstrated in the sequences assigned for other families (*Cytophagaceae*, *Weekesllaceae* and *Alicyclobaciliaceae)* between these two-time points.

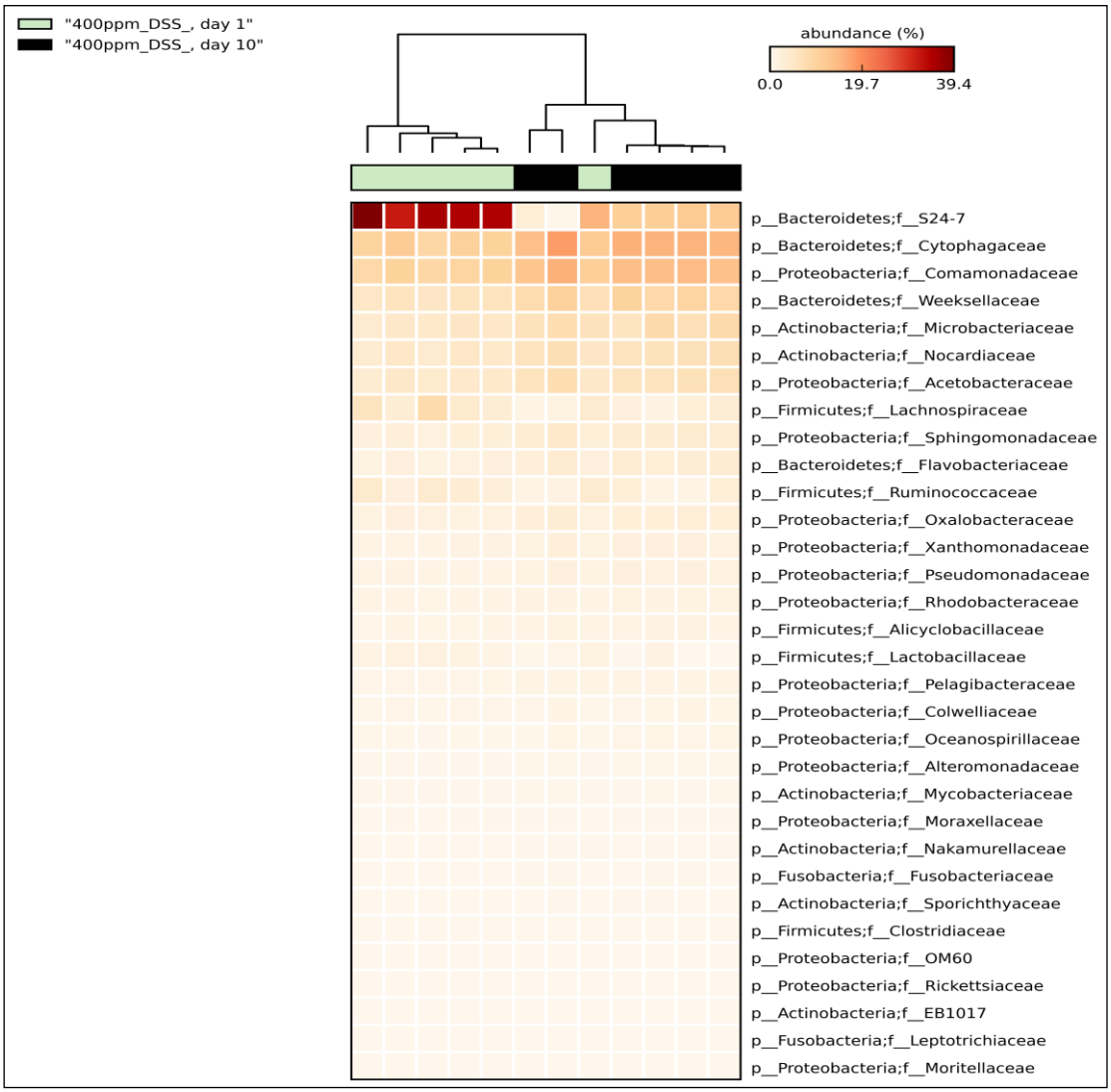

Figure 4-13: Heat map at Phylum-level, phylogenetic classification of 16S rRNA gene sequences representing relative abundances for each pre- or post-DSS intervention for the 400ppm iron group. Statistical differences were assessed by Welch's t-test followed by Storey's FDR multiple test correction.

4.3.2.1 Families belonging to Bacteroidetes phylum

The mean proportion of sequences assigned to the four families (*S24-7*, *Cytophagaceae*, *Weekesllaceae* and *Flavobacteriaceae*) is represented in Figure 4-7. A significant reduction in the *S24-7* family was observed at day-1 vs. day-10 (P<2.15e-3). By contrast, *Cytophagaceae*, *Weekesllaceae* and *Flavobacteriaceae* showed an increasing manner at day-10 vs. day-1.

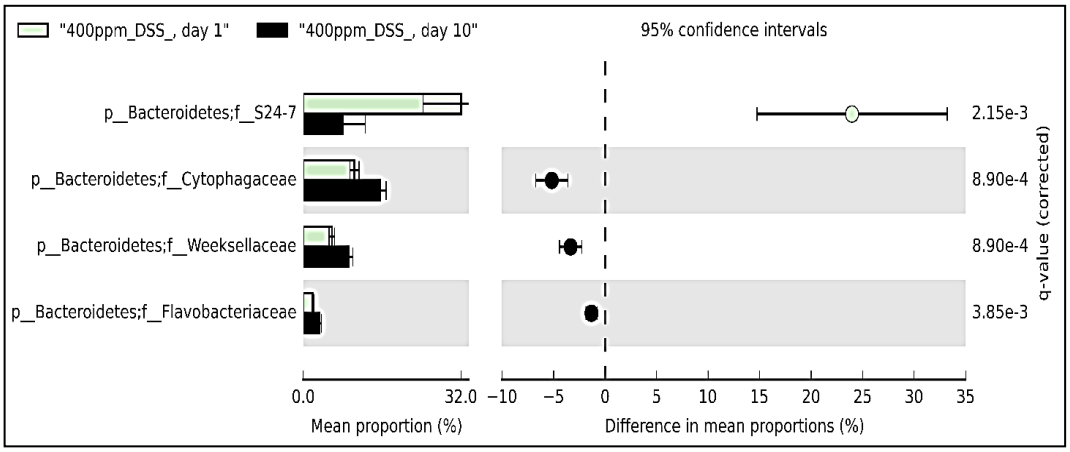

Figure 4-14: Extended error bar plot for the four families (*S24-7*, *Cytophagaceae*, *Weekesllaceae* and *Flavobacteriaceae*) that have a difference between the proportions of day-1 and day-10 for 400pm iron DSS-treated mice. This Post-hoc plot for each family indicating *1)* the mean proportion of sequences at day-1 and 10, *2)* the difference in mean proportions for each family comparing pre-and post-DSS treatment, and *3)* a p-value indicating if the mean proportion is equal for each time point. Statistical differences were assessed by Welch's t-test followed by Storey's FDR multiple test correction.

4.3.2.2 Families belonging to Firmicutes phylum

Five families in the *Firmicutes* phylum (*Lachnospiraceae*, *Ruminococcaceae*, *Lactobacillaceae*, *Mogibacteriaceae* and *Clostridiaceae*) showed a significant decline in their mean proportion of sequences (P<0.037, 0.017, 6.92e-3, 0.046 and 0.035 respectively).

However, the *Alicyclobaciliaceae* family increased at day-10 vs. day-1 (P<2.15e-3) as presented in Figure 4-15.

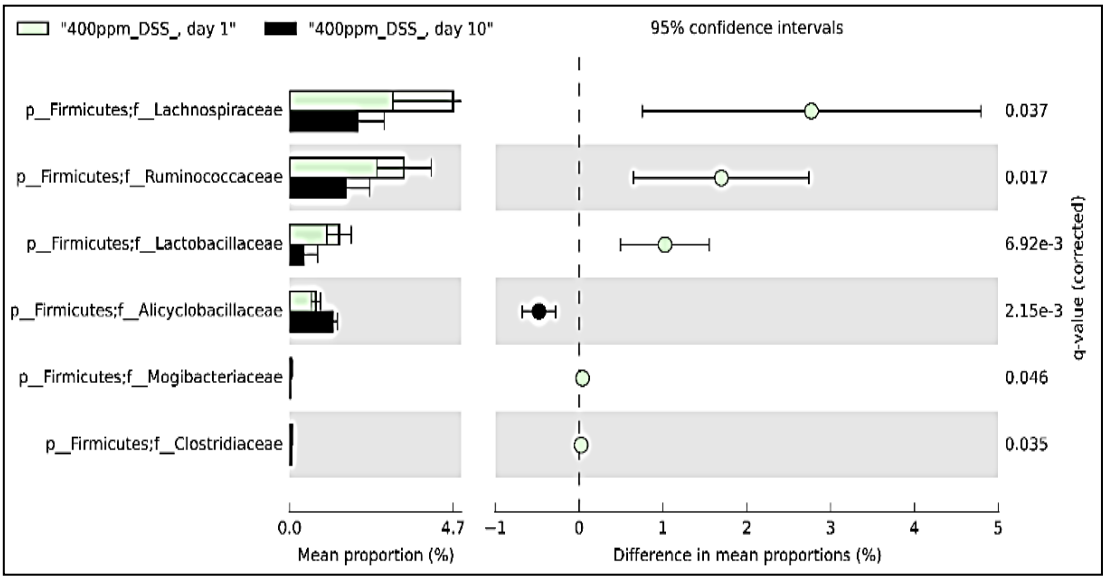

Figure 4-15: Extended error bar plot for six families (*Lachnospiraceae*, *Ruminococcaceae*, *Lactobacillaceae*, *Mogibacteriaceae*, *Alicyclobaciliaceae* and *Clostridiaceae*) that have a difference between the proportions at day-1 and day-10 for 400pm iron DSS-treated mice. This Post-hoc plot for each family indicates *1)* the mean proportion of sequences at day-1 and-10, *2)* the difference in mean proportions for each family comparing pre-and post-DSS treatment, and *3)* a p-value indicating if the mean proportion is equal for each time point. Statistical differences were assessed by Welch's t-test followed by Storey's FDR multiple test correction.

4.3.2.3 Families belonging to Actinobacteria phylum

The mean proportion of sequences assigned to the six families (*Microbacteriaceae*, *Nocardiaceae*, *Mycobacteriaceae*, *Sporichthyaceae*, *Nakamurellaceae* and *EB1017*) is represented in Figure 4-16 where a significant increase for all families at day-10 vs. day-1 was seen.

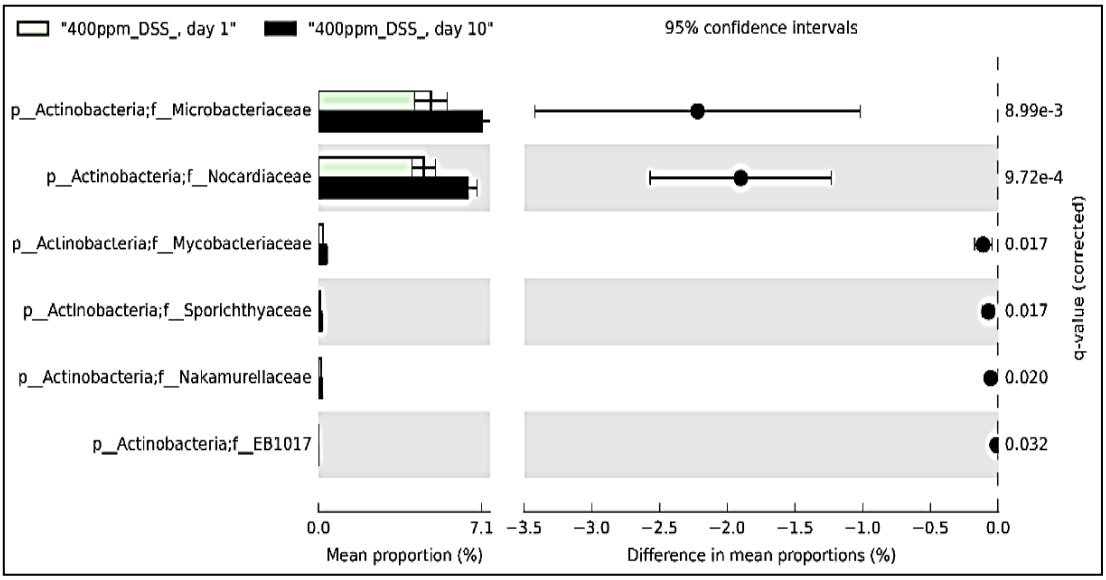

Figure 4-1: Extended error bar plot for the six Families (*Microbacteriaceae*, *Nocardiaceae*, *Mycobacteriaceae*, *Sporichthyaceae*, *Nakamurellaceae* and *EB1017*) that have a difference between the proportions of day-1 and day-10 for 400pm iron DSS-treated mice. This Post-hoc plot for each family indicates *1)* the mean proportion of sequences at day-1 and 10, *2)* the difference in mean proportions for each family comparing pre-and post-DSS treatment, and *3)* a p-value indicating if the mean proportion is equal for each time point. Statistical differences were assessed by Welch's t-test followed by Storey's FDR multiple test correction.

4.3.2.4 Families belonging to Fusobacteria phylum

The families belonging to *Fusobacteria* were low in number (*Fusobacteriaceae* and *Leptotrichiaceae*). However, they showed a high percentage of sequences that were assigned to these families as represented in Figure 4-17. A significant reduction was seen in the *Fusobacteriaceae* family at day-1 vs. day-10 (P<1e-15), whereas *Leptotrichiaceae* displayed a significant increase (P<1e-15) on day-10 vs. day-1.

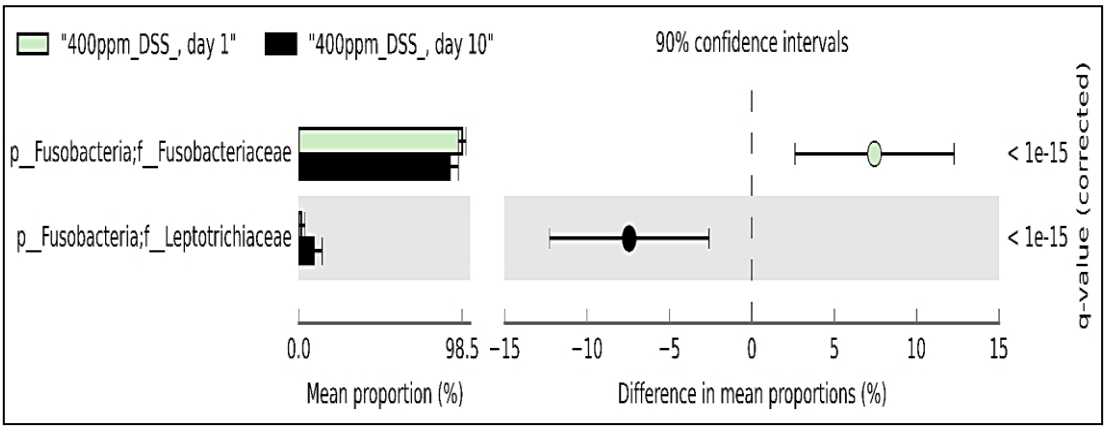

Figure 4-2: Extended error bar plot for two families (*Fusobacteriaceae* and *Leptotrichiaceae*) that have a difference between the proportions of day-1 and day-10 for 400pm iron DSS-treated mice. This Post-hoc plot for each family indicates *1)* the mean proportion of sequences at day-1 and 10, *2)* the difference in mean proportions for each family comparing pre-and post-DSS treatment, and *3)* a p-value indicating if the mean proportion is equal for each time point. Statistical differences were assessed by Welch's t-test followed by Storey's FDR multiple test correction.

4.3.2.5 Families belonging to Proteobacteria phylum

15 families were shown to have a significant increase in the mean proportion of sequences assigned to each family at day-1 vs. day-10 as demonstrated in Figure 4-18. The highest most abundant three families were (*Comamonadaceae*, *Acetobacteraceae* and *Sphingomonadaceae*) with P<8.90e-4 for each.

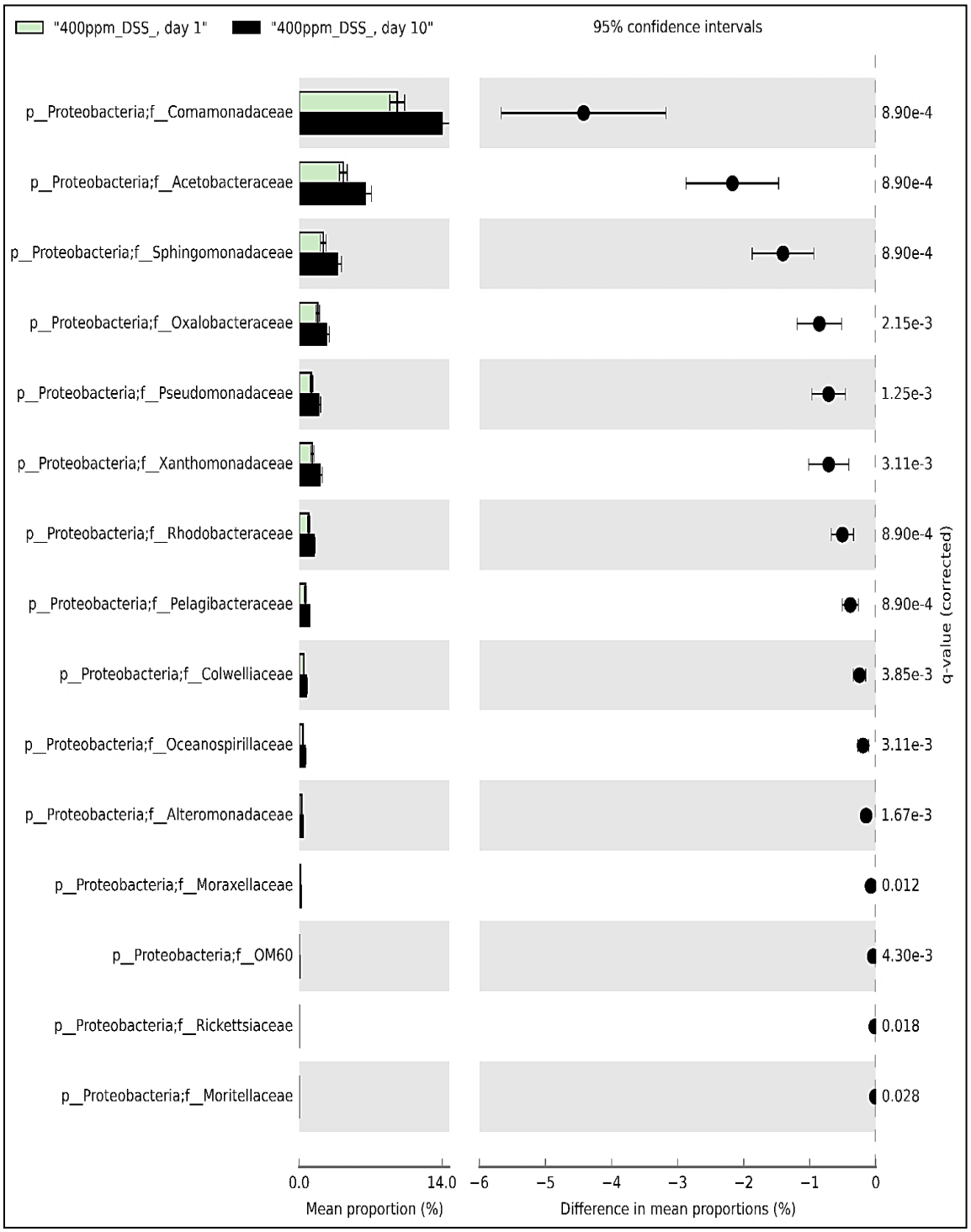

Figure 4-3: Extended error bar plot for 15 families (belong to *Proteobacteria* level), where, each family has a difference between the proportions of day-1 and day-10 for 400pm iron DSS-treated mice. This Post-hoc plot for each family indicates *1)* the mean proportion of sequences at day 1 and 10, *2)* the difference in mean proportions for each family comparing pre and post-DSS treatment, and *3)* a p-value indicating if the mean proportion is equal for each time point.

4.4 Discussion

Laboratory mice are frequently used as experimental models for diseases such as inflammatory bowel disease, where the gut microbiota composition, as well as function, has been found to be a significant contributory factor [135]. Nevertheless, currently, there is a knowledge gap concerning the degree of similarity between the human and mouse gut microbiota particularly at the deeper levels of taxonomy such as genera and species [135]. However, many gut microbiota associated illnesses have been related to bacterial dysbiosis on a higher taxonomic level, providing evidence for the efficacy of sequencing the gut microbiota to the Phylum and Family levels [136].

Therefore, in this chapter, we analysed inter- and intragroup differences and similarities between the gut microbiota composition of 36 laboratory wild-type mice (6 mice per group). Qualitative and quantitative-based analysis of the faecal gut microbiota at two different time points (day-1 and day-10) for DSS-treated groups (100, 200 and 400ppm iron) and untreated mice (controls) on the same diets was undertaken. PCA revealed overlap of all microbial profiles, except for the 400ppm iron DSS-treated mice, which seemed to be the only group that had clear separation with significant differences observed (Figure 4-8).

Previously the gut microbiota composition has been shown to be influenced by multiple factors including environmental factors and host genetics. Recently, researchers have suggested that diet is one of many environmental factors which strongly affects the composition of the gut microbiota [137]. However, the mice used in this project received the same diet, except for its iron content. The effect was most notable after the DSS treatment.

Further analysis was applied to compare the day-10 data for different doses of iron. However, this analysis did not reveal any significant findings.

Some studies have shown significant results indicating that a subset of CD and UC samples contain abnormal gut microbiotas, characterised by depletion of commensal bacteria, particular members of the phyla *Firmicutes* and *Bacteroidetes* and an increase in *Proteobacteria* [68]. These results agreed with our project's data analysis, where *Proteobacteria* increased by 1.62-fold, *Firmicutes* levels decreased by 2.7-fold and *Bacteroidetes* also reduced by 1.26-fold on day-10 vs. day-1 in 400ppm iron DSS-treated mice (Figure 4-10). Although similar trends were found in the other groups of mice, without any no significance.

The relative distribution of the gut microbiota in each group was calculated, combined, and summarised at the family level in OTU tables. Further statistical analysis was applied using STAMP software and various statistical tests for each group at day-1 vs. day-10. Correspondingly, only the 400ppm iron DSS-treated mice samples showed any significant differences and these were in families belonging to the phyla *Bacteroidetes*, *Firmicutes*, *Proteobacteria*, *Actinobacteria* and *Fusobacteria*.

In conclusion, this chapter reports the use of high-throughput 16S rRNA gene sequencing of the gut microbiome in mice treated with iron and or DSS. Increasing the iron content of the diet led to a change in the microbiota after colitis was induced with DSS: this was not observed in the normal or low-iron diet groups of mice.

5 Induction of chronic intestinal inflammation using repeated cycles of dextran sulphate sodium (DSS)

5.1 Introduction

Millions of people worldwide have been diagnosed with inflammatory bowel disease (IBD), which is considered to be a chronic inflammatory illness of the gastrointestinal tract. However, its pathophysiology remains unclear, and usually, IBD takes a relatively benign course with either a single attack or perhaps periods of long-term remission. The experimental models of colitis have contributed crucially to a better understanding of the disease (IBD), as well as the investigation of new therapies [138]. Oral consumption of dextran sulphate sodium (DSS) in drinking water is widely used as a model to induce colitis in animals. DSS induction can cause both acute and chronic colitis in rodents by causing inflammation and the recruitment of immune cells, which are then activated directly via epithelial cell damage and macrophage function alterations [139].

In chronic DSS-induced colitis, the induction phase is characterised by mild-moderate disease activity with significant colonic polymorph nuclear leucocyte infiltration [82]. Variations in the composition of microbiota associated with IBD is recognised as dysbiosis. However, until now the mechanism by which IBD-associated dysbiosis develops is uncertain, and it is unclear whether this dysbiosis should be considered a cause or consequence of IBD [140].

Over the past 20 years, many types of research have highlighted why the understanding of the IBD pathogenesis is imperative to the production of efficient and safe pharmacological treatments. In this chapter, some of the clinical, as well as molecular inflammatory actions, that occur during the acute and chronic stages as well as the remission period have been investigated using a widely employed experimental model of DSS-induced colitis.

5.2 Aims

The aims were to:

1- Investigate the effects of dextran sodium sulphate (DSS) on clinical, histological and molecular features during acute and chronic phases of colitis.

2- Study the effect of iron on DSS-induced colitis, during both acute and chronic phases.

5.3 Induction of chronic colitis in three different iron diet groups

The chronic DSS colitis model (3 cycles of 1.25% DSS (5-days), each followed by a 16-day recovery period (Figure 5-1)) has previously been established in our department and has been documented previously [83].

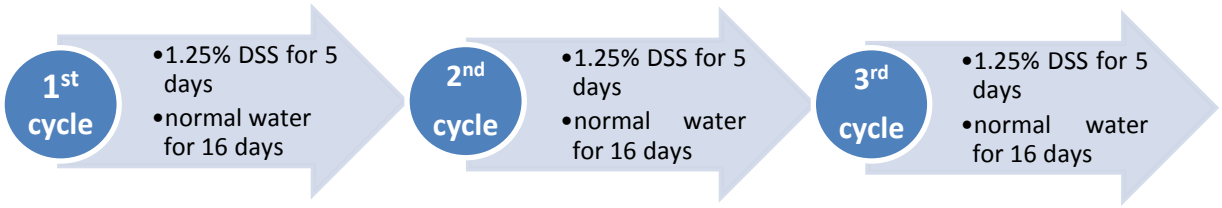

Figure 5-1: Chronic DSS-induced colitis model

48 individually-housed, wild-type C57BL/6 female mice aged 8-9 weeks were divided into six groups of 8 mice each. Group (A) mice were given 100ppm iron diet; Group (B) a 200ppm iron diet and Group (C) a 400ppm iron diet. All these groups were administered 3 cycles of 1.25% DSS treatment (Figure 5-1). Control mice were given distilled water without DSS. Of these, Group (D) had a 100ppm iron diet; Group (E) a 200ppm iron diet and Group (F) mice a 400ppm iron diet (Figure 5-2).

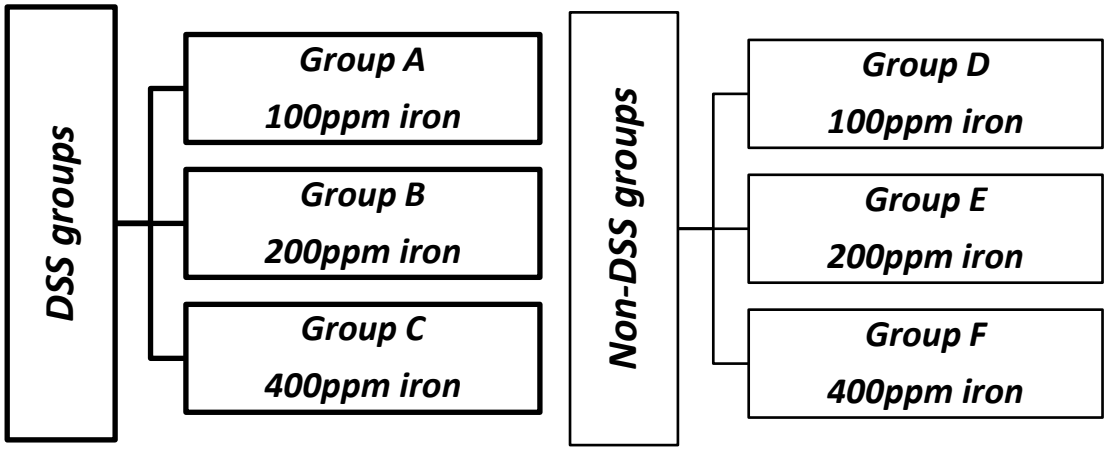

Figure 5-2: Different diet groups with and without DSS treatment

DSS treated animals (Group (A) 100ppm iron, (B) 200ppm iron and (C) 400ppm iron) were fed with their diet from day-1 until day-63. All mice were administered 1.25% DSS in distilled water as the sole source of drinking fluid for 5-days, and then normal drinking water for 16-days. This 21-day period was defined as one cycle of acute DSS as illustrated in Figure 5-1. During the whole 63-day experiment, the mice were caged separately and placed on paper bedding, which was changed daily to collect fresh samples and observe any signs of rectal bleeding. Daily body weight was recorded as well as any clinical signs of colitis at the end of the experiment (day-63) when all mice were euthanised using a Home Office approved schedule 1 method.

5.3.1 The effect of repeated cycles of low dose (1.25%) dextran sulphate sodium (DSS) on the body weight of wild-type C57BL/6 mice supplemented with different iron diets

The body weight of the DSS-treated mice was recorded daily to monitor the percentage of body weight change (weight loss) for each cycle as outlined in Figures 5-3, 5-4 and 5-5. In the first DSS cycle, all mice lost the most weight on day-8: 2.3%, 1% and 0.75% weight loss for mice taking 100ppm iron, 200ppm iron and 400ppm iron diets, respectively. In each group, this was followed by a steady increase in body weight during the 16-day recovery period (Figure 5-3).

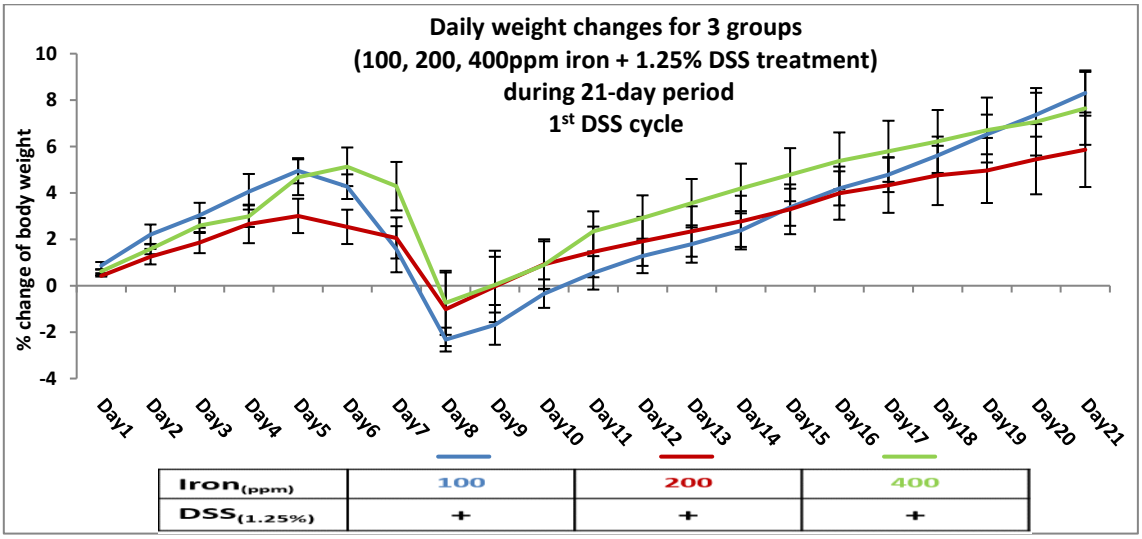

Figure 5-3: Percentage of weight change in mice (100ppm iron (blue), 200ppm iron (red) and 400ppm iron (green)) during 1.25% dextran sulphate sodium-induced colitis. Data are presented as a mean ± standard error of the mean. Statistical differences were assessed by Kruskal–Wallis test followed by Dunn's multiple comparison tests. (n=8 female mice per group).

On the second DSS cycle, all mice again developed maximum weight loss at day-8: mice on the 400ppm iron diet, appeared as if they lost more weight than mice taking 100ppm iron and 200ppm iron diets. From day-9 to day-21 of this cycle mice in all groups started to regain their body weight (Figure 5-4).

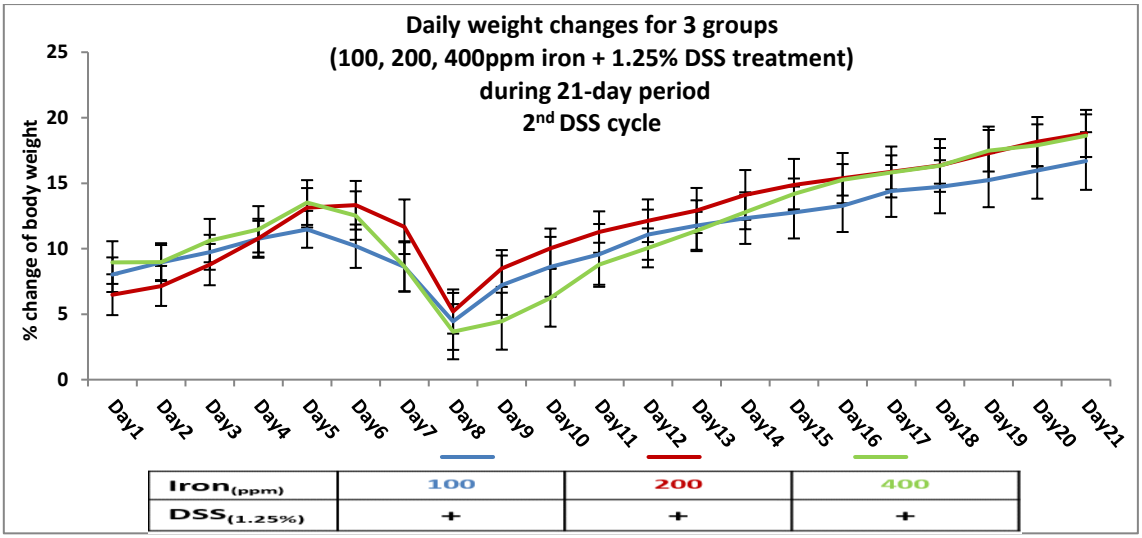

Figure 5-4: Percentage of weight change in mice (100ppm iron (blue), 200ppm iron (red) and 400ppm iron (green)) during 1.25% dextran sulphate sodium-induced colitis. Data are presented as a mean ± standard error of the mean. Statistical differences were assessed by Kruskal–Wallis test followed by Dunn's multiple comparison tests. (n=8 female mice per group).

In the last (third) DSS cycle, the mice on the 100ppm iron diet lost most body weight followed by the 400ppm iron and 200ppm iron diet groups. However, the percentage of body weight loss was more than that lost in the previous two cycles for all animals. Again, from day-9 to day-21 of this cycle, all mice started to gain in their body weight (Figure 5-5).

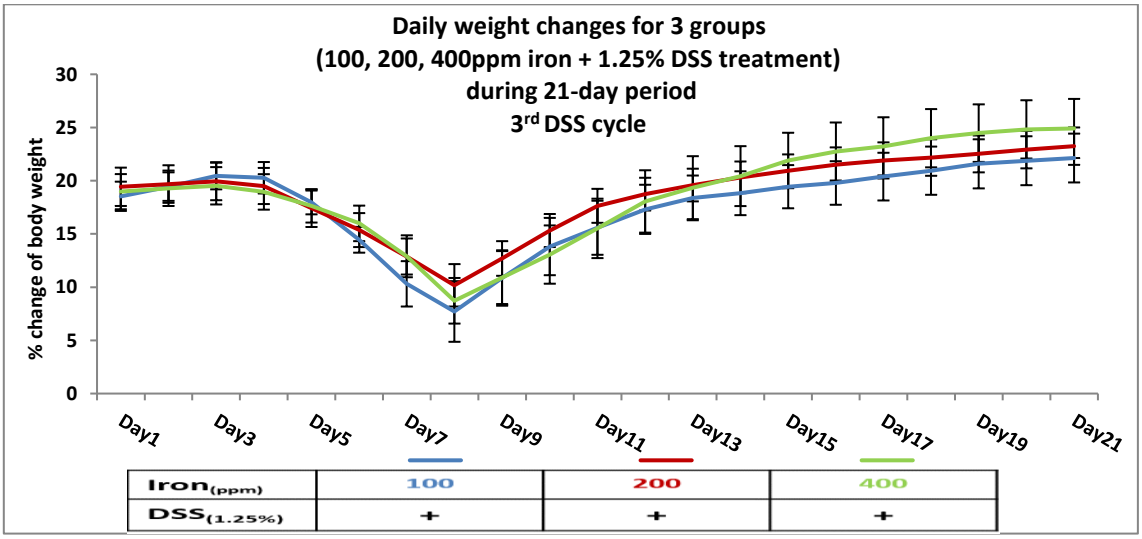

Figure 5-5: Percentage of weight change in mice (100ppm iron (blue), 200ppm iron (red) and 400ppm iron (green)) during 1.25% dextran sulphate sodium-induced colitis. Data are presented as a mean ± standard error of the mean. Statistical differences were assessed by Kruskal–Wallis test followed by Dunn's multiple comparison tests. (n=8 female mice per group).

Recurrent acute colitis was therefore induced in mice that received 1.25% DSS in their drinking water for 5-days, and this was followed by recovery in the following 16-days on plain drinking water. All DSS-treated mice lost body weight from day-6 with the maximal loss occurring on day-8 in each cycle. Group A (100ppm iron) mice appeared to lose more weight overall than the other groups, but this difference was not statistically significant (Figure 5-6).

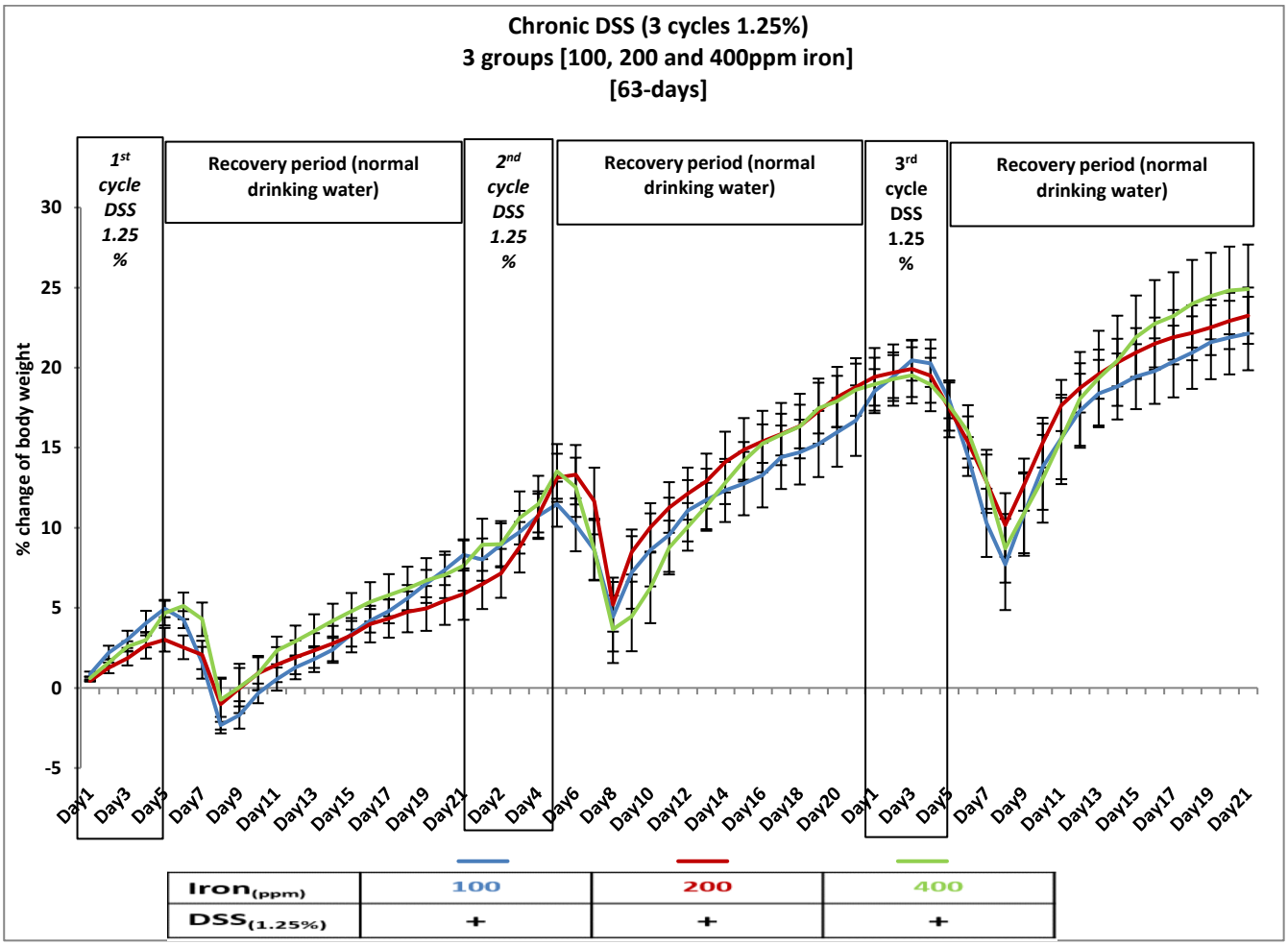

Figure 5-6: Percentage of weight change in mice (100ppm iron (blue), 200ppm iron (red) and 400ppm iron (green)) during three cycles of 1.25% dextran sulphate sodium-induced colitis during the 63-day period. Data are presented as a mean ± standard error of the mean. Statistical differences were assessed by Kruskal–Wallis test followed by Dunn's multiple comparison tests. (n=8 female mice per group).

5.3.2 The effect of different iron diets on the body weight of wild-type C57BL/6 mice without DSS treatment during a 63-day period

Control mice (Groups D-F) were given drinking water without DSS, but with varying amounts of dietary iron, as described above. Daily observations and measures were completed in the same way as for the mice receiving DSS. At day-53 the control groups were divided further into 2 groups (consisting of 4 mice each). 3 groups (Group (G) 100ppm iron, (H) 200ppm iron and (I) 400ppm iron) had colitis induced with 2% DSS in a single acute cycle [2% DSS in drinking water for 5 days followed by another 5 days on plain drinking water]. The other three groups (D, E and F) were maintained on their diets for a total of 63-days. These mice increased in body weight in a dose-dependent manner, illustrating the importance of iron as a nutrient. Group (D) mice (100ppm iron) however gained significantly less weight between day-7-49 than the other non-DSS-treatment groups. All mice were euthanised using a Home Office approved schedule 1 method on day-63 (Figure 5-7).

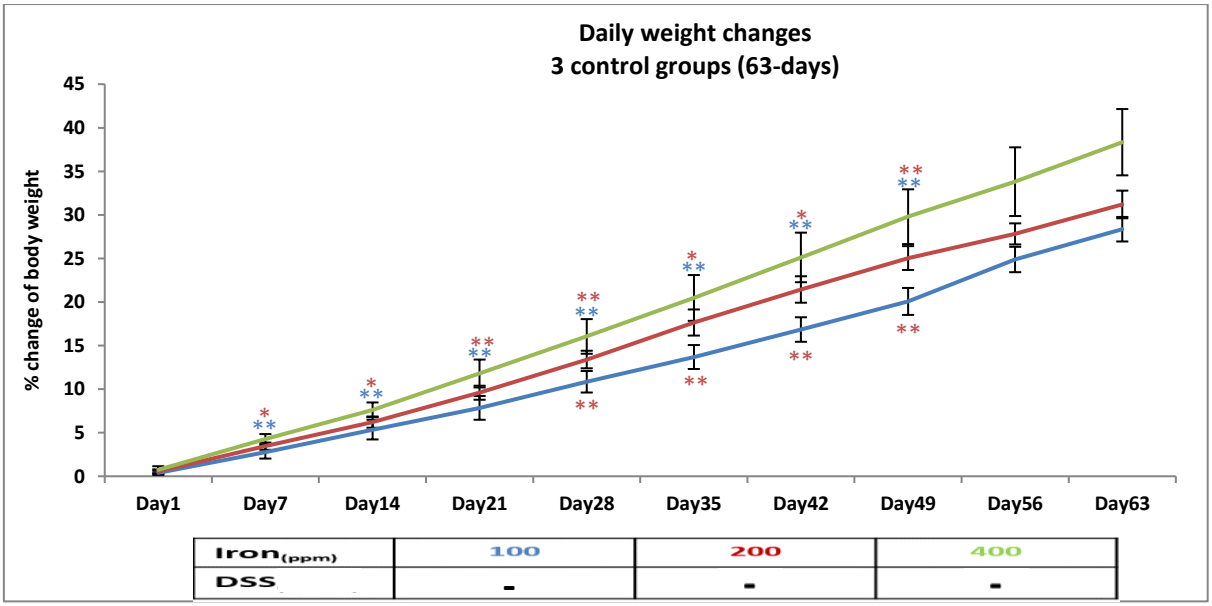

Figure 5-7: Percentage of weight change in mice (100ppm iron (blue), 200ppm iron (red) and 400ppm iron (green) without DSS treatment during the 63-day period. Data are presented as a mean ± standard error of the mean. Statistical differences were assessed by Kruskal–Wallis test followed by Dunn's multiple comparison tests (*P<0.05, **P<0.01). (n=8 until day-54, then 4 female mice per group).

5.3.3 The effect of a long period (53-days) on iron modification diets on the body weight of wild-type mice (C57BL/6) during the 10-day period of acute dextran sulphate sodium (DSS) induced colitis

After feeding mice diets for 53 days an acute DSS cycle applied to mimic the human (IBD iron deficient patients) scenario. During the 10-day period, the body weight of the DSS-treated mice was recorded daily. All these DSS-treated mice developed colitis. There was an earlier onset of weight loss day-3 and greater magnitude of weight loss in group G (100ppm iron). Group H (200ppm iron) and the group I (400ppm iron) did not start to lose weight until day-5 (Figure 5-8).

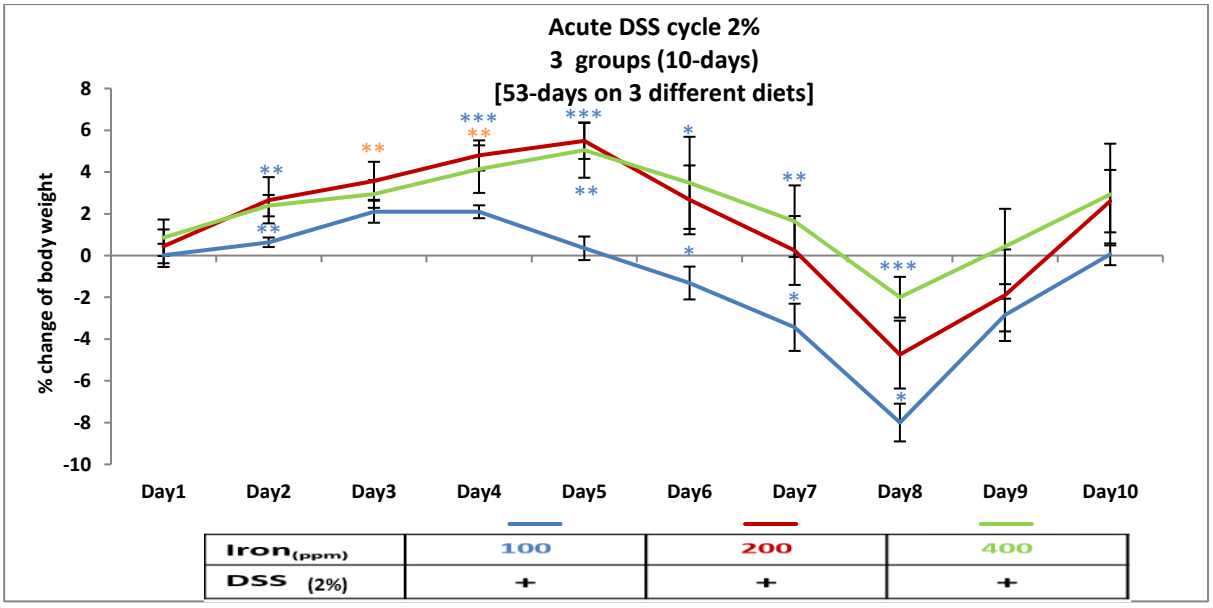

Figure 5-8: Percentage of weight change in mice (100ppm iron (blue), 200ppm iron (red) and 400ppm iron (green)) during 2% dextran sulphate sodium-induced colitis. Data are presented as a mean ± standard error of the mean. Statistical differences were assessed by Kruskal–Wallis test followed by Dunn's multiple comparison tests. (n=4 female mice per group).

During this acute DSS cycle, the mice fed 100ppm iron lost more weight than other groups with significance difference observed from day-2 until day-8 as it illustrated in Figure 5-8.

5.4 Histopathological changes caused by colonic inflammation following repetitive cycles of Dextran Sulphate Sodium administration

The colons of the mice were examined for features of colitis by light microscopy after staining with H & E as described in Chapters 2 and 3.

5.4.1 100ppm iron diet DSS-treated mice displayed more colonic inflammation than mice on 200ppm iron and 400ppm iron diets

After 63-days, all mice were killed, and their colons examined, chronic DSS groups reflect mild colitis, and acute DSS reflects the sever colitis has been shown in Chapter 3, while controls demonstrate the longer effects of diets on mucosal tissues. H&E slides were observed under light microscopy. Untreated mice had no signs of colitis (Figure 5-9 IV, V and VI). On the other hand, all the mice treated with repeated cycles of 1.25% DSS developed features of mild colitis, but there was no mortality (Figure 5-9 I, II and III).

Histological examination of colonic tissue sections from the mice treated with a single 2% DSS cycle (Groups G-I) also established the presence of moderate DSS-induced colitis, which as usual, was located in the distal part of the colon with areas of mucosal loss, increased muscle thickness, oedema and inflammatory cell infiltration (Figure 5-9 VII, VIII and IX).

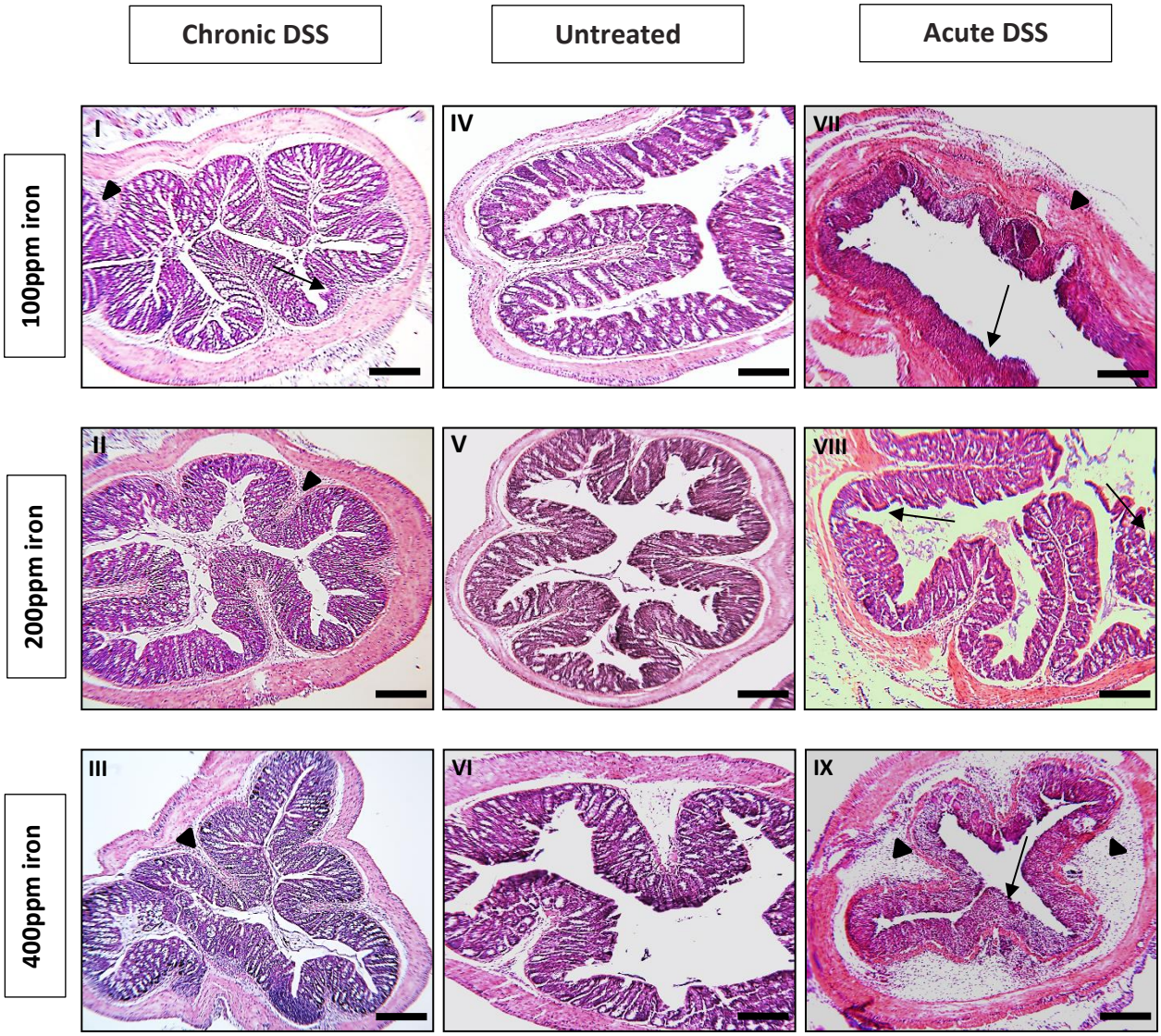

Figure 5-9: Illustrative H&E-stained segments of distal colon from untreated (n=4), 1.25% (n=8) and 2% DSS-treated mice (n=4). Mice received either water (control) (IV, V, VI), 1.25% DSS for 5 days and full recovery period 16 days on normal water (I, II, III) or 2% DSS for 5 days and followed by another 5 days on plain drinking water before they were euthanised (VII, VIII, IX). Arrowheads highlight submucosal oedema; arrows highlight almost complete loss of colonic epithelium (20x magnification).

The researcher assessed the degree of inflammation blinded to diets and treatment using the histological inflammatory scoring system (Table 5-1) [91].

Score	Cell infiltration	Tissue damage
0	None	None
1	Focally increased numbers of inflammatory cells in the lamina propria	Discrete epithelial lesions
2	Confluence of inflammatory cells extending into the submucosa	Mucosal erosions
3	Transmural extension of the infiltrates	Extensive mucosal damage and/or extension through deeper structures of the bowel wall

Table 5-1: Colitis scoring system adapted from [90]

Mild inflammatory reaction occurred with every 1.25% DSS cycle as shown under the light microscope. Group B (200ppm iron and 1.25% DSS treatment) had significantly more moderate colitis than Group E (200ppm iron, no DSS). The colitis score was significantly greater than baseline for all three treated groups: the difference, compared to baseline, was greatest for the mice receiving 100ppm iron DSS-treated mice (Group A) (Figure 5-10).

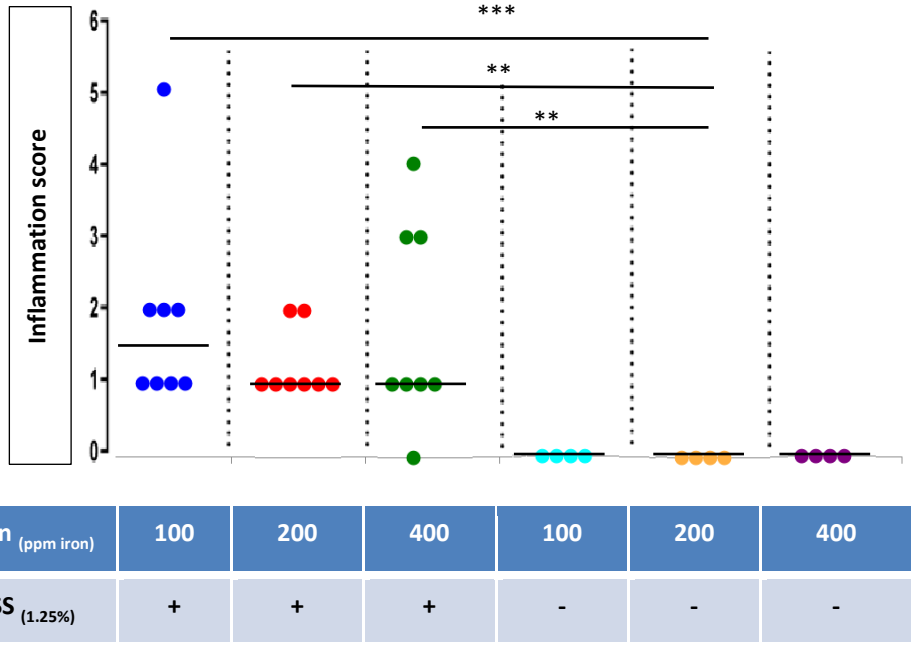

Figure 5-10: Inflammation (colitis) scores for all groups 1.25% DSS-treated and untreated (controls) mice on different iron diets. Horizontal lines at the median. Differences tested by Kruskal-Wallis test followed by multiple comparisons Dunn's test. ** P<0.01, *** P<0.001 versus control (200ppm iron).

Acute 2% DSS caused severe colitis in all mice when delivered towards the end of the 63-day experiment. There was a significant difference in the colitis scores between the 200ppm iron DSS-treated and 200ppm iron DSS-untreated groups. The 100ppm iron and 400ppm iron DSS-treated mice had more significant increases in intestinal inflammation similarly compared with DSS-untreated mice on the 200ppm iron diet. However, comparing 100 and 400ppm iron DSS-treated mice vs. 200ppm iron DSS-treated mice showed no significance difference (Figure 5-11).

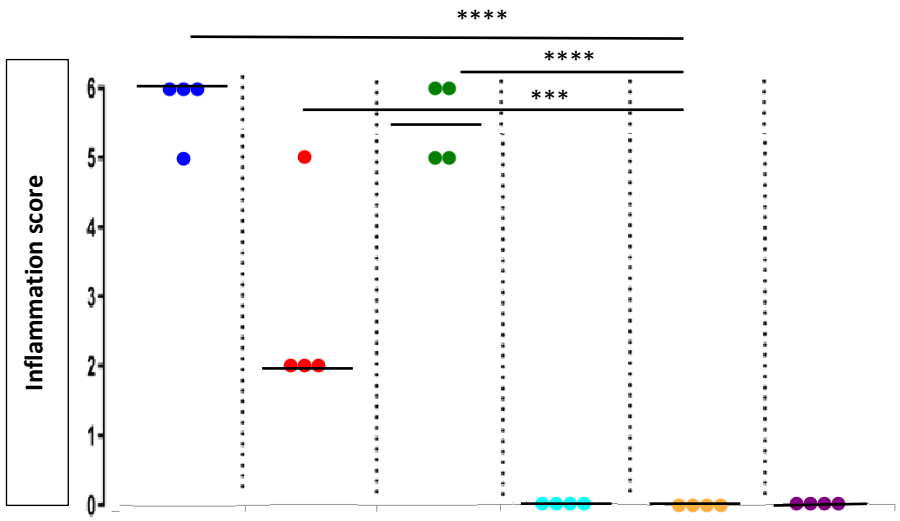

Iron (ppm iron)	100	200	400	100	200	400
DSS (2%)	+	+	+	-	-	-

Figure 5-11: Inflammation (colitis) scores for all groups 2% DSS-treated and untreated (controls) mice on different iron diets. Horizontal lines at the median. Differences tested by Kruskal– Wallis test followed by multiple comparisons Dunn's test. *** P<0.001, **** P<0.0001 versus control (200ppm iron).

5.4.2 Analysis of intestinal fibrosis in chronic colitis in mice treated with repeated cycles of dextran sulphate sodium

Masson's trichrome staining was used to assess the degree of fibrosis following chronic DSS treatment. Collagen deposition was shown by blue staining in the mucosa and submucosa (Figure 5-12).

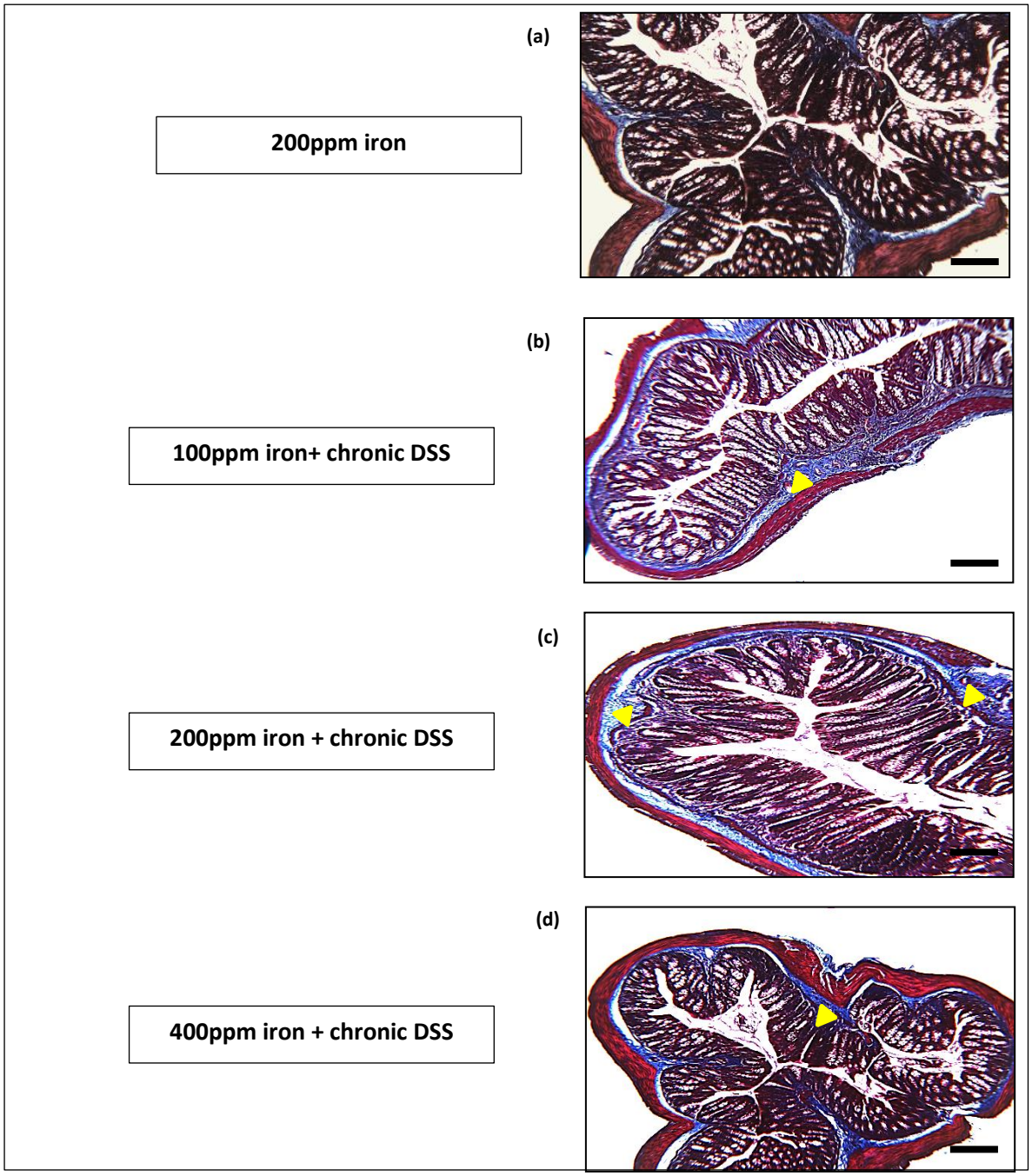

Figure 5--12: Masson's trichrome staining of the colonic tissues of (b) 100ppm iron; (c) 200ppm iron; (d) 400ppm iron mice with dextran sulphate sodium (DSS)-induced colitis at day-63, and 200ppm iron controls (a). The extracellular matrix is blue in colour in the mucosal and submucosal layers. Arrowheads (yellow) highlight submucosal fibrosis. (10x magnification).

In chronic Crohn's disease (CD) intestinal fibrosis may occur [124]. In this research, we observed thickening of the colon of mice with chronic DSS-induced colitis. Masson's trichrome staining was used to assess fibrosis (Table 5-2) [141] and slides were scored by a researcher blinded to the treatment group.

Category	Score	Description
Collagen (fibrosis)	0	No increase
	1	Increased in the submucosa
	2	Increased in the mucosa
	3	Increased in the muscularis mucosa; thickening/disorganisation of the muscularis mucosa
	4	Increased in the muscularis propria (evident increase in collagen fibrils for Sirius red)
	5	Gross disorganisation of muscularis propria; increased Sirius red/GFP or thickening of the serosa
Percent involvement	1	1-25% of section
	2	26-50% of section
	3	51-75% of section
	4	76-100% of section

Table 5-2: Histological fibrosis scoring system adapted from Ding S. *et al.* [122]

Mice in the 100ppm iron DSS-treated group had significantly more fibrosis than the DSS-treated mice receiving 200ppm iron and 400ppm iron diets (Figure 5-13).

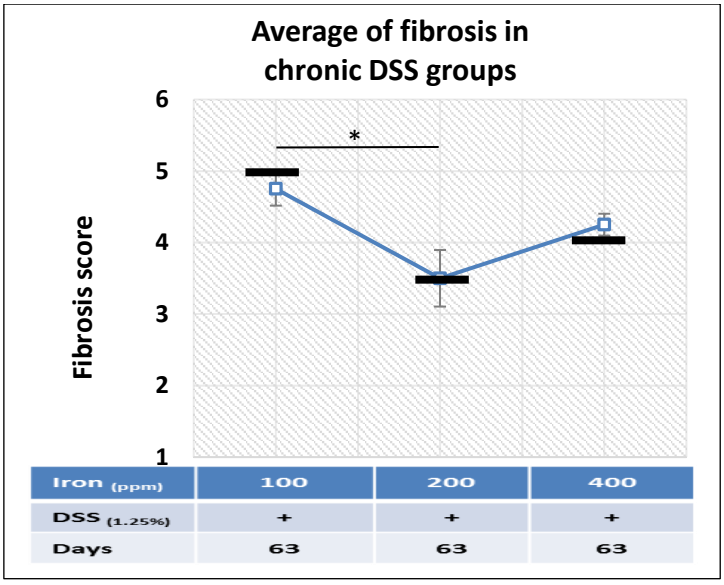

Figure 5-13: Fibrosis scores for all groups of DSS-treated mice on different iron diets. Horizontal lines at the median. Data are presented as a mean ± standard error of the mean. Differences were tested by Kruskal–Wallis test followed by multiple comparison Dunn's test. ($P<0.05$)

5.5 Measuring the faecal calprotectin concentration in chronic DSS-treated wild-type (C57BL/6) mice at different time points during the 63-day course

Faecal calprotectin concentrations were measured using the S100A8/S100A9 ELISA as described in Chapters 2 and 3. Faecal pellets were collected from the cage of each mouse in all groups at days-1, 21, 42 and 63. Faecal calprotectin concentration was measured and the difference between samples taken at different time points was used to assess the degree of inflammation in DSS-treated animals after each cycle. However, any difference in untreated groups will show whether the diet has any effect on intestinal cells and their response during the time course as shown in Figure 5-14.

In mice treated with DSS, faecal calprotectin levels increased after each cycle of treatment in those receiving 100 and 400ppm iron, but not in those taking 200ppm iron. However, there was no any statistical significance between any of the groups as illustrated in Figure 5-14.

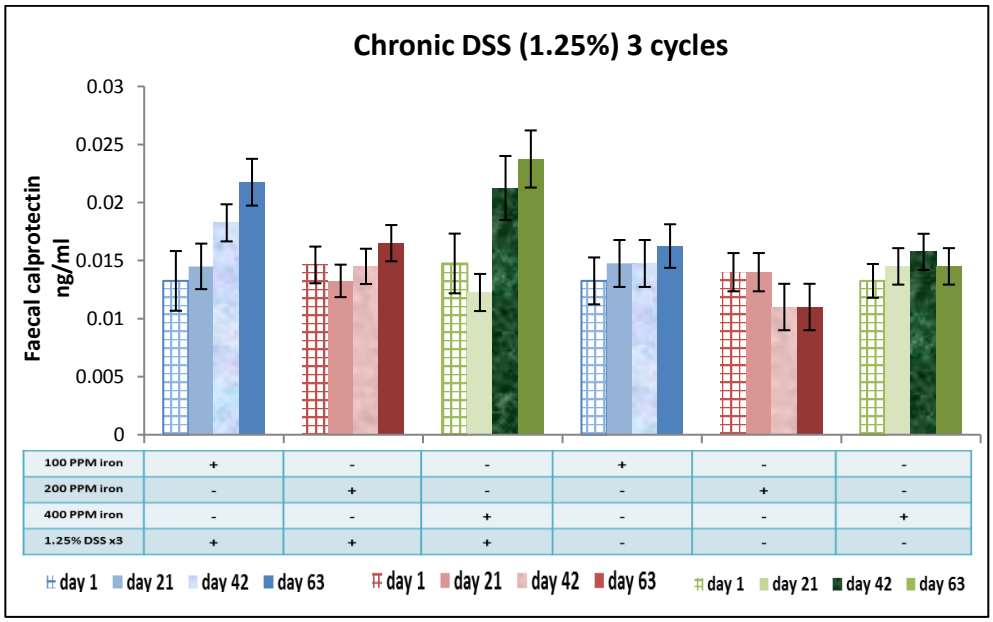

Figure 5-14: Faecal calprotectin at four different time points (day-1, 21, 42 and 63) for six groups, three DSS-treated and three untreated controls. Data are presented as a mean ± standard error of the mean. Differences were tested by Kruskal– Wallis test followed by multiple comparison Dunn's test.

Comparison of faecal calprotectin concentration in each pair of groups taking similar diets (DSS-treated and untreated) showed the effects of DSS for a given amount of iron. Only the comparison in mice taking 400ppm iron showed a difference between day-21 and day-63 in the mice receiving DSS (Figure 5-15).

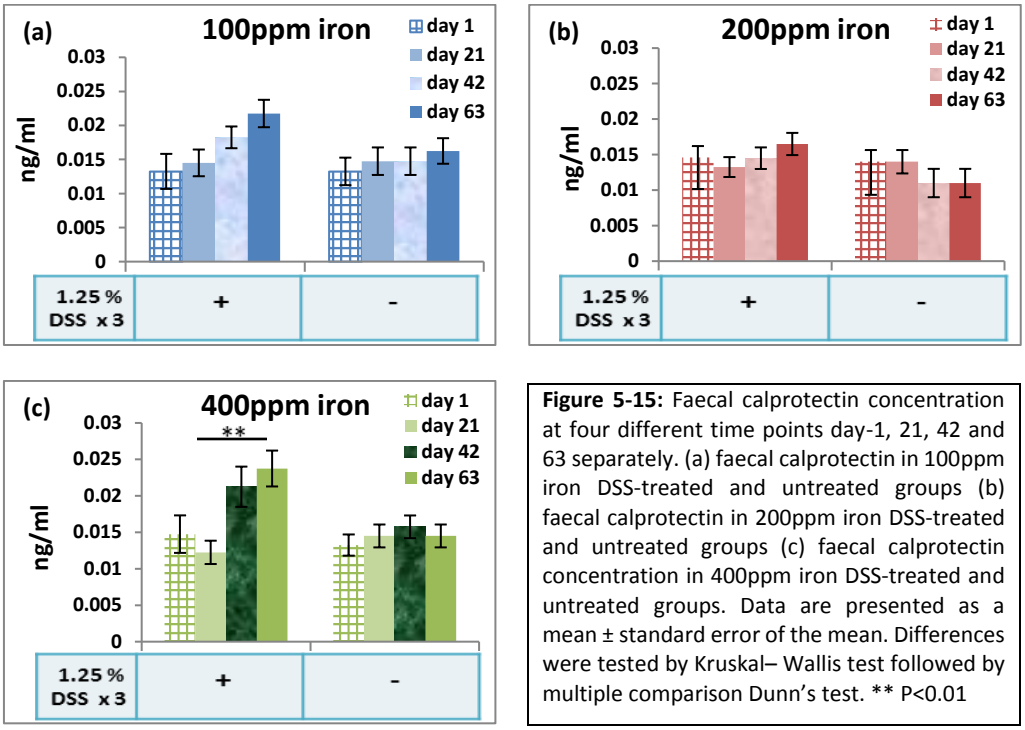

Figure 5-15: Faecal calprotectin concentration at four different time points day-1, 21, 42 and 63 separately. (a) faecal calprotectin in 100ppm iron DSS-treated and untreated groups (b) faecal calprotectin in 200ppm iron DSS-treated and untreated groups (c) faecal calprotectin concentration in 400ppm iron DSS-treated and untreated groups. Data are presented as a mean ± standard error of the mean. Differences were tested by Kruskal– Wallis test followed by multiple comparison Dunn's test. ** P<0.01

5.5.1 Evaluating gut inflammation at the molecular level by measuring faecal calprotectin in 2% DSS-treated (53-days on diets) and untreated mice during 10-day course

Faecal calprotectin concentrations measured from samples taken at two different time points' day-1 and day-10 for all groups. However, samples did not show any significant differences when comparing all groups together (Figure 5-16). However the study is likely to be underpowered.

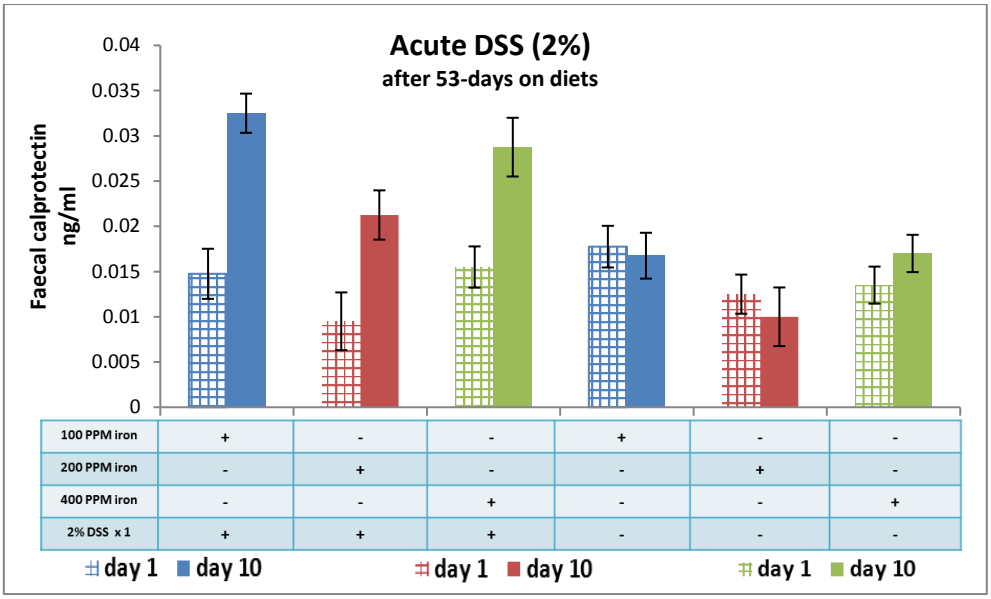

Figure 5-16: Faecal calprotectin at two different time points (day-1 and 10) for n=4 mice each group. Data are presented as a mean ± standard error of the mean. Differences were tested by Kruskal–Wallis test followed by multiple comparison Dunn's test.

However, comparing faecal calprotectin in each pair of groups taking similar diets (DSS-treated and untreated) revealed that, the change in faecal calprotectin concentration from day-1 vs. day -10 was significant for each DSS-treated group. The 100ppm iron diet DSS-treated mice had a greater difference between time points than that the other groups are receiving 200 and 400ppm iron (Figure 5-17).

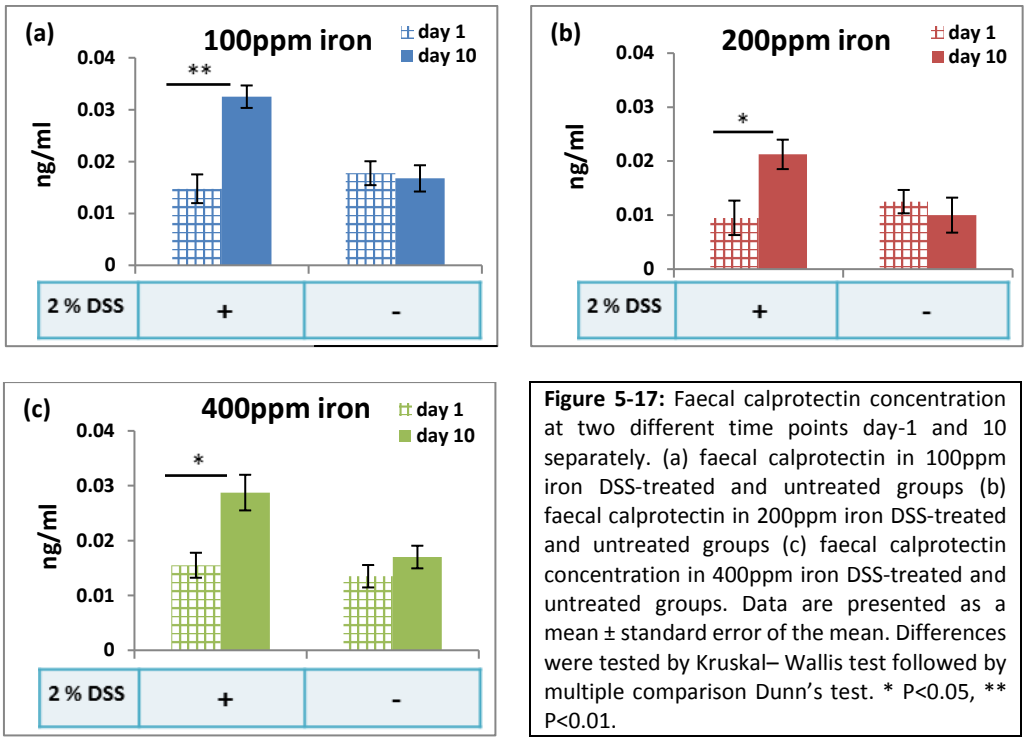

Figure 5-17: Faecal calprotectin concentration at two different time points day-1 and 10 separately. (a) faecal calprotectin in 100ppm iron DSS-treated and untreated groups (b) faecal calprotectin in 200ppm iron DSS-treated and untreated groups (c) faecal calprotectin concentration in 400ppm iron DSS-treated and untreated groups. Data are presented as a mean ± standard error of the mean. Differences were tested by Kruskal– Wallis test followed by multiple comparison Dunn's test. * P<0.05, ** P<0.01.

5.6 The measurement of the total faecal iron concentration in chronic DSS-treated and untreated mice during 63-day course at different time points

Faecal iron was measured using the same kit [MAK025, Sigma-Aldrich] as described previously (Chapters 2 and 3). Faecal iron concentrations were measured at days-1, 21, 42 and 63. The difference between samples taken at these time points can reflect colitis severity (luminal bleeding) in DSS-treated animals. The difference in untreated mice can be used to indicate the effect of dietary iron consumption. However, by comparing all groups together, no statistical significance was shown (Figure 5-18).

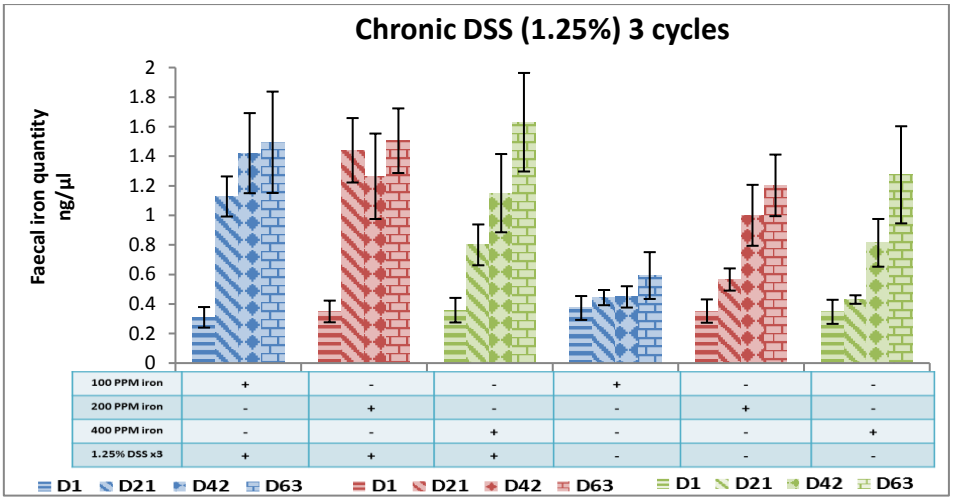

Figure 5-18: Faecal iron concentration at four different time points (day-1, 21, 42 and 63) for six groups, three DSS-treated and three untreated controls. Data are presented as a mean ± standard error of the mean. Differences were tested by Kruskal– Wallis test followed by multiple comparison Dunn's test.

Comparing faecal iron in each pair of groups taking similar diets (DSS-treated and untreated) showed the effects of DSS for a given amount of iron consumed. DSS-treated mice taking 400ppm iron showed a difference between day-1 and day-63 only, while 100 and 200ppm iron mice receiving DSS both showed significant differences at day-1 vs. day-21, 42 and 63 (Figure 5-19). A significant increase in faecal iron concentration was observed over the course of the experiment in control mice with fed 200ppm iron and 400ppm iron, but this was not seen in mice on 100ppm iron (Figure 5-19).

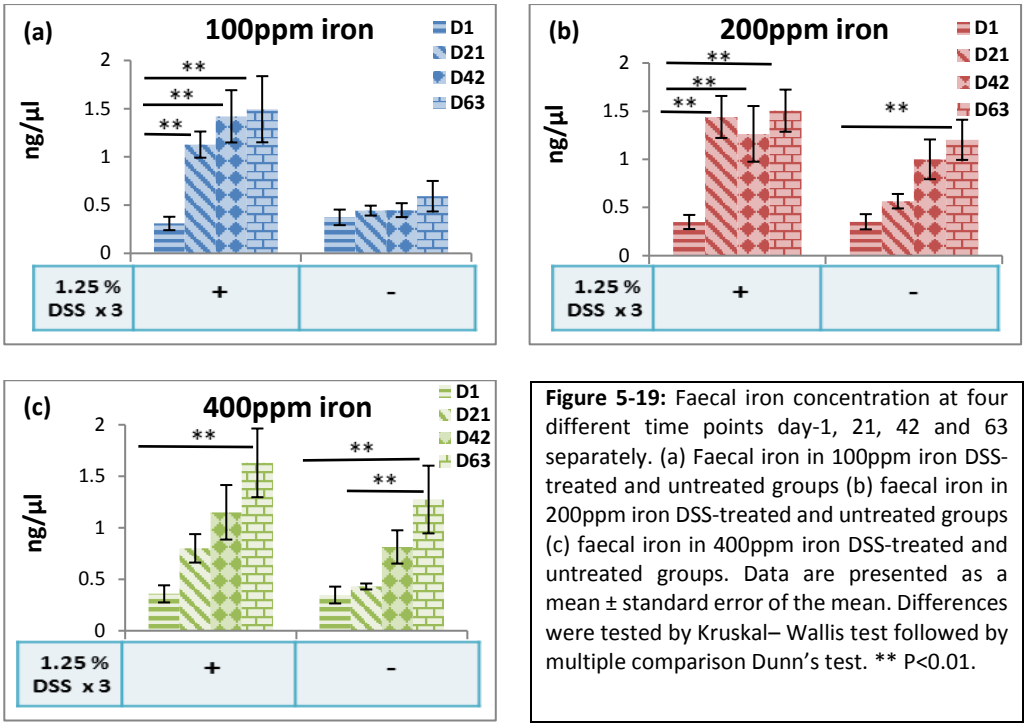

Figure 5-19: Faecal iron concentration at four different time points day-1, 21, 42 and 63 separately. (a) Faecal iron in 100ppm iron DSS-treated and untreated groups (b) faecal iron in 200ppm iron DSS-treated and untreated groups (c) faecal iron in 400ppm iron DSS-treated and untreated groups. Data are presented as a mean ± standard error of the mean. Differences were tested by Kruskal– Wallis test followed by multiple comparison Dunn's test. ** P<0.01.

5.6.1 The measurement of the total faecal iron concentration in 2% DSS-treated and untreated mice (on diets 53-days) during 10 -day course

The bar chart below illustrates the difference between samples taken at two different time points, day-1 at the start of 2% DSS treatment and day-10 when mice were euthanised and same points for the controls. When the DSS-treated and untreated groups were compared together, there was no any significant difference (Figure 5-20). However the study is likely to be underpowered.

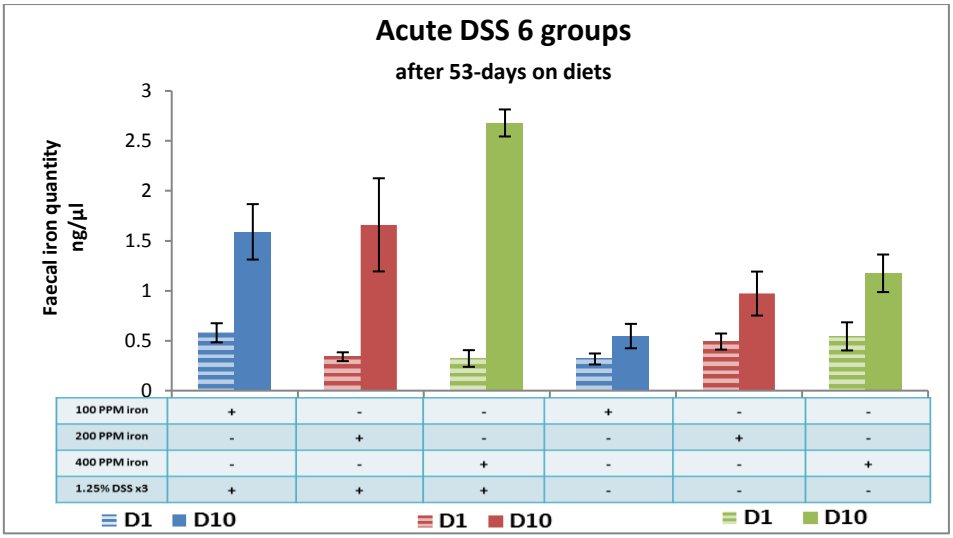

Figure 5-20: Faecal iron concentration at two different time points (day-1 and 10) for six groups (n=4 mice each) three DSS-treated and three untreated controls. Data are presented as a mean ± standard error of the mean. Differences were tested by Kruskal– Wallis test followed by multiple comparison Dunn's test.

Once again, when all diet-matched groups were compared, DSS-treated mice showed significant differences between day-1 and day-10 for each group. This was more pronounced in the 400ppm iron group. Untreated mice did not reveal any differences apart from the 400ppm iron group which has a statistical difference between day-1 and-10 (Figure 5-21).

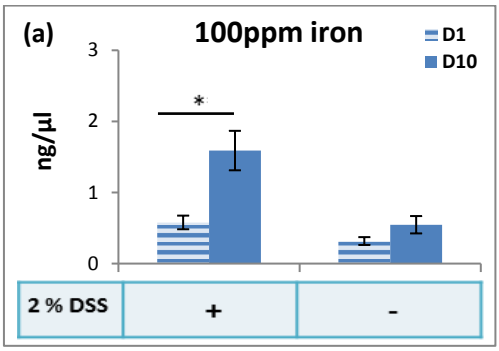

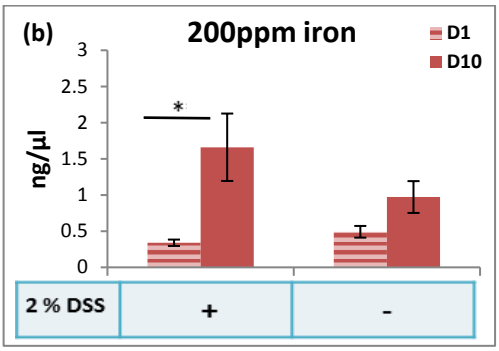

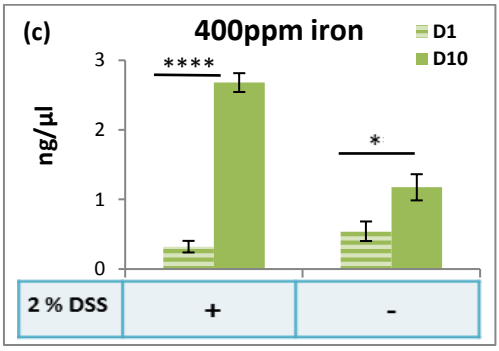

Figure 5-21: Faecal iron concentration at two different time points day-1 and 10 separately. (a) Faecal iron in 100ppm iron DSS-treated and untreated groups (b) faecal iron in 200ppm iron DSS-treated and untreated groups (c) faecal iron in 400ppm iron DSS-treated and untreated groups. Data are presented as a mean ± standard error of the mean. Differences were tested by Kruskal– Wallis test followed by multiple comparison Dunn's test.
* P<0.05, **** P<0.0001.

5.7 Discussion

DSS-induced colitis in mice is a popular model for human ulcerative colitis. The mechanism by which DSS induces colitis is unclear. There are several theories including by direct toxic effects on colonic epithelial cells, by activation of macrophage inflammatory responses and by altering the gut microbiota [89]. The majority of published work has used acute IBD animal models. But CD and UC are known as chronic pathologies. In 1990, Okayasu and colleagues described a model in which mice that were given DSS orally developed acute and chronic colitis similar to UC [89].

DSS-induced colitis in mice is characterised by clinical and histological manifestations that are similar to those observed in humans. Therefore, it is important to induce a chronic intestinal inflammation model by administering repetitive cycles of DSS. This model allows observations about the adaptive immune system, mediators and cell Influx involved in the chronification process of IBD [142].

Exposure to dextran sulphate sodium (DSS) induces acute colitis in mice, which usually resolves when DSS is stopped. In order to obtain the chronicity in DSS-induced colitis, mice are classically exposed to three to five cycles of DSS, followed by rest periods [124].

This chapter presents data that clearly demonstrate the importance of both keeping mice longer on different iron diets and repeating DSS cycles to investigate the real influence of iron on chronic as well as acute colonic intestinal inflammatory responses (as it seen be in Figures 5-10 & 5-11). Alterations to the iron level in standard chow diet (200ppm iron) resulted in

increased susceptibility of mice to developing DSS-induced colitis. In chronic DSS phase, 100ppm iron diet DSS-treated wild-type mice showed more weight loss than other DSS-treated mice (on 200 and 400ppm iron diets) at days-8 following DSS administration during the first and third DSS cycles (as it shown in Figure 5-6). However, in the second DSS cycle, the 400ppm iron DSS group lost more weight than the other groups at the same time point (day-8). However, administration of acute DSS treatment to mice that had been established on a 100ppm iron diet for-53 days induced more significant colitis. Thus any modifications in iron consumption can potentially exacerbate the severity of DSS-induced colitis.

The data show two forms of colitis, acute and chronic, as well as recovery phases. This classification is built on clinical symptoms and histopathological changes (epithelial architecture, type of inflammatory infiltrate, and fibrosis) [143]. Microscopic examination revealed extensive damage and increased inflammatory cell infiltration (mononuclear cells (MNC)) in wild-type mice treated with 2% DSS (acute phase), especially the 100ppm iron group which showed worse colitis scores than the other mice. When looking at chronic colitis, after three cycles of 1.25% DSS, all mice exhibited mild-moderate colitis, as shown by weight loss. By histological examination, the colitis score was highest in the 100ppm iron DSS-treated group. Chronic intestinal inflammation resulted in fibrosis in submucosal tissue and the lamina propria as shown by Masson's trichrome stain in all chronic DSS-treated mice [141]. However, these fibrotic changes were more pronounced in the 100ppm iron groups followed by the 400ppm iron then 200ppm iron groups.

To increase the accuracy of this study, colitis was assessed by measuring faecal calprotectin concentrations. DSS-induced colitis leads to cell infiltration by mononuclear cells (MNC) which contain abundant calprotectin molecules. Therefore, when inflammation occurs neutrophils release calprotectin which can be used as an indicator of the degree of inflammation within tissues [129]. The 2% DSS induction phase was characterised by an increase in faecal calprotectin concentration for each group which was significantly higher for those mice on the 100ppm iron diet.

A correlation between the amount of dietary iron consumed and faecal iron excretion in healthy individuals has been proposed. In patients with IBD, faecal iron may also be increased as a result of luminal bleeding during flares of the disease [123]. Iron has a role in intestinal inflammation by producing free radicals which can destroy DNA and damage cells [111]. The iron assay kit gives the option to measure Fe^{3+}, Fe^{2+} or total iron concentration. Therefore, total faecal iron was measured at the end of each DSS cycle to assess bleeding (luminal) as a feature of colitis and dietary iron consumed.

To conclude, in the present chapter, changes in dietary iron intake enhanced both chronic and acute phases of colonic inflammation. The low iron diet had the most major effects on colitis courses (acute and chronic) in terms of body weight changes, histology (colitis and fibrosis) and faecal calprotectin concentration (acute course) in DSS-treated mice. The high iron diet also exacerbated colitis (acute and chronic) but had the most major effects on faecal calprotectin concentration and faecal iron concentration in the untreated control groups.

6 Longitudinal investigation of microbiota dynamics in a model of mild chronic DSS-induced colitis in wild-type C57BL/6 mice receiving diets different with iron contents

6.1 Introduction

Dextran sulphate sodium (DSS) may be used to study colitis in laboratory rodents. The severity of the colitis is influenced by many factors (DSS; MW, concentration, lenghth of exposure) and these may be used to induce different kinds of colitis (severe acute colitis, chronic or semi-chronic colitis). This model (DSS-induced colitis) of colitis has been used to translate murine data to human inflammatory bowel disease (IBD) [82].

The intestinal pathology observed in the acute DSS model remain for a few days after the DSS treatment has been stopped. Therefore, they do not provide a subtle system to assess new therapeutics or the role of the numerous parameters that are involved in intestinal healing [144]. In contrast, the milder chronic DSS treatment model seems to be ideal for assessing the influence of drugs as well as the repair phase of colitis. Moreover, it is now clear that models characterised by mild intestinal damage are more accurate for studying the effects of several therapeutic agents [145].

The importance of the microbiota in the pathogenesis of IBD is supported by the study of several animal models, where the severity of colitis depends on the commensal bacterial strains that are maintained in animals [146]. DSS treatment is associated with a major shift in gut microbiota composition, which leads to an unhealthy state [147]. The administration of antibiotics has been shown to improve both IBD and DSS-induced colitis, indicating the importance of the microbiota's role in disease [148]. This interpretation was supported by a group of researchers from North Carolina University who reported that the simple ingestion

of a lysate of bacterial cells belonging to the *Firmicutes* phylum (which is considered to be a healthy-type phylum), reduced the severity of DSS-induced experimental colitis in mice [149].

In this chapter, we used a reproducible mild chronic colitis model, which allowed us to evaluate intestinal repair processes and the gut microbiota.

6.2 Aims

The aims were to:

1- Characterise the inflammation and the gut microbiota dynamics longitudinally in a DSS-induced murine model of chronic colitis using 16S ribosomal RNA (rRNA) gene surveys.

2- Investigate the effects of long-term supplementation of various iron diets on chronic colitis as well as the gut microbial structure.

6.3 Murine and genomics methods

Groups of C57BL/6 mice were repeatedly (3 cycles) treated with a small dose of DSS (1.25%) dissolved in their drinking water to induce colitis for 5-days, followed by a full (16-days) recovery period. After-53 days on a diet alone, the comparator control groups were divided into two. Four mice in each group continued as controls, and the other four were subjected to an acute (2%) DSS cycle for the last ten days of the chronic experiment (details provided in Chapter 5). Bacterial DNA was extracted from the stool (pellets) collected and 16S rRNA gene sequencing was performed. Operational taxonomic unit (OTU) selection, microbial composition and community structure analyses and metagenome inference were conducted in collaboration with the CGR. For details on DNA extraction and sequencing, see Methods chapter. Finally, statistical analysis in this chapter was undertaken in a similar way to that used for the microbiome data generated after acute DSS exposure (Chapter 4).

6.4 Statistical analysis of metagenomic profiles for two as well as multiple groups

The STatistical Analysis of Metagenomic Profiles (STAMP) software package was used for metagenomic profiles analysis. This generated phylogenetic profiles representing the number of indicator genes allocated to different taxonomic units or functional outlines representing the number of sequences assigned to various subsystems or pathways [132]. The bioinformatic analysis of the microbiota data for chronic groups used Kruskal-Wallis H-test to compare day-1, 21, 42 and 63 together. The false discovery rate (FDR) (multiple correction tests) was used

for all groups to produce a prioritised list of OTUs that summarise observed differences between user-defined populations. The q-value is the adjusted p-value based on FDR calculation, where differences were considered statistically significant at $P<0.05$.

For paired-end sequence data, there are three sequence file types. The files labelled R1 and R2 contain the corresponding paired-end sequences. The singlet files contain sequences whose pair has been removed due to poor sequence quality or adapter contamination. If a sample has been sequenced several times, there will be several sets of sequence files in the sample directory. These will need to be concatenated before downstream analysis. (See Appendix-5 and-6).

6.4.1 Bacterial diversity data analysis at phylum level (Summary and plot of the taxonomic content of each sample) for chronic experiments

The intestinal microbiota of mice was characterised using the fully-validated 16S ribosomal RNA (rRNA) gene surveys. We investigated the effects of long-term adjustments to luminal iron content on mild-chronic as well as severe acute colitis status and gut microbial structure in wild-type mice. A linear analysis was undertaken for gut microbial communities, pre- and post-treatment with three cycles of 1.25% DSS i.e. day-1, 21, 42 and 63 along with control groups at the same time points.

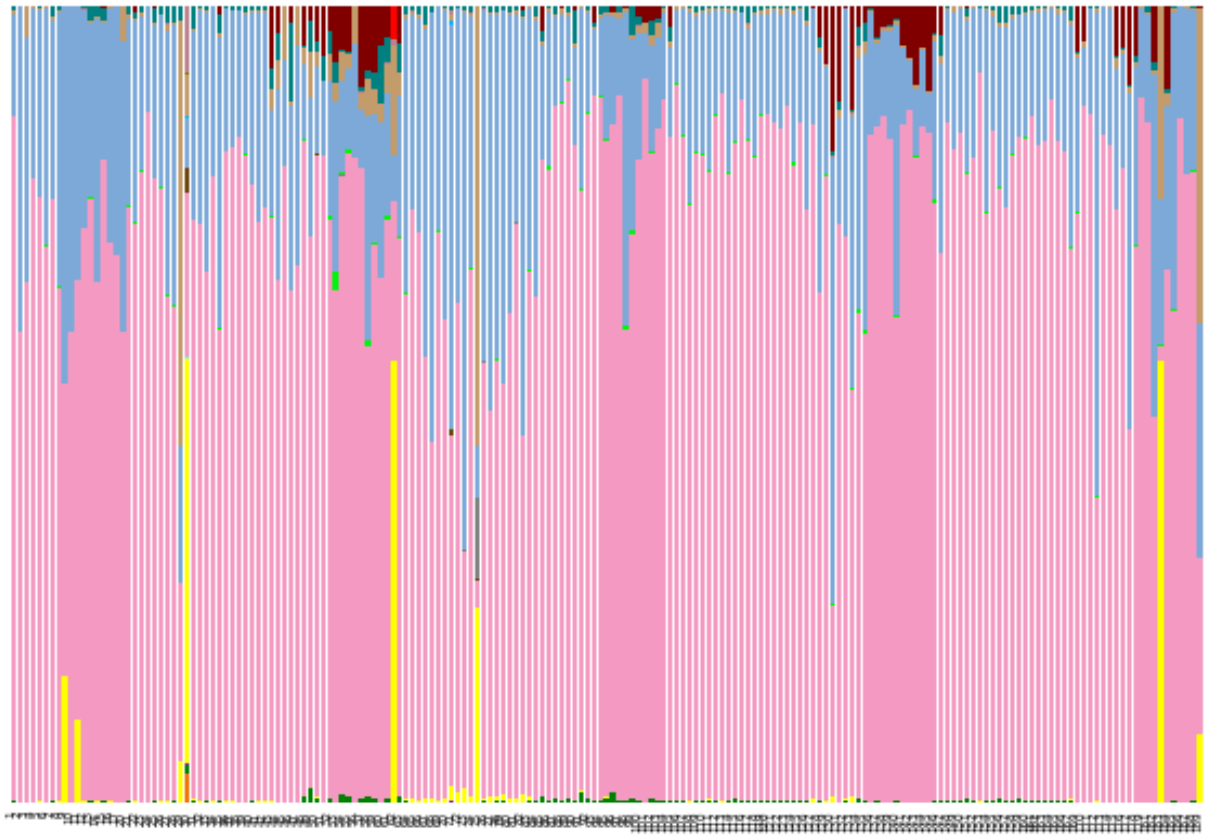

Figure 6-1: Phylum-level taxonomic composition of all samples (relative abundance).
Note: all samples identifications are listed in appendix -4 and legends in appendix -2

6.4.1.1 Alpha diversity estimation and alpha rarefaction analyses

To negate the effect of sample size and to estimate species richness within each sample (alpha diversity), OTU tables were repeatedly sub-sampled (rarefied). For each rarefied OTU table, three measures of alpha diversity were estimated: chao1, the observed number of species, and the phylogenetic distance. These estimates were plotted as rarefaction curves using Qiime (Figures 6-2,-3 and -4).

Chao1

Chao1 is a nonparametric estimator that predicts the minimum species richness of a sample.

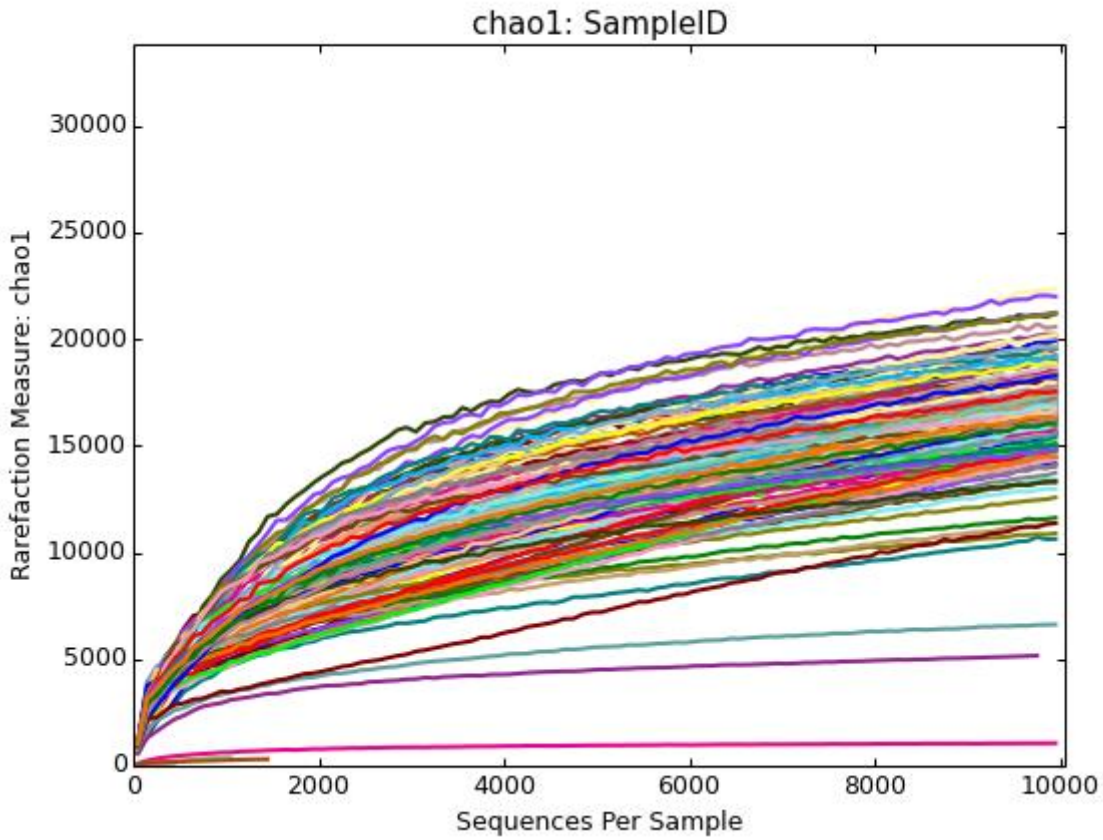

Figure 6-2: Rarefaction curves of the observed number of species metric for all samples (> 500 reads). The plot shows the average number of distinct OTUs found in sub-samples of increasing number of sequences.

Observed species

The observed number of species is defined as the number of distinct OTUs within a sample.

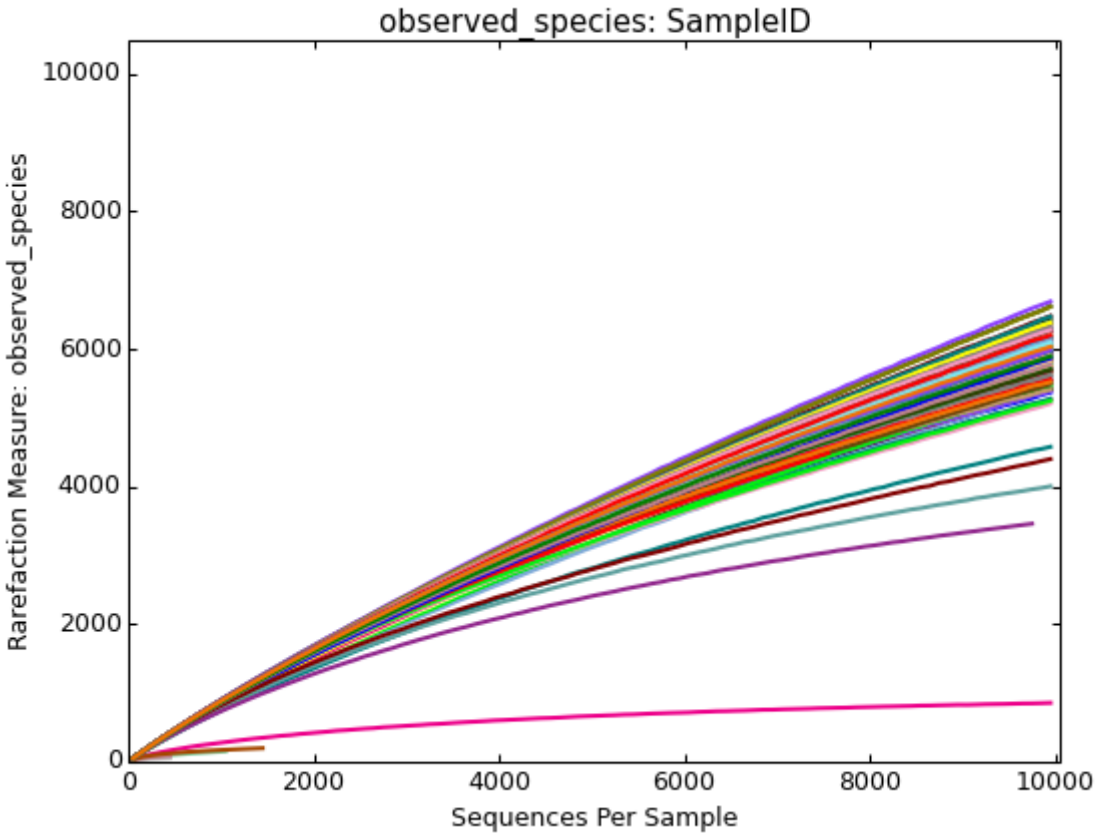

Figure 6-3: Rarefaction curves of the observed number of species metric for all samples (> 500 reads). The plot shows the average number of distinct OTUs found in sub-samples of increasing number of sequences.

PD (phylogenetic diversity)

The PD metric represents the minimum total branch length that covers all taxa within the sample on a phylogenetic tree (Faith *et. al., 1992*). A smaller PD value therefore indicates a reduced expected taxonomic diversity whilst a large PD value indicates a higher expected diversity.

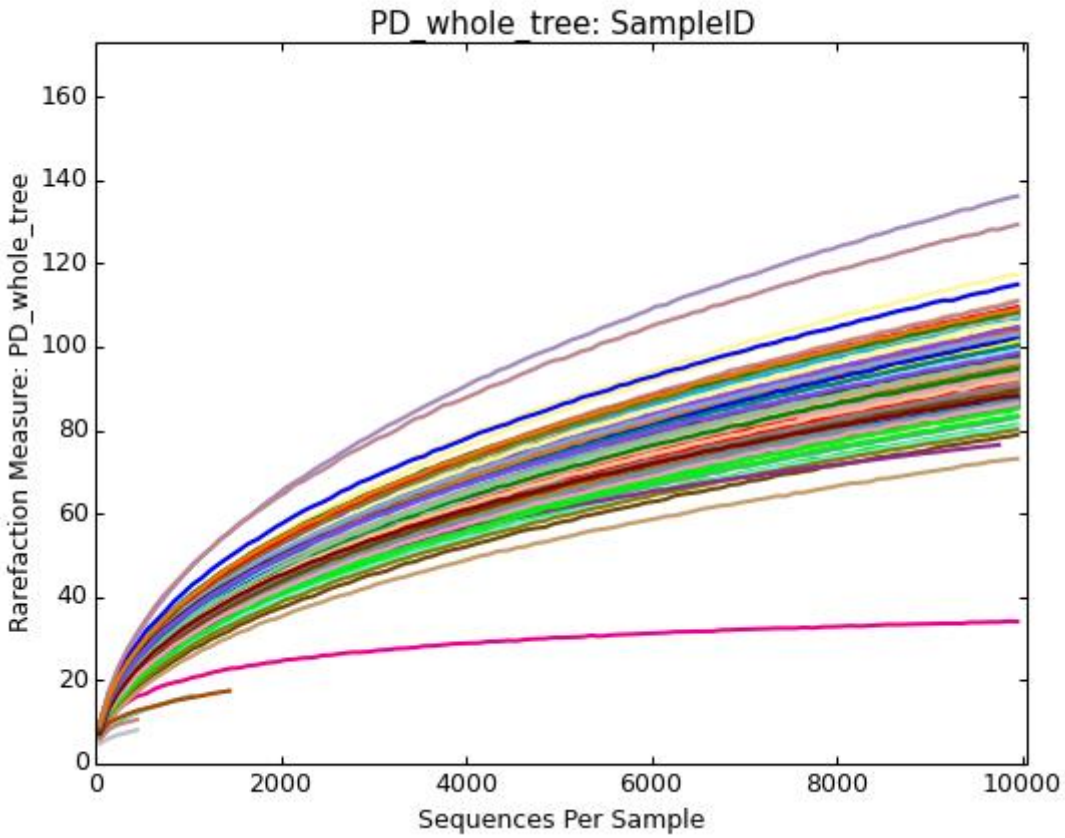

Figure 6-4: Rarefaction curves of the PD metric represents the minimum total branch length that covers all taxa within the sample on a phylogenetic tree. The plot shows the average number of distinct OTUs found in sub-samples of increasing number of sequences.

6.4.1.2 Estimate of beta diversity, generate UPGMA trees and 2D PCoA plots

To allow inter-sample comparisons (beta-diversity), all datasets were sub-sampled (rarefied) using the Qiime script. Rarefied OTU tables were used to calculate weighted and unweighted pair-wise UniFrac matrices using Qiime. UniFrac matrices were then used to generate UPGMA (Unweighted Pair-Group Method with Arithmetic mean) trees and 2D principal coordinates plots (PCoA).

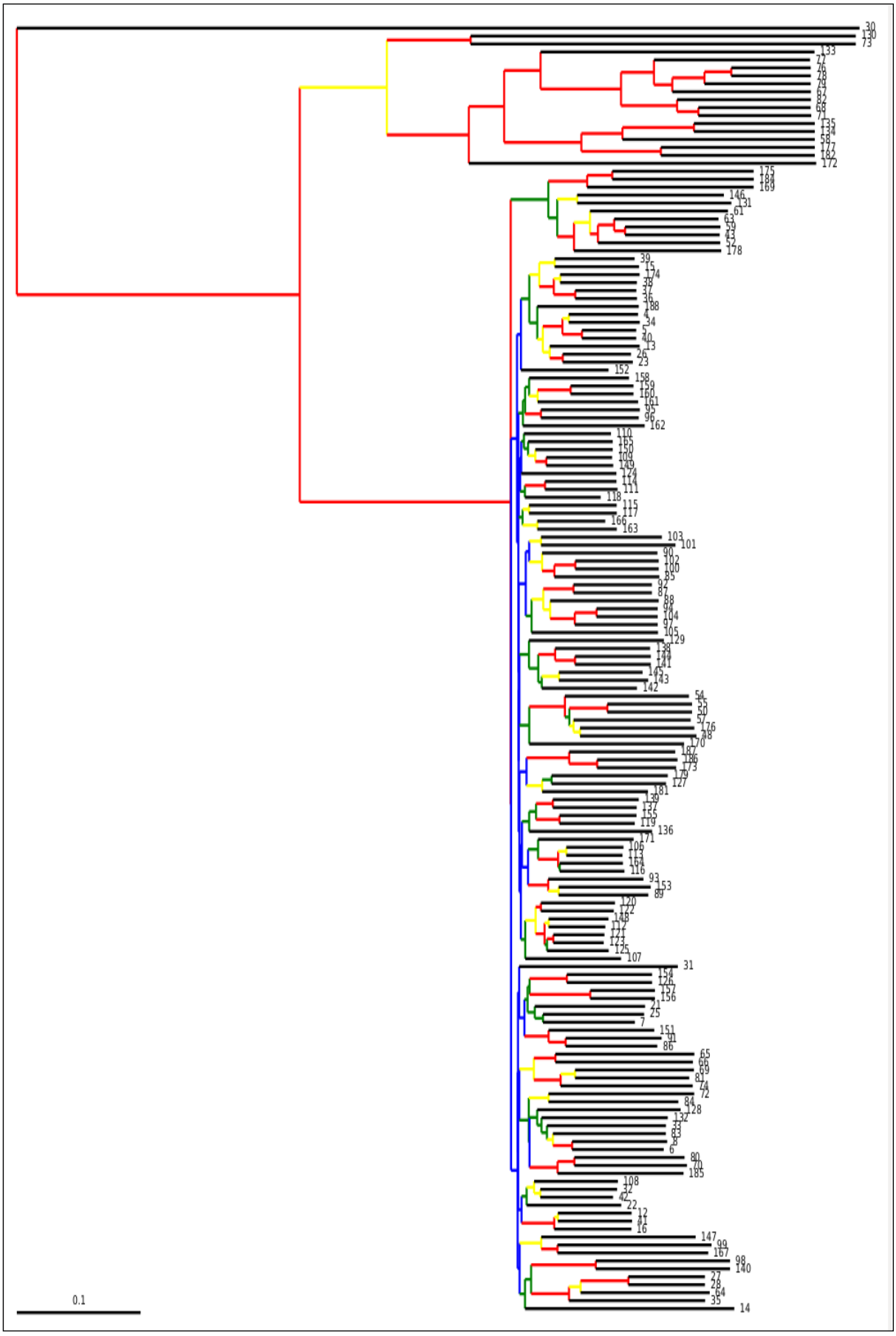

Figure 6-5: UPGMA (Unweighted Pair-Group Method with Arithmetic mean) trees.

The multidimensionality of the data was reduced first by an OTU-based method - Principal Component Analysis (PCA) for each group separately. Principal component analysis was used to identify linear combinations of gut microbial taxa associated with the duration on a diet. The phylogeny-based method, UniFrac, was then applied, where UniFrac accounts for the phylogenetic divergence between OTUs. Our data showed an overlap in the samples of 100 and 200ppm iron DSS-untreated and 200ppm iron DSS-treated mice in PCAs on unweighted (qualitative) UniFrac distances (Figure 6-6 a, c and d). There was clustering with little separation of samples pre and post-DSS treatment for 100 and the 400ppm iron DSS-treated groups as well as with control mice fed a 400ppm iron diet (Figure 6-6 b, e and f). Interestingly, the high iron diet disturbed the microbial community in both DSS-treated and untreated mice.

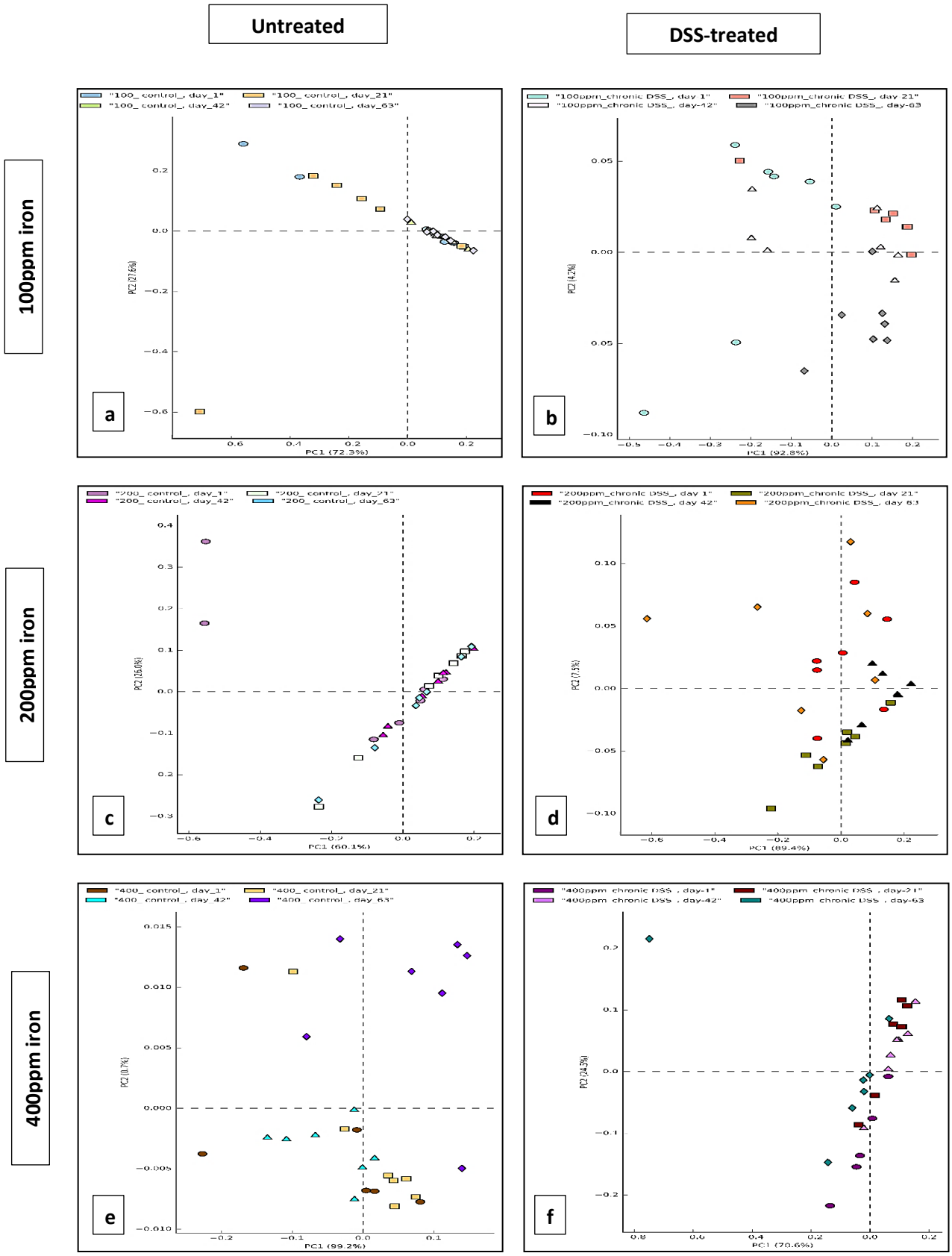

Figure 6-6: PCA plots of the unweighted UniFrac distances of pre-and post DSS-intervention stool samples from chronic (3 cycles) DSS-treated mice (b, d, and f) and (a, c and e) untreated mice at Phylum-level, phylogenetic classification of 16S rRNA gene sequences. Symbols represent data from individual mice, color-coded by the indicated metadata. Statistical differences were assessed by Kruskal-Wallis H-test followed by Storey's FDR multiple test correction.

6.4.1.3 Increased bacterial diversity at phylum level for 100ppm iron DSS-treated mice

Post-hoc test revealed the only significance difference in 100ppm iron chronic DSS-treated mice was for the phylum (*Proteobacteria*). The extended error bar plot for the 100ppm iron DSS-treated group (Figure 6-7), illustrates the mean proportion of sequences assigned to one phylum (*Proteobacteria*) within this group. Moreover, the graph shows the difference in mean proportion between the two-time points along with the associated confidence interval of this effect size and the p-value of the specified statistical test. There was a significant increase in day-63 vs. days-1 and 21 with P<0.05.

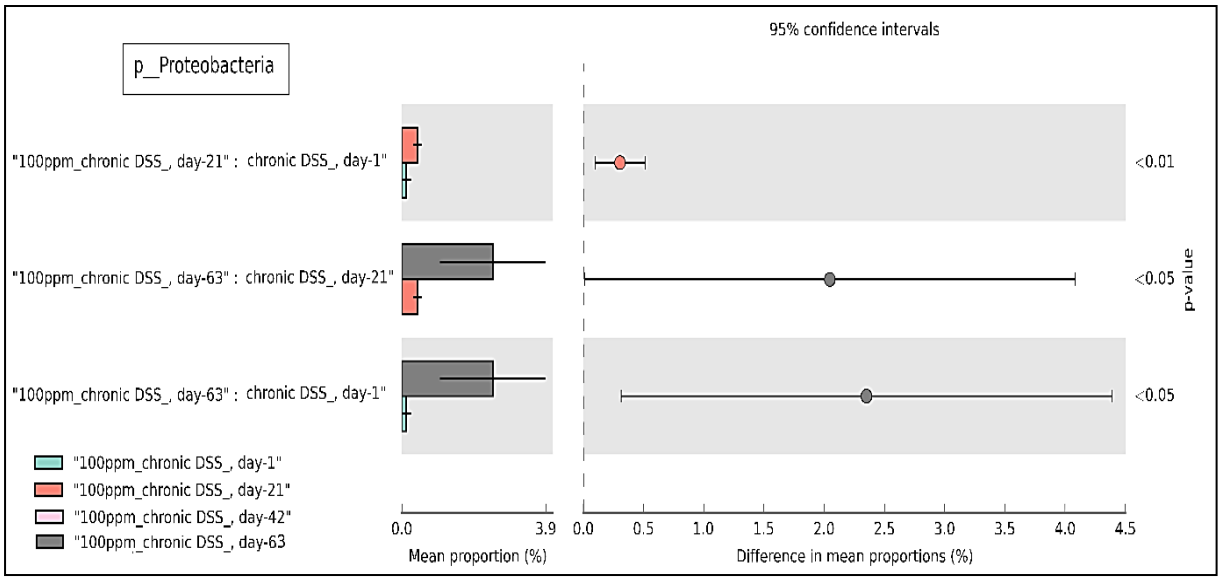

Figure 6-7: Extended error bar plot for one phylum (*Proteobacteria*) that showed a difference between the proportions on days-1, 21 and day-63 for 100pm iron DSS-treated mice. This Post-hoc plot for this phylum indicates *1)* the mean proportion of sequences at four-time points, *2)* the difference in mean proportions for *Proteobacteria* comparing pre-and post-DSS treatment, and *3)* a p-value indicating if the mean proportion is equal for each time point. Statistical differences were assessed by Kruskal-Wallis H-test followed by Storey's FDR multiple test correction.

The box plot graph below (Figure 6-8) shows a concise summary of the allocation of the proportions of *Proteobacteria* at various time-points within the 100ppm iron DSS-treated group.

There was a variation in assigned sequences for *Proteobacteria* within the 100ppm iron DSS-treated group when comparing days-1, 21, 42 and 63 samples. There were differences between the pre and post-DSS intervention: analysis of the experimental murine microbiota at the phylum level indicated that the abundance was increased significantly at day-63 for *Proteobacteria* (P<0.017) as shown in Figure 6-8.

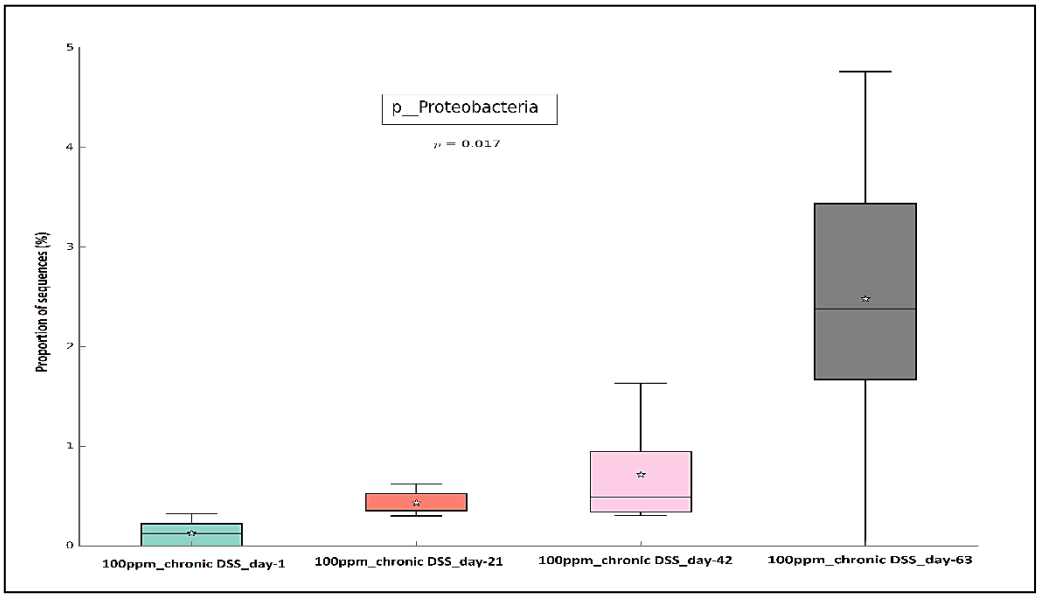

Figure 6-8: Box plot showing the distribution in the proportion of *Proteobacteria* assigned to samples at day-1, 21, 42 and 63 from 100ppm iron DSS-treated mice. The boxes show the IQR (75^{th} to 25^{th} of the data), whiskers extend to the most extreme value within 1.5*IQR, and any outliers are shown as crosses. The median value appears as a line within the box and the mean value as a star. Statistical differences were assessed by Kruskal-Wallis H-test followed by Storey's FDR multiple test correction.

6.4.1.4 The effect of high iron diet (400ppm iron) on gut microbiota composition

The heat map is useful for the graphical display of data from 16S rRNA high-throughput sequencing studies such as microbial analysis. Therefore, the heat map (Figure 6-9) represents the relative abundance (0.0-1.3%) of 2 phyla (*Proteobacteria* and *Actinobacteria*) for 400ppm iron untreated mice at days-1, 21, 42 and 63. An increase is shown in the sequences assigned for *Proteobacteria* and *Actinobacteria* starting from day-1 until day-63 as it was shown by the post-hoc test.

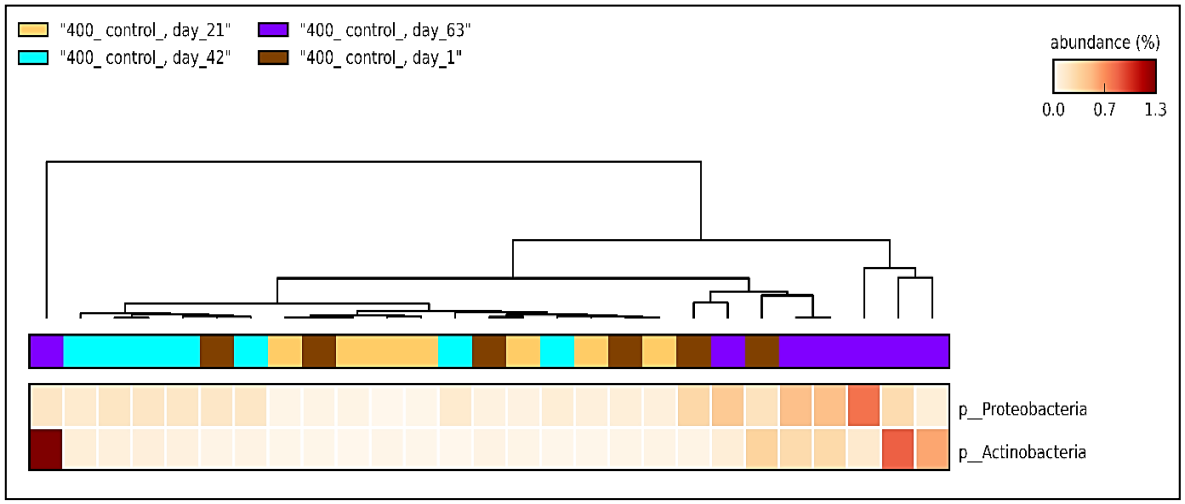

Figure 6-9: Heat map at Phylum-level, phylogenetic classification of 16S rRNA gene sequences representing relative abundances for the 400ppm iron group. Statistical differences were assessed by Kruskal-Wallis H-test followed by Storey's FDR multiple test correction.

A post hoc test showing the mean proportion of sequences assigned only to *Proteobacteria* is represented in Figure 6-10. This showed a significant rise in this phylum at day-42 vs. day-21 ($P<0.001$) and day-63 vs. day-21 ($P<0.05$).

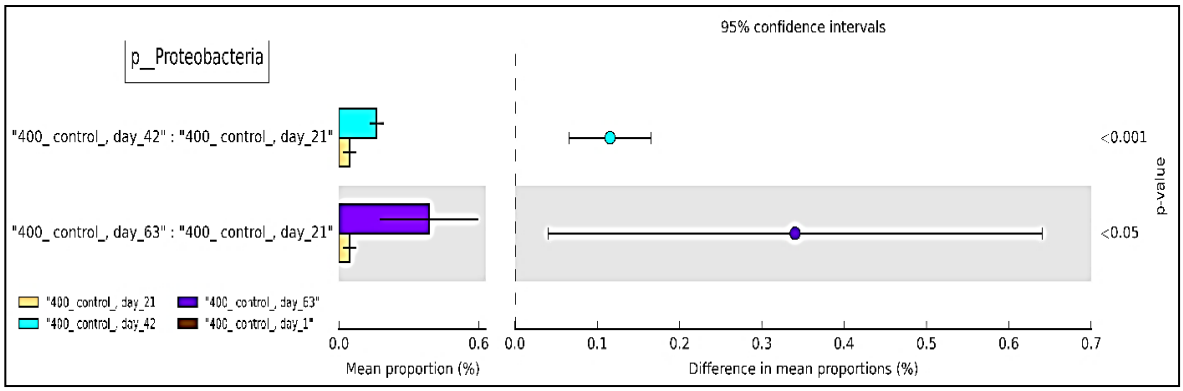

Figure 6-10: Extended error bar plot for *Proteobacteria* that have a difference between the proportions of day-21, 42 and 63 for 400pm iron untreated mice. This Post-hoc plot for *Proteobacteria* indicating *1)* the mean proportion of sequences at day-21, 42 and 63, *2)* the difference in mean proportions, and *3)* a p-value indicating if the mean proportion is equal for each time point. Statistical differences were assessed by Kruskal-Wallis H-test followed by Storey's FDR multiple test correction.

However, a clearer summary of the proportions for *Proteobacteria* and *Actinobacteria* in 400ppm iron DSS-untreated mice is presented in the box plot graph (Figure 6-11), showing a variation in those two phyla comparing day-1, 21, 42 and 63 samples. Nevertheless, analysis of the experimental murine microbiota indicated that the proportion increased significantly over time-course for *Proteobacteria* and *Actinobacteria* with P<0.011 each. The significant differences were observed most in the day-63 samples as illustrated in Figure 6-11.

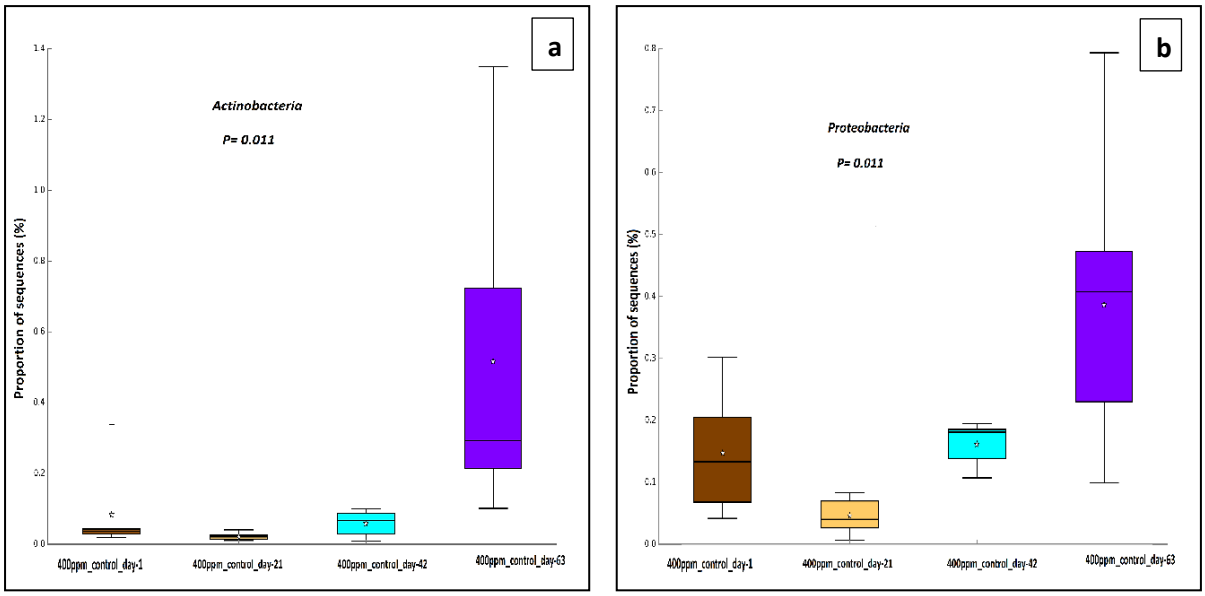

Figure 6-11: Box plot showing the distribution in the proportion of two phyla (*Actinobacteria* **(a)** and *Proteobacteria* **(b)**) assigned to samples from 400ppm iron untreated mice. Statistical differences were assessed by Kruskal-Wallis H-test followed by Storey's FDR multiple test correction.

6.4.1.5 Dysbiosis of microbiota composition at phylum level in 400ppm iron DSS- treated wild-type mice

The analysis of faecal samples at day-1, 21, 42 and 63 for mice in the 400ppm iron DSS-treated group showed a big relative abundance range (0.0-90.8%) as demonstrated in Figure 6-12. However, the proportion of the sequences for the two phyla (*Bacteroidetes* and *Proteobacteria*) was increased from day-1 until day-63.

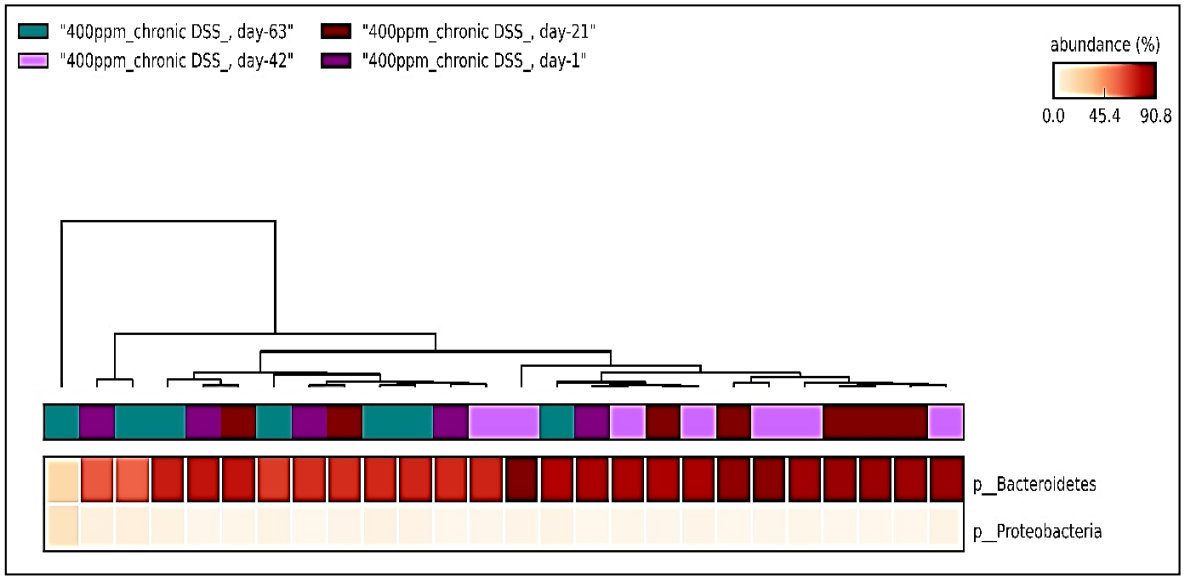

Figure 6-12: Heat map at Phylum-level, phylogenetic classification of 16S rRNA gene sequences representing relative abundances for each pre- or post-DSS intervention for the 400ppm iron group. Statistical differences were assessed by Kruskal-Wallis H-test followed by Storey's FDR multiple test correction.

In the box plot graphs below, the distribution of proportions at different time points for each phylum in the 400ppm iron DSS-treated group is indicated using a box-and-whiskers graphic (Figure 6-13). There were differences in *Bacteroidetes* and *Proteobacteria* comparing day-1, 21, 42 and 63 within the 400ppm iron DSS-treated group. However the differences between the pre and post-DSS intervention samples indicated that the proportion was increased significantly with time for *Proteobacteria* (P<0.016), and decreased for *Bacteroidetes* (P<0.028) as shown in Figure 6-13.

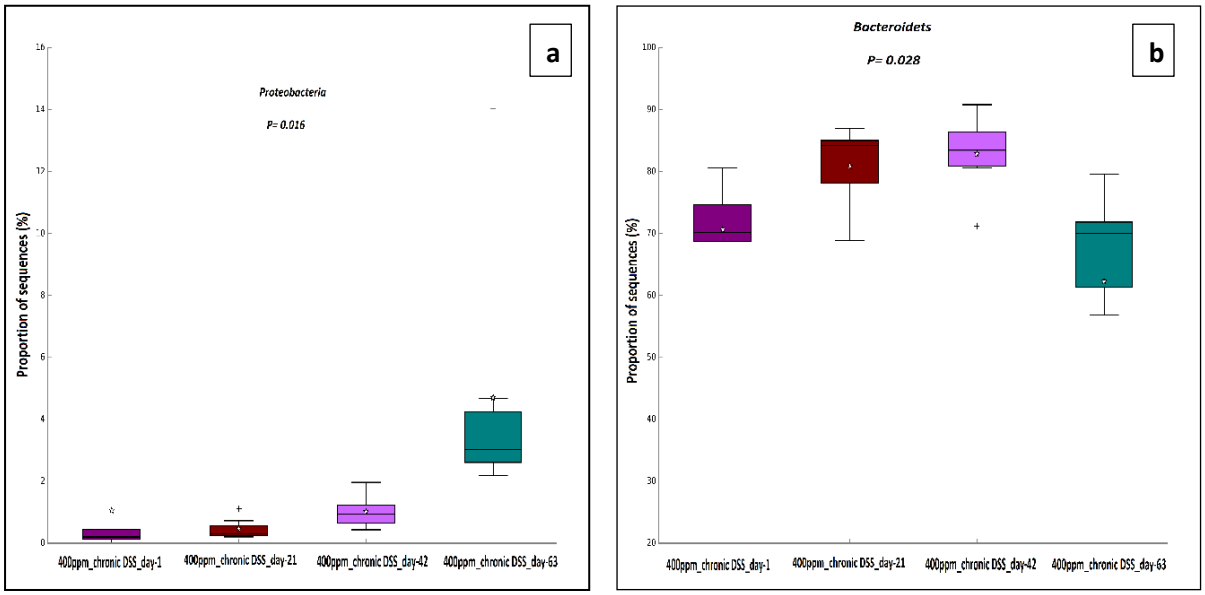

Figure 6-13: Box plot showing the distribution in the proportion of two phyla (*Proteobacteria* **(a)** and *Bacteroidetes* **(b)**) assigned to samples from 400ppm iron DSS-treated mice. Statistical differences were assessed by Kruskal-Wallis H-followed by Storey's FDR multiple test correction.

6.4.2 Microbiota composition at taxonomic level (genus) lower than phylum level in faecal samples of chronic DSS experiments

To further evaluate the performance of gut microbiota, we analysed high-throughput 16S amplicon reads data that were generated from sets of murine faecal samples by the Illumina MiSeq platform. Analysis of the bioinformatics data started from the Phylum taxonomic level and continued deeper to reach the lowest level that showed significance differences. Ultimately, we found that the number of genus level assignations was higher and statistically significant in both the 100ppm iron and 400ppm iron DSS-treated mice as well as in the 400ppm iron untreated animals.

The Kruskal-Wallis H-test post-hoc test along with effect size, and multiple test correction method (Storeys FDR) were used after quality filtering steps resulted in the identification of four phyla and 15 taxa (genera). Of the four phyla [*Firmicutes*, *Bacteroidetes*, *Proteobacteria*, and *Actinobacteria*], one phylum (*Firmicutes*) was highly abundant among all groups while the lowest abundance phylum was *Actinobacteria*. However, 100ppm iron and 400ppm iron DSS groups showed seven different genera apart from the three genera (*Bacteroides*, *Lactobacillus* and *Bilophila*) that they shared. The results of the relative abundances of various phyla and identified genera are summarised in Table 6-1, 2 and 3.

STAMP encourages the use of effect sizes and confidence intervals in evaluating biological importance. Effect size is a simple method of quantifying the difference between groups, which has several advantages over the use of tests of statistical significance [150].

100ppm iron DSS-treated group			
Taxon	**p-values**	**p-values (corrected)**	**Effect size**
p_*Bacteroidetes*; g_*Bacteroides*	0.003	0.047	0.496
p_*Bacteroidetes*; g_*Odoribacter*	0.002	0.04	0.620
p_*Bacteroidetes*; g_*Prevotella*	0.0002	0.008	0.669
p_*Firmicutes*; g_*Clostridium*	0.002	0.04	0.431
p_*Firmicutes*; g_*Dorea*	0.003	0.047	0.138
p_*Firmicutes*; g_*Lactobacillus*	0.00002	0.002	0.880
p_*Proteobacteria*; g_*Bilophila*	0.0002	0.008	0.766

Table 6-1: Genus-level taxonomic composition of faecal samples from 100ppm iron DSS-treated mice (Day-1 vs. 21, 42 and 63 samples)

400ppm iron DSS-treated group			
Taxon	**p-values**	**p-values (corrected)**	**Effect size**
p_*Firmicutes*; g_*Lactobacillus*	0.0001	0.01	0.74

Table 6-2: Genus-level taxonomic composition of faecal samples from 400ppm iron DSS-treated mice (Day-1 vs. 21, 42 and 63 samples)

400ppm iron untreated group (Controls)			
Taxon	**p-values**	**p-values (corrected)**	**Effect size**
p_*Actinobacteria*; g_*Adlercreutzia*	0.002	0.04	0.49
p_*Bacteroidetes*; g_*Bacteroides*	0.0005	0.02	0.68
p_*Firmicutes*; g_*Candidatus Arthromitus*	0.003	0.04	0.54
p_*Firmicutes*; g_*Lactobacillus*	0.0002	0.02	0.77
p_*Firmicutes*; g_*Oscillospira*	0.001	0.03	0.61
p_*Firmicutes*; g_*Ruminococcus*	0.002	0.04	0.46
p_*Proteobacteria*; g_*Bilophila*	0.001	0.03	0.55

Table 6-3: Genus-level taxonomic composition of faecal samples from 400ppm iron untreated mice (Day-1 vs. 21, 42 and 63 samples)

6.5 The influence of long-term modification of the iron composition of diets on gut microbiota in a 10-day acute DSS (2%) experiment

Here, we investigated the effects of 53-days alterations in dietary iron intake on acute DSS-induced colitis: as described in Chapter 5. However, in this chapter, we have investigated the effects on gut microbial structure through 16S ribosomal RNA (rRNA) gene surveys. We analysed gut microbial communities, pre and post treatment with 2% DSS in 100, 200 and 400ppm iron groups. These were compared with control groups (consuming 100, 200 and 400ppm iron) on day-1 and day-10.

The multidimensionality of the data was reduced first by an OTU-based method-Principal Component Analysis (PCA) for each group separately. Principal component analysis was used to identify linear combinations of gut microbial taxa that were associated with duration on a diet. The phylogeny-based method UniFrac was then applied to the data, where UniFrac accounts for the phylogenetic divergence between the OTUs. No separation of samples in PCA on unweighted (qualitative) UniFrac distances for all groups was seen (Figure 6-14 a, b, c, d and e). There were also no active features or degenerate plot (i.e. no PCA) for 200ppm iron control mice.

As can be seen from the PCA plots in Figure 6-14, samples at day-1 clustered together in most of the groups, whereas samples at day-10 showed separation in all groups. However, the post-hoc test did not show any significant differences between day-1 vs. day-10 for any of the six groups.

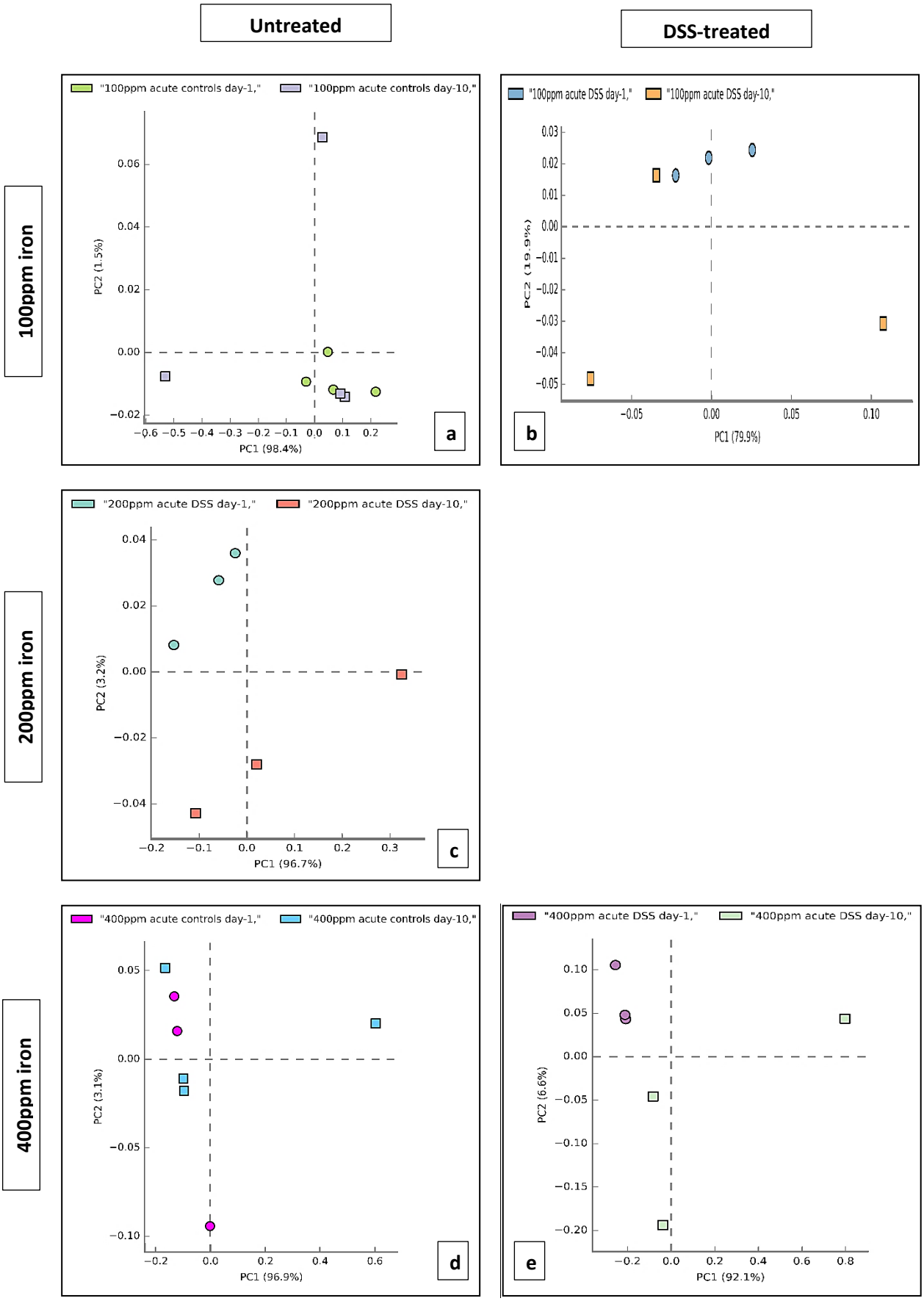

Figure 6-14: PCA plots of the unweighted UniFrac distances of pre-and post DSS-intervention stool samples from acute (2%) DSS-treated mice (b, c, and e) and (a, and d) untreated mice at Phylum-level, phylogenetic classification of 16S rRNA gene sequences. Symbols represent data from individual mice, color-coded by the indicated metadata. Statistical differences were assessed by Welch's t-test followed by Storey's FDR multiple test correction.

6.6 Discussion

The incidence of IBD continues to increase in the developed world areas and is appearing in developing areas as a Westernised lifestyle is becoming implemented. However, despite significant advances in the understanding of the pathogenesis of IBD and the development of new treatments, a cure for IBD remains elusive. Taking into consideration the implications of the microbiota in intestinal inflammation, and the fact that diets play a major factor in recognition of bacterial influence and induction of inflammation, we, therefore, investigated the role of iron as an environmental factor in the pathogenesis of colitis and its effect on the composition of the gut microbiota.

The dextran sulphate sodium (DSS) model involves damaging the mucosal epithelium during colitis. For that reason, it can be used as a model to examine the effect of environmental change on the commensal microbiota of the colon. Bacteria play a complex role in the commonly used acute model of DSS-induced colitis [151]. Antibiotic treatment improves DSS-induced colitis, suggesting that bacteria drive inflammation as well as epithelial damage [149].

The use of repeated cycles of small doses of DSS (1.25%) provokes a mild form of colitis that replicates some features of human IBD, as shown in Chapter 5. We found that analysis of sequence pools revealed significant differences in microbial community composition at the phylum taxonomic level between the tested time points (days-1, 21, 42 and 63) in both the 100 and 400ppm iron DSS-treated and 400ppm iron untreated groups of animals. However, according to a study done by Dirk Haller and his team, major alterations in microbial

composition occurred when mice received an iron depleted diet, whereas host genotype, inflammatory response, and systemic iron administration had smaller effects [152].

However, in our study, principal component analysis (PCA), based on the normalised abundance of dominant bacterial phyla with a colour code according to iron and DSS treatment, illustrated the major separation of samples according to their collection time in 100 and 400ppm iron DSS groups. Control group analysis indicated that a high iron diet (400ppm iron) led to most of the alterations in microbial population regardless of DSS treatment (Figure 6-6). These data were consistent with the results from a study of anaemic African children, which showed that iron fortification led to a potentially more pathogenic gut microbiota profile and gut inflammation [153].

The population structure of the bacterial gut community and the intestinal ecosystem were affected by gut inflammation. In particular, intestinal pathogens (some types of *Proteobacteria*) appeared to take advantage of this shift (inflammation). This observation is in agreement with the 'food hypothesis' and 'differential killing' hypothesis: these two mechanisms are likely to contribute to the loss of colonisation resistance in the inflamed gut [154]. Nonetheless, the post-hoc analysis of our data revealed that one bacterial phylum (*Proteobacteria)* was increased significantly ($P<0.01$) in the 100ppm iron and 400ppm iron DSS-treated and 400ppm iron untreated groups (Figure 6-8, -11 (b) and -13 (a)). However, *Actinobacteria* were increased significantly ($P<0.011$) in the samples from 400ppm iron untreated mice (Figure 6-11 (a)), whereas *Bacteroidetes* decreased significantly ($P<0.028$) in the 400ppm iron DSS-treated group (Figure 6-13 (b)).

Dirk Haller and his team studied the depletion of luminal iron and its effects on the gut microbiota and how it prevents Crohn's disease-like ileitis: the analysis revealed that eight bacterial families and nine bacterial genera were significantly (P<0.01) affected by the luminal iron (ferrous sulphate) deficiency. The genera *Bifidobacterium* (P<0.0018), *Succinivibrio* (P<0.0027), *Turicibacter* (P<0.0020) and *Clostridium* (P<0.0017) were significantly increased in mice supplemented with an iron depleted diet, whereas the genera *Desulfovibrio* (P<0.0001), *Dorea* (P<0.01) and *Bacteroides* related were greatly reduced. They concluded that all significant differences in bacterial abundance in wild-type mice appeared as a result of the interaction between treatment and Host-mediated inflammation [152].

However, our analysis showed that seven genera were significantly different. We found reductions in *Lactobacillus* (P<0.002), *Dorea*, *Clostridium*, *Bacteroides* and *Odoribacter* (P<0.04), *Bilophila* (P<0.008), and an increase in (*Prevotella* P<0.008), all belonging to three phyla [*Firmicutes*, *Bacteroidetes* and *Proteobacteria*] in 100ppm iron DSS-treated mice (Table 6-1). A significant reduction was shown in the *Firmicutes* with one genus (*Lactobacillus* P<0.01) in the 400ppm iron DSS group (Table 6-2). The only control group in which significant differences were found was the 400ppm iron group, where four phyla [*Firmicutes*, *Bacteroidetes*, *Proteobacteria*, and *Actinobacteria*] with seven genera showed statistically significant differences. Increases were shown in *Lactobacillus* (P<0.02), *Oscillospira* (P<0.03), *Adlercreutzia* and *Candidatus Arthromitus* (P<0.04) whereas, reductions occurred in *Bacteroides* (P<0.02), *Bilophila* (P<0.03) and *Ruminococcus* (P<0.04) (Table 6-3).

Our results suggest that any modifications of iron that is consumed in the diet can exacerbate colitis in mice and disturb the gut microbiota. Collectively these findings explore some mechanisms responsible for the disruption in intestinal epithelial homoeostasis and provide a new perspective on host-commensal symbiosis.

7 General discussion

IBD (ulcerative colitis and Crohn's disease) is a long-term condition that damages the gastrointestinal tract. IBD is becoming a global problem which affects around 240,000 people in the UK [155]. About one-third of IBD patients suffer from anaemia. Intestinal bleeding is a significant symptom in IBD, and a fall in the red blood cell count is common during relapse [156]. Iron deficiency (ID) is the most frequent cause of anaemia in IBD. Therefore, intravenous iron and oral replacements are often used for the treatment of IDA [157]. Regardless of the new recommendations by international expert guidelines, intravenous iron preparations are associated with safety issues and thus are widely considered as a last option [158].

Iron is an essential requirement for most organisms, including bacteria. Unabsorbed iron from supplements and gastrointestinal bleeding puts iron into the colon and causes undesirable effects on the intestinal host–microbiota interface, which can excite the growth and virulence of some bacterial pathogens within the intestine and exacerbate inflammation in IBD [159]. Any alterations of the gut microbial composition cause a condition called "dysbiosis", which may contribute to the pathogenesis of IBD [160].

We hypothesised that iron supplementation (and or bleeding) in IBD patients could change the composition of the gut microbiota and potentially influence the natural history of IBD. In this context, we assessed the intestinal microbiota in murine models (acute and chronic DSS) of inflammatory bowel disease, and in mice given different doses of iron supplements.

Acute colitis was effectively induced in wild-type mice fed with different doses of iron (100, 200 and 400ppm iron), by administering 2% DSS in drinking water for 5-days followed by another 3 or 5-days of plain drinking water. All DSS-treated mice started losing body weight

from day-6: the maximal weight loss occurred on day-8. Mice receiving 100ppm iron lost significantly more weight than other groups (Chapter 3). These findings were consistent with a study by a Norwegian group who found that intestinal inflammation in DSS-induced colitis in rats was aggravated by using low-dose oral ferrous fumarate [128]. In the same study [128], there was an increase in histologic colitis scores in DSS-treated Wistar rats after receiving low-dose oral ferrous fumarate, while no changes were observed in control animals. Higher doses of iron caused an increase in histological intestinal inflammation [128]. In our study, mice had significantly greater inflammation at day-10 after receiving 100ppm iron with DSS than DSS-treated mice that received 200 or 400ppm iron.

In humans, faecal calprotectin measurement is common for the assessment of IBD disease activity [161]. We, therefore, measured faecal calprotectin concentrations to examine whether dietary iron affected inflammation by an additional technique. Interestingly, similar to the histological changes, faecal calprotectin levels were increased at day-8 compared to day-10 and this occurred most prominently in the high- and low-iron DSS groups ($P<0.001$): these groups also had significantly ($P<0.05$) greater colitis score than the regular (200ppm iron) iron DSS group at day-10 (Figure 3-11 Chapter 3).

Jaeggi *et al.*[127] reported that oral iron supplementation had been associated with increased levels of faecal calprotectin (demonstrating augmented gut inflammation) and with an increased rate of diarrhoea [127]. In contrast, a study by Kortman *et al.*[162] showed that faecal calprotectin levels were not influenced by dietary iron intervention alone, but after enteric infection faecal calprotectin was significantly lower in mice on an iron-deficient diet.

Moreover, *Kortman* found that *Enterorhabdus* appeared only after enteric infection and its relative abundance and faecal calprotectin levels were highest in the regular iron group [162].

Anaemia is a common clinical feature of IBD, whereas intestinal bleeding (either visible or occult blood) is a key symptom of IBD during a flare. We, therefore, measured total faecal iron concentrations in our mice. Our data showed a difference in total faecal iron concentration between samples taken at day-1 vs. day-10 which reflected colitis severity (luminal bleeding) in DSS-treated animals. The increase in faecal iron from day-1 to day-8 (the maximum weight loss point) was significant in the 100 and 400ppm iron groups ($P<0.0001$) as well as the 200ppm iron DSS-treated groups ($P<0.01$). There was little change in faecal iron concentration in mice that did not receive DSS: $P<0.05$, only in mice receiving 400ppm iron (Chapter 3).

In recent research, Kortman *et al.*[162] investigated the effects of iron on pathology, host intestinal immune responses and gut microbiota composition in non-inflamed and inflamed colon mouse models. They reported that iron diets alone had a clear influence on luminal iron content and tissue iron stores, but found no effects on general health as reflected by body weight, immunological factors such as lipocalin-2 and calprotectin [162]. In agreement with these results, we found that different amounts of iron in the diet alone did not affect body weight, histology or faecal calprotectin, in the absence of DSS (acute).

However, as mentioned, the DSS-induced colitis groups showed an effect of the amount of iron in the diet on faecal iron concentration as demonstrated by the severity of inflammation where luminal iron was increased due to luminal bleeding. These results were highest at day-8, when weight loss was greatest for low (100ppm iron) as well as high (400ppm iron) iron

groups. We have shown, therefore, that low, as well as high, iron diets, exacerbate the severity of colitis in the DSS murine model.

Quantitative and qualitative changes in the composition of the intestinal microbial community (bacteria, viruses, yeast, and parasites) are referred to as a dysbiotic microbiota. The gut microbiota is susceptible to invasion and to blooms of pathogens affecting the niches that are left open after disturbances. So dysbiosis is considered as a potential trigger of disease and is commonly linked to other illnesses. For example, inflammatory bowel disease may arise as the result of inflammation that was caused by an altered immune response to the gut bacteria [121, 163].

Therefore, 16S sequencing of our samples (acute DSS-induced colitis) was performed. Bioinformatic analysis indicated that the only significant difference was for 400ppm iron DSS-treated mice at day-1 vs. day-10, with significant reductions in the proportions of *Bacteroidetes* and *Firmicutes* (P<5.98e-3 and P<6.96e-3 respectively). In contrast, a significant increase was found in the sequences assigned to other phyla; *Proteobacteria* (P<1.38-e3), *Actinobacteria* (P<5.13-e3) and *Fusobacteria* (P<3.25-e3) (Chapter 4). Such findings were consistent with recent studies that have characterised the microbiota in IBD patients revealing that a reduction in the biodiversity of commensal bacteria has occurred, particularly in the phyla *Bacteroidetes* and *Firmicutes* [74]. Also, recent research on rodents has also shown that bacterial compositional changes occur with colonic inflammation and/or infection [164].

Patterns of gut microbiome dysbiosis in the murine acute IBD model (DSS) vary among published studies. However, in our research, we used samples collected before and after DSS treatment and then studied the microbiome via 16S rDNA sequencing. An axis (luminal iron-intestinal colitis) defined by an increased abundance of bacteria which include *Proteobacteria*, *Actinobacteria* and *Fusobacteria* and decreased abundance in *Bacteroidetes* and *Firmicutes* correlates strongly with disease status.

Having already established the acute colitis mouse model, which allowed us to elucidate the impact of DSS-induced colitis on the intestinal microbiota and the proposed impact of iron on dysbiosis, we subsequently investigated a chronic DSS-induced colitis model to investigate the long-term effect of dietary iron consumption on the same parameters.

Our data showed that chronic colitis was induced successfully in all mice that received 1.25% DSS as indicated by weight loss from day-6 and reaching a maximum at day-8 before mice started gaining weight throughout the recovery periods. However, body weight changes showed no statistically significant differences between DSS groups, although 100ppm iron treated mice appeared to lose more weight than other groups (Figure 5-6). In agreement with these data Erichsen *et al.* showed that a low dose of iron aggravated DSS-induced colitis in rats [128]. Our untreated-DSS mice (controls) fed with different iron diets for a 63-day period showed increases in body weight in a dose-dependent manner (Figure 5-7). Therefore, these results demonstrate the importance of iron as a nutrient, and its level, in turn, affects the course of inflammation.

After 53-days on different diets, the control mice were split into six groups of four mice each. Three groups received 2% DSS to induce acute colitis and to investigate the influence of an extended period of iron depletion/supplementation upon the acute phase of colitis as well as on the microbiome, and the remaining mice continued as untreated controls. Surprisingly, our data showed significant differences in weight among all DSS-treated groups which developed colitis: weight loss was maximal at day-8 for all mice. However, the 100ppm iron DSS-treated mice again appeared to be the most severely affected group as shown by weight loss (Figure 5-8). Our observations demonstrated the importance of luminal iron and inflammation, where low and high dietary iron administration for a longer period did exacerbate intestinal inflammation significantly, suggesting that the time of iron supplementation may be crucial in aggravating colitis.

Histologically, mild inflammation occurred after three cycles of 1.25% DSS. Inflammation was significantly increased in 100ppm iron ($P<0.001$), 200ppm iron ($P<0.01$) and 400ppm iron ($P<0.01$) DSS-treated mice vs. untreated animals. These findings demonstrate first that the DSS model had successfully worked to induce colitis, and secondly that a low iron diet (100ppm iron) resulted in the highest histological inflammation score. Such results imply that the degree of inflammation in the low iron group was worse than in the higher and regular iron diet groups; this is consistent with the weight chart results.

However, inducing colitis with 2% DSS (severe colitis) after a prolonged period on different doses of oral iron was associated with significantly more histological colitis than occurred during the chronic colitis regimen. Acute DSS-treatment after the prolonged dietary manipulation resulted in colitis scores that were significantly greater ($P<0.0001$) in those mice

taking 100ppm iron and 400ppm iron and ($P<0.001$) for 200ppm iron DSS-treated groups vs. untreated 200ppm iron group. Accordingly, histological changes reflected the level of inflammation, as noted for the weight change.

In this research, we identified the degree of thickening (fibrosis) in the colon of mice after chronic DSS-colitis was induced by staining the tissues with Masson's trichrome [141]. All slides were treatment and group blinded to the researcher to assess fibrosis using a histological fibrosis score (Table 5-2 Chapter 5). The results revealed fibrosis in all DSS-treated sections with statistical significance ($P<0.05$) between the 100ppm iron and 200ppm iron DSS-treated mice. However, the fibrotic score median value was higher for the low iron group followed by the high iron group then the standard iron group (5, 4 and 3.5 respectively).

Collectively, all parameters established that low iron (100ppm iron) mice suffered from more colitis followed by high iron (400ppm iron) mice then regular iron diet (200ppm iron). This is in agreement with data reported by Erichsen *et al.* and his group which showed that a low iron diet aggravated colitis regarding body weight and histology [128].

Our statistics showed no significant differences in faecal calprotectin levels in chronic DSS-treated mice. However, the calprotectin level appeared to increase gradually after each cycle of DSS treatment in mice receiving 100 and 400ppm iron, but not in those taking 200ppm iron. Comparison of the samples taken at day-21 vs. day-63 in DSS-treated mice consuming 400ppm iron showed a significant difference ($P<0.01$) (Figure 5-17). Once more, calprotectin signified the presence of more faecal neutrophils, i.e. more inflammation in mice that were receiving high iron diets [129]. No differences were noted in the untreated chronic groups.

The levels of faecal calprotectin in mice fed long term 100ppm iron and 400ppm iron diets followed by acute DSS (2%) were consistent with our acute DSS experimental results (reported in Chapter 3) where faecal calprotectin day-1 vs. day-10 showed significant differences in each DSS-treated group. However, the highest difference was for 100ppm iron diet DSS-treated mice.

We measured total faecal iron concentrations to assess the level of inflammation by using the presence of luminal bleeding [111]. Data in this research showed that all DSS-treated group revealed a significant difference between cycles. However, the 400ppm iron group had lower significance than those with 100 and 200ppm iron groups. In contrast, untreated mice receiving 200 and 400ppm iron showed significant differences ($P<0.01$) and not in those taking 100ppm iron (Figure 5-19 Chapter 5).

After 63-days on diets, the samples were taken from mice that received 2% DSS displayed a significant difference (day-1 vs. 10) reflecting the severity of colitis. The 400ppm iron group showed the most significant difference ($P<0.0001$) whereas the 100ppm iron and 200ppm iron DSS groups had a difference of similar significance ($P<0.01$). However, faecal iron concentration data for untreated mice were only significant in the mice supplemented with 400ppm iron which was statistically significant ($P<0.05$) (Figure 5-21 Chapter 5).

Microbiome analysis for chronic DSS samples was carried out using the same technique and software employed in the acute DSS experiments (Chapter 4). Chronic samples were taken at four different time points (days-1, 21, 42 and 63) which represented the beginning and the end of each DSS cycle. Thorough analysis started at an upper taxonomic level such as phylum

with principal component analysis (PCA) for each group separately to identify linear combinations of gut microbial taxa that were associated with the duration on a diet. A clear separation was seen for the samples from 100ppm iron and 400ppm iron DSS-treated groups as well as from 400ppm iron control mice. Thus, high dietary iron disturbs the microbial community in both DSS-treated and untreated mice, while low dietary iron only affects gut microbiota in the presence of colitis (DSS-induce).

Further post hoc tests applied to each group showed that the mean proportion of sequences was significantly assigned to *Proteobacteria* in 100ppm iron DSS group with an increase in day-63 vs. day-1 and 21 ($P<0.05$). This suggests that at the end of each DSS cycle, the level of inflammation was associated with an increase in *Proteobacteria.* In a study, *Proteobacteria* appeared to have a growth advantage from this shift (low iron) [154]. These observations are in agreement with our other findings (weight loss, histology, calprotectin and microbiome analysis), proposing that a low iron diet exacerbates colitis and causes dysbiosis.

The data from research on anaemic African children where iron fortification in their food was applied, revealed that a pathogenic intestinal bacterial profile and gut inflammation were increased as a result of extra iron in the diet [153]. This is consistent with our findings in which the 400ppm iron DSS-treated group had significantly reduced *Bacteroidetes* ($P<0.078$) and increased *Proteobacteria* ($P<0.016$), where the difference between each pre and post-DSS intervention was observed in day-63 samples.

However, the only DSS-untreated group that showed a significant difference in the phyla was the 400ppm iron group: these mice showed an increase in both *Proteobacteria* and

Actinobacteria (P<0.011 each). Nevertheless, the increase in *Proteobacteria* was significant at day-42 vs. 21 (P<0.001) and day-63 vs. 21 (P<0.05). However the changes seen in the gut microbiome in this group are contrary to data reported by Dirk Haller and his team: they found that a depleted iron diet caused significant dysbiosis without a major effect on host genotype, inflammatory response and systemic iron application [152].

When studying probiotics and IBD, Toumi *et al.*[165] stated that administration of some strains of *Lactobacillus* and *Bifidobacterium* had not only beneficial effects on maintenance of the integrity of the epithelial barrier and tissue repair but also had anti-inflammatory effects and improved DSS-induced colitis [165]. Devkota *et al.*[166] also demonstrated that diet could alter the intestinal microbiota which contributes to the development of colitis in mice, and any reduction in bacteria *Bilophila wadsworthia* could increase the incidence of colitis [166].

These results support our data. When a further lower taxonomic analysis was done, seven genera belonging to three phyla were significantly different in 100ppm iron DSS-treated and 400ppm iron DSS-untreated mice. Three of these genera reduced over time and were present in both groups (*Lactobacillus*, *Bacteroides* and *Bilophila).* However, the differences were changed in the low iron DSS-treated mice for *Lactobacillus* (P<0.002) and *Bilophila* (P<0.008) than in untreated fed with a high iron diet *(Lactobacillus* (P<0.02) and *Bilophila* (P<0.03)).

As previously mentioned iron is an essential nutrient for various gut bacteria that compete for unabsorbed dietary iron. Iron acquisition plays a key role in determining the virulence and colonisation of the majority of enteric Gram-negative bacteria (e.g. *Shigella, Salmonella* and pathogenic *Escherichia coli*) [76]. Other commensal gut bacteria belonging to the genera

Lactobacillus and *Bifidobacterium* play a major role (barrier effect) against colonisation by such pathogens. Interestingly *Lactobacilli* do not require iron but instead, use manganese [167].

The *Bifidobacterium* species (*Bifidobacterium breve*) can sequester luminal iron. However, the majority of *Bifidobacterium* species do not produce siderophores or other active iron carriers. Therefore, unabsorbed dietary iron may modify the colonic microbiota equilibrium and help the growth of pathogenic strains more than healthy 'barrier' strains.

Interestingly, the 400ppm iron DSS group had only one phylum (*Firmicutes)* with one genus that showed a statistically significant difference (*Lactobacillus* $P<0.01$). These data suggest that 400ppm iron led to a relative suppression of *Lactobacilli*. Also, in a recent study by Werner T *et al.* data analysis found that depleted luminal iron only significantly affected a few genera, for example, *Clostridium* ($P<0.0017$) [152]. This was also consistent with our findings where 100ppm iron DSS-treated mice showed a significant reduction in *Clostridium* ($P<0.04$).

In the case of high grades of inflammation and infection, iron absorption is likely to be even lower, as inflammation results in elevated circulating hepcidin and this further reduces iron absorption [168]. So, in DSS-induced colitis, the level of absorbed iron was probably decreased. This leads to an increase in pathogenic bacteria and reduced immunity against infection.

In this project, we investigated the effects of different dietary iron interventions (for 53-days) on the severity of acute DSS-induced colitis and its impact on the gut microbial structure in wild-type mice. However, the bioinformatics analysis at day-1 vs. day-10 for each group showed no significance. The inflammation was severe as shown by colitis scores (Chapter 5)

as a result of 2% DSS-induced colitis. The absence of difference may, therefore, be due to the small sample size (n=4) and also due to a failure to obtain bacterial DNA: the latter may be a result of DSS in the sample or disruption of the microbiome. However the study is also likely to be underpowered

7.1 Potential medical implications

Certainly, there is evidence to support the notion that the quality of life in anaemic IBD patients can be very poor and that treatment of anaemia will improve this [38]. The best therapy for anaemia of chronic disease (ACD) is curing the underlying illness, and treating anaemia might be a therapeutic target for treating IBD. However, a cure may not be possible [35]. Oral iron supplementation is often preferred by clinicians to treat IDA because of its relative safety, efficacy, and cost. Common oral iron preparations that are used to treat iron deficiency in IBD patients such as ferrous salts e.g.; sulphate, fumarate and gluconate, however, have multiple gastrointestinal side effects [34]. Recent studies have also shown that oral iron supplements can increase intestinal tissue injury by catalysing the production of reactive oxygen species (ROS) and can affect the immune system as well as intestinal inflammation in IBD [38]. Moreover, advanced molecular techniques have illustrated changes in the gut microbiota (dysbiosis) in IBD patients [68].

To provide a more rational approach, it is essential to distinguish between the role of iron in aggravating intestinal inflammation and the inflammation-associated dysbiosis. The data in this thesis have shown differential and unique influences of different iron diets upon murine models of colitis and colitis-associated microbiota. It is too early for our results to suggest that

reducing the amount of consumed (luminal) iron to the optimal range may be a promising novel strategy to manage IBD and minimise the risk of dysbiosis in these patients. Therefore, we need to extend these observations toward a prospective study in humans (IBD patients) comparing faecal samples before and after taking iron supplements.

7.2 Future research directions

Numerous potential future experiments have already been discussed with my supervisor and carrying out these experiments could help to answer several important research questions and explain the molecular mechanisms responsible for the different intestinal responses to injury that were observed among animals consuming different amounts of iron in their diet. Data in this thesis have demonstrated that modifications of standard iron diet can exacerbate DSS-induced colitis as well as the balance of the intestinal microbial community in wild-type (C57BL/6) mice. It is well documented that NF-kB signalling pathways make important contributions to inflammatory responses. Pritchard *et al.*[169] demonstrated that NF-κB2-mediated signalling seems to be critical for DSS-induced colitis [169]. Consequently, it would be interesting to investigate the effect of administering a different range of iron diets on the development of DSS-induced colitis in NFκB null mice as well as study the consequences of deleting various NFκB family members on gut microbiota.

Ferric maltol is a new oral iron treatment containing a stable complex of ferric iron (Fe^{3+}) with maltol. This preparation allows ferric iron to be absorbed properly by enterocytes at relatively low dose levels enabling IBD patients to be treated with iron deficiency [170]. Also, ferric maltol has good tolerability and has less impact on inflammatory bowel disease severity [171].

Therefore, it would be interesting to look at (1) the effect of ferric iron supplementation upon murine colitis, by assessing the severity of colitis and dysbiosis, and (2) the impact of ferric iron on the microbiota of humans with IBD.

The fundamental aim of our studies was to increase understanding of the pathogenesis of inflammatory bowel disease and its associated dysbiosis. Thus, it is now necessary to extend these studies to more types of murine IBD models along with further manipulations in iron diets. Several IBD models such as TNBS colitis have previously been established and can be used to study colitis in mice. Moreover, some bacteria have been associated with iron concentrations and inflammation development in this research, so *in vitro* experiments using techniques such as cell culture could also be used to assess the function of a particular organism (*S. Typhimurium*) in response to iron. This could provide another window to look through on the pathogenesis of inflammatory bowel disease and dysbiosis.

7.3 Limitations of presented studies

Iron concentrations in animals are controlled by regulation of intestinal iron absorption. Haemochromatosis is considered when total body iron is widely increased due to inappropriately high levels of intestinal iron absorption [172]. In contrast, low levels of intestinal iron absorption cause iron deficiency (ID) with or without anaemia. In this research, diets low (100ppm iron) and high (400ppm iron) in iron were formulated according to literature and previous studies in this area. The low iron diet (100ppm iron) was the lowest that we could obtain based on the standard chow (200ppm iron) already used in maintaining animals and high iron diet (400ppm iron) was created by doubling the standard chow (200ppm iron) iron content to prevent hemochromatosis. This apparent limitation, however, allows for investigating the iron influence on the study of colitis in both acute as well as chronic experiments.

The majority of the ingested iron (ferrous) passes unabsorbed on to the ileum and colon, where sites of inflammation in Crohn's disease (CD) and ulcerative colitis (UC) occur, before appearing in the stool. Iron attaches to the intestinal surface (ulcerated), increasing the local production of reactive oxygen species (ROS) and thus augmenting inflammation [173]. We suggested that the immunoassay technique may be required for assessing faecal iron concentrations using the best commercially available iron assay kit (as it described in Chapter 2), which is a cheap, simple and relatively consistent way to measure luminal iron i.e. from food and any intestinal bleeding, but other methods such as Coulter counter may be preferable to assess iron deficiency anaemia (IDA) or Hem-occult test (Beckman Coulter, Inc., Fullerton, CA) to detect any intestinal bleeding, however the Biomedical Services Unit (BSU)

lack of such tool. As discussed in previous chapters, particular time points (pre and post-DSS treatment) utilised to address these important research questions.

The successful and reproducible induction of DSS-induced colitis was achieved in this project and allowed us to obtain faecal samples to assess microbiota disturbances at various time-points. During DSS-induced colitis day-8 was the showed the most weight loss and histological changes (as it described in Chapter 3). However, we could not study the microbiota at this stage as the PCR appeared to be inhibited, perhaps by DSS. It would, therefore, be helpful to find other means of assessing the microbiota at this time point.

7.4 Conclusions

In this thesis, I have demonstrated that dietary iron plays a role in DSS-induced colitis and intestinal responses to various types of inflammation. Low iron was clinically (body weight and histology) significantly worsened colitis while high iron had a great impact on intestinal microbiota disturbance as summarised in Table 7.1. Although we do not have an ultimate explanation for this observation, it could reflect the consequences of differences in blood loss from the inflamed colon, differences in food intake or the influence of iron regulating mechanisms. In the setting of inflammation, any modifications of iron in the diet exacerbated the severity of experimental acute and chronic colitis in wild-type mice. However, long-term high iron diet (400ppm iron) resulted in increased inflammation associated with dysbiosis induced by DSS and dysbiosis with diet alone as summarised in Table 7.2. These findings how oral iron supplements exacerbate IBD.

Acute DSS-induced colitis	100ppm iron		200ppm iron		400ppm iron	
	DSS	Ctr.	DSS	Ctr.	DSS	Ctr.
Body weight	↓↓↓	—	↓	—	↓↓	—
Histology (colitis)	↑↑↑	—	↑	—	↑↑	—
Faecal calprotectin	↑↑	—	↑	—	↑↑	—
Faecal iron	↑↑	—	↑	—	↑↑	—
Microbiome significance	—	—	—	—	↑	—

Table 7-1: Summary of the main observations from acute 2% DSS-induce colitis experiments. Ctr. (control), the dash (—) no change and microbiome significance represent statistical significance.

Chronic DSS-induced colitis	100ppm iron		200ppm iron		400ppm iron	
	DSS	Ctr.	DSS	Ctr.	DSS	Ctr.
Body weight	↓↓↓	↑	↓	↑↑	↓↓	↑↑↑
Histology (colitis)	↑↑	—	↑	—	↑	—
Histology (fibrosis)	↑↑	—	↑	—	↑	—
Faecal calprotectin	↑↑	—	—	—	↑	—
Faecal iron	↑↑↑	—	↑↑	↑	↑↑	↑
Microbiome significance	↑↑	—	—	—	↑	↑↑

Table 7-2: Summary of the main observations from chronic 1.25% DSS-induce colitis experiments. Ctr. (control), the dash (—) no change and microbiome significance represent statistical significance.

8 Publications arising from this thesis

8.1 List of published abstracts

1. **Mahalhal A.**, Campbell B., Pritchard D.M., Probert C. *Influence of Iron Supplementation on The Natural History of Colitis*. BSG 2016 Liverpool. Gut 2016; 65: A244. PTH-051 (abstract of distinction) (poster of distinction).

2. **Mahalhal A.**, Campbell B.J., Pritchard D.M., Probert C. *Influence of iron supplementation on gut microbiota and the natural history of colitis.* European Microbiome Congress, 18-19 November 2015 (Poster of distinction).

3. **Mahalhal A.**, Aggio R., Reade S., Campbell B., Pritchard D.M., Probert C. *The influence of iron supplementation on the severity of a murine model of colitis*. ITM research day July 6, 2015, University of Liverpool. S1-P06 (Poster of distinction).

4. **Mahalhal A.**, Reade S., Campbell B., Pritchard D.M., Probert C. *The influence of iron supplementation on the severity of a murine model of colitis*. DDF 2015 conference London. Gut 2015; 64: A92. PTU-072 (poster).

9 References

1. Baumgart DC, Carding SR. Inflammatory bowel disease: cause and immunobiology. The Lancet 2007;369:1627-1640.
2. Molodecky NA, Soon IS, Rabi DM, et al. Increasing incidence and prevalence of the inflammatory bowel diseases with time, based on systematic review. Gastroenterology 2012;142:46-54 e42; quiz e30.
3. Ghosh N, Leonard S, Miles G, et al. A cost of care model for inflammatory bowel disease. Journal of Crohns & Colitis 2014;8:S309-S310.
4. Geboes K, De Hertogh G. Indeterminate colitis. Inflammatory Bowel Diseases 2003;9:324-331.
5. Loftus EV, Jr. Clinical epidemiology of inflammatory bowel disease: Incidence, prevalence, and environmental influences. Gastroenterology 2004;126:1504-17.
6. Wardwell LH, Huttenhower C, Garrett WS. Current concepts of the intestinal microbiota and the pathogenesis of infection. Curr Infect Dis Rep 2011;13:28-34.
7. Strober W. Immunology. Unraveling gut inflammation. Science 2006;313:1052-4.
8. Loftus EV, Jr., Sandborn WJ. Epidemiology of inflammatory bowel disease. Gastroenterol Clin North Am 2002;31:1-20.
9. Krishnan A, Korzenik JR. Inflammatory bowel disease and environmental influences. Gastroenterol Clin North Am 2002;31:21-39.
10. Sonnenberg A. Occupational distribution of inflammatory bowel disease among German employees. Gut 1990;31:1037-40.
11. Hold GL. The gut microbiota, dietary extremes and exercise. Gut 2014;63:1838-9.

12. Persson PG, Ahlbom A, Hellers G. Diet and inflammatory bowel disease: a case-control study. Epidemiology 1992;3:47-52.

13. Nos P, Domenech E. Management of Crohn's disease in smokers: is an alternative approach necessary? World J Gastroenterol 2011;17:3567-74.

14. Seksik P, Nion-Larmurier I, Sokol H, et al. Effects of light smoking consumption on the clinical course of Crohn's disease. Inflamm Bowel Dis 2009;15:734-41.

15. Pullan RD, Rhodes J, Ganesh S, et al. Transdermal nicotine for active ulcerative colitis. N Engl J Med 1994;330:811-5.

16. Madretsma GS, Donze GJ, van Dijk AP, et al. Nicotine inhibits the in vitro production of interleukin 2 and tumour necrosis factor-alpha by human mononuclear cells. Immunopharmacology 1996;35:47-51.

17. Binder V. Genetic epidemiology in inflammatory bowel disease. Dig Dis 1998;16:351-5.

18. Yang H, McElree C, Roth MP, et al. Familial empirical risks for inflammatory bowel disease: differences between Jews and non-Jews. Gut 1993;34:517-24.

19. Tysk C, Lindberg E, Jarnerot G, et al. Ulcerative colitis and Crohn's disease in an unselected population of monozygotic and dizygotic twins. A study of heritability and the influence of smoking. Gut 1988;29:990-6.

20. Lagercrantz R, Perlmann P, Hammarstrom S. Immunological studies in ulcerative colitis. V. Family studies. Gastroenterology 1971;60:381-9.

21. Fiocchi C, Roche JK, Michener WM. High prevalence of antibodies to intestinal epithelial antigens in patients with inflammatory bowel disease and their relatives. Ann Intern Med 1989;110:786-94.

22. Jostins L, Ripke S, Weersma RK, et al. Host-microbe interactions have shaped the genetic architecture of inflammatory bowel disease. Nature 2012;491:119-24.

23. Franke A, McGovern DP, Barrett JC, et al. Genome-wide meta-analysis increases to 71 the number of confirmed Crohn's disease susceptibility loci. Nat Genet 2010;42:1118-25.

24. Anderson CA, Boucher G, Lees CW, et al. Meta-analysis identifies 29 additional ulcerative colitis risk loci, increasing the number of confirmed associations to 47. Nat Genet 2011;43:246-52.

25. O'Neil DA, Porter EM, Elewaut D, et al. Expression and regulation of the human beta-defensins hBD-1 and hBD-2 in intestinal epithelium. J Immunol 1999;163:6718-24.

26. Jones DE, Bevins CL. Paneth cells of the human small intestine express an antimicrobial peptide gene. J Biol Chem 1992;267:23216-25.

27. Harder J, Bartels J, Christophers E, et al. A peptide antibiotic from human skin. Nature 1997;387:861.

28. Rastall RA. Bacteria in the gut: friends and foes and how to alter the balance. J Nutr 2004;134:2022S-2026S.

29. Bik EM. Composition and function of the human-associated microbiota. Nutr Rev 2009;67 Suppl 2:S164-71.

30. Lupp C, Robertson ML, Wickham ME, et al. Host-mediated inflammation disrupts the intestinal microbiota and promotes the overgrowth of Enterobacteriaceae. Cell Host Microbe 2007;2:204.

31. Fredricks DN, Relman DA. Sequence-based identification of microbial pathogens: a reconsideration of Koch's postulates. Clin Microbiol Rev 1996;9:18-33.

32. Schenk M, Bouchon A, Birrer S, et al. Macrophages expressing triggering receptor expressed on myeloid cells-1 are underrepresented in the human intestine. J Immunol 2005;174:517-24.

33. Babbs CF. Oxygen radicals in ulcerative colitis. Free Radic Biol Med 1992;13:169-81.

34. Stein J, Dignass AU. Management of iron deficiency anemia in inflammatory bowel disease - a practical approach. Ann Gastroenterol 2013;26:104-113.

35. Kulnigg S, Teischinger L, Dejaco C, et al. Rapid recurrence of IBD-associated anemia and iron deficiency after intravenous iron sucrose and erythropoietin treatment. Am J Gastroenterol 2009;104:1460-7.

36. Weiss G, Gasche C. Pathogenesis and treatment of anemia in inflammatory bowel disease. Haematologica 2010;95:175-8.

37. Weiss G, Goodnough LT. Anemia of chronic disease. N Engl J Med 2005;352:1011-23.

38. Gasche C, Lomer MC, Cavill I, et al. Iron, anaemia, and inflammatory bowel diseases. Gut 2004;53:1190-7.

39. Gomollon F, Gisbert JP. Anemia and inflammatory bowel diseases. World J Gastroenterol 2009;15:4659-65.

40. Ponka P, Lok CN. The transferrin receptor: role in health and disease. Int J Biochem Cell Biol 1999;31:1111-37.

41. Rizvi S, Schoen RE. Supplementation with oral vs. intravenous iron for anemia with IBD or gastrointestinal bleeding: is oral iron getting a bad rap? Am J Gastroenterol 2011;106:1872-9.

42. Lobo V, Patil A, Phatak A, et al. Free radicals, antioxidants and functional foods: Impact on human health. Pharmacogn Rev 2010;4:118-26.

43. Manfred Wick WP, Paul Lehmann. Clinical Aspects and Laboratory – Iron Metabolism. SpingerWienNewYork: Springer Vienna, 2011.

44. Anderson GJ, Frazer DM, McKie AT, et al. Mechanisms of haem and non-haem iron absorption: lessons from inherited disorders of iron metabolism. Biometals 2005;18:339-48.

45. Hansen TM, Hansen NE, Birgens HS, et al. Serum ferritin and the assessment of iron deficiency in rheumatoid arthritis. Scand J Rheumatol 1983;12:353-9.

46. Thomson AB, Brust R, Ali MA, et al. Iron deficiency in inflammatory bowel disease. Diagnostic efficacy of serum ferritin. Am J Dig Dis 1978;23:705-9.

47. Weiss G, Wachter H, Fuchs D. Linkage of cell-mediated immunity to iron metabolism. Immunol Today 1995;16:495-500.

48. Weiss G, Houston T, Kastner S, et al. Regulation of cellular iron metabolism by erythropoietin: activation of iron-regulatory protein and upregulation of transferrin receptor expression in erythroid cells. Blood 1997;89:680-7.

49. Macdougall IC, Cavill I, Hulme B, et al. Detection of functional iron deficiency during erythropoietin treatment: a new approach. BMJ 1992;304:225-6.

50. Ratledge C, Dover LG. Iron metabolism in pathogenic bacteria. Annu Rev Microbiol 2000;54:881-941.

51. Crichton RR, Ward RJ. Iron homeostasis. Met Ions Biol Syst 1998;35:633-65.

52. Dhople AM, Ibanez MA, Poirier TC. Role of iron in the pathogenesis of Mycobacterium avium infection in mice. Microbios 1996;87:77-87.

53. Weinberg ED. The development of awareness of iron-withholding defense. Perspect Biol Med 1993;36:215-21.

54. Payne SM. Iron acquisition in microbial pathogenesis. Trends Microbiol 1993;1:66-9.

55. Carrano CJ, Bohnke R, Matzanke BF. Fungal ferritins: the ferritin from mycelia of Absidia spinosa is a bacterioferritin. FEBS Lett 1996;390:261-4.

56. Chambers CE, Sokol PA. Comparison of siderophore production and utilization in pathogenic and environmental isolates of Yersinia enterocolitica. J Clin Microbiol 1994;32:32-9.

57. Carrier J, Aghdassi E, Platt I, et al. Effect of oral iron supplementation on oxidative stress and colonic inflammation in rats with induced colitis. Aliment Pharmacol Ther 2001;15:1989-99.

58. Dethlefsen L, McFall-Ngai M, Relman DA. An ecological and evolutionary perspective on human-microbe mutualism and disease. Nature 2007;449:811-8.

59. Savage DC. Microbial ecology of the gastrointestinal tract. Annu Rev Microbiol 1977;31:107-33.

60. Gao Z, Tseng CH, Pei Z, et al. Molecular analysis of human forearm superficial skin bacterial biota. Proc Natl Acad Sci U S A 2007;104:2927-32.

61. Cribby S, Taylor M, Reid G. Vaginal microbiota and the use of probiotics. Interdiscip Perspect Infect Dis 2008;2008:256490.

62. Beaugerie L, Flahault A, Barbut F, et al. Antibiotic-associated diarrhoea and Clostridium difficile in the community. Aliment Pharmacol Ther 2003;17:905-12.

63. Aas JA, Paster BJ, Stokes LN, et al. Defining the normal bacterial flora of the oral cavity. J Clin Microbiol 2005;43:5721-32.

64. Bik EM, Eckburg PB, Gill SR, et al. Molecular analysis of the bacterial microbiota in the human stomach. Proc Natl Acad Sci U S A 2006;103:732-7.

65. Eckburg PB, Bik EM, Bernstein CN, et al. Diversity of the human intestinal microbial flora. Science 2005;308:1635-8.

66. Turnbaugh PJ, Ley RE, Mahowald MA, et al. An obesity-associated gut microbiome with increased capacity for energy harvest. Nature 2006;444:1027-31.

67. Ley RE, Backhed F, Turnbaugh P, et al. Obesity alters gut microbial ecology. Proc Natl Acad Sci U S A 2005;102:11070-5.

68. Frank DN, St Amand AL, Feldman RA, et al. Molecular-phylogenetic characterization of microbial community imbalances in human inflammatory bowel diseases. Proc Natl Acad Sci U S A 2007;104:13780-5.

69. Xavier RJ, Podolsky DK. Unravelling the pathogenesis of inflammatory bowel disease. Nature 2007;448:427-34.

70. Strober W, Fuss I, Mannon P. The fundamental basis of inflammatory bowel disease. J Clin Invest 2007;117:514-21.

71. Sartor RB. Microbial influences in inflammatory bowel diseases. Gastroenterology 2008;134:577-94.

72. Prescott NJ, Fisher SA, Franke A, et al. A nonsynonymous SNP in ATG16L1 predisposes to ileal Crohn's disease and is independent of CARD15 and IBD5. Gastroenterology 2007;132:1665-71.

73. Cadwell K, Liu JY, Brown SL, et al. A key role for autophagy and the autophagy gene Atg16l1 in mouse and human intestinal Paneth cells. Nature 2008;456:259-63.

74. Packey CD, Sartor RB. Commensal bacteria, traditional and opportunistic pathogens, dysbiosis and bacterial killing in inflammatory bowel diseases. Curr Opin Infect Dis 2009;22:292-301.

75. Andrews SC, Robinson AK, Rodriguez-Quinones F. Bacterial iron homeostasis. FEMS Microbiol Rev 2003;27:215-37.

76. Naikare H, Palyada K, Panciera R, et al. Major role for FeoB in Campylobacter jejuni ferrous iron acquisition, gut colonization, and intracellular survival. Infect Immun 2006;74:5433-44.

77. Lee SH, Shinde P, Choi J, et al. Effects of dietary iron levels on growth performance, hematological status, liver mineral concentration, fecal microflora, and diarrhea incidence in weanling pigs. Biol Trace Elem Res 2008;126 Suppl 1:S57-68.

78. Reid CA HK. The effects of retrogradation and amylose/amylopectin ratio of starches on carbohydrate fermentation and microbial populations in the porcine colon. Animal Science 1999;68:503-510.

79. Jurjus AR, Khoury NN, Reimund JM. Animal models of inflammatory bowel disease. J Pharmacol Toxicol Methods 2004;50:81-92.

80. Wirtz S, Neurath MF. Mouse models of inflammatory bowel disease. Adv Drug Deliv Rev 2007;59:1073-83.

81. Stefan Wirtz CN, Benno Weigmann & Markus F Neurath. Chemically induced mouse models of intestinal inflammation. Volume 2 No.3: Nature Publishing Group, 2007:541 - 546.

82. Kanneganti M, Mino-Kenudson M, Mizoguchi E. Animal models of colitis-associated carcinogenesis. J Biomed Biotechnol 2011;2011:342637.

83. Perse M, Cerar A. Dextran sodium sulphate colitis mouse model: traps and tricks. J Biomed Biotechnol 2012;2012:718617.

84. Kitajima S, Takuma S, Morimoto M. Histological analysis of murine colitis induced by dextran sulfate sodium of different molecular weights. Exp Anim 2000;49:9-15.

85. Hirono I, Kuhara K, Yamaji T, et al. Carcinogenicity of dextran sulfate sodium in relation to its molecular weight. Cancer Lett 1983;18:29-34.

86. Aharoni R, Kayhan B, Brenner O, et al. Immunomodulatory therapeutic effect of glatiramer acetate on several murine models of inflammatory bowel disease. J Pharmacol Exp Ther 2006;318:68-78.

87. LEE Y-K. Effects of Diet on Gut Microbiota Profile and the Implications for Health and Disease. Bioscience of Microbiota 2013; 32 (1):1–12.

88. Kitajima S, Morimoto M, Sagara E. A model for dextran sodium sulfate (DSS)-induced mouse colitis: bacterial degradation of DSS does not occur after incubation with mouse cecal contents. Exp Anim 2002;51:203-6.

89. Okayasu I, Hatakeyama S, Yamada M, et al. A novel method in the induction of reliable experimental acute and chronic ulcerative colitis in mice. Gastroenterology 1990;98:694-702.

90. Murthy SN, Cooper HS, Shim H, et al. Treatment of dextran sulfate sodium-induced murine colitis by intracolonic cyclosporin. Dig Dis Sci 1993;38:1722-34.

91. Bauer C, Duewell P, Mayer C, et al. Colitis induced in mice with dextran sulfate sodium (DSS) is mediated by the NLRP3 inflammasome. Gut 2010;59:1192-9.

92. Seril DN, Liao J, Ho KL, et al. Dietary iron supplementation enhances DSS-induced colitis and associated colorectal carcinoma development in mice. Dig Dis Sci 2002;47:1266-78.

93. Carrier JC, Aghdassi E, Jeejeebhoy K, et al. Exacerbation of dextran sulfate sodium-induced colitis by dietary iron supplementation: role of NF-kappaB. Int J Colorectal Dis 2006;21:381-7.

94. Mazmanian SK, Round JL, Kasper DL. A microbial symbiosis factor prevents intestinal inflammatory disease. Nature 2008;453:620-5.

95. Hold GL. Western lifestyle: a 'master' manipulator of the intestinal microbiota? Gut 2014;63:5-6.

96. Hold GL, Smith M, Grange C, et al. Role of the gut microbiota in inflammatory bowel disease pathogenesis: what have we learnt in the past 10 years? World J Gastroenterol 2014;20:1192-210.

97. Sartor RB. Gut microbiota: Diet promotes dysbiosis and colitis in susceptible hosts. Nat Rev Gastroenterol Hepatol 2012;9:561-2.

98. Turnbaugh PJ, Hamady M, Yatsunenko T, et al. A core gut microbiome in obese and lean twins. Nature 2009;457:480-4.

99. Wills ES, Jonkers DM, Savelkoul PH, et al. Fecal microbial composition of ulcerative colitis and Crohn's disease patients in remission and subsequent exacerbation. PLoS One 2014;9:e90981.

100. Staley JT, Konopka A. Measurement of in situ activities of nonphotosynthetic microorganisms in aquatic and terrestrial habitats. Annu Rev Microbiol 1985;39:321-46.

101. Van de Peer Y, Chapelle S, De Wachter R. A quantitative map of nucleotide substitution rates in bacterial rRNA. Nucleic Acids Res 1996;24:3381-91.

102. Hold GL, Pryde SE, Russell VJ, et al. Assessment of microbial diversity in human colonic samples by 16S rDNA sequence analysis. FEMS Microbiol Ecol 2002;39:33-9.

103. Williams JM, Duckworth CA, Vowell K, et al. Intestinal Preparation Techniques for Histological Analysis in the Mouse. Curr Protoc Mouse Biol 2016;6:148-68.

104. Dostal A, Chassard C, Hilty FM, et al. Iron depletion and repletion with ferrous sulfate or electrolytic iron modifies the composition and metabolic activity of the gut microbiota in rats. J Nutr 2012;142:271-7.

105. Yuan S, Cohen DB, Ravel J, et al. Evaluation of methods for the extraction and purification of DNA from the human microbiome. PLoS One 2012;7:e33865.

106. Kennedy NA, Walker AW, Berry SH, et al. The impact of different DNA extraction kits and laboratories upon the assessment of human gut microbiota composition by 16S rRNA gene sequencing. PLoS One 2014;9:e88982.

107. Oldenburg B, Koningsberger JC, Van Berge Henegouwen GP, et al. Iron and inflammatory bowel disease. Aliment Pharmacol Ther 2001;15:429-38.

108. Gasche C. Anemia in IBD: the overlooked villain. Inflamm Bowel Dis 2000;6:142-150; discussion 151.

109. Huang J, Simcox J, Mitchell TC, et al. Iron regulates glucose homeostasis in liver and muscle via AMP-activated protein kinase in mice. FASEB J 2013;27:2845-54.

110. Rezaie A, Parker RD, Abdollahi M. Oxidative stress and pathogenesis of inflammatory bowel disease: an epiphenomenon or the cause? Dig Dis Sci 2007;52:2015-21.

111. Bullen JJ, Rogers HJ, Spalding PB, et al. Natural resistance, iron and infection: a challenge for clinical medicine. J Med Microbiol 2006;55:251-8.

112. Ruseler-van Embden JG, Schouten WR, van Lieshout LM. Pouchitis: result of microbial imbalance? Gut 1994;35:658-64.

113. Sokol H, Seksik P, Furet JP, et al. Low counts of Faecalibacterium prausnitzii in colitis microbiota. Inflamm Bowel Dis 2009;15:1183-9.

114. Sokol H, Seksik P, Rigottier-Gois L, et al. Specificities of the fecal microbiota in inflammatory bowel disease. Inflamm Bowel Dis 2006;12:106-11.

115. Rehman A, Lepage P, Nolte A, et al. Transcriptional activity of the dominant gut mucosal microbiota in chronic inflammatory bowel disease patients. J Med Microbiol 2010;59:1114-22.

116. Seksik P, Rigottier-Gois L, Gramet G, et al. Alterations of the dominant faecal bacterial groups in patients with Crohn's disease of the colon. Gut 2003;52:237-42.

117. Sokol H, Lay C, Seksik P, et al. Analysis of bacterial bowel communities of IBD patients: what has it revealed? Inflamm Bowel Dis 2008;14:858-67.

118. Martinez-Medina M, Aldeguer X, Gonzalez-Huix F, et al. Abnormal microbiota composition in the ileocolonic mucosa of Crohn's disease patients as revealed by polymerase chain reaction-denaturing gradient gel electrophoresis. Inflamm Bowel Dis 2006;12:1136-45.

119. Willing BP, Dicksved J, Halfvarson J, et al. A pyrosequencing study in twins shows that gastrointestinal microbial profiles vary with inflammatory bowel disease phenotypes. Gastroenterology 2010;139:1844-1854 e1.

120. Ott SJ, Musfeldt M, Wenderoth DF, et al. Reduction in diversity of the colonic mucosa associated bacterial microflora in patients with active inflammatory bowel disease. Gut 2004;53:685-93.

121. Manichanh C, Rigottier-Gois L, Bonnaud E, et al. Reduced diversity of faecal microbiota in Crohn's disease revealed by a metagenomic approach. Gut 2006;55:205-11.

122. Cross JH, Bradbury RS, Fulford AJ, et al. Oral iron acutely elevates bacterial growth in human serum. Sci Rep 2015;5:16670.

123. Sharp P, Srai SK. Molecular mechanisms involved in intestinal iron absorption. World J Gastroenterol 2007;13:4716-24.

124. Melgar S, Karlsson A, Michaelsson E. Acute colitis induced by dextran sulfate sodium progresses to chronicity in C57BL/6 but not in BALB/c mice: correlation between symptoms and inflammation. Am J Physiol Gastrointest Liver Physiol 2005;288:G1328-38.

125. Vermeire S, Vermeulen N, Van Assche G, et al. (Auto)antibodies in inflammatory bowel diseases. Gastroenterol Clin North Am 2008;37:429-38, vii.

126. Roseth AG, Fagerhol MK, Aadland E, et al. Assessment of the neutrophil dominating protein calprotectin in feces. A methodologic study. Scand J Gastroenterol 1992;27:793-8.

127. Jaeggi T, Kortman GA, Moretti D, et al. Iron fortification adversely affects the gut microbiome, increases pathogen abundance and induces intestinal inflammation in Kenyan infants. Gut 2015;64:731-42.

128. Erichsen K, Milde AM, Arslan G, et al. Low-dose oral ferrous fumarate aggravated intestinal inflammation in rats with DSS-induced colitis. Inflamm Bowel Dis 2005;11:744-8.

129. von Roon AC, Karamountzos L, Purkayastha S, et al. Diagnostic precision of fecal calprotectin for inflammatory bowel disease and colorectal malignancy. Am J Gastroenterol 2007;102:803-13.

130. Rooks MG, Veiga P, Wardwell-Scott LH, et al. Gut microbiome composition and function in experimental colitis during active disease and treatment-induced remission. ISME J 2014;8:1403-17.

131. Garrett WS, Lord GM, Punit S, et al. Communicable ulcerative colitis induced by T-bet deficiency in the innate immune system. Cell 2007;131:33-45.

132. Parks DH, Beiko RG. Identifying biologically relevant differences between metagenomic communities. Bioinformatics 2010;26:715-21.

133. Hartmann M, Howes CG, Abarenkov K, et al. V-Xtractor: an open-source, high-throughput software tool to identify and extract hypervariable regions of small

subunit (16S/18S) ribosomal RNA gene sequences. J Microbiol Methods 2010;83:250-3.

134. Tringe SG, von Mering C, Kobayashi A, et al. Comparative metagenomics of microbial communities. Science 2005;308:554-7.

135. Bleich A, Hansen AK. Time to include the gut microbiota in the hygienic standardisation of laboratory rodents. Comp Immunol Microbiol Infect Dis 2012;35:81-92.

136. Turnbaugh PJ, Ridaura VK, Faith JJ, et al. The effect of diet on the human gut microbiome: a metagenomic analysis in humanized gnotobiotic mice. Sci Transl Med 2009;1:6ra14.

137. Scott KP, Gratz SW, Sheridan PO, et al. The influence of diet on the gut microbiota. Pharmacol Res 2013;69:52-60.

138. Kaser A, Zeissig S, Blumberg RS. Inflammatory bowel disease. Annu Rev Immunol 2010;28:573-621.

139. Byrne FR, Viney JL. Mouse models of inflammatory bowel disease. Curr Opin Drug Discov Devel 2006;9:207-17.

140. Lombardi VR, Etcheverria I, Carrera I, et al. Prevention of chronic experimental colitis induced by dextran sulphate sodium (DSS) in mice treated with FR91. J Biomed Biotechnol 2012;2012:826178.

141. Ding S, Walton KL, Blue RE, et al. Mucosal healing and fibrosis after acute or chronic inflammation in wild type FVB-N mice and C57BL6 procollagen alpha1(I)-promoter-GFP reporter mice. PLoS One 2012;7:e42568.

142. Tanaka T, Kohno H, Suzuki R, et al. A novel inflammation-related mouse colon carcinogenesis model induced by azoxymethane and dextran sodium sulfate. Cancer Sci 2003;94:965-73.

143. Geboes K, Dalle I. Influence of treatment on morphological features of mucosal inflammation. Gut 2002;50 Suppl 3:III37-42.

144. Rose WA, 2nd, Sakamoto K, Leifer CA. Multifunctional role of dextran sulfate sodium for in vivo modeling of intestinal diseases. BMC Immunol 2012;13:41.

145. Melgar S, Karlsson L, Rehnstrom E, et al. Validation of murine dextran sulfate sodium-induced colitis using four therapeutic agents for human inflammatory bowel disease. Int Immunopharmacol 2008;8:836-44.

146. Samanta AK, Torok VA, Percy NJ, et al. Microbial fingerprinting detects unique bacterial communities in the faecal microbiota of rats with experimentally-induced colitis. J Microbiol 2012;50:218-25.

147. Berry D, Schwab C, Milinovich G, et al. Phylotype-level 16S rRNA analysis reveals new bacterial indicators of health state in acute murine colitis. ISME J 2012;6:2091-106.

148. De Fazio L, Cavazza E, Spisni E, et al. Longitudinal analysis of inflammation and microbiota dynamics in a model of mild chronic dextran sulfate sodium-induced colitis in mice. World J Gastroenterol 2014;20:2051-61.

149. Rath HC, Schultz M, Freitag R, et al. Different subsets of enteric bacteria induce and perpetuate experimental colitis in rats and mice. Infect Immun 2001;69:2277-85.

150. Califf K GA, Knight R, Caporaso JG. The human microbiome: getting personal. Microbe 2014;9:410–5.

151. Chassaing B, Aitken JD, Malleshappa M, et al. Dextran sulfate sodium (DSS)-induced colitis in mice. Curr Protoc Immunol 2014;104:Unit 15 25.

152. Werner T, Wagner SJ, Martinez I, et al. Depletion of luminal iron alters the gut microbiota and prevents Crohn's disease-like ileitis. Gut 2011;60:325-33.

153. Dostal A, Baumgartner J, Riesen N, et al. Effects of iron supplementation on dominant bacterial groups in the gut, faecal SCFA and gut inflammation: a randomised, placebo-controlled intervention trial in South African children. Br J Nutr 2014;112:547-56.

154. Stecher B, Hardt WD. The role of microbiota in infectious disease. Trends Microbiol 2008;16:107-14.

155. Mowat C, Cole A, Windsor A, et al. Guidelines for the management of inflammatory bowel disease in adults. Gut 2011;60:571-607.

156. Gasche C, Reinisch W, Lochs H, et al. Anemia in Crohn's disease. Importance of inadequate erythropoietin production and iron deficiency. Dig Dis Sci 1994;39:1930-4.

157. Kulnigg S, Gasche C. Systematic review: managing anaemia in Crohn's disease. Aliment Pharmacol Ther 2006;24:1507-23.

158. Gasche C, Berstad A, Befrits R, et al. Guidelines on the diagnosis and management of iron deficiency and anemia in inflammatory bowel diseases. Inflamm Bowel Dis 2007;13:1545-53.

159. Erichsen K, Ulvik RJ, Grimstad T, et al. Effects of ferrous sulphate and non-ionic iron-polymaltose complex on markers of oxidative tissue damage in patients with inflammatory bowel disease. Aliment Pharmacol Ther 2005;22:831-8.

160. Comito D, Romano C. Dysbiosis in the pathogenesis of pediatric inflammatory bowel diseases. Int J Inflam 2012;2012:687143.

161. Kopylov U, Rosenfeld G, Bressler B, et al. Clinical utility of fecal biomarkers for the diagnosis and management of inflammatory bowel disease. Inflamm Bowel Dis 2014;20:742-56.

162. Kortman GA, Mulder ML, Richters TJ, et al. Low dietary iron intake restrains the intestinal inflammatory response and pathology of enteric infection by food-borne bacterial pathogens. Eur J Immunol 2015;45:2553-67.

163. Hill DA, Artis D. Intestinal bacteria and the regulation of immune cell homeostasis. Annu Rev Immunol 2010;28:623-67.

164. Lupp C, Robertson ML, Wickham ME, et al. Host-mediated inflammation disrupts the intestinal microbiota and promotes the overgrowth of Enterobacteriaceae. Cell Host Microbe 2007;2:119-29.

165. Toumi R, Soufli I, Rafa H, et al. Probiotic bacteria lactobacillus and bifidobacterium attenuate inflammation in dextran sulfate sodium-induced experimental colitis in mice. Int J Immunopathol Pharmacol 2014;27:615-27.

166. Devkota S, Wang Y, Musch MW, et al. Dietary-fat-induced taurocholic acid promotes pathobiont expansion and colitis in Il10-/- mice. Nature 2012;487:104-8.

167. Anderson RC, Cookson AL, McNabb WC, et al. Lactobacillus plantarum DSM 2648 is a potential probiotic that enhances intestinal barrier function. FEMS Microbiol Lett 2010;309:184-92.

168. Nemeth E, Tuttle MS, Powelson J, et al. Hepcidin regulates cellular iron efflux by binding to ferroportin and inducing its internalization. Science 2004;306:2090-3.

169. Burkitt MD, Hanedi AF, Duckworth CA, et al. NF-kappaB1, NF-kappaB2 and c-Rel differentially regulate susceptibility to colitis-associated adenoma development in C57BL/6 mice. J Pathol 2015;236:326-36.

170. Barrand MA, Callingham BA, Dobbin P, et al. Dissociation of a ferric maltol complex and its subsequent metabolism during absorption across the small intestine of the rat. Br J Pharmacol 1991;102:723-9.

171. Gasche C, Ahmad T, Tulassay Z, et al. Ferric maltol is effective in correcting iron deficiency anemia in patients with inflammatory bowel disease: results from a phase-3 clinical trial program. Inflamm Bowel Dis 2015;21:579-88.

172. Edwards CQ, Dadone MM, Skolnick MH, et al. Hereditary haemochromatosis. Clin Haematol 1982;11:411-35.

173. Oldenburg B, van Berge Henegouwen GP, Rennick D, et al. Iron supplementation affects the production of pro-inflammatory cytokines in IL-10 deficient mice. Eur J Clin Invest 2000;30:505-10.

10 Appendices

Appendix 1- Samples identifications (Chapter 4)

Sample ID According to 96 well plate	Barcode Sequence	Linker Primer Sequence	Treatment	DOB	Description
A1			Control	25/02/2014	Control mouse, colon content –I.D MA01,1,CC
A2			Control	25/02/2014	Control mouse, colon content –I.D MA01,2,CC
A3			Control	25/02/2014	Control mouse, colon content –I.D MA01,3,CC
A4			Control	25/02/2014	Control mouse, colon content –I.DMA01,4,CC
A5			Control	25/02/2014	Control mouse, colon content –I.D MA01,5,CC
A6			Control	25/02/2014	Control mouse, colon content –I.D MA01,6,CC
A7			DSS/low iron diet	25/02/2014	DSS/low iron mouse, colon content –I.D MA03,1,CC
A8			DSS/low iron diet	25/02/2014	DSS/low iron mouse, colon content –I.D MA03,2,CC
A9			DSS/normal diet	25/02/2014	DSS normal diet mouse, colon content –I.D MA02,1,CC
A10			DSS/normal diet	25/02/2014	DSS normal diet mouse, colon content –I.D MA02,2,CC
A11			DSS/normal diet	25/02/2014	DSS normal diet mouse, colon content –I.D MA02,3,CC
A12			DSS/normal diet	25/02/2014	DSS normal diet mouse, colon content –I.D MA02,4,CC
B1			DSS/normal diet	25/02/2014	DSS normal diet mouse, colon content –I.D MA02,5,CC
B2			DSS/normal diet	25/02/2014	DSS normal diet mouse, colon content –I.D MA02,6,CC

B3			DSS/low iron diet	25/02/2014	DSS/low iron mouse, colon content –I.D MA03,3,CC
B4			DSS/low iron diet	25/02/2014	DSS/low iron mouse, colon content –I.D MA03,4,CC
B5			DSS/high iron diet	25/02/2014	DSS/high iron mouse, colon content – I.DMA04,1,CC
B6			DSS/high iron diet	25/02/2014	DSS/high iron mouse, colon content – I.DMA04,2,CC
B7			DSS/high iron diet	25/02/2014	DSS/high iron mouse, colon content – I.DMA04,3,CC
B8			DSS/high iron diet	25/02/2014	DSS/high iron mouse, colon content – I.DMA04,4,CC
B9			DSS/high iron diet	25/02/2014	DSS/high iron mouse, colon content – I.DMA04,5,CC
B10			DSS/high iron diet	25/02/2014	DSS/high iron mouse, colon content – I.DMA04,6,CC
B11			DSS/low iron diet	25/02/2014	DSS/low iron mouse, colon content –I.D MA03,5,CC
B12			DSS/low iron diet	25/02/2014	DSS/low iron mouse, colon content –I.D MA03,6,CC
C1			Low iron diet	25/02/2014	low iron mouse, colon content –I.D MA05,1,CC
C2			Low iron diet	25/02/2014	low iron mouse, colon content –I.D MA05,2,CC
C3			Low iron diet	25/02/2014	low iron mouse, colon content –I.D MA05,3,CC
C4			Low iron diet	25/02/2014	low iron mouse, colon content –I.D MA05,4,CC
C5			Low iron diet	25/02/2014	low iron mouse, colon content –I.D MA05,5,CC
C6			Low iron diet	25/02/2014	low iron mouse, colon content –I.D MA05,6,CC
C7			High iron diet	25/02/2014	high iron mouse, colon content –I.D MA06,1,CC
C8			High iron diet	25/02/2014	high iron mouse, colon content –I.D MA06,2,CC
C9			High iron diet	25/02/2014	high iron mouse, colon content –I.D MA06,3,CC
C10			High iron diet	25/02/2014	high iron mouse, colon content –I.D MA06,4,CC

C11			High iron diet	25/02/2014	high iron mouse, colon content –I.D MA06,5,CC
C12			High iron diet	25/02/2014	high iron mouse, colon content –I.D MA06,6,CC
D1			Control	25/02/2014	Control mouse, Faecal pellet day 0–I.D MA01,1,P_0
D2			Control	25/02/2014	Control mouse, Faecal pellet day 0–I.D MA01,2,P_0
D3			Control	25/02/2014	Control mouse, Faecal pellet day 0–I.D MA01,3,P_0
D4			Control	25/02/2014	Control mouse, Faecal pellet day 0–I.D MA01,4,P_0
D5			Control	25/02/2014	Control mouse, Faecal pellet day 0–I.D MA01,5,P_0
D6			Control	25/02/2014	Control mouse, Faecal pellet day 0–I.D MA01,6,P_0
D7			DSS/normal diet	25/02/2014	DSS mouse, Faecal pellet day 0–I.D MA02,1,P_0
D8			DSS/normal diet	25/02/2014	DSS mouse, Faecal pellet day 0–I.D MA02,2,P_0
D9			DSS/normal diet	25/02/2014	DSS mouse, Faecal pellet day 0–I.D MA02,3,P_0
D10			DSS/normal diet	25/02/2014	DSS mouse, Faecal pellet day 0–I.D MA02,4,P_0
D11			DSS/normal diet	25/02/2014	DSS mouse, Faecal pellet day 0–I.D MA02,5,P_0
D12			DSS/normal diet	25/02/2014	DSS mouse, Faecal pellet day 0–I.D MA02,6,P_0
E1			DSS/low iron diet	25/02/2014	DSS low iron mouse, Faecal pellet day 0–I.D MA03,1,P_0
E2			DSS/low iron diet	25/02/2014	DSS low iron mouse, Faecal pellet day 0–I.D MA03,2,P_0
E3			DSS/low iron diet	25/02/2014	DSS low iron mouse, Faecal pellet day 0–I.D MA03,3,P_0

E4			DSS/low iron diet	25/02/2014	DSS low iron mouse, Faecal pellet day 0–I.D MA03,4,P_0
E5			DSS/low iron diet	25/02/2014	DSS low iron mouse, Faecal pellet day 0–I.D MA03,5,P_0
E6			DSS/low iron diet	25/02/2014	DSS low iron mouse, Faecal pellet day 0–I.D MA03,6,P_0
E7			DSS/high iron diet	25/02/2014	DSS high iron mouse, Faecal pellet day 0–I.D MA04,1,P_0
E8			DSS/high iron diet	25/02/2014	DSS high iron mouse, Faecal pellet day 0–I.D MA04,2,P_0
E9			DSS/high iron diet	25/02/2014	DSS high iron mouse, Faecal pellet day 0–I.D MA04,3,P_0
E10			DSS/high iron diet	25/02/2014	DSS high iron mouse, Faecal pellet day 0–I.D MA04,4,P_0
E11			DSS/high iron diet	25/02/2014	DSS high iron mouse, Faecal pellet day 0–I.D MA04,5,P_0
E12			DSS/high iron diet	25/02/2014	DSS high iron mouse, Faecal pellet day 0–I.D MA04,6,P_0
F1			Low iron diet	25/02/2014	Low iron mouse, Faecal pellet day 0–I.D MA05,1,P_0
F2			Low iron diet	25/02/2014	Low iron mouse, Faecal pellet day 0–I.D MA05,2,P_0
F3			Low iron diet	25/02/2014	Low iron mouse, Faecal pellet day 0–I.D MA05,3,P_0
F4			Low iron diet	25/02/2014	Low iron mouse, Faecal pellet day 0–I.D MA05,4,P_0
F5			Low iron diet	25/02/2014	Low iron mouse, Faecal pellet day 0–I.D MA05,5,P_0
F6			Low iron diet	25/02/2014	Low iron mouse, Faecal pellet day 0–I.D MA05,6,P_0
F7			High iron diet	25/02/2014	High iron mouse, Faecal pellet day 0–I.D MA06,1,P_0
F8			High iron diet	25/02/2014	High iron mouse, Faecal pellet day 0–I.D MA06,2,P_0

F9			High iron diet	25/02/2014	High iron mouse, Faecal pellet day 0–I.D MA06,3,P_0
F10			High iron diet	25/02/2014	High iron mouse, Faecal pellet day 0–I.D MA06,4,P_0
F11			High iron diet	25/02/2014	High iron mouse, Faecal pellet day 0–I.D MA06,5,P_0
F12			High iron diet	25/02/2014	High iron mouse, Faecal pellet day 0–I.D MA06,6,P_0
G1			-	-	-VE control
G2, G3			-	-	-VE control

Appendix 2- Phyla (legends) Chapter 4 and 5

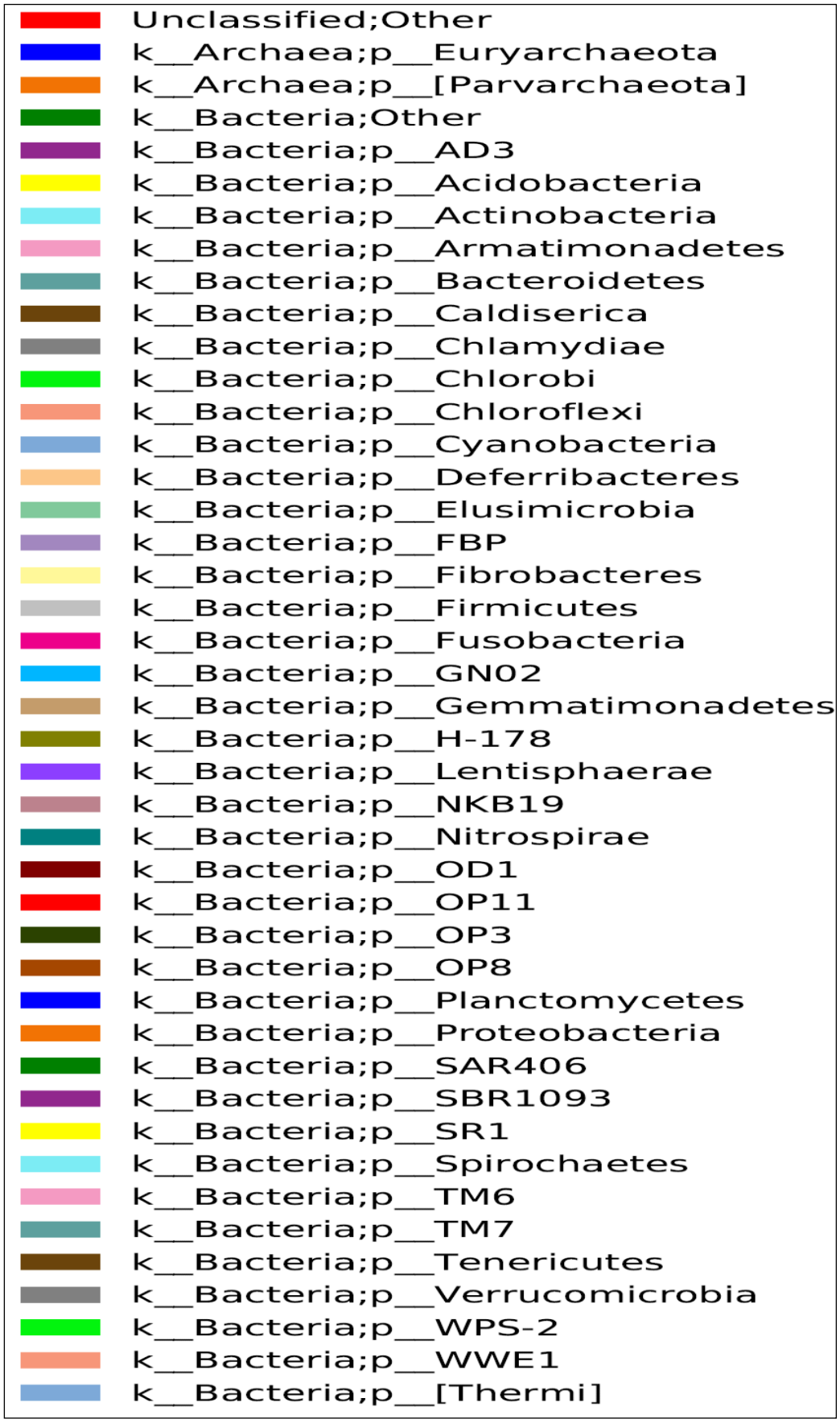

Appendix 3- Families (legends) Chapter 4

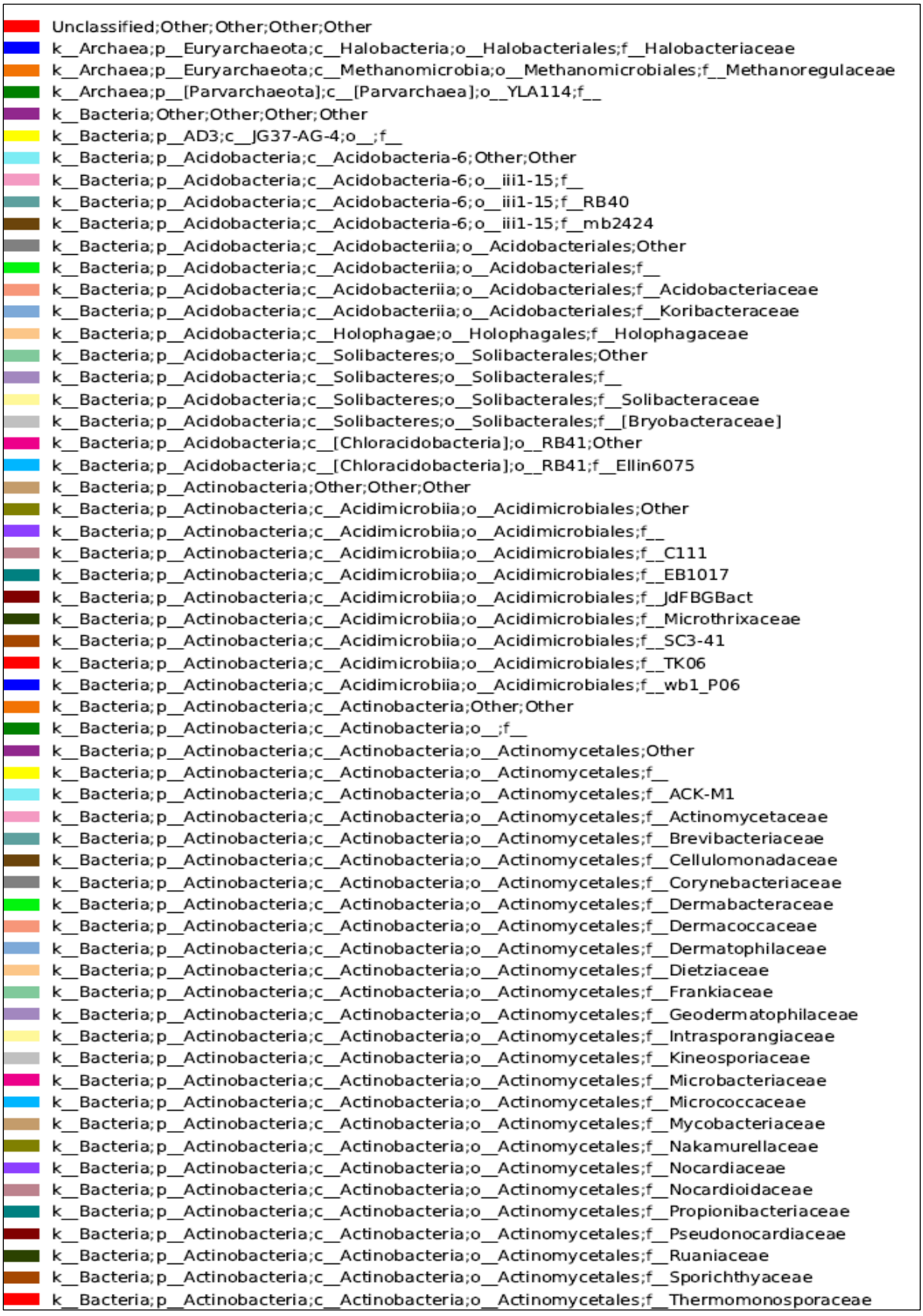

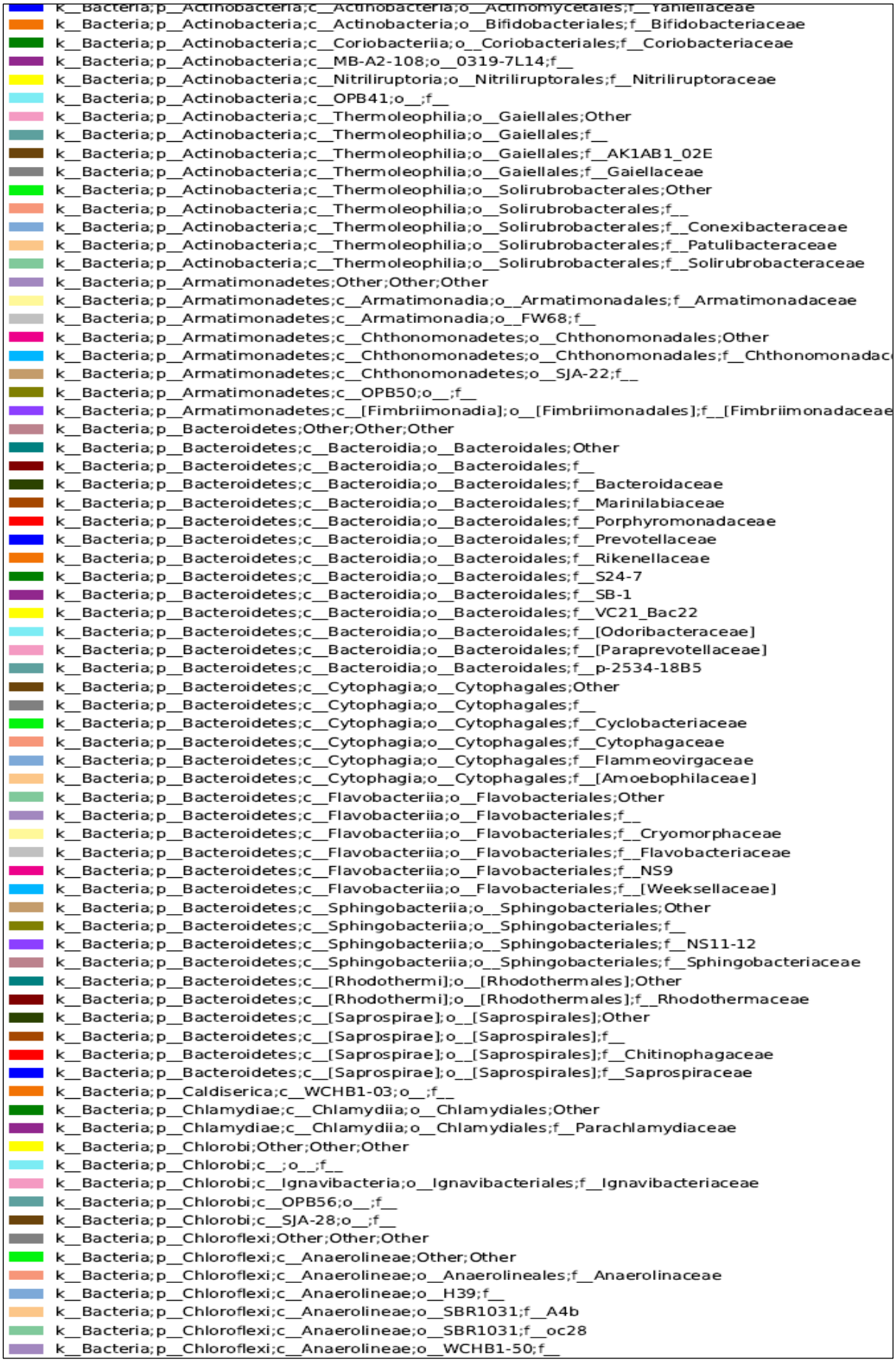
k__Bacteria;p__Actinobacteria;c__Actinobacteria;o__Actinomycetales;f__Yaniellaceae
k__Bacteria;p__Actinobacteria;c__Actinobacteria;o__Bifidobacteriales;f__Bifidobacteriaceae
k__Bacteria;p__Actinobacteria;c__Coriobacteriia;o__Coriobacteriales;f__Coriobacteriaceae
k__Bacteria;p__Actinobacteria;c__MB-A2-108;o__0319-7L14;f__
k__Bacteria;p__Actinobacteria;c__Nitriliruptoria;o__Nitriliruptorales;f__Nitriliruptoraceae
k__Bacteria;p__Actinobacteria;c__OPB41;o__;f__
k__Bacteria;p__Actinobacteria;c__Thermoleophilia;o__Gaiellales;Other
k__Bacteria;p__Actinobacteria;c__Thermoleophilia;o__Gaiellales;f__
k__Bacteria;p__Actinobacteria;c__Thermoleophilia;o__Gaiellales;f__AK1AB1_02E
k__Bacteria;p__Actinobacteria;c__Thermoleophilia;o__Gaiellales;f__Gaiellaceae
k__Bacteria;p__Actinobacteria;c__Thermoleophilia;o__Solirubrobacterales;Other
k__Bacteria;p__Actinobacteria;c__Thermoleophilia;o__Solirubrobacterales;f__
k__Bacteria;p__Actinobacteria;c__Thermoleophilia;o__Solirubrobacterales;f__Conexibacteraceae
k__Bacteria;p__Actinobacteria;c__Thermoleophilia;o__Solirubrobacterales;f__Patulibacteraceae
k__Bacteria;p__Actinobacteria;c__Thermoleophilia;o__Solirubrobacterales;f__Solirubrobacteraceae
k__Bacteria;p__Armatimonadetes;Other;Other;Other
k__Bacteria;p__Armatimonadetes;c__Armatimonadia;o__Armatimonadales;f__Armatimonadaceae
k__Bacteria;p__Armatimonadetes;c__Armatimonadia;o__FW68;f__
k__Bacteria;p__Armatimonadetes;c__Chthonomonadetes;o__Chthonomonadales;Other
k__Bacteria;p__Armatimonadetes;c__Chthonomonadetes;o__Chthonomonadales;f__Chthonomonadac
k__Bacteria;p__Armatimonadetes;c__Chthonomonadetes;o__SJA-22;f__
k__Bacteria;p__Armatimonadetes;c__OPB50;o__;f__
k__Bacteria;p__Armatimonadetes;c__[Fimbriimonadia];o__[Fimbriimonadales];f__[Fimbriimonadaceae
k__Bacteria;p__Bacteroidetes;Other;Other;Other
k__Bacteria;p__Bacteroidetes;c__Bacteroidia;o__Bacteroidales;Other
k__Bacteria;p__Bacteroidetes;c__Bacteroidia;o__Bacteroidales;f__
k__Bacteria;p__Bacteroidetes;c__Bacteroidia;o__Bacteroidales;f__Bacteroidaceae
k__Bacteria;p__Bacteroidetes;c__Bacteroidia;o__Bacteroidales;f__Marinilabiaceae
k__Bacteria;p__Bacteroidetes;c__Bacteroidia;o__Bacteroidales;f__Porphyromonadaceae
k__Bacteria;p__Bacteroidetes;c__Bacteroidia;o__Bacteroidales;f__Prevotellaceae
k__Bacteria;p__Bacteroidetes;c__Bacteroidia;o__Bacteroidales;f__Rikenellaceae
k__Bacteria;p__Bacteroidetes;c__Bacteroidia;o__Bacteroidales;f__S24-7
k__Bacteria;p__Bacteroidetes;c__Bacteroidia;o__Bacteroidales;f__SB-1
k__Bacteria;p__Bacteroidetes;c__Bacteroidia;o__Bacteroidales;f__VC21_Bac22
k__Bacteria;p__Bacteroidetes;c__Bacteroidia;o__Bacteroidales;f__[Odoribacteraceae]
k__Bacteria;p__Bacteroidetes;c__Bacteroidia;o__Bacteroidales;f__[Paraprevotellaceae]
k__Bacteria;p__Bacteroidetes;c__Bacteroidia;o__Bacteroidales;f__p-2534-18B5
k__Bacteria;p__Bacteroidetes;c__Cytophagia;o__Cytophagales;Other
k__Bacteria;p__Bacteroidetes;c__Cytophagia;o__Cytophagales;f__
k__Bacteria;p__Bacteroidetes;c__Cytophagia;o__Cytophagales;f__Cyclobacteriaceae
k__Bacteria;p__Bacteroidetes;c__Cytophagia;o__Cytophagales;f__Cytophagaceae
k__Bacteria;p__Bacteroidetes;c__Cytophagia;o__Cytophagales;f__Flammeovirgaceae
k__Bacteria;p__Bacteroidetes;c__Cytophagia;o__Cytophagales;f__[Amoebophilaceae]
k__Bacteria;p__Bacteroidetes;c__Flavobacteriia;o__Flavobacteriales;Other
k__Bacteria;p__Bacteroidetes;c__Flavobacteriia;o__Flavobacteriales;f__
k__Bacteria;p__Bacteroidetes;c__Flavobacteriia;o__Flavobacteriales;f__Cryomorphaceae
k__Bacteria;p__Bacteroidetes;c__Flavobacteriia;o__Flavobacteriales;f__Flavobacteriaceae
k__Bacteria;p__Bacteroidetes;c__Flavobacteriia;o__Flavobacteriales;f__NS9
k__Bacteria;p__Bacteroidetes;c__Flavobacteriia;o__Flavobacteriales;f__[Weeksellaceae]
k__Bacteria;p__Bacteroidetes;c__Sphingobacteriia;o__Sphingobacteriales;Other
k__Bacteria;p__Bacteroidetes;c__Sphingobacteriia;o__Sphingobacteriales;f__
k__Bacteria;p__Bacteroidetes;c__Sphingobacteriia;o__Sphingobacteriales;f__NS11-12
k__Bacteria;p__Bacteroidetes;c__Sphingobacteriia;o__Sphingobacteriales;f__Sphingobacteriaceae
k__Bacteria;p__Bacteroidetes;c__[Rhodothermi];o__[Rhodothermales];Other
k__Bacteria;p__Bacteroidetes;c__[Rhodothermi];o__[Rhodothermales];f__Rhodothermaceae
k__Bacteria;p__Bacteroidetes;c__[Saprospirae];o__[Saprospirales];Other
k__Bacteria;p__Bacteroidetes;c__[Saprospirae];o__[Saprospirales];f__
k__Bacteria;p__Bacteroidetes;c__[Saprospirae];o__[Saprospirales];f__Chitinophagaceae
k__Bacteria;p__Bacteroidetes;c__[Saprospirae];o__[Saprospirales];f__Saprospiraceae
k__Bacteria;p__Caldiserica;c__WCHB1-03;o__;f__
k__Bacteria;p__Chlamydiae;c__Chlamydiia;o__Chlamydiales;Other
k__Bacteria;p__Chlamydiae;c__Chlamydiia;o__Chlamydiales;f__Parachlamydiaceae
k__Bacteria;p__Chlorobi;Other;Other;Other
k__Bacteria;p__Chlorobi;c__;o__;f__
k__Bacteria;p__Chlorobi;c__Ignavibacteria;o__Ignavibacteriales;f__Ignavibacteriaceae
k__Bacteria;p__Chlorobi;c__OPB56;o__;f__
k__Bacteria;p__Chlorobi;c__SJA-28;o__;f__
k__Bacteria;p__Chloroflexi;Other;Other;Other
k__Bacteria;p__Chloroflexi;c__Anaerolineae;Other;Other
k__Bacteria;p__Chloroflexi;c__Anaerolineae;o__Anaerolineales;f__Anaerolinaceae
k__Bacteria;p__Chloroflexi;c__Anaerolineae;o__H39;f__
k__Bacteria;p__Chloroflexi;c__Anaerolineae;o__SBR1031;f__A4b
k__Bacteria;p__Chloroflexi;c__Anaerolineae;o__SBR1031;f__oc28
k__Bacteria;p__Chloroflexi;c__Anaerolineae;o__WCHB1-50;f__


k__Bacteria;p__Chloroflexi;c__C0119;o__;f__
k__Bacteria;p__Chloroflexi;c__Chloroflexi;Other;Other
k__Bacteria;p__Chloroflexi;c__Chloroflexi;o__AKIW781;f__
k__Bacteria;p__Chloroflexi;c__Chloroflexi;o__Herpetosiphonales;f__
k__Bacteria;p__Chloroflexi;c__Chloroflexi;o__[Roseiflexales];Other
k__Bacteria;p__Chloroflexi;c__Chloroflexi;o__[Roseiflexales];f__[Kouleothrixaceae]
k__Bacteria;p__Chloroflexi;c__Ellin6529;o__;f__
k__Bacteria;p__Chloroflexi;c__Gitt-GS-136;o__;f__
k__Bacteria;p__Chloroflexi;c__Ktedonobacteria;Other;Other
k__Bacteria;p__Chloroflexi;c__Ktedonobacteria;o__Ktedonobacterales;f__Ktedonobacteraceae
k__Bacteria;p__Chloroflexi;c__P2-11E;o__;f__
k__Bacteria;p__Chloroflexi;c__S085;o__;f__
k__Bacteria;p__Chloroflexi;c__Thermomicrobia;o__;f__
k__Bacteria;p__Chloroflexi;c__Thermomicrobia;o__JG30-KF-CM45;f__
k__Bacteria;p__Cyanobacteria;Other;Other;Other
k__Bacteria;p__Cyanobacteria;c__;o__;f__
k__Bacteria;p__Cyanobacteria;c__4C0d-2;o__MLE1-12;f__
k__Bacteria;p__Cyanobacteria;c__4C0d-2;o__SM1D11;f__
k__Bacteria;p__Cyanobacteria;c__4C0d-2;o__YS2;f__
k__Bacteria;p__Cyanobacteria;c__Chloroplast;Other;Other
k__Bacteria;p__Cyanobacteria;c__Chloroplast;o__;f__
k__Bacteria;p__Cyanobacteria;c__Chloroplast;o__Chlorophyta;Other
k__Bacteria;p__Cyanobacteria;c__Chloroplast;o__Chlorophyta;f__
k__Bacteria;p__Cyanobacteria;c__Chloroplast;o__Chlorophyta;f__Chlamydomonadaceae
k__Bacteria;p__Cyanobacteria;c__Chloroplast;o__Chlorophyta;f__Mamiellaceae
k__Bacteria;p__Cyanobacteria;c__Chloroplast;o__Chlorophyta;f__Trebouxiophyceae
k__Bacteria;p__Cyanobacteria;c__Chloroplast;o__Cryptophyta;f__
k__Bacteria;p__Cyanobacteria;c__Chloroplast;o__Haptophyceae;f__
k__Bacteria;p__Cyanobacteria;c__Chloroplast;o__Rhodophyta;f__
k__Bacteria;p__Cyanobacteria;c__Chloroplast;o__Stramenopiles;f__
k__Bacteria;p__Cyanobacteria;c__Chloroplast;o__Streptophyta;f__
k__Bacteria;p__Cyanobacteria;c__ML635J-21;o__;f__
k__Bacteria;p__Cyanobacteria;c__Nostocophycideae;o__Nostocales;f__Nostocaceae
k__Bacteria;p__Cyanobacteria;c__Oscillatoriophycideae;Other;Other
k__Bacteria;p__Cyanobacteria;c__Oscillatoriophycideae;o__Chroococcales;Other
k__Bacteria;p__Cyanobacteria;c__Oscillatoriophycideae;o__Chroococcales;f__Xenococcaceae
k__Bacteria;p__Cyanobacteria;c__Oscillatoriophycideae;o__Oscillatoriales;f__Phormidiaceae
k__Bacteria;p__Cyanobacteria;c__Synechococcophycideae;Other;Other
k__Bacteria;p__Cyanobacteria;c__Synechococcophycideae;o__Pseudanabaenales;Other
k__Bacteria;p__Cyanobacteria;c__Synechococcophycideae;o__Pseudanabaenales;f__Pseudanabaenaceae
k__Bacteria;p__Cyanobacteria;c__Synechococcophycideae;o__Synechococcales;f__Chamaesiphonaceae
k__Bacteria;p__Deferribacteres;c__Deferribacteres;o__Deferribacterales;f__Deferribacteraceae
k__Bacteria;p__Elusimicrobia;Other;Other;Other
k__Bacteria;p__Elusimicrobia;c__Elusimicrobia;Other;Other
k__Bacteria;p__Elusimicrobia;c__Elusimicrobia;o__Elusimicrobiales;f__
k__Bacteria;p__FBP;c__;o__;f__

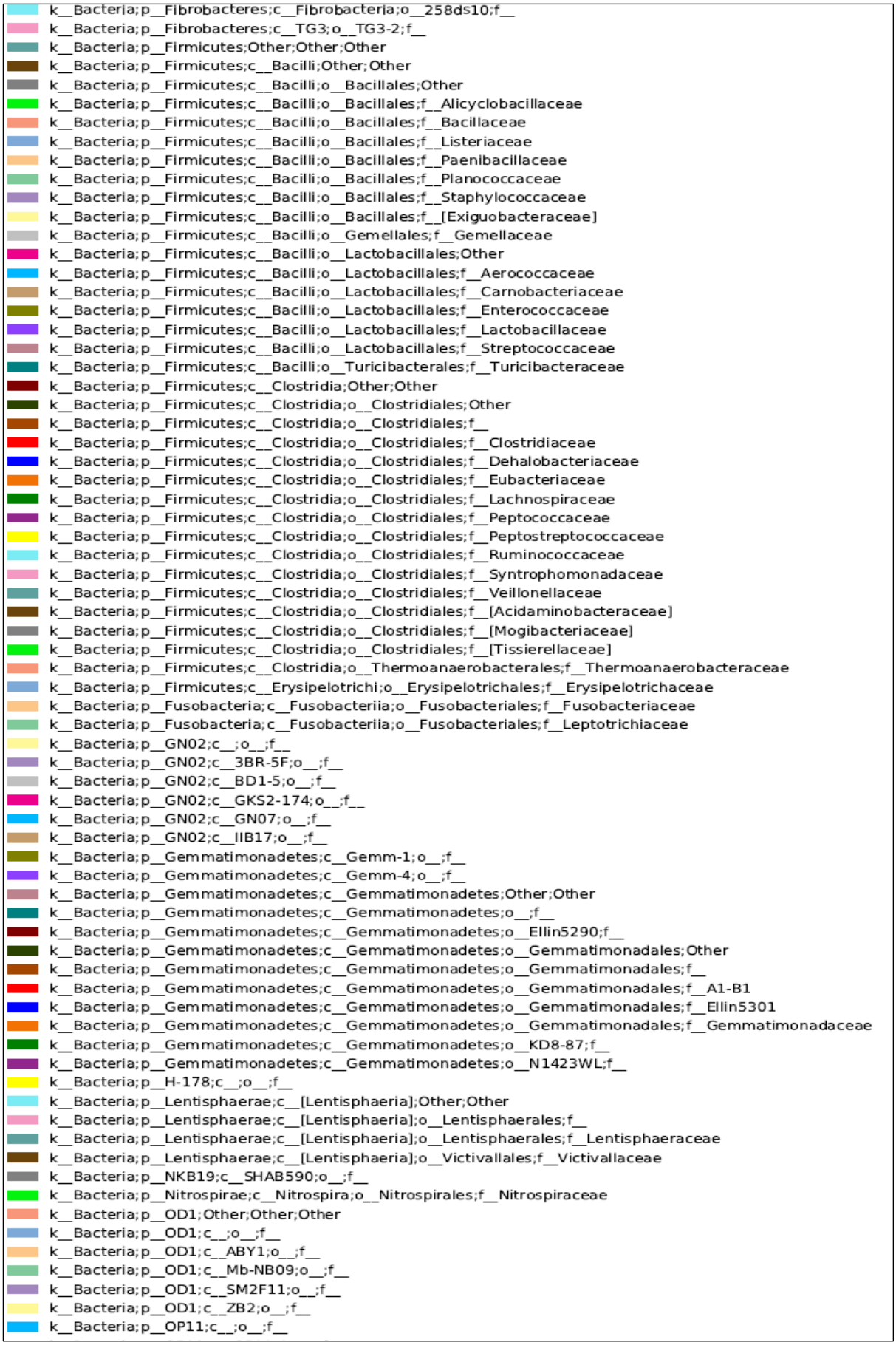
k__Bacteria;p__Fibrobacteres;c__Fibrobacteria;o__258ds10;f__
k__Bacteria;p__Fibrobacteres;c__TG3;o__TG3-2;f__
k__Bacteria;p__Firmicutes;Other;Other;Other
k__Bacteria;p__Firmicutes;c__Bacilli;Other;Other
k__Bacteria;p__Firmicutes;c__Bacilli;o__Bacillales;Other
k__Bacteria;p__Firmicutes;c__Bacilli;o__Bacillales;f__Alicyclobacillaceae
k__Bacteria;p__Firmicutes;c__Bacilli;o__Bacillales;f__Bacillaceae
k__Bacteria;p__Firmicutes;c__Bacilli;o__Bacillales;f__Listeriaceae
k__Bacteria;p__Firmicutes;c__Bacilli;o__Bacillales;f__Paenibacillaceae
k__Bacteria;p__Firmicutes;c__Bacilli;o__Bacillales;f__Planococcaceae
k__Bacteria;p__Firmicutes;c__Bacilli;o__Bacillales;f__Staphylococcaceae
k__Bacteria;p__Firmicutes;c__Bacilli;o__Bacillales;f__[Exiguobacteraceae]
k__Bacteria;p__Firmicutes;c__Bacilli;o__Gemellales;f__Gemellaceae
k__Bacteria;p__Firmicutes;c__Bacilli;o__Lactobacillales;Other
k__Bacteria;p__Firmicutes;c__Bacilli;o__Lactobacillales;f__Aerococcaceae
k__Bacteria;p__Firmicutes;c__Bacilli;o__Lactobacillales;f__Carnobacteriaceae
k__Bacteria;p__Firmicutes;c__Bacilli;o__Lactobacillales;f__Enterococcaceae
k__Bacteria;p__Firmicutes;c__Bacilli;o__Lactobacillales;f__Lactobacillaceae
k__Bacteria;p__Firmicutes;c__Bacilli;o__Lactobacillales;f__Streptococcaceae
k__Bacteria;p__Firmicutes;c__Bacilli;o__Turicibacterales;f__Turicibacteraceae
k__Bacteria;p__Firmicutes;c__Clostridia;Other;Other
k__Bacteria;p__Firmicutes;c__Clostridia;o__Clostridiales;Other
k__Bacteria;p__Firmicutes;c__Clostridia;o__Clostridiales;f__
k__Bacteria;p__Firmicutes;c__Clostridia;o__Clostridiales;f__Clostridiaceae
k__Bacteria;p__Firmicutes;c__Clostridia;o__Clostridiales;f__Dehalobacteriaceae
k__Bacteria;p__Firmicutes;c__Clostridia;o__Clostridiales;f__Eubacteriaceae
k__Bacteria;p__Firmicutes;c__Clostridia;o__Clostridiales;f__Lachnospiraceae
k__Bacteria;p__Firmicutes;c__Clostridia;o__Clostridiales;f__Peptococcaceae
k__Bacteria;p__Firmicutes;c__Clostridia;o__Clostridiales;f__Peptostreptococcaceae
k__Bacteria;p__Firmicutes;c__Clostridia;o__Clostridiales;f__Ruminococcaceae
k__Bacteria;p__Firmicutes;c__Clostridia;o__Clostridiales;f__Syntrophomonadaceae
k__Bacteria;p__Firmicutes;c__Clostridia;o__Clostridiales;f__Veillonellaceae
k__Bacteria;p__Firmicutes;c__Clostridia;o__Clostridiales;f__[Acidaminobacteraceae]
k__Bacteria;p__Firmicutes;c__Clostridia;o__Clostridiales;f__[Mogibacteriaceae]
k__Bacteria;p__Firmicutes;c__Clostridia;o__Clostridiales;f__[Tissierellaceae]
k__Bacteria;p__Firmicutes;c__Clostridia;o__Thermoanaerobacterales;f__Thermoanaerobacteraceae
k__Bacteria;p__Firmicutes;c__Erysipelotrichi;o__Erysipelotrichales;f__Erysipelotrichaceae
k__Bacteria;p__Fusobacteria;c__Fusobacteriia;o__Fusobacteriales;f__Fusobacteriaceae
k__Bacteria;p__Fusobacteria;c__Fusobacteriia;o__Fusobacteriales;f__Leptotrichiaceae
k__Bacteria;p__GN02;c__;o__;f__
k__Bacteria;p__GN02;c__3BR-5F;o__;f__
k__Bacteria;p__GN02;c__BD1-5;o__;f__
k__Bacteria;p__GN02;c__GKS2-174;o__;f__
k__Bacteria;p__GN02;c__GN07;o__;f__
k__Bacteria;p__GN02;c__IIB17;o__;f__
k__Bacteria;p__Gemmatimonadetes;c__Gemm-1;o__;f__
k__Bacteria;p__Gemmatimonadetes;c__Gemm-4;o__;f__
k__Bacteria;p__Gemmatimonadetes;c__Gemmatimonadetes;Other;Other
k__Bacteria;p__Gemmatimonadetes;c__Gemmatimonadetes;o__;f__
k__Bacteria;p__Gemmatimonadetes;c__Gemmatimonadetes;o__Ellin5290;f__
k__Bacteria;p__Gemmatimonadetes;c__Gemmatimonadetes;o__Gemmatimonadales;Other
k__Bacteria;p__Gemmatimonadetes;c__Gemmatimonadetes;o__Gemmatimonadales;f__
k__Bacteria;p__Gemmatimonadetes;c__Gemmatimonadetes;o__Gemmatimonadales;f__A1-B1
k__Bacteria;p__Gemmatimonadetes;c__Gemmatimonadetes;o__Gemmatimonadales;f__Ellin5301
k__Bacteria;p__Gemmatimonadetes;c__Gemmatimonadetes;o__Gemmatimonadales;f__Gemmatimonadaceae
k__Bacteria;p__Gemmatimonadetes;c__Gemmatimonadetes;o__KD8-87;f__
k__Bacteria;p__Gemmatimonadetes;c__Gemmatimonadetes;o__N1423WL;f__
k__Bacteria;p__H-178;c__;o__;f__
k__Bacteria;p__Lentisphaerae;c__[Lentisphaeria];Other;Other
k__Bacteria;p__Lentisphaerae;c__[Lentisphaeria];o__Lentisphaerales;f__
k__Bacteria;p__Lentisphaerae;c__[Lentisphaeria];o__Lentisphaerales;f__Lentisphaeraceae
k__Bacteria;p__Lentisphaerae;c__[Lentisphaeria];o__Victivallales;f__Victivallaceae
k__Bacteria;p__NKB19;c__SHAB590;o__;f__
k__Bacteria;p__Nitrospirae;c__Nitrospira;o__Nitrospirales;f__Nitrospiraceae
k__Bacteria;p__OD1;Other;Other;Other
k__Bacteria;p__OD1;c__;o__;f__
k__Bacteria;p__OD1;c__ABY1;o__;f__
k__Bacteria;p__OD1;c__Mb-NB09;o__;f__
k__Bacteria;p__OD1;c__SM2F11;o__;f__
k__Bacteria;p__OD1;c__ZB2;o__;f__
k__Bacteria;p__OP11;c__;o__;f__

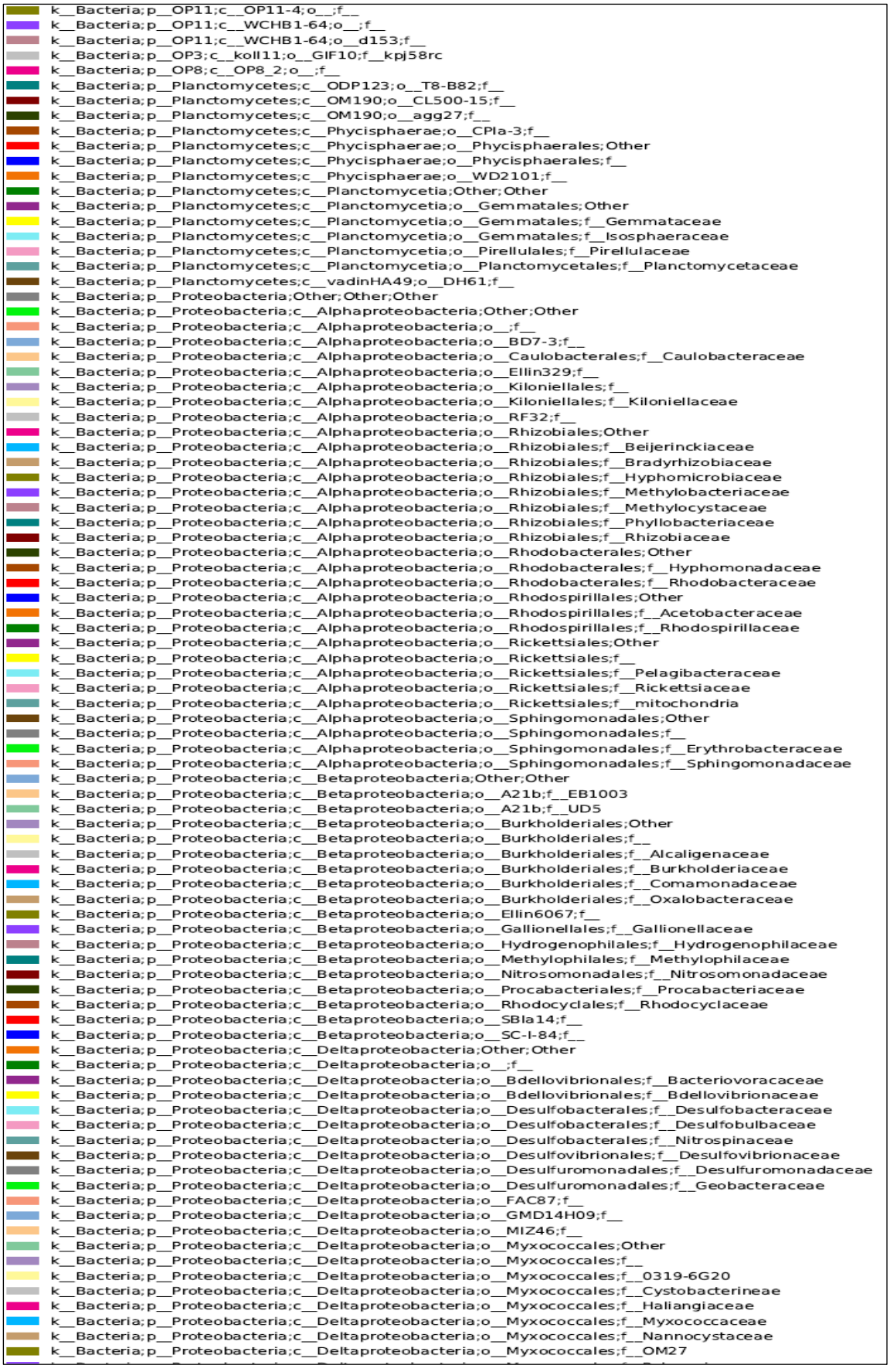
k__Bacteria;p__OP11;c__OP11-4;o__;f__
k__Bacteria;p__OP11;c__WCHB1-64;o__;f__
k__Bacteria;p__OP11;c__WCHB1-64;o__d153;f__
k__Bacteria;p__OP3;c__koll11;o__GIF10;f__kpj58rc
k__Bacteria;p__OP8;c__OP8_2;o__;f__
k__Bacteria;p__Planctomycetes;c__ODP123;o__T8-B82;f__
k__Bacteria;p__Planctomycetes;c__OM190;o__CL500-15;f__
k__Bacteria;p__Planctomycetes;c__OM190;o__agg27;f__
k__Bacteria;p__Planctomycetes;c__Phycisphaerae;o__CPla-3;f__
k__Bacteria;p__Planctomycetes;c__Phycisphaerae;o__Phycisphaerales;Other
k__Bacteria;p__Planctomycetes;c__Phycisphaerae;o__Phycisphaerales;f__
k__Bacteria;p__Planctomycetes;c__Phycisphaerae;o__WD2101;f__
k__Bacteria;p__Planctomycetes;c__Planctomycetia;Other;Other
k__Bacteria;p__Planctomycetes;c__Planctomycetia;o__Gemmatales;Other
k__Bacteria;p__Planctomycetes;c__Planctomycetia;o__Gemmatales;f__Gemmataceae
k__Bacteria;p__Planctomycetes;c__Planctomycetia;o__Gemmatales;f__Isosphaeraceae
k__Bacteria;p__Planctomycetes;c__Planctomycetia;o__Pirellulales;f__Pirellulaceae
k__Bacteria;p__Planctomycetes;c__Planctomycetia;o__Planctomycetales;f__Planctomycetaceae
k__Bacteria;p__Planctomycetes;c__vadinHA49;o__DH61;f__
k__Bacteria;p__Proteobacteria;Other;Other;Other
k__Bacteria;p__Proteobacteria;c__Alphaproteobacteria;Other;Other
k__Bacteria;p__Proteobacteria;c__Alphaproteobacteria;o__;f__
k__Bacteria;p__Proteobacteria;c__Alphaproteobacteria;o__BD7-3;f__
k__Bacteria;p__Proteobacteria;c__Alphaproteobacteria;o__Caulobacterales;f__Caulobacteraceae
k__Bacteria;p__Proteobacteria;c__Alphaproteobacteria;o__Ellin329;f__
k__Bacteria;p__Proteobacteria;c__Alphaproteobacteria;o__Kiloniellales;f__
k__Bacteria;p__Proteobacteria;c__Alphaproteobacteria;o__Kiloniellales;f__Kiloniellaceae
k__Bacteria;p__Proteobacteria;c__Alphaproteobacteria;o__RF32;f__
k__Bacteria;p__Proteobacteria;c__Alphaproteobacteria;o__Rhizobiales;Other
k__Bacteria;p__Proteobacteria;c__Alphaproteobacteria;o__Rhizobiales;f__Beijerinckiaceae
k__Bacteria;p__Proteobacteria;c__Alphaproteobacteria;o__Rhizobiales;f__Bradyrhizobiaceae
k__Bacteria;p__Proteobacteria;c__Alphaproteobacteria;o__Rhizobiales;f__Hyphomicrobiaceae
k__Bacteria;p__Proteobacteria;c__Alphaproteobacteria;o__Rhizobiales;f__Methylobacteriaceae
k__Bacteria;p__Proteobacteria;c__Alphaproteobacteria;o__Rhizobiales;f__Methylocystaceae
k__Bacteria;p__Proteobacteria;c__Alphaproteobacteria;o__Rhizobiales;f__Phyllobacteriaceae
k__Bacteria;p__Proteobacteria;c__Alphaproteobacteria;o__Rhizobiales;f__Rhizobiaceae
k__Bacteria;p__Proteobacteria;c__Alphaproteobacteria;o__Rhodobacterales;Other
k__Bacteria;p__Proteobacteria;c__Alphaproteobacteria;o__Rhodobacterales;f__Hyphomonadaceae
k__Bacteria;p__Proteobacteria;c__Alphaproteobacteria;o__Rhodobacterales;f__Rhodobacteraceae
k__Bacteria;p__Proteobacteria;c__Alphaproteobacteria;o__Rhodospirillales;Other
k__Bacteria;p__Proteobacteria;c__Alphaproteobacteria;o__Rhodospirillales;f__Acetobacteraceae
k__Bacteria;p__Proteobacteria;c__Alphaproteobacteria;o__Rhodospirillales;f__Rhodospirillaceae
k__Bacteria;p__Proteobacteria;c__Alphaproteobacteria;o__Rickettsiales;Other
k__Bacteria;p__Proteobacteria;c__Alphaproteobacteria;o__Rickettsiales;f__
k__Bacteria;p__Proteobacteria;c__Alphaproteobacteria;o__Rickettsiales;f__Pelagibacteraceae
k__Bacteria;p__Proteobacteria;c__Alphaproteobacteria;o__Rickettsiales;f__Rickettsiaceae
k__Bacteria;p__Proteobacteria;c__Alphaproteobacteria;o__Rickettsiales;f__mitochondria
k__Bacteria;p__Proteobacteria;c__Alphaproteobacteria;o__Sphingomonadales;Other
k__Bacteria;p__Proteobacteria;c__Alphaproteobacteria;o__Sphingomonadales;f__
k__Bacteria;p__Proteobacteria;c__Alphaproteobacteria;o__Sphingomonadales;f__Erythrobacteraceae
k__Bacteria;p__Proteobacteria;c__Alphaproteobacteria;o__Sphingomonadales;f__Sphingomonadaceae
k__Bacteria;p__Proteobacteria;c__Betaproteobacteria;Other;Other
k__Bacteria;p__Proteobacteria;c__Betaproteobacteria;o__A21b;f__EB1003
k__Bacteria;p__Proteobacteria;c__Betaproteobacteria;o__A21b;f__UD5
k__Bacteria;p__Proteobacteria;c__Betaproteobacteria;o__Burkholderiales;Other
k__Bacteria;p__Proteobacteria;c__Betaproteobacteria;o__Burkholderiales;f__
k__Bacteria;p__Proteobacteria;c__Betaproteobacteria;o__Burkholderiales;f__Alcaligenaceae
k__Bacteria;p__Proteobacteria;c__Betaproteobacteria;o__Burkholderiales;f__Burkholderiaceae
k__Bacteria;p__Proteobacteria;c__Betaproteobacteria;o__Burkholderiales;f__Comamonadaceae
k__Bacteria;p__Proteobacteria;c__Betaproteobacteria;o__Burkholderiales;f__Oxalobacteraceae
k__Bacteria;p__Proteobacteria;c__Betaproteobacteria;o__Ellin6067;f__
k__Bacteria;p__Proteobacteria;c__Betaproteobacteria;o__Gallionellales;f__Gallionellaceae
k__Bacteria;p__Proteobacteria;c__Betaproteobacteria;o__Hydrogenophilales;f__Hydrogenophilaceae
k__Bacteria;p__Proteobacteria;c__Betaproteobacteria;o__Methylophilales;f__Methylophilaceae
k__Bacteria;p__Proteobacteria;c__Betaproteobacteria;o__Nitrosomonadales;f__Nitrosomonadaceae
k__Bacteria;p__Proteobacteria;c__Betaproteobacteria;o__Procabacteriales;f__Procabacteriaceae
k__Bacteria;p__Proteobacteria;c__Betaproteobacteria;o__Rhodocyclales;f__Rhodocyclaceae
k__Bacteria;p__Proteobacteria;c__Betaproteobacteria;o__SBla14;f__
k__Bacteria;p__Proteobacteria;c__Betaproteobacteria;o__SC-I-84;f__
k__Bacteria;p__Proteobacteria;c__Deltaproteobacteria;Other;Other
k__Bacteria;p__Proteobacteria;c__Deltaproteobacteria;o__;f__
k__Bacteria;p__Proteobacteria;c__Deltaproteobacteria;o__Bdellovibrionales;f__Bacteriovoracaceae
k__Bacteria;p__Proteobacteria;c__Deltaproteobacteria;o__Bdellovibrionales;f__Bdellovibrionaceae
k__Bacteria;p__Proteobacteria;c__Deltaproteobacteria;o__Desulfobacterales;f__Desulfobacteraceae
k__Bacteria;p__Proteobacteria;c__Deltaproteobacteria;o__Desulfobacterales;f__Desulfobulbaceae
k__Bacteria;p__Proteobacteria;c__Deltaproteobacteria;o__Desulfobacterales;f__Nitrospinaceae
k__Bacteria;p__Proteobacteria;c__Deltaproteobacteria;o__Desulfovibrionales;f__Desulfovibrionaceae
k__Bacteria;p__Proteobacteria;c__Deltaproteobacteria;o__Desulfuromonadales;f__Desulfuromonadaceae
k__Bacteria;p__Proteobacteria;c__Deltaproteobacteria;o__Desulfuromonadales;f__Geobacteraceae
k__Bacteria;p__Proteobacteria;c__Deltaproteobacteria;o__FAC87;f__
k__Bacteria;p__Proteobacteria;c__Deltaproteobacteria;o__GMD14H09;f__
k__Bacteria;p__Proteobacteria;c__Deltaproteobacteria;o__MIZ46;f__
k__Bacteria;p__Proteobacteria;c__Deltaproteobacteria;o__Myxococcales;Other
k__Bacteria;p__Proteobacteria;c__Deltaproteobacteria;o__Myxococcales;f__
k__Bacteria;p__Proteobacteria;c__Deltaproteobacteria;o__Myxococcales;f__0319-6G20
k__Bacteria;p__Proteobacteria;c__Deltaproteobacteria;o__Myxococcales;f__Cystobacterineae
k__Bacteria;p__Proteobacteria;c__Deltaproteobacteria;o__Myxococcales;f__Haliangiaceae
k__Bacteria;p__Proteobacteria;c__Deltaproteobacteria;o__Myxococcales;f__Myxococcaceae
k__Bacteria;p__Proteobacteria;c__Deltaproteobacteria;o__Myxococcales;f__Nannocystaceae
k__Bacteria;p__Proteobacteria;c__Deltaproteobacteria;o__Myxococcales;f__OM27

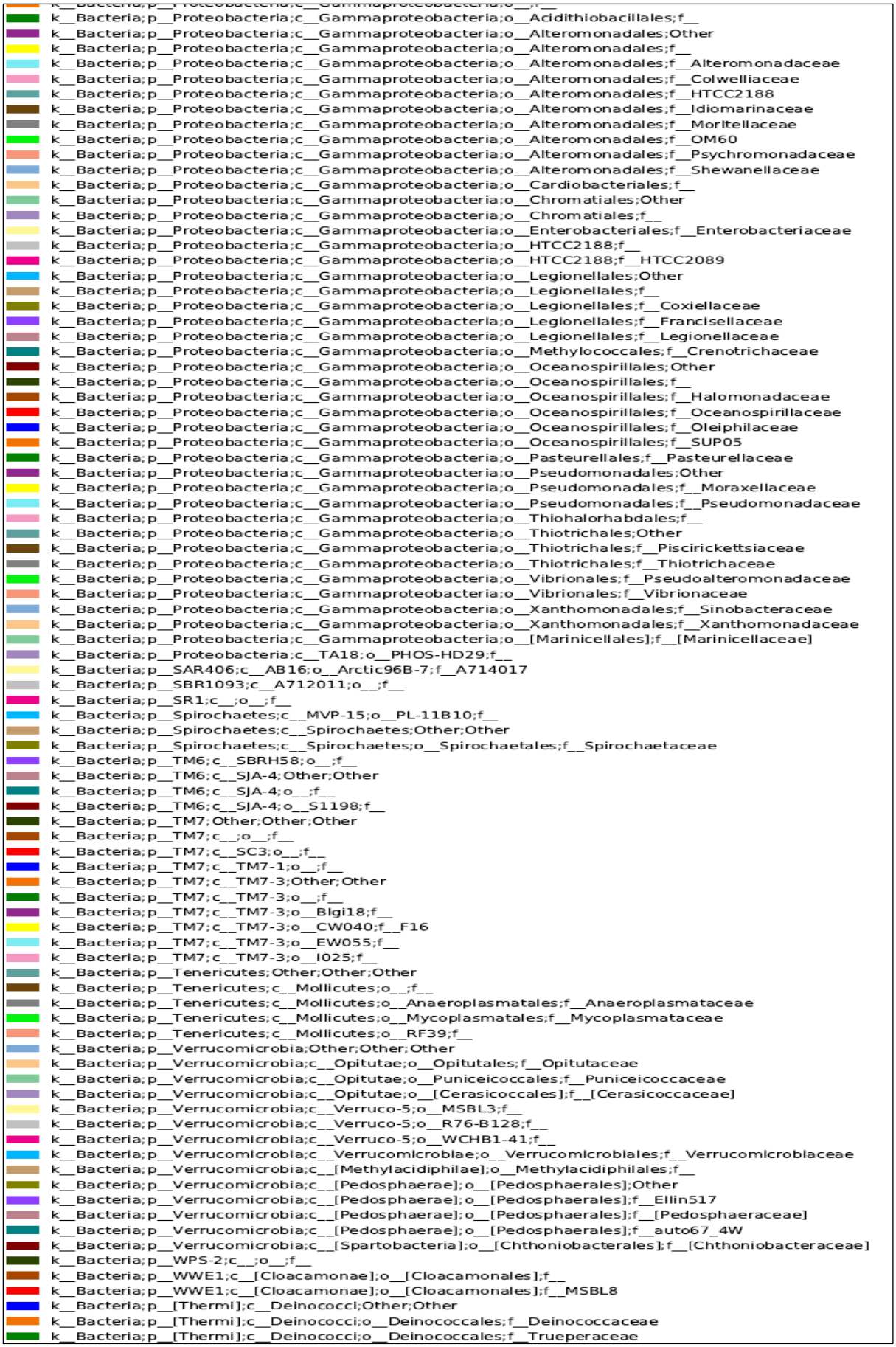
k__Bacteria;p__Proteobacteria;c__Gammaproteobacteria;o__Acidithiobacillales;f__
k__Bacteria;p__Proteobacteria;c__Gammaproteobacteria;o__Alteromonadales;Other
k__Bacteria;p__Proteobacteria;c__Gammaproteobacteria;o__Alteromonadales;f__
k__Bacteria;p__Proteobacteria;c__Gammaproteobacteria;o__Alteromonadales;f__Alteromonadaceae
k__Bacteria;p__Proteobacteria;c__Gammaproteobacteria;o__Alteromonadales;f__Colwelliaceae
k__Bacteria;p__Proteobacteria;c__Gammaproteobacteria;o__Alteromonadales;f__HTCC2188
k__Bacteria;p__Proteobacteria;c__Gammaproteobacteria;o__Alteromonadales;f__Idiomarinaceae
k__Bacteria;p__Proteobacteria;c__Gammaproteobacteria;o__Alteromonadales;f__Moritellaceae
k__Bacteria;p__Proteobacteria;c__Gammaproteobacteria;o__Alteromonadales;f__OM60
k__Bacteria;p__Proteobacteria;c__Gammaproteobacteria;o__Alteromonadales;f__Psychromonadaceae
k__Bacteria;p__Proteobacteria;c__Gammaproteobacteria;o__Alteromonadales;f__Shewanellaceae
k__Bacteria;p__Proteobacteria;c__Gammaproteobacteria;o__Cardiobacteriales;f__
k__Bacteria;p__Proteobacteria;c__Gammaproteobacteria;o__Chromatiales;Other
k__Bacteria;p__Proteobacteria;c__Gammaproteobacteria;o__Chromatiales;f__
k__Bacteria;p__Proteobacteria;c__Gammaproteobacteria;o__Enterobacteriales;f__Enterobacteriaceae
k__Bacteria;p__Proteobacteria;c__Gammaproteobacteria;o__HTCC2188;f__
k__Bacteria;p__Proteobacteria;c__Gammaproteobacteria;o__HTCC2188;f__HTCC2089
k__Bacteria;p__Proteobacteria;c__Gammaproteobacteria;o__Legionellales;Other
k__Bacteria;p__Proteobacteria;c__Gammaproteobacteria;o__Legionellales;f__
k__Bacteria;p__Proteobacteria;c__Gammaproteobacteria;o__Legionellales;f__Coxiellaceae
k__Bacteria;p__Proteobacteria;c__Gammaproteobacteria;o__Legionellales;f__Francisellaceae
k__Bacteria;p__Proteobacteria;c__Gammaproteobacteria;o__Legionellales;f__Legionellaceae
k__Bacteria;p__Proteobacteria;c__Gammaproteobacteria;o__Methylococcales;f__Crenotrichaceae
k__Bacteria;p__Proteobacteria;c__Gammaproteobacteria;o__Oceanospirillales;Other
k__Bacteria;p__Proteobacteria;c__Gammaproteobacteria;o__Oceanospirillales;f__
k__Bacteria;p__Proteobacteria;c__Gammaproteobacteria;o__Oceanospirillales;f__Halomonadaceae
k__Bacteria;p__Proteobacteria;c__Gammaproteobacteria;o__Oceanospirillales;f__Oceanospirillaceae
k__Bacteria;p__Proteobacteria;c__Gammaproteobacteria;o__Oceanospirillales;f__Oleiphilaceae
k__Bacteria;p__Proteobacteria;c__Gammaproteobacteria;o__Oceanospirillales;f__SUP05
k__Bacteria;p__Proteobacteria;c__Gammaproteobacteria;o__Pasteurellales;f__Pasteurellaceae
k__Bacteria;p__Proteobacteria;c__Gammaproteobacteria;o__Pseudomonadales;Other
k__Bacteria;p__Proteobacteria;c__Gammaproteobacteria;o__Pseudomonadales;f__Moraxellaceae
k__Bacteria;p__Proteobacteria;c__Gammaproteobacteria;o__Pseudomonadales;f__Pseudomonadaceae
k__Bacteria;p__Proteobacteria;c__Gammaproteobacteria;o__Thiohalorhabdales;f__
k__Bacteria;p__Proteobacteria;c__Gammaproteobacteria;o__Thiotrichales;Other
k__Bacteria;p__Proteobacteria;c__Gammaproteobacteria;o__Thiotrichales;f__Piscirickettsiaceae
k__Bacteria;p__Proteobacteria;c__Gammaproteobacteria;o__Thiotrichales;f__Thiotrichaceae
k__Bacteria;p__Proteobacteria;c__Gammaproteobacteria;o__Vibrionales;f__Pseudoalteromonadaceae
k__Bacteria;p__Proteobacteria;c__Gammaproteobacteria;o__Vibrionales;f__Vibrionaceae
k__Bacteria;p__Proteobacteria;c__Gammaproteobacteria;o__Xanthomonadales;f__Sinobacteraceae
k__Bacteria;p__Proteobacteria;c__Gammaproteobacteria;o__Xanthomonadales;f__Xanthomonadaceae
k__Bacteria;p__Proteobacteria;c__Gammaproteobacteria;o__[Marinicellales];f__[Marinicellaceae]
k__Bacteria;p__Proteobacteria;c__TA18;o__PHOS-HD29;f__
k__Bacteria;p__SAR406;c__AB16;o__Arctic96B-7;f__A714017
k__Bacteria;p__SBR1093;c__A712011;o__;f__
k__Bacteria;p__SR1;c__;o__;f__
k__Bacteria;p__Spirochaetes;c__MVP-15;o__PL-11B10;f__
k__Bacteria;p__Spirochaetes;c__Spirochaetes;Other;Other
k__Bacteria;p__Spirochaetes;c__Spirochaetes;o__Spirochaetales;f__Spirochaetaceae
k__Bacteria;p__TM6;c__SBRH58;o__;f__
k__Bacteria;p__TM6;c__SJA-4;Other;Other
k__Bacteria;p__TM6;c__SJA-4;o__;f__
k__Bacteria;p__TM6;c__SJA-4;o__S1198;f__
k__Bacteria;p__TM7;Other;Other;Other
k__Bacteria;p__TM7;c__;o__;f__
k__Bacteria;p__TM7;c__SC3;o__;f__
k__Bacteria;p__TM7;c__TM7-1;o__;f__
k__Bacteria;p__TM7;c__TM7-3;Other;Other
k__Bacteria;p__TM7;c__TM7-3;o__;f__
k__Bacteria;p__TM7;c__TM7-3;o__Blgi18;f__
k__Bacteria;p__TM7;c__TM7-3;o__CW040;f__F16
k__Bacteria;p__TM7;c__TM7-3;o__EW055;f__
k__Bacteria;p__TM7;c__TM7-3;o__I025;f__
k__Bacteria;p__Tenericutes;Other;Other;Other
k__Bacteria;p__Tenericutes;c__Mollicutes;o__;f__
k__Bacteria;p__Tenericutes;c__Mollicutes;o__Anaeroplasmatales;f__Anaeroplasmataceae
k__Bacteria;p__Tenericutes;c__Mollicutes;o__Mycoplasmatales;f__Mycoplasmataceae
k__Bacteria;p__Tenericutes;c__Mollicutes;o__RF39;f__
k__Bacteria;p__Verrucomicrobia;Other;Other;Other
k__Bacteria;p__Verrucomicrobia;c__Opitutae;o__Opitutales;f__Opitutaceae
k__Bacteria;p__Verrucomicrobia;c__Opitutae;o__Puniceicoccales;f__Puniceicoccaceae
k__Bacteria;p__Verrucomicrobia;c__Opitutae;o__[Cerasicoccales];f__[Cerasicoccaceae]
k__Bacteria;p__Verrucomicrobia;c__Verruco-5;o__MSBL3;f__
k__Bacteria;p__Verrucomicrobia;c__Verruco-5;o__R76-B128;f__
k__Bacteria;p__Verrucomicrobia;c__Verruco-5;o__WCHB1-41;f__
k__Bacteria;p__Verrucomicrobia;c__Verrucomicrobiae;o__Verrucomicrobiales;f__Verrucomicrobiaceae
k__Bacteria;p__Verrucomicrobia;c__[Methylacidiphilae];o__Methylacidiphilales;f__
k__Bacteria;p__Verrucomicrobia;c__[Pedosphaerae];o__[Pedosphaerales];Other
k__Bacteria;p__Verrucomicrobia;c__[Pedosphaerae];o__[Pedosphaerales];f__Ellin517
k__Bacteria;p__Verrucomicrobia;c__[Pedosphaerae];o__[Pedosphaerales];f__[Pedosphaeraceae]
k__Bacteria;p__Verrucomicrobia;c__[Pedosphaerae];o__[Pedosphaerales];f__auto67_4W
k__Bacteria;p__Verrucomicrobia;c__[Spartobacteria];o__[Chthoniobacterales];f__[Chthoniobacteraceae]
k__Bacteria;p__WPS-2;c__;o__;f__
k__Bacteria;p__WWE1;c__[Cloacamonae];o__[Cloacamonales];f__
k__Bacteria;p__WWE1;c__[Cloacamonae];o__[Cloacamonales];f__MSBL8
k__Bacteria;p__[Thermi];c__Deinococci;Other;Other
k__Bacteria;p__[Thermi];c__Deinococci;o__Deinococcales;f__Deinococcaceae
k__Bacteria;p__[Thermi];c__Deinococci;o__Deinococcales;f__Trueperaceae

Appendix 4- Samples identifications (Chapter 6)

	Sample	Plate
Plate 1	Name	Location
9676_1	Chronic DSS, 100, d1,1	A1
9676_2	Chronic DSS, 100, d1,2	A2
9676_3	Chronic DSS, 100, d1,3	A3
9676_4	Chronic DSS, 100, d1,4	A4
9676_5	Chronic DSS, 100, d1,5	A5
9676_6	Chronic DSS, 100, d1,6	A6
9676_7	Chronic DSS, 100, d1,7	A7
9676_8	Chronic DSS, 200, d1,1	A8
9676_9	Chronic DSS, 200, d1,2	A9
9676_10	Chronic DSS, 200, d1,3	A10
9676_11	Chronic DSS, 200, d1,4	A11
9676_12	Chronic DSS, 200, d1,5	A12
9676_13	Chronic DSS, 200, d1,6	B1
9676_14	Chronic DSS, 200, d1,7	B2
9676_15	Chronic DSS, 400, d1,1	B3
9676_16	Chronic DSS, 400, d1,2	B4
9676_17	Chronic DSS, 400, d1,3	B5
9676_18	Chronic DSS, 400, d1,4	B6
9676_19	Chronic DSS, 400, d1,5	B7
9676_20	Chronic DSS, 400, d1,6	B8
9676_21	Chronic DSS, 400, d1,7	B9
9676_22	Chronic control, 100, d1,1	B10
9676_23	Chronic control, 100, d1,2	B11
9676_24	Chronic control, 100, d1,3	B12
9676_25	Chronic control, 100, d1,4	C1
9676_26	Chronic control, 100, d1,5	C2
9676_27	Chronic control, 100, d1,6	C3
9676_28	Chronic control, 100, d1,7	C4
9676_29	Chronic control, 200, d1,1	C5
9676_30	Chronic control, 200, d1,2	C6
9676_31	Chronic control, 200, d1,3	C7
9676_32	Chronic control, 200, d1,4	C8
9676_33	Chronic control, 200, d1,5	C9
9676_34	Chronic control, 200, d1,6	C10
9676_35	Chronic control, 200, d1,7	C11
9676_36	Chronic control, 400, d1,1	C12
9676_37	Chronic control, 400, d1,2	D1
9676_38	Chronic control, 400, d1,3	D2
9676_39	Chronic control, 400, d1,4	D3

9676_40	Chronic control, 400, d1,5	D4
9676_41	Chronic control, 400, d1,6	D5
9676_42	Chronic control, 400, d1,7	D6
9676_43	Chronic DSS, 100, d21,1	D7
9676_44	Chronic DSS, 100, d21,2	D8
9676_45	Chronic DSS, 100, d21,3	D9
9676_46	Chronic DSS, 100, d21,4	D10
9676_47	Chronic DSS, 100, d21,5	D11
9676_48	Chronic DSS, 100, d21,6	D12
9676_49	Chronic DSS, 100, d21,7	E1
9676_50	Chronic DSS, 200, d21,1	E2
9676_51	Chronic DSS, 200, d21,2	E3
9676_52	Chronic DSS, 200, d21,3	E4
9676_53	Chronic DSS, 200, d21,4	E5
9676_54	Chronic DSS, 200, d21,5	E6
9676_55	Chronic DSS, 200, d21,6	E7
9676_56	Chronic DSS, 200, d21,7	E8
9676_57	Chronic DSS, 400, d21,1	E9
9676_58	Chronic DSS, 400, d21,2	E10
9676_59	Chronic DSS, 400, d21,3	E11
9676_60	Chronic DSS, 400, d21,4	E12
9676_61	Chronic DSS, 400, d21,5	F1
9676_62	Chronic DSS, 400, d21,6	F2
9676_63	Chronic DSS, 400, d21,7	F3
9676_64	Chronic control, 100, d21,1	F4
9676_65	Chronic control, 100, d21,2	F5
9676_66	Chronic control, 100, d21,3	F6
9676_67	Chronic control, 100, d21,4	F7
9676_68	Chronic control, 100, d21,5	F8
9676_69	Chronic control, 100, d21,6	F9
9676_70	Chronic control, 100, d21,7	F10
9676_71	Chronic control, 200, d21,1	F11
9676_72	Chronic control, 200, d21,2	F12
9676_73	Chronic control, 200, d21,3	G1
9676_74	Chronic control, 200, d21,4	G2
9676_75	Chronic control, 200, d21,5	G3
9676_76	Chronic control, 200, d21,6	G4
9676_77	Chronic control, 200, d21,7	G5
9676_78	Chronic control, 400, d21,1	G6
9676_79	Chronic control, 400, d21,2	G7
9676_80	Chronic control, 400, d21,3	G8
9676_81	Chronic control, 400, d21,4	G9
9676_82	Chronic control, 400, d21,5	G10
9676_83	Chronic control, 400, d21,6	G11
9676_84	Chronic control, 400, d21,7	G12

9676_85	Chronic DSS, 100, d42,1	H1
9676_86	Chronic DSS, 100, d42,2	H2
9676_87	Chronic DSS, 100, d42,3	H3
9676_88	Chronic DSS, 100, d42,4	H4
9676_89	Chronic DSS, 100, d42,5	H5
9676_90	Chronic DSS, 100, d42,6	H6
9676_91	Chronic DSS, 100, d42,7	H7
9676_92	Chronic DSS, 200, d42,1	H8
9676_93	Chronic DSS, 200, d42,2	H9
9676_94	Chronic DSS, 200, d42,3	H10
9676_95	Chronic DSS, 200, d42,4	H11
9676_96	Chronic DSS, 200, d42,5	H12

	Sample	Plate
Plate 2	Name	Location
9676_97	Chronic DSS, 200, d42,6	A1
9676_98	Chronic DSS, 200, d42,7	A2
9676_99	Chronic DSS, 400, d42,1	A3
9676_100	Chronic DSS, 400, d42,2	A4
9676_101	Chronic DSS, 400, d42,3	A5
9676_102	Chronic DSS, 400, d42,4	A6
9676_103	Chronic DSS, 400, d42,5	A7
9676_104	Chronic DSS, 400, d42,6	A8
9676_105	Chronic DSS, 400, d42,7	A9
9676_106	Chronic control, 100, d42,1	A10
9676_107	Chronic control, 100, d42,2	A11
9676_108	Chronic control, 100, d42,3	A12
9676_109	Chronic control, 100, d42,4	B1
9676_110	Chronic control, 100, d42,5	B2
9676_111	Chronic control, 100, d42,6	B3
9676_112	Chronic control, 100, d42,7	B4
9676_113	Chronic control, 200, d42,1	B5
9676_114	Chronic control, 200, d42,2	B6
9676_115	Chronic control, 200, d42,3	B7
9676_116	Chronic control, 200, d42,4	B8
9676_117	Chronic control, 200, d42,5	B9
9676_118	Chronic control, 200, d42,6	B10
9676_119	Chronic control, 200, d42,7	B11
9676_120	Chronic control, 400, d42,1	B12
9676_121	Chronic control, 400, d42,2	C1
9676_122	Chronic control, 400, d42,3	C2
9676_123	Chronic control, 400, d42,4	C3

9676_124	Chronic control, 400, d42,5	C4
9676_125	Chronic control, 400, d42,6	C5
9676_126	Chronic control, 400, d42,7	C6
9676_127	Chronic DSS, 100, d63,1	C7
9676_128	Chronic DSS, 100, d63,2	C8
9676_129	Chronic DSS, 100, d63,3	C9
9676_130	Chronic DSS, 100, d63,4	C10
9676_131	Chronic DSS, 100, d63,5	C11
9676_132	Chronic DSS, 100, d63,6	C12
9676_133	Chronic DSS, 100, d63,7	D1
9676_134	Chronic DSS, 200, d63,1	D2
9676_135	Chronic DSS, 200, d63,2	D3
9676_136	Chronic DSS, 200, d63,3	D4
9676_137	Chronic DSS, 200, d63,4	D5
9676_138	Chronic DSS, 200, d63,5	D6
9676_139	Chronic DSS, 200, d63,6	D7
9676_140	Chronic DSS, 200, d63,7	D8
9676_141	Chronic DSS, 400, d63,1	D9
9676_142	Chronic DSS, 400, d63,2	D10
9676_143	Chronic DSS, 400, d63,3	D11
9676_144	Chronic DSS, 400, d63,4	D12
9676_145	Chronic DSS, 400, d63,5	E1
9676_146	Chronic DSS, 400, d63,6	E2
9676_147	Chronic DSS, 400, d63,7	E3
9676_148	Chr.ctr.d63,acute DSS d1, 100, 1	E4
9676_149	Chr.ctr.d63,acute DSS d1, 100, 2	E5
9676_150	Chr.ctr.d63,acute DSS d1, 100, 3	E6
9676_151	Chr.ctr.d63,acute ctr. d1, 100, 1	E7
9676_152	Chr.ctr.d63,acute ctr. d1, 100, 2	E8
9676_153	Chr.ctr.d63,acute ctr. d1, 100, 3	E9
9676_154	Chr.ctr.d63,acute ctr. d1, 100, 4	E10
9676_155	Chr.ctr.d63,acute DSS d1, 200, 1	E11
9676_156	Chr.ctr.d63,acute DSS d1, 200, 2	E12
9676_157	Chr.ctr.d63,acute DSS d1, 200, 3	F1
9676_158	Chr.ctr.d63,acute ctr. d1, 200, 1	F2
9676_159	Chr.ctr.d63,acute ctr. d1, 200, 2	F3
9676_160	Chr.ctr.d63,acute ctr. d1, 200, 3	F4
9676_161	Chr.ctr.d63,acute ctr. d1, 200, 4	F5
9676_162	Chr.ctr.d63,acute DSS d1, 200, 1	F6
9676_163	Chr.ctr.d63,acute DSS d1, 200, 2	F7
9676_164	Chr.ctr.d63,acute DSS d1, 200, 3	F8
9676_165	Chr.ctr.d63,acute ctr. d1, 200, 1	F9
9676_166	Chr.ctr.d63,acute ctr. d1, 200, 2	F10
9676_167	Chr.ctr.d63,acute ctr. d1, 200, 3	F11
9676_168	Chr.ctr.d63,acute ctr. d1, 200, 4	F12

9676_169	Acute DSS d10, 100, 1	G1
9676_170	Acute DSS d10, 100, 2	G2
9676_171	Acute DSS d10, 100, 3	G3
9676_172	Control d63,d10, 100, 1	G4
9676_173	Control d63,d10, 100, 2	G5
9676_174	Control d63,d10, 100, 3	G6
9676_175	Control d63,d10, 100, 4	G7
9676_176	Acute DSS d10, 200, 1	G8
9676_177	Acute DSS d10, 200, 2	G9
9676_178	Acute DSS d10, 200, 3	G10
9676_179	Control d63,d10, 200, 1	G11
9676_180	Control d63,d10, 200, 2	G12
9676_181	Control d63,d10, 200, 3	H1
9676_182	Control d63,d10, 200, 4	H2
9676_183	Acute DSS d10, 400, 1	H3
9676_184	Acute DSS d10, 400, 2	H4
9676_185	Acute DSS d10, 400, 3	H5
9676_186	Control d63,d10, 400, 1	H6
9676_187	Control d63,d10, 400, 2	H7
9676_188	Control d63,d10, 400, 3	H8
9676_189	Control d63,d10, 400, 4	H9

Appendix 5- Total number of reads (Chapter 6)

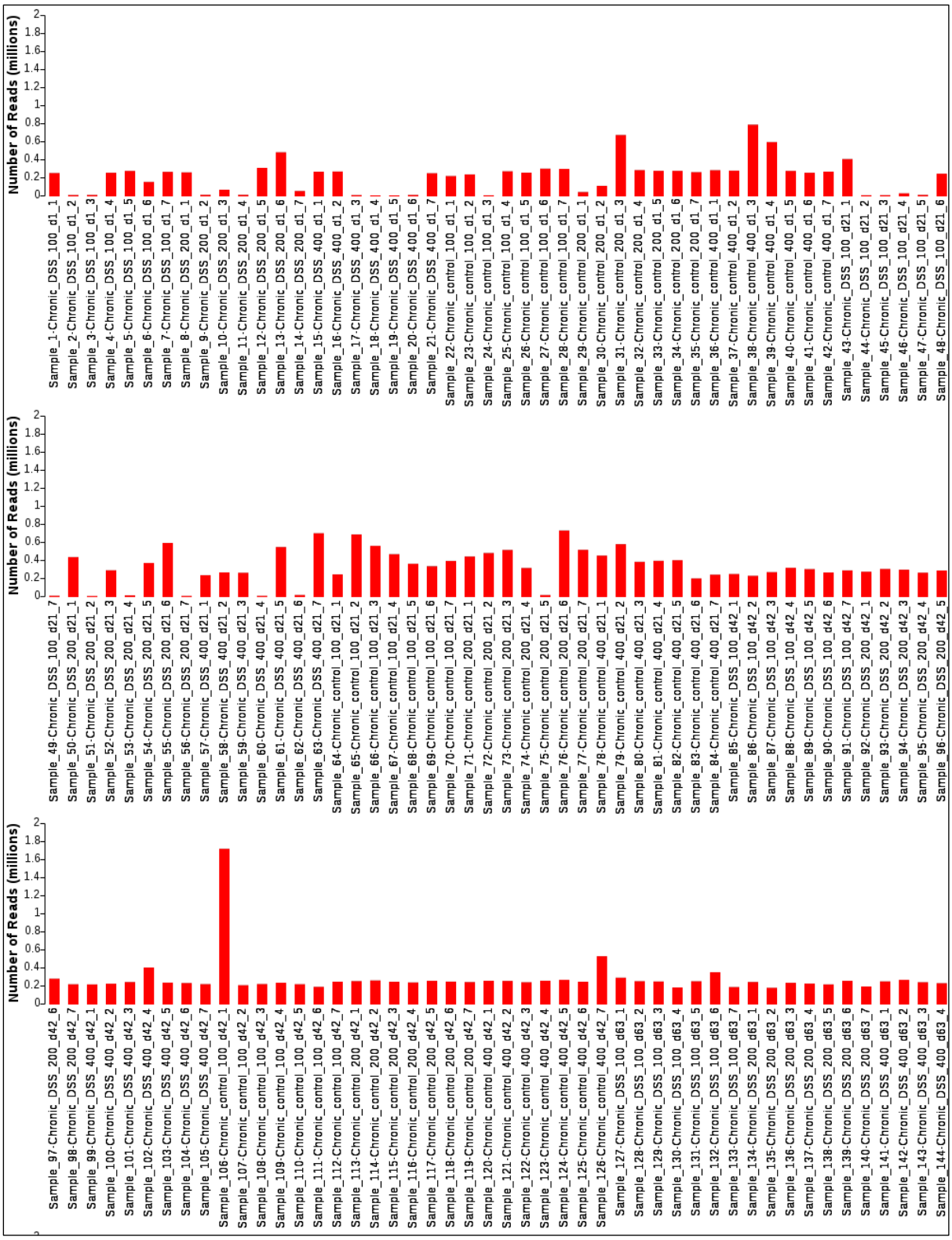

Diagram illustrating the total number of reads obtained for each sample.

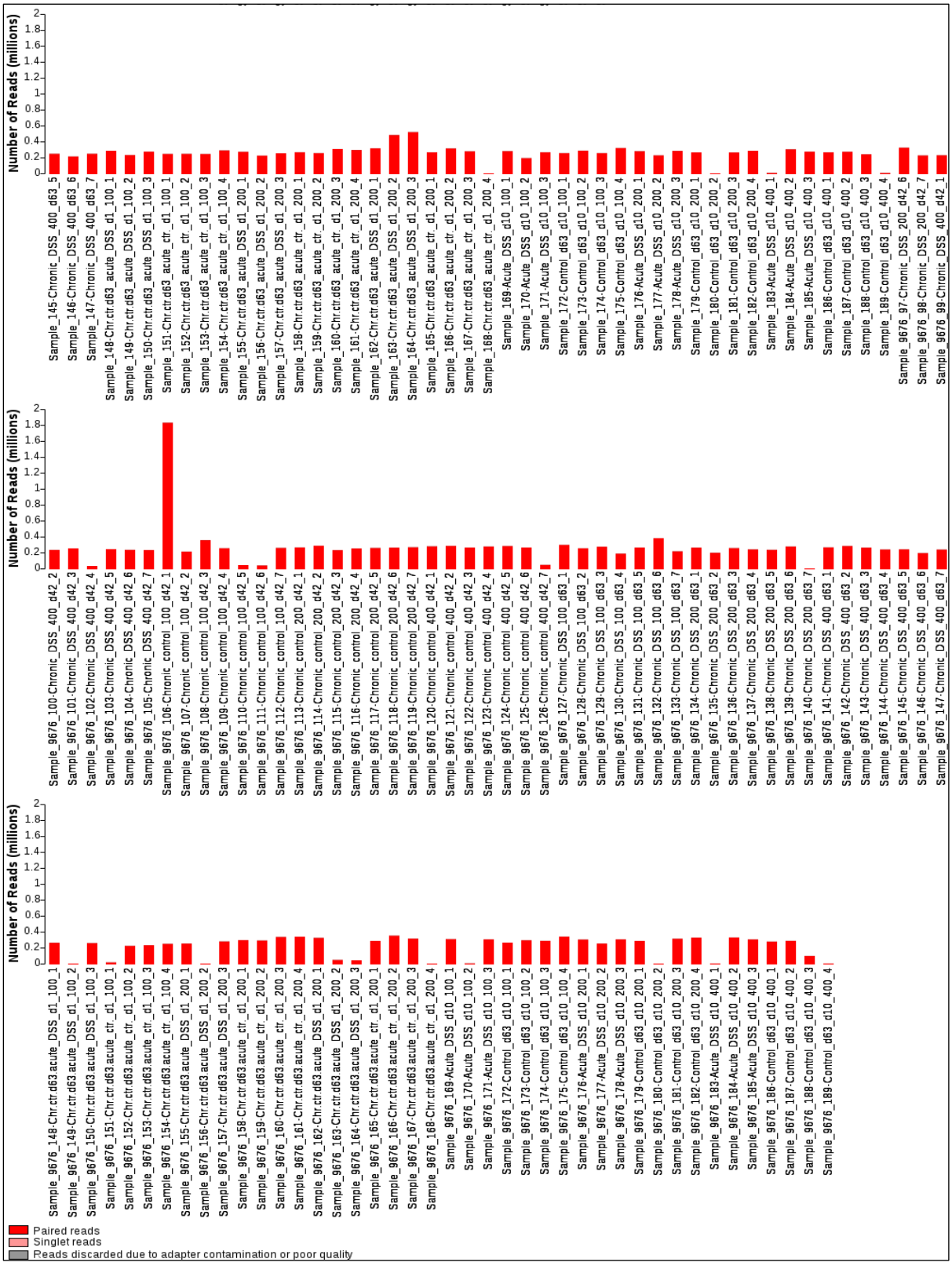

Diagram illustrating the total number of reads obtained for each sample.

Appendix 6- Distribution of trimmed read lengths (Chapter 6)

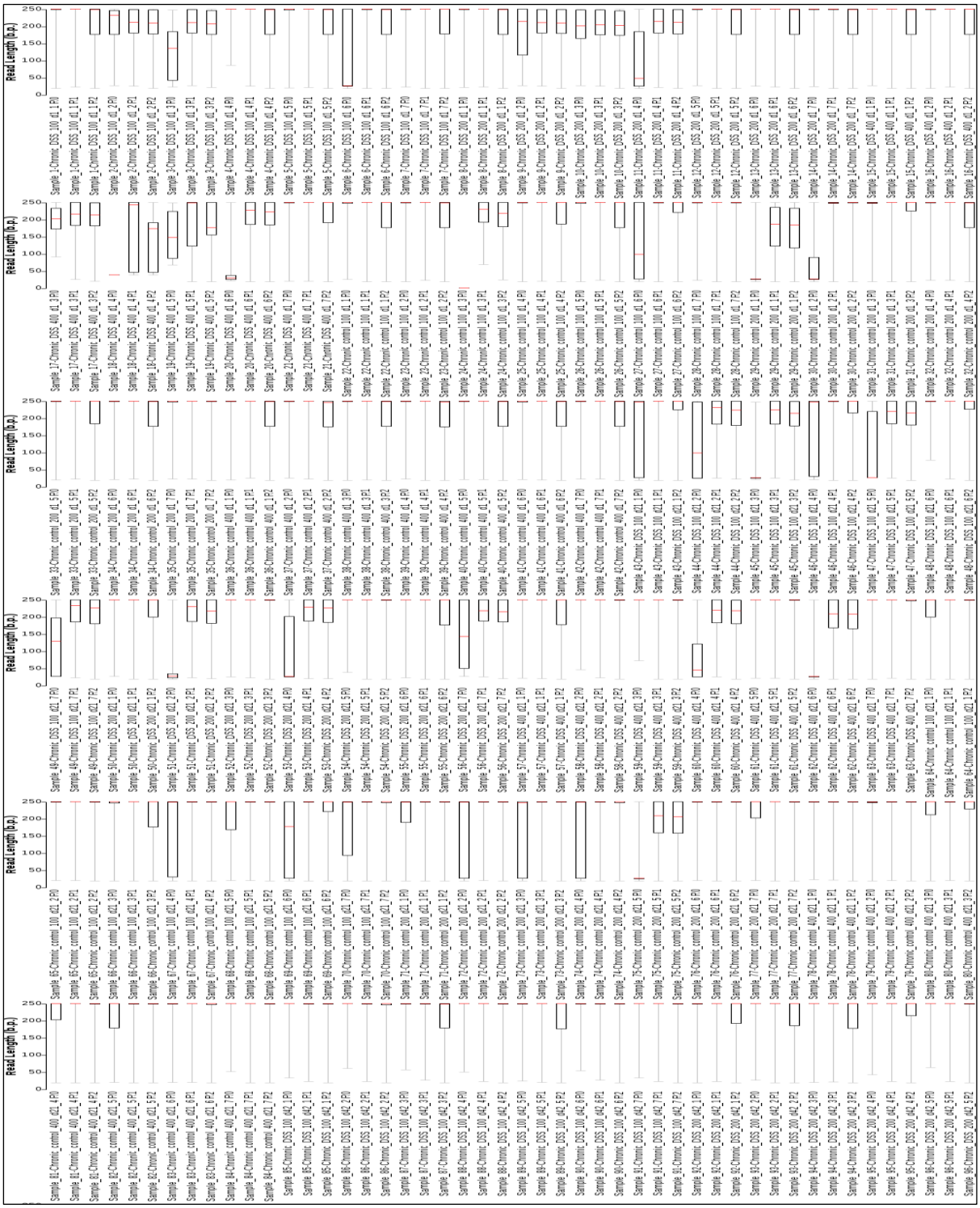

Box plot showing the distribution of trimmed read lengths for the forward (R1), reverse (R2) and singlet (R0) reads.

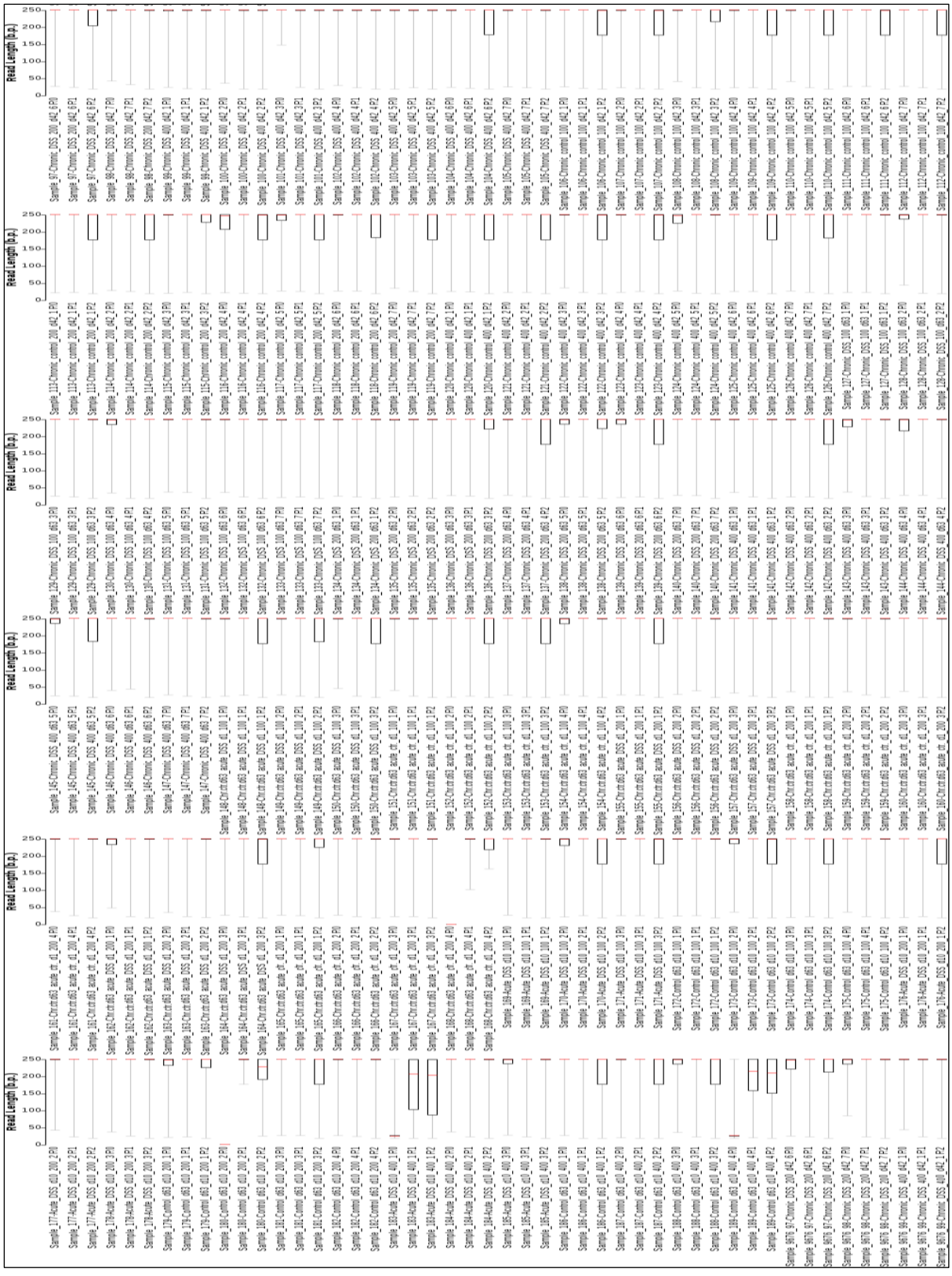

Box plot showing the distribution of trimmed read lengths for the forward (R1), reverse (R2) and singlet (R0) reads.

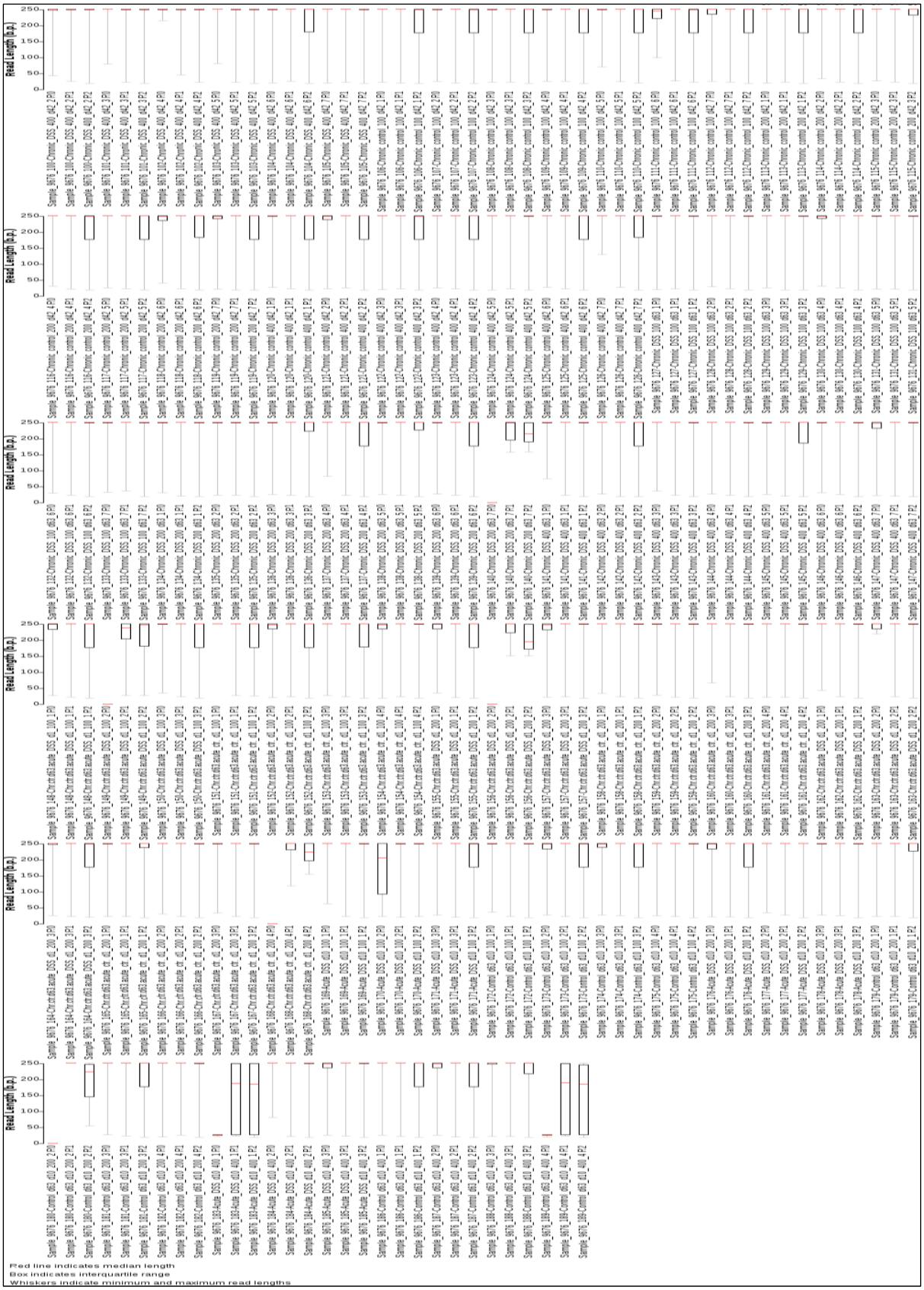

Box plot showing the distribution of trimmed read lengths for the forward (R1), reverse (R2) and singlet (R0) reads.